N° D'ORDRE : 866

THESE

présentée à

L'UNIVERSITE DES SCIENCES ET TECHNIQUES DE LILLE
FLANDRES ARTOIS

pour obtenir le grade de

DOCTEUR DE L'UNIVERSITE

en

LASERS, MOLECULES ET
RAYONNEMENT ATMOSPHERIQUE

par

Mireille LE GUENNEC

SPECTROSCOPIE DE ROTATION ET STRUCTURES DE :

$BrCN$, $OCSe$, $FClO_3$, GeH_3F, CH_3CN, CH_2CHPH_2

Soutenue le 21 Février 1992 devant la commission d'examen

M. P. GLORIEUX	Professseur à l'Université de Lille I	Président du jury
M. D. BOUGEARD	Directeur de Recherches CNRS, Lille I	Rapporteur
M. J. L. TEFFO	Maître de Conférences à l'Université Pierre et Marie Curie, Paris	Rapporteur
M. M. BOGEY	Directeur de Recherches CNRS, Lille I	Rapporteur
M. J. M. DENIS	Directeur de Recherches CNRS, Rennes I	Examinateur
M. J. DEMAISON	Directeur de Recherches CNRS, Lille I	Directeur de Thèse

Ce travail a été réalisé au LABORATOIRE DE SPECTROSCOPIE HERTZIENNE (U.A. 249) de l'Université de Lille I, dirigé par Monsieur le Professeur P. GLORIEUX qui me fait l'honneur de présider le jury de cette thèse.

Je souhaite également remercier Monsieur le Professeur B. MACKE pour m'avoir accueillie dans ce laboratoire.

Qu'ils trouvent ici l'expression de ma profonde gratitude.

Je remercie très vivement Messieurs J.L. TEFFO, D. BOUGEARD et M. BOGEY qui me font l'honneur de juger ce travail.

Je tiens à remercier tout partivculièrement Messieurs J. DEMAISON et J. M. DENIS, Directeurs de Recherches au CNRS. Que ce mémoire soit l'occasion de leur exprimer ma sincère reconnaissance pour avoir assuré la direction de cette thèse et pour les conseils qu'ils m'ont prodigués tout au long de ce travail.

Que Monsieur le Professeur H. BÜRGER et Messieurs K. BURCZYK, R. EUJEN et H. WILLNER soient remerciés pour leur collaboration et la synthèse des composés inorganiques.

J'adresse aussi mes remerciements à Messieurs les Professeurs J. L. ALONSO et J. C. LOPEZ ainsi qu'à Monsieur J. C. GUILLEMIN pour l'accueil et la constante disponibilité qu'ils m'ont toujours réservés.

Enfin, j'exprime ma plus profonde sympathie à Monsieur le Professeur D. BOUCHER et Messieurs G. WLODARCZAK, J. BURIE et R. BOCQUET grâce à qui les résultats présentés ont pu être obtenus. J'ai également eu la chance de connaître et de travailler avec W. CHEN, J. COSLEOU et H. DELBARRE. Qu'ils trouvent ici l'expression de mon amical souvenir.

Mes remerciements vont également à l'ensemble du personnel technique et administratif du laboratoire et de l'UFR de Physique grâce auquel ce travail s'est effectué dans les meilleures conditions, et en particulier à Mademoiselle S. DESCHAMPS qui s'est chargée de la dactylographie de ce mémoire.

SOMMAIRE

C - Aspects expérimentaux

1°) Obtention des molécules - Synthèses -

1.1. Le séléniure de carbonyle : OCSe

1.2. Le fluorure de germyle : GeH_3F

1.3. Le fluorure de perchloryle : $FClO_3$

1.4. L'acétonitrile monodeutéré : CH_2DCN

1.5. Les propynes monodeutérés

a) propyne - 3D

b) propyne - 1D

1.6. Les molécules phosphorées

a) Cl-C≡P

b) $H_2C=CH(PH_2)$

c) $(CH_3)CH=PH$

d) synthèse et isomérisation de l'yne phosphine

e) schéma du montage utilisé pour la mise en évidence des dérivés de basse coordinence du phosphore non stabilisés

2°) Les spectromètres utilisés

3°) Le traitement du signal par le logiciel LabVIEW

4°) Les calculs "ab initio" avec Gaussian 82

Bibliographie

D - Analyse des spectres et structures géométriques

1°) Molécules linéaires

1.1. Etat fondamental et structures géométriques du bromure de cyanogène

1.2. Etat fondamental et structures géométriques du séléniure de carbonyle

2°) Molécules symétriques

2.1. Le fluorure de perchoryle

2.2. Le fluorure de germyle

2.3. L'acétonitrile

E - Analyse de composés de basse coordinence du phosphore non stabilisés

Introduction

La spectroscopie de rotation est à juste titre considérée comme la technique la plus précise de détermination de la structure géométrique des molécules isolées (en phase gazeuse). Cependant la structure déterminée est le plus souvent une structure empirique (dite "effective") car même lorsque les données expérimentales sont suffisantes pour déterminer tous les paramètres géométriques (ce qui n'est pas le cas général), on est souvent amené à négliger les interactions de rotation-vibration. Or il est bien établi que ces interactions ne sont pas négligeables et qu'en particulier elles peuvent avoir une influence importante sur la structure obtenue.

Le but de ce travail est :

- d'étudier expérimentalement l'influence de ces interactions sur la structure de molécules assez simples pour pouvoir être utilisées comme modèles,
- de comparer les différentes méthodes permettant de calculer une structure expérimentale,
- et finalement, de montrer que, pour des molécules simples et possèdant un nombre suffisant d'isotopomères, l'analyse des résidus du calcul des moindres carrés permet de modéliser de façon simple l'influence des vibrations sur les moments d'inertie et donc de déterminer une structure qui est une très bonne approximation de la structure à l'équilibre.

Après quelques généralités spectroscopiques, présentées dans un premier chapitre afin de mieux comprendre ce qui va suivre, nous verrons dans le chapitre suivant les différentes méthodes dont on dispose pour déterminer la structure d'une molécule. C'est ainsi que l'on définit quatre grandes familles de structures géométriques selon le type d'approximation effectué :

- la structure à l'équilibre (dite structure r_e) est la structure de référence car elle correspond au minimum de l'énergie potentielle,
- la structure effective (r_0), obtenue directement à partir des constantes de rotation de l'état fondamental et dans laquelle les interactions de rotation-vibration sont négligées,
- les structures de substitution déterminées en substituant différents atomes de la molécule. Il est possible de substituer soit chaque atome successivement (r_s), soit deux atomes différents simultanément (r_{ss}), soit les atomes symétriquement équivalents simultanément (polysubstitution),
- les structures "moyennes" correspondant à la configuration moléculaire moyenne dans un état de vibration donné et calculée à partir des moments d'inertie expérimentaux.

Dans un troisième chapitre, nous aborderons les aspects expérimentaux de ce travail : la synthèse des molécules étudiées, les différents spectromètres utilisés, ...

Nous présenterons ensuite les résultats obtenus pour quelques molécules simples : BrCN, OCSe, $FClO_3$, GeH_3F et CH_3CN. Pour chacune d'entre elles, le grand nombre de constantes

de rotation déterminées grâce à une analyse des spectres dans les domaines millimétrique et submillimétrique a permis de faire une étude comparative des différentes structures .

Enfin, dans un dernier chapitre nous étudierons la possibilité de caractériser des composés de basse coordinence du phosphore à partir de leur spectre de rotation. Ces molécules, très instables, ne peuvent pas être isolées mais sont néanmoins des intermédiaires de réaction importants et la détermination de leur structure pourrait permettre de mieux comprendre les mécanismes réactionnels.

CHAPITRE A

SPECTROSCOPIE DE ROTATION

Introduction

Les états d'énergie d'une molécule polyatomique sont calculés à partir de la résolution de l'équation de Schrödinger :

$$H\Psi = E\Psi \qquad (A\text{-}1)$$

où H est l'hamiltonien quantique
Ψ est la fonction d'onde
E est la valeur propre de l'hamiltonien.

Pour faciliter sa résolution, l'hamiltonien global peut se décomposer en une somme de trois termes principaux :

$$H = H_V + H_R + H_{RV} \qquad (A\text{-}2)$$

où H est l'hamiltonien global
H_V est l'hamiltonien de vibration (dans l'approximation de l'oscillateur harmonique)
H_R est l'hamiltonien de rotation pure (dans le modèle du rotateur rigide)
H_{RV} est l'hamiltonien de l'interaction de rotation-vibration.

Nous ne ferons que rappeler ici les aspects de la spectroscopie de rotation qui nous sont indispensables à une bonne compréhension du travail présenté. Il est toutefois possible de les compléter en consultant les références suivantes : [77 Wat] et [84 Gor].

Ainsi nous aborderons les thèmes suivants :

- l'approximation du rotateur rigide,
- la distorsion centrifuge,
- les corrections vibrationnelles, de distorsion centrifuge, et magnétique à apporter aux constantes de rotation en vue de déterminer une structure.

bibliographie p. 19

1°) L'approximation du rotateur rigide

En première approximation, on peut considérer que les distances interatomiques ne varient pas pendant la rotation de la molécule : c'est le modèle du rotateur rigide.

On repère la position des différents atomes dans un repère (a, b, c) lié à la molécule et centré sur le centre de gravité. Ce système d'axes est choisi de manière que le tenseur d'inertie soit diagonal. L'hamiltonien de rotation de la molécule s'écrit alors :

$$H_R = A J_a^2 + B J_b^2 + C J_c^2 \quad \text{avec } A \geq B \geq C \qquad \text{(A-3)}$$

où J_a, J_b, J_c sont les composantes du moment cinétique J selon les axes principaux a, b, c
A, B, C sont les constantes de rotation de la molécule.

Selon la symétrie de la molécule, certaines simplifications sont possibles, réduisant ainsi le nombre de constantes de rotation différentes (Tableau AI).

une toupie	possède	exemples
asymétrique	$A \neq B \neq C$	H_2O, SO_2, O_3, ...
symétrique	$A = B \neq C$	molécules "oblate" (aplaties) : NH_3, C_6H_6, ...
	$A \neq B = C$	molécules "prolate" (allongées) : CH_3X (X = F, Cl, Br, I), CH_3CN, ...
sphérique	$A = B = C$	CH_4, SF_6, ...
linéaire	$A = \infty$; $B = C$	CO_2, OCS, HCN, ...

Tableau AI : Constantes de rotation des molécules

2°) La distorsion centrifuge

Dans l'analyse des spectres de rotation, le modèle rigide devient très vite insuffisant et on doit recourir au modèle semi-rigide dans lequel les déformations induites par le mouvement de rotation sont prises en compte. Cela amène à introduire dans l'hamitonien des termes correctifs de distorsion centrifuge, soit :

$$H = H_{rot} + H_{dist} \qquad \text{(A-4)}$$

bibliographie p. 19

où $H_{rot} = A J_a^2 + B J_b^2 + C J_c^2$ avec $A \geq B \geq C$

$H_{dist} = \frac{1}{4} \sum_{(\alpha, \beta, \gamma, \delta)} \tau_{\alpha\beta\gamma\delta} J_\alpha J_\beta J_\gamma J_\delta + ...$ avec $\alpha, \beta, \gamma, \delta$ = a, b, c (pour un hamiltonien de distorsion centrifuge limité à l'ordre 4)

où $\tau_{\alpha\beta\gamma\delta}$ sont les constantes de Kivelson et Wilson de distorsion centrifuge [84 Gor].

L'hamiltonien quantique ainsi obtenu se présente sous la forme d'un développement de 81 termes, mais peut toutefois être réduit selon la symétrie de la molécule étudiée et les propriétés des coefficients $\tau_{\alpha\beta\gamma\delta}$ [84 Gor].

Les différentes formes d'hamiltonien sont présentés dans l'article de revue de Watson [77 Wat] ainsi que dans [84 Gor].

3°) Les corrections à apporter aux constantes de rotation en vue de déterminer une structure

3.1. Correction vibrationnelle

Chaque état de vibration a des constantes de rotation différentes. Par exemple, pour un molécule diatomique, l'anharmonicité de l'oscillateur implique une augmentation de la distance interatomique moyenne dans l'état excité v par rapport à la distance à l'équilibre. Dans le cas général d'une molécule polyatomique, ceci se traduit par l'expression [82 Pap] :

$$B_v^g = B_e^g - \sum_s^{3N-6} \alpha_s^g (v_s + \frac{d_s}{2}) + \sum_{r,s}^{3N-6} \gamma_{rs}^g (v_r + \frac{d_r}{2})(v_s + \frac{d_s}{2}) + \sum_{t,t'} \gamma_{l_t l_{t'}} l_t l_{t'} + ... \qquad \text{(A-5)}$$

avec g = a, b, c

avec B_e^g constantes de rotation à l'équilibre (A_e, B_e, C_e)

B_v^g constantes de rotation (A_v, B_v, C_v) dans le niveau de vibration $v = (v_1, v_2, ...v_s, ...)$

α_s^g constantes d'interaction rotation-vibration du 1er ordre

γ_{rs}^g constantes d'interaction rotation-vibration du 2ème ordre

d_r, d_s dégénérescences des états de vibration v_r et v_s

$\gamma_{l_t l_{t'}}$ constantes d'interaction rovibrationnelle

bibliographie p. 19

l_t et $l_{t'}$ nombres quantiques entiers de même parité que v et soumis à la condition $-v \leq l \leq +v$ (concernent les états dégénérés de vibration).

En général les termes γ_{rs}^g sont négligés car leur ordre de grandeur est souvent inférieur à l'erreur expérimentale. Cependant cette approximation n'est pas toujours valable. Par exemple, pour le dioxyde de soufre SO_2 (Tableau AII) [88 Mor], on peut remarquer que certains termes α_s^g sont du même ordre de grandeur que certains termes γ_{rs}^g qu'il ne faudra donc pas négliger.

On peut admettre en première approximation que ceci est dû aux vibrations de déformation où les angles de valence varient.

	A	B	C
B_0^g (MHz)	60778,5270 (29)	10317,9370 (13)	8799,8485 (13)
$t_g = \frac{\sigma_{B_0^g}}{B_0^g}$	4,77 10^{-7}	1,26 10^{-6}	1,48 10^{-7}
α_1^g / B_0^g	-5,839 10^{-4}	4,881 10^{-3}	4,822 10^{-3}
α_2^g / B_0^g	-1,856 10^{-2}	-2,518 10^{-4}	1,793 10^{-3}
α_3^g / B_0^g	1,012 10^{-2}	3,375 10^{-3}	3,702 10^{-3}
γ_{11}^g / B_0^g	-3,633 10^{-5}	3,964 10^{-5}	4,341 10^{-5}
γ_{22}^g / B_0^g	4,642 10^{-4}	-1,405 10^{-5}	1,136 10^{-6}
γ_{33}^g / B_0^g	3,746 10^{-5}	3,848 10^{-5}	6,318 10^{-5}
γ_{12}^g / B_0^g	-3,070 10^{-5}	-1,745 10^{-6}	3,932 10^{-5}
γ_{13}^g / B_0^g	-1,316 10^{-7}	1,224 10^{-4}	1,455 10^{-5}
γ_{23}^g / B_0^g	-3,088 10^{-4}	-1,105 10^{-5}	-5.841 10^{-5}

Tableau AII : Termes α_s^g et γ_{rs}^g de SO_2 (g = a, b, c)

bibliographie p. 19

3.2. Correction de la distorsion centrifuge

L'influence de la distorsion centrifuge se répercute bien entendu sur les constantes de rotation. Ainsi dans le cas d'une molécule asymétrique par exemple, les constantes de rotation expérimentales doivent être corrigées afin d'obtenir les constantes de rotation qui vont servir à déterminer la structure géométrique de la molécule [84 Gor] :

$$A' = A^{(A)} + 2\Delta_J + \frac{1}{2}\,(\tau_{bbcc} + 2\tau_{bcbc}) + \frac{1}{4}\,(3\tau_{bcbc} - 2\tau_{abab} - 2\,\tau_{acac}) \qquad \text{(A-6a)}$$

$$B' = B^{(A)} + 2\Delta_J + \Delta_{JK} - 2\delta_J - 2\delta_K + \frac{1}{2}\,(\tau_{aacc} + 2\,\tau_{acac}) + \frac{1}{4}\,(3\tau_{acac} - 2\,\tau_{bcbc} - 2\,\tau_{abab}) \qquad \text{(A-6b)}$$

$$C' = C^{(A)} + 2\Delta_J + \Delta_{JK} + 2\delta_J + 2\delta_K + \frac{1}{2}\,(\tau_{aabb} + 2\,\tau_{abab}) + \frac{1}{4}\,(3\tau_{abab} - 2\,\tau_{bcbc} - 2\,\tau_{acac}) \qquad \text{(A-6c)}$$

où $A^{(A)}$, $B^{(A)}$, $C^{(A)}$ sont les constantes de rotation expérimentales dans la reduction A (dépendant de la distorsion centrifuge)

A', B', C' sont les constantes de rotation structurales (indépendantes de la distorsion centrifuge)

Δ_J, Δ_{JK}, δ_J, δ_K sont 4 des 5 constantes quartiques "déterminables" de distorsion centrifuge

$\tau_{\alpha\beta\gamma\delta}$ (α, β, γ, δ = a, b, c) sont les constantes de Kivelson et Wilson de distorsion centrifuge (ces constantes ne sont en général pas déterminables expérimentalement).

3.3. La correction magnétique

Dans le calcul des structures moléculaires à partir des moments d'inertie expérimentaux, on considère que la masse des électrons est concentrée dans le noyau de l'atome. C'est une bonne approximation pour la plupart des molécules mais dans certains cas, en particulier pour les molécules légères, des corrections sont nécessaires.

L'effet Zeeman permet l'évaluation de ces corrections d'ordre supérieur.

L'hypothèse que les électrons peuvent être regroupés avec le noyau n'est qu'une approximation. Ses limites de validité sont mises en évidence par un moment magnétique (facteur g), différent de zéro, causé par la rotation des électrons.

On peut alors introduire une correction magnétique aux constantes de rotation, qui tient compte de cet effet [84 Gor], et dont l'expression est :

bibliographie p. 19

$$B^{\alpha} = \frac{B^{\alpha}_{eff}}{1 + \frac{m}{M_p} g_{\alpha\alpha}} \cong B^{\alpha}_{eff}\left(1 - \frac{g_{\alpha\alpha}}{1836}\right) \qquad \text{avec } \alpha = a, b, c \qquad \text{(A-7)}$$

où B^{α} constantes de rotation corrigées selon l'axe α

B^{α}_{eff} constantes de rotation expérimentales selon l'axe α

m est la masse de l'électron

M_p est la masse du proton

$g_{\alpha\alpha}$ est le moment magnétique rotationnel selon l'axe α.

Comme on l'a signalé au début de ce paragraphe, cet effet est la plupart du temps négligé mais son importance varie toutefois suivant la molécule, comme le montre le tableau AIII.

	g_{bb}	B_{eff} (MHz)	$\lvert B_{eff} - B \rvert$ (MHz)	référence
$^{16}O^{12}C^{32}S$	-0,028826	6081,492106 (12)	0,095	[74 Dav], [84 Tan]
$^{12}C^{16}O$	-0,26895	57635,9660 (34)	8,44	[77 Mee], [87 Nol]
^{7}LiD	-0,27674	126905,36 (4)	19,1	[69 Pea], [74 Doc]
CH_3CN	g_{aa} = 0 ,310	A_{eff} = 158099,2 (6)	26,7	[70 Poc], [91 Hor]
	g_{bb} = -0 ,0338	B_{eff} = 9198 ,899378 (70)	0 ,169	[70 Poc], [88 Bro]

Tableau AIII : Correction magnétique pour quelques molécules

On remarque donc qu'il est préférable d'évaluer l'importance de cet effet avant de déterminer les constantes de rotation qui vont servir au calcul de la structure géométrique d'une molécule.

bibliographie p. 19

Depuis que la spectroscopie microonde existe, les progrès de la technologie et de l'informatique ont contribué à l'amélioration de la qualité des spectres et des résultats expérimentaux obtenus. Le tableau AIV montre, dans le cas de l'acétonitrile (CH_3CN), l'évolution de la précision de sa constante de rotation B de l'état fondamental en fonction de la fréquence maximale explorée.

n[a]	B(σ) en MHz	J_{max}	ν_{max} (GHz)	référence
2	9198.83	1	37	[50 Kes]
2	9198.70	1	37	[50 Col]
3	9198.899	11	220.5	[61 Ven]
3	9198.90	2	55	[66 Bau]
3	9198.8970(64)	7	147	[69 Bau]
5	9198.899299(50)	12	239	[77 Bou]
5	9198.899439(64)	49	918	[88 Boc]
7	9198.899378(70)	68	1263	[88 Bro]
7	9198.899236(137)[b]	80	1480	[90 Pav]
8	9198.899284(34)	80	1480	[90 Sch]

a) n est le nombre de paramètres déterminés
b) combinaison de données infra-rouge lointain (transformée de Fourier) et submillimétriques

Tableau AIV : Evolution de la constante de rotation B de CH_3CN en fonction de la fréquence maximale explorée

bibliographie p. 19

BIBLIOGRAPHIE

[50 Col] D. K. COLES, W. E. GOOD & R. H. HUGHES
Phys. Rev. 1950, 79, 224-224

[50 Kes] M. KESSLER, H. RING, R. TRAMBARULO & W. GORDY
Phys. Rev. 1950, 79, 54-56

[61 Ven] P. VENKATESWARLU, J. G. BAKER & W. GORDY
J. Mol. Spectrosc. 1961, 6, 215-228

[66 Bau] A. BAUER, A. MOISES & S. MAES
C. R. Acad. Sc. 1966, 262, 558-561

[69 Bau] A. BAUER & S. MAES
J. Phys. (Paris) 1969, 30, 169-180

[69 Pea] E. F. PEARSON & W. GORDY
Phys. Rev. 1969, 177, 59-61

[70 Poc] J. M. POCHAN, R. L. SHOEMAKER, R. G. STONE & W. H. FLYGARE
J. Chem. Phys. 1970, 52, 2478-2484

[74 Dav] R. E. DAVIS & J. S. MUENTER
Chem. Phys. lett. 1974, 24, 343-345

[74 Doc] K. K. DOCKEN & R. R. FREEMAN
J. Chem. Phys. 1974, 61, 4217-4223

[77 Bou] D. BOUCHER, J. BURIE, J. DEMAISON, A. DUBRULLE, J. LEGRAND & B. SEGARD
J. Mol. Spectrosc. 1977, 64, 290-294

[77 Mee] W. L. MEERTS, F. H. DE LEEUW & A. DYMANUS
Chem. Phys. 1977, 22, 319-324

[77 Wat] J. K. G. WATSON
"In Vibrational Spectra and Structure"
J. D. Durig Ed, New York 1977

[82 Pap] D. PAPOUSEK & M. R. ALIEV
"Molecular Vibrational-Rotational Spectra"
Elsevier Scientific Publishing Company 1982

[84 Gor] W. GORDY & R. L. COOK
"Microwave Molecular Spectra"
Wiley, New York 1984

[84 Tan] K. TANAKA, H. ITO & T. TANAKA
J. Mol. Spectrosc. 1984, 107, 324-332

[87 Nol] I. G. NOLT, J. V. RADOSTITZ, G. DI LONARDO, K. N. EVENSON, D. A. JENNINGS, K. R. LEOPOLD, M. D. VANEK, L. R. ZINK, A. KINZ & K. V. CHANCE
J. Mol. Spectrosc. 1987, 125, 274-287

[88 Boc] R. BOCQUET, G. WLODARCZAK, A. BAUER & J. DEMAISON
J. Mol. Spectrsoc. 1988, 127, 382-389

[88 Bro] F. X. BROWN, D. DANGOISSE & J. DEMAISON
J. Mol. Spectrosc. 1988, 129, 483-485

[88 Mor] Y. MORINO, M. TANIMOTO & S. SAITO
Acta Chem. Scand. 1988, A42, 346-351

[90 Pav] F. S. PAVONE, L. R. ZINK, M. PREVEDELLI, I. INGUSCIO & L. FUSINA
J. Mol. Spectrosc. 1990, 144, 45-50

[90 Sch] G. SCHWAAB
Thèse, Novembre 1990, Université de Bonn (Allemagne)

[91 Hor] V. M. HORNEMAN, M. KOIVUSAARI & R. ANTTILA
"12ème Colloque sur la Spectroscopie Moléculaire à Haute Résolution"
Septembre 1991, poster O-20, Dijon (France)

CHAPITRE B

METHODES DE DETERMINATION DES STRUCTURES GEOMETRIQUES

Introduction

L'une des applications les plus importantes de la spectroscopie de rotation est la détermination de la géométrie des molécules.

L'analyse des spectres de rotation permet de déterminer les moments principaux d'inertie de la molécule étudiée et de ses espèces isotopiques.

$$I_g = \frac{h}{8\pi^2 B_g} = \frac{505379}{B_g} \qquad \text{avec } g = a, b, c \qquad \text{(B-1)}$$

où I_g sont les moments d'inertie en u Å^2 le long des axes a, b, c

B_g sont les constantes de rotation A, B, C en MHz.

De part leur définition [84 Gor], les moments d'inertie contiennent l'information structurale de toute molécule quelle qu'elle soit puisque :

$$I_a = \sum_i m_i (b_i^2 + c_i^2) \qquad \text{(B-2a)}$$

$$I_b = \sum_i m_i (a_i^2 + c_i^2) \qquad \text{(B-2b)}$$

$$I_c = \sum_i m_i (a_i^2 + b_i^2) \qquad \text{(B-2c)}$$

où a_i, b_i, c_i sont les coordonnées cartésiennes de l'atome i, et m_i sa masse.

En fonction des approximations effectuées, il existe plusieurs types de structures géométriques :

- La structure à l'équilibre (dite structure r_e)

C'est la structure de référence. Elle est isotopiquement invariante et peut être déterminée dans certains cas avec une très grande précision ; mais elle est souvent très difficile à obtenir car il faut au moins étudier tous les modes fondamentaux de la molécule en plus de son état fondamental. La spectroscopie infra-rouge à haute résolution s'avère alors souvent nécessaire.

bibliographie p. 41

- La structure effective (r_0)

C'est la structure obtenue directement à partir des constantes de rotation de l'état fondamental. C'est la plus ancienne et la plus simple à déterminer mais elle n'est pas très précise (environ 0,01 Å) car les interactions de rotation-vibration y sont négligées.

- Les structures de substitution

Les structures de substitution sont déterminées en substituant différents atomes de la molécule. Il est possible de substituer soit chaque atome successivement (r_s), soit deux atomes différents simultanément (r_{ss}), soit les atomes symétriquement équivalents simultanément (polysubstitution).

- Les structures "moyennes"

En 1962, plusieurs équipes ont considéré une structure "moyenne", correspondant à la configuration moléculaire moyenne dans un état de vibration donné et calculée à partir des moments d'inertie expérimentaux.

Lorsque nous aurons présenté chacune de ces structures, nous les déterminerons dans un prochain chapitre pour plusieurs types de molécules. Nous verrons alors que :

- le fait de combiner des résultats issus de la spectroscopie microonde avec ceux de la spectroscopie infra-rouge à haute résolution, nous permet de déterminer des constantes de rotation, puis des structures géométriques, extrêmement précises,
- une analyse très fine des spectres millimétriques et submillimétriques donne des constantes de rotation d'une telle précision que l'on peut visualiser la variation des coordonnées cartésiennes d'un atome lors de sa substitution [90 Dem] et [91 LeG].

bibliographie p. 41

1°) La structure à l'équilibre (structure r_e)

C'est la structure de référence car c'est lorsque la molécule est dans son état d'équilibre que son énergie potentielle est minimale.

Pour une molécule diatomique, on observe la courbe de potentiel suivante, en fonction de la distance interatomique (figure BI) :

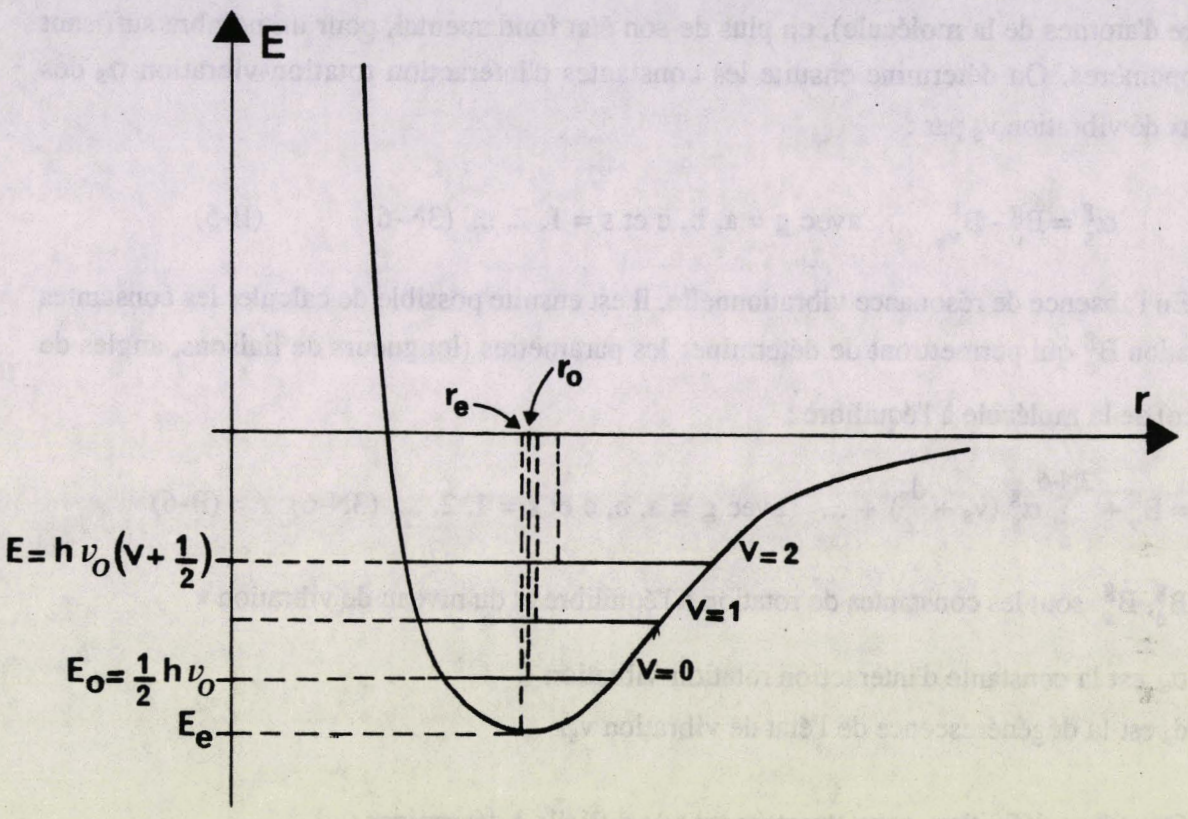

Figure BI : Courbe de potentiel d'une molécule diatomique

Comme le potentiel est anharmonique, on peut montrer que la distance interatomique moyenne varie avec l'état de vibration de la molécule :

$$r_e \neq r_0 \neq \langle r_v \rangle \qquad \text{(B-3)}$$

Il s'en suit une différence au niveau des constantes de rotation, que l'on traduit par la relation :

$$B_v = \frac{h}{8\pi^2 \mu} \left\langle \frac{1}{r_v^2} \right\rangle \qquad \text{(B-4)}$$

bibliographie p. 41

où B_v est la constante de rotation dans l'état de vibration v

h est la constante de Planck

μ est la masse réduite

$< r_v >$ est la moyenne quantique de la distance interatomique dans l'état de vibration v.

Pour déterminer la structure à l'équilibre d'une molécule quelconque, on analyse donc les spectres de rotation dans chacun de ses états excités $v_s = 1$ (s = 1, 2, ..., (3N-6) où N est le nombre d'atomes de la molécule), en plus de son état fondamental, pour un nombre suffisant d'isotopomères. On détermine ensuite les constantes d'interaction rotation-vibration α_s des niveaux de vibration v_s par :

$$\alpha_s^g = B_0^g - B_{v_s}^g \qquad \text{avec g = a, b, c et s = 1, 2, ..., (3N-6)} \qquad \text{(B-5)}$$

En l'absence de résonance vibrationnelle, il est ensuite possible de calculer les constantes de rotation B_e^g qui permettront de déterminer les paramètres (longueurs de liaisons, angles de valence) de la molécule à l'équilibre :

$$B_e^g = B_v^g + \sum_s^{3N-6} \alpha_s^g \, (v_s + \frac{d_s}{2}) + \ldots \quad \text{avec g = a, b, c et s = 1, 2, ..., (3N-6)} \qquad \text{(B-6)}$$

où B_e^g, B_v^g sont les constantes de rotation à l'équilibre et du niveau de vibration v

α_s est la constante d'interaction rotation-vibration

d_s est la dégénérescence de l'état de vibration v_s.

De part sa définition, cette structure est très difficile à déterminer :

- il faut analyser un très grand nombre de spectres [(3N-6) + 1] par isotopomère, et ce n'est faisable que pour de petites molécules,
- certains états de vibration, trop hauts en énergie, ne sont plus accessibles en spectroscopie microonde : le peuplement de ces niveaux élevés, vérifiant la loi de Boltzmann, est faible ; ce qui donne des spectres de faible intensité.

$$\frac{n_{v_i}}{n_0} = e^{-\frac{E_{v_i} - E_0}{kT}} \qquad \text{(B-7)}$$

où n_0 et n_{v_i} sont les populations des niveaux de vibration v = 0 et v_i

E_0 et E_{v_i} sont les énergies des niveaux v = 0 et v_i

k est la constante de Boltzmann

T est la température absolue.

bibliographie p. 41

La spectroscopie infrarouge à haute résolution s'avère alors nécessaire pour l'analyse de ces niveaux d'énergie élevée.

Quand on ne peut pas déterminer toutes les constantes d'interaction rotation-vibration α_s^g directement par l'analyse des spectres de rotation (ou des structures fines de rotation-vibration en infrarouge), on essaie de calculer autrement celles qui manquent :

1) à partir du champ de force anharmonique obtenu à partir de données expérimentales existantes :

Hoy a développé cette méthode en 1972 et l'a appliquée à H_2O et NH_3 [72 Hoy]. C'est ainsi qu'ont été déterminées, entre autres, les structures à l'équilibre de SiF_3H [73 Hoy] et de HCCH [76 Str].

2) à partir du champ de force anharmonique "ab initio" :

Les calculs "ab initio" permettent de déterminer une structure géométrique avec une précision rarement meilleure que quelques pourcents [86 Gaw]. Ceci reste valable pour les autres propriétés moléculaires, en particulier le champ de force [84 Kon 2]. Mais la constante d'interaction rotation-vibration α étant elle-même une correction de la constante de rotation B de l'ordre de quelques pourcents, l'erreur ainsi introduite semble admissible. Cette méthode a déjà été utilisée pour quelques molécules et radicaux : CH_3F, CH_3Cl [84 Kon 1], HCN [86 Gaw], H_2O, H_2CO [86 Gaw] et [88 Cla], H_2S, $H_2C{=}CH_2$, CH_2, HCO [88 Cla], N_2O [89 Tef].

Par ailleurs, Botschwina a récemment utilisé la méthode CEPA (Coupled Electron Pair Approximation), qu'il combine avec des données expérimentales afin de déterminer les structures à l'équilibre de C_3O, HC_5^+, HCO^+, NCCN, CNCN, HC_2Si^+ et SiCC [91 Bot].

3) à partir d'une relation empirique :

Pour calculer la structure à l'équilibre d'une molécule à partir de ses constantes expérimentales, il est nécessaire de corriger les moments d'inertie obtenus d'un terme, noté ε, dû aux vibrations et variant lors de la substitution isotopique. Nous avons alors vérifié que dans certains cas, il est possible de déterminer une pseudo-structure r_e en utilisant la relation de Demaison et Nemes [79 Dem 1], écrite sous la forme :

$$\varepsilon' = \varepsilon \sqrt{\frac{I'_0}{I_0}} \qquad \text{avec } \varepsilon = I_0 - I_e = \frac{I_e}{2B_e} \sum_s \alpha_s d_s \qquad \text{(B-8)}$$

bibliographie p. 41

où I_0 est le moment d'inertie expérimental de la molécule mère dans l'état fondamental
I_e est le moment d'inertie à l'équilibre
ε est la correction vibrationnelle
I'_0 et ε' concernent les molécules filles substituées
α_s est la constante d'interaction rotation-vibration
d_s est la dégénérescence du niveau de vibration v_s,

Ensuite une analyse par moindres carrés de l'expression $I_e = I_0 - \varepsilon = f(r_i ; \theta_i)$ permet de déterminer une bonne approximation de la structure r_e, [91 Bur] et [91 LeG].

2°) La structure effective (structure r_0)

Expérimentalement, l'analyse des spectres de rotation de l'état fondamental (v = 0) permet de déterminer les constantes de rotation (et par conséquent, les moments d'inertie) de la molécule et de ses espèces isotopiques. Lorsque l'on possède un nombre de moments d'inertie au minimum égal au nombre de paramètres à déterminer, une analyse par moindres carrés permet de calculer les longueurs de liaisons (r_i) et les angles de valence (θ_i) grâce aux relations $I_0^g = f(r_i, \theta_i)$ avec g = a, b, c.

Nous avons étudié un grand nombre d'espèces isotopiques du séléniure de carbonyle OCSe. L'analyse des résidus a alors montré (voir chapitre D) que la régression n'était pas bonne et que le modèle théorique devait inclure au moins un terme linéaire du type :

$$\varepsilon + \sum_i \frac{\partial \varepsilon}{\partial m_i} (\Delta m_i) + \ldots \qquad \text{(B-9)}$$

En effet, en négligeant le terme d'interaction rotation-vibration ε dans $I_0 = I_e + \varepsilon$, on suppose la molécule rigide. Ceci introduit une erreur systématique non négligeable dans la détermination d'une structure géométrique. Pour pallier cet inconvénient, plusieurs améliorations, plus ou moins complexes, ont été proposées : la structure r_s tout d'abord, puis les structures r_{ss}, r_m, r_m^{ρ}, $r_{\varepsilon,I}$, etc.

bibliographie p. 41

3°) Les structures de substitution

3.1. La structure de monosubstitution (structure r_s)

Kraitchman a élaboré une méthode [53 Kra] qui permet de calculer les coordonnées cartésiennes d'un atome par rapport aux axes principaux d'inertie de la molécule, en utilisant les variations des moments d'inertie lors de la substitution isotopique.

Dans cette méthode, il considère que, lors de la substitution, la variation des moments d'inertie est due uniquement à celle de la masse de l'atome substitué. Il écrit alors que :

$$I_0 = I_e + \varepsilon \qquad \text{(B–10)}$$

où ε = 3 à 5% de I et est supposé isotopiquement invariant,

donc
$$I'_0 - I_0 = (I'_e - I_e) + (\varepsilon' - \varepsilon)$$
$$\cong I'_e - I_e \qquad \text{(B-11)}$$

On peut donc, pour une molécule linéaire, déterminer la coordonnée cartésienne de l'atome substitué i par [84 Gor] :

$$z_s^2 (i) = \frac{I'_0 - I_0}{\mu} \qquad \text{avec } \mu = \frac{M\,\Delta m}{M + \Delta m} \qquad \text{(B-12)}$$

où I_0 est le moment d'inertie de la molécule mère
I'_0 est le moment d'inertie de la molécule fille
μ est la masse réduite (M la masse de la molécule mère et Δm la variation de masse de l'atome i).

Pour une molécule diatomique, on peut montrer que :

$$r_e < r_s < r_0 \qquad \text{et} \qquad r_s = \frac{r_e + r_0}{2} \qquad \text{(B-13)}$$

Pour une molécule polyatomique, cette hypothèse (ε = constante) n'est bonne que si $\Delta I_e >> \Delta\varepsilon$, c'est à dire si :
- un atome "lourd" est substitué (donc non valable pour la substitution H → D),
- cet atome est loin d'un axe ou du centre de gravité de la molécule. L'incertitude de sa coordonnée cartésienne est estimée par la formule de Costain [66 Cos] :

bibliographie p. 41

$$\sigma(z(i)) = \frac{K}{z(i)} \qquad \text{avec } K = 0{,}0012 \text{ Å}^2 \qquad \text{(B-14)}$$

donc plus la coordonnée z(i) est petite, plus sa précision est faible. La validité de cette formule a été analysée par Van Eijck [82 Van] qui l'estime pessimiste excepté pour une substitution classique H → D où il propose K = 0,003 Å^2. Il a en effet montré par exemple que dans le cas des cycles rigides insaturés K = 0,0005 Å^2 pour la substitution des carbones et 0,0007Å^2 pour celle des hydrogènes directement liés au cycle.

Expérimentalement, on constate que la structure r_s de molécules sans hydrogène a une précision meilleure que 0,005 Å [90 Dem].

Un autre problème peut se poser pour déterminer cette structure : il faut pouvoir substituer tous les atomes. Or ils ne possèdent pas nécessairement des isotopes (ex : P, F, As, I, ...) ou alors la synthèse chimique peut s'avérer coûteuse ou difficile.

La coordonnée manquante peut toutefois être déterminée en utilisant la relation du centre de gravité $\sum_i m_i z_i = 0$.

3.2. La structure de double substitution (structure r_{ss})

Un peu plus tard, Pierce a établi une méthode [59 Pie] qui utilise les molécules doublement substituées. Il ne considère plus que les interactions de rotation-vibration sont constantes mais au contraire qu'elles varient lors de la substitution. Il pense que de ce fait, les coordonnées cartésiennes des atomes sont bien déterminées, même s'ils sont près d'un axe ou du centre de gravité.

Soit une molécule mère, linéaire et contenant les atomes ^iX et ^kY ($i \neq k$), son moment d'inertie s'écrit :

$$I_0(ik) = I_e(ik) + \varepsilon \qquad \text{(B-15)}$$

Lors de la substitution i → j, le moment d'inertie varie de :

$$\begin{aligned} \Delta I_0(ik) &= I_0(jk) - I_0(ik) \\ &= I_e(jk) - I_e(ik) + \frac{\partial \varepsilon}{\partial m_i}(\Delta m_i) + \frac{\partial^2 \varepsilon}{\partial m_i^2}(\Delta m_i)^2 \end{aligned} \qquad \text{(B-16)}$$

Lors de la seconde substitution k → l, l'expression devient :

$$\Delta I_0 (il) = I_e (jl) - I_e (il) + \frac{\partial \varepsilon}{\partial m_i} (\Delta m_i) + \frac{\partial \varepsilon}{\partial m_k} (\Delta m_k) \qquad \text{(B-17)}$$

$$+ \frac{\partial^2 \varepsilon}{\partial m_i^2} (\Delta m_i)^2 + \frac{\partial^2 \varepsilon}{\partial m_k^2} (\Delta m_k)^2 + \frac{\partial^2 \varepsilon}{\partial m_i \, \partial m_k} (\Delta m_i) (\Delta m_k)$$

d'où $\Delta(\Delta I_0) = \Delta I_0(il) - \Delta I_0 (ik)$

$$= \Delta I_e (il) - \Delta I_e (ik) + \frac{\partial^2 \varepsilon}{\partial m_i \, \partial m_k} (\Delta m_i) (\Delta m_k) \qquad \text{(B-18)}$$

Si on néglige le terme croisé, la coordonnée cartésienne de l'atome i se calcule alors grâce à l'équation :

$$\frac{\Delta(\Delta I_0)}{\mu'} = \left(1 - \frac{\mu}{\mu'}\right) z_{ss}^2 (i) - \frac{2\Delta m_k \, z_s(k)}{M_{(ik)} + \Delta m_k} z_{ss} (i) + \left(\frac{\Delta m_k \, z_s (k)}{M_{(ik)} + \Delta m_k} \right)^2 \qquad \text{(B-19)}$$

$$\text{avec } \mu = \frac{M(ik) \, \Delta m_i}{M(ik) + \Delta m_i} \text{ et } \mu' = \frac{M(il) \, \Delta m_i}{M(il) + \Delta m_i}$$

Cette structure, bien qu'à première vue plus proche de la structure à l'équilibre que la structure r_s, n'est toutefois pas facile à déterminer (souvent coûteux et parfois impossible chimiquement).

La faible amélioration de la précision s'explique par plusieurs raisons qui peuvent coexister :

- le terme $\Delta (\Delta I_0)$, très petit, est très sensible aux erreurs existant sur les constantes de rotation expérimentales,
- pour obtenir la coordonnée cartésienne de double substitution de l'atome i, il faut connaitre celle de simple substitution de l'atome k ; donc l'erreur sur z_s (k) se répercute sur z_{ss} (i),
- les termes croisés du type $\frac{\partial^2 \varepsilon}{\partial m_i \partial m_k}$ ne sont pas toujours négligeables (voir OCSe au chapitre D et [90 Dem]).

Pour toutes ces raisons , la structure r_{ss} est peu utilisée.

Récemment, Kirby et Kroto ont utilisé une formule analogue à celle de Pierce pour déterminer la structure de double substitution de Cl-B=S [80 Kir], et de Br-B=S [91 Coo].

Partant de la définition du moment d'inertie d'une molécule triatomique linéaire XYZ, écrite sous la forme :

bibliographie p. 41

$$I = \frac{1}{M}\left[m_x m_y d_{xy}^2 + m_y m_z d_{yz}^2 + m_x m_z (d_{xy}+d_{yz})^2\right] \qquad \text{(B-20)}$$

ils considèrent : - une molécule mère de masse M et de moment d'inertie I

- deux molécules filles monosubstituées où les atomes substitués sont différents (masses M_1^* et M_2^* et moments d'inertie I_1^* et I_2^*)

- la molécule fille disubstituée correspondante (masse M_{12}^{**} et moment d'inertie I_{12}^{**})

et définissent la structure de double substitution telle que :

$$(\Delta m_1)\,(\Delta m_2)\, r_{ss}^2 = MI - M_1^* I_1^* - M_2^* I_2^* + M_{12}^{**} I_{12}^{**} \qquad \text{(B-21)}$$

où Δm est la variation de la masse de l'atome substitué et le nombre d'astérisques indique le nombre de substitution.

C'est une structure dont les résultats sont discutables. Alors qu'elle donne de bons résultats dans le cas de Cl-B=S [80 Kir], on a pu voir qu'elle n'est pas toujours applicable. En effet, dans le cas de O=C=Se par exemple, les résultats que l'on obtient sont en désaccord avec ceux des autres structures. Ce point sera discuté dans le chapitre D.

3.3. La structure de polysubstitution

Chutjian [64 Chu] a étendu la méthode de Kraitchman à la polysubstitution simultanée d'atomes symétriquement équivalents dans une molécule.

Dans le cas, par exemple, d'une molécule ZXY_3, de symétrie C_{3v} (l'axe a étant l'axe de symétrie), les coordonnées cartésiennes des trois atomes équivalents Y sont données par les relations (B-22a, b, c) ci-dessous :

$$Y_1 : \begin{vmatrix} a = -\sqrt{\frac{1}{\mu_3}\left(\Delta I_b - \frac{\Delta I_a}{2}\right)} \quad \text{avec } \mu_3 = \frac{3\,\Delta m\, M}{M + 3\,\Delta m} \\ b = \sqrt{\frac{\Delta I_a}{3\,\Delta m}} \\ c = 0 \end{vmatrix} \qquad Y_2 : \begin{vmatrix} a \\ \frac{-b}{2} \\ \frac{b\sqrt{3}}{2} \end{vmatrix} \qquad Y_3 : \begin{vmatrix} a \\ \frac{-b}{2} \\ \frac{-b\sqrt{3}}{2} \end{vmatrix}$$

bibliographie p. 41

où $\Delta Ig = I'_g - I_g$ (g = a, b, c) où I_g sont les moments d'inertie de la molécule mère selon les axes a, b, c, et I'_g ceux de la molécule fille

M est la masse de la molécule mère
Δm est la variation de la masse de l'atome substitué Y.

Cette méthode donne en général de bons résultats. Elle n'est toutefois pas très utilisée car le moment d'inertie le long de l'axe de symétrie de la molécule est difficile à déterminer. Sa détermination se fait habituellement en infrarouge. Citons par exemple [88 Gra] et [89 Bra] pour CH_3CCH, [90 Ant] pour CH_3I et [91 Bur] pour $FClO_3$.

3.4. La structure r_m

La structure r_m, élaborée par Watson [73 Wat] est une extension des méthodes de substitution.

De même que dans la structure r_s, où la coordonnée cartésienne d'un atome i pour une molécule linéaire est définie par :

$$z_s^2(i) = \frac{I'_0 - I_0}{\mu} \qquad \text{avec } \mu = \frac{M\Delta m}{M + \Delta m} \tag{B-12}$$

où I_0 est le moment d'inertie de la molécule mère
I'_0 est le moment d'inertie de la molécule fille
μ est la masse réduite,

à l'équilibre, on a $z_e^2(i) = \frac{I'_e - I_e}{\mu}$ (B-23)

d'où $$z_s^2(i) = \frac{I'_e - I_e}{\mu} + \frac{\varepsilon' - \varepsilon}{\mu} = z_e^2(i) + \frac{\varepsilon' - \varepsilon}{\mu} \tag{B-24}$$

on a alors :

$$I_s = \sum_i m_i z_s^2(i)$$
$$= I_e + \sum_i m_i \left(\frac{\varepsilon'-\varepsilon}{\mu}\right) \tag{B-25}$$

bibliographie p. 41

Si on développe $\Delta\varepsilon = \varepsilon' - \varepsilon$ en une série de Taylor [77 Wat], l'expression devient après utilisation du théorème d'Euler ($\sum_i m_i \frac{\partial \varepsilon}{\partial m_i} = \frac{1}{2}\varepsilon$) :

$$2I_s - I_0 = I_e + \frac{1}{M}\sum_i m_i \left(\frac{\partial^2(M\varepsilon)}{\partial m_i^2}\right)(\Delta m_i) + ... \qquad \text{(B-26)}$$

Si on néglige les termes d'ordre supérieur dans le développement en série, on a $I_e = 2I_s - I_o$. La structure r_m a alors été définie telle que :

$$I_m = 2I_s - I_0 \qquad \text{(B-27)}$$

Cette relation reste valable pour une molécule quelconque (possédant trois moments d'inertie). Il suffit de considérer les relations (B-2a, b, c) et (B-28):

$$I_m^g = 2\, I_s^g - I_0^g \qquad \text{(B-28)}$$

Cette structure possède des conditions de validité très strictes. Il faut en effet :
- pouvoir substituer tous les atomes de la molécule,
- que le développement en série de $\Delta\varepsilon$ converge très vite, ce qui correspond aux atomes "lourds", d'où le problème lors de la substitution $H \rightarrow D$.

De plus, les imprécisions sur I_s^g et I_0^g se répercutent sur I_m^g.

En fait Smith et Watson [78 Smi] ont montré que la structure r_m n'était proche de la structure r_e que dans des cas très particuliers (molécules triatomiques non linéaires). En général, le terme Δm_i n'est pas négligeable et la structure r_m n'est pas meilleure que la structure r_s .

Kuchitsu a proposé une méthode qui fait appel à de nombreuses substitutions isotopiques pour éliminer les termes en Δm_i. Etudiée tout d'abord pour $COCl_2$ [80 Nak 2], cette structure, dite structure r_c, a ensuite été calculée pour Cl_2O et SO_2 [81 Nak] et pour H_2O, H_2CO et H_2CS [84 Nak]. Cette structure r_m modifiée est très proche de la structure r_e, même pour une molécule hydrogénée.

3.5. La structure r_m^ρ

Harmony a, en 1986, proposé une structure r_m modifiée [86 Har] qui la rend plus facile d'utilisation et surtout plus générale. Ses principaux intérêts sont qu'elle nécessite beaucoup moins d'isotopomères et qu'elle devient applicable aux molécules hydrogénées [88 Ber].

bibliographie p. 41

Partant de la relation (B-27) écrite sous la forme :

$$I_m = \left(2 \frac{I_s}{I_0} - 1 \right) I_0 \qquad \text{(B-29)}$$

il a observé que le rapport $\frac{I_s}{I_0}$ pouvait être considéré comme isotopiquement invariant [86 Har]. Il a alors introduit un nouveau moment d'inertie I_m^ρ tel que :

$$\left[I_m^\rho \right]_\alpha = (2\rho - 1) \left[I_0 \right]_\alpha \quad \text{avec } \rho = \frac{\left[I_s \right]_1}{\left[I_0 \right]_1} \qquad \text{(B-30)}$$

où $\alpha = 1$ pour la molécule mère

$\alpha \neq 1$ pour les molécules filles

I_s sont les moments d'inertie (I_a, I_b, I_c) de la molécule dans la structure r_s

I_0 sont les moments d'inertie expérimentaux.

Il s'est ensuite rendu compte que cette nouvelle structure introduisait des erreurs systématiques pour des liaisons faisant intervenir l'hydrogène.

En effet, lors de la substitution H → D, la fréquence de vibration de déformation de la liaison diminue et tout se passe comme si la valeur moyenne de la liaison C-D était plus courte que la liaison C-H :

$$r_0 (X\text{-}H) = r_0 (X\text{-}D) + \eta \qquad \text{avec } 0{,}003 < \eta < 0{,}005 \text{ Å} \qquad \text{(B-31)}$$

Harmony a donc introduit une correction empirique du moment d'inertie [89 Ber] qui tient compte de cette élongation. Pour une molécule linéaire, cette correction vaut :

$$\Delta = (I_m^\rho)^D_{corr} - (I_m^\rho)^D$$

$$= 2\, m_D\, z_D\, (\delta z_D) \qquad \text{(B-32)}$$

où (δz_D) est l'élongation de la liaison due à la substitution H→D

m_D est la masse de deutérium et z_D sa coordonnée cartésienne.

Cette relation reste valable pour une molécule quelconque. Il suffit de considérer que le long de l'axe a, on a :

bibliographie p. 41

$$\Delta a = \left[(I_m^\rho)^D_{corr}\right]^a - \left[(I_m^\rho)^D\right]^a$$

$$= 2\, m_D \left[b_D\, (\delta b_D) + c_D\, (\delta c_D)\right] \qquad \text{(B-33)}$$

Par permutation cyclique, on obtient aussi Δb et Δc. L'erreur systématique observée dans la structure r_m^ρ initiale est alors égale à :

$$(\delta r_D) = \sqrt{(\delta a_D)^2 + (\delta b_D)^2 + (\delta c_D)^2} \qquad \text{(B-34)}$$

$\equiv 0{,}003$ Å pour la liaison C-H

3.6. La structure $r_{\varepsilon,I}$

De calcul tout aussi facile que la structure r_0, la structure $r_{\varepsilon,I}$, élaborée par Rudolph [92 Rud], se détermine par analyse par moindres carrés de la relation :

$$I_0 = I_e + \varepsilon = f\,(r_i, \theta_i, \varepsilon) \qquad \text{(B-35)}$$

où les paramètres déterminés sont les longueurs de liaisons (r_i), les angles de valence (θ_i) et le terme ε, supposé isotopiquement invariant et qui représente les interactions de rotation-vibration.

Cette structure est équivalente à la structure r_s, et souvent même meilleure, d'autant plus qu'elle peut être déterminée même lorsqu'un atome ne possède pas d'isotope ou qu'il est difficile à substituer.

La valeur obtenue pour ε peut être comparée à celle calculée à partir de la formule empirique de Demaison et Nemes [79 Dem 1] :

$$\log \varepsilon = 1{,}247(5) \log I_0 - 2{,}651\ (13) \qquad \text{(B-36)}$$

D'autres variantes de la structure r_s ont été comparées par Rudolph [92 Rud] : les structures $r_{0,I}$, $r_{0,B}$, $r_{\Delta I}$, $r_{\Delta B}$, qu'il définit, pour une molécule diatomique, par :

bibliographie p. 41

$$r_0 = \sqrt{\frac{I_0}{\mu}} = \sqrt{\frac{1}{\mu}\frac{K}{B_0}} = \sqrt{\frac{\Delta I_0}{\mu^{(2)} - \mu^{(1)}}} = \sqrt{\left(\frac{1}{\mu^{(2)}} - \frac{1}{\mu^{(1)}}\right)\frac{K}{\Delta B_0}} \qquad \text{(B-37)}$$

$\rightarrow r_{0,I}$ $\rightarrow r_{0,B}$ $\rightarrow r_{\Delta I}$ $\rightarrow r_{\Delta B}$

où $I_0 = I_e + \varepsilon$ et $B_0 = B_e - \alpha$, tels que $K = BI = 505379$ MHz uÅ^2.

Il en conclue que certaines structures sont équivalentes :

$$r_{0,I} = r_{0,B} \approx r_0 \qquad \text{(B-38a)}$$

$$r_{\Delta I} = r_{\varepsilon,I} \approx r_s \qquad \text{(B-38b)}$$

et qu'en particulier, pour une molécule diatomique, on a :

$$r_e < r_{\Delta I} = r_s < r_0 < r_{\Delta B} \qquad \text{(B-39)}$$

Cette inégalité reste souvent valable dans le cas des molécules polyatomiques.

4°) Les structures "moyennes"

4.1. La structure r_z

Un des inconvénients des structures de substitution est qu'elles ne possèdent pas de sens physique bien défini tel que la structure à l'équilibre. La possibilité de calculer une structure "moyenne" (notée r_z) à partir des moments d'inertie effectifs a été considérée par Herschbach et Laurie [62 Her] et [62 Lau], et par Oka et Morino [60 Oka] et [62 Oka]. Une telle structure possède une signification physique claire puisqu'elle correspond à la configuration moléculaire moyenne dans un état de vibration donné. Cette structure ne diffère donc de la structure à l'équilibre que par l'anharmonicité des vibrations de la molécule.

On part de la relation :

$$I_e^g = I_0^g - \varepsilon g \qquad \text{avec } g = a, b, c \qquad \text{(B-10)}$$

Le terme εg dû à la vibration de la molécule peut être considéré comme la somme de deux composantes, l'une harmonique et l'autre anharmonique, soit :

$$\varepsilon^g = \varepsilon^g_{harm} + \varepsilon^g_{anharm} \qquad \text{(B-40)}$$

Le moment d'inertie de la configuration moyenne est alors défini par :

$$I^g_z = I^g_0 - \varepsilon^g_{harm} = I^g_e + \varepsilon^g_{anharm} \quad \text{avec } g = a, b, c \qquad \text{(B-41)}$$

On se contente alors de calculer à partir du champ de force la contribution harmonique de la correction de vibration ε^g afin de déterminer les moments d'inertie I^g_z à partir des moments d'inertie expérimentaux I^g_0.

Cette structure r_z a été calculée pour un certain nombre de molécules simples, comme par exemple H_2CO [60 Oka] et [84 Nak], H_2Se [62 Oka], C_2H_6, B_2H_6 [68 Kuc], CH_3CN [79 Dem 2], $COCl_2$ [80 Nak 1], OCl_2 [83 Nak], H_2O, H_2CS [84 Nak], etc.

Dans le cas de molécules diatomiques, la distance interatomique s'écrit :

$$r_z = r_e \left(1 - \frac{3}{2} a_1 \frac{B_e}{\omega_e}\right) \qquad \text{avec } a_1 = \frac{\varepsilon_{anharm}}{\varepsilon_{harm}} = -\left(\frac{\alpha_e \omega_e}{6B_e^2} + 1\right) \qquad \text{(B-42)}$$

où r_e est la distance interatomique de la molécule à l'équilibre
a_1 est la constante d'anharmonicité
B_e est la constante de rotation à l'équilibre
ω_e est la fréquence de vibration harmonique
α_e est la constante d'interaction rotation-vibration,

et on observe alors que :

$$r_z > r_0 > r_s > r_e. \qquad \text{(B-43)}$$

Il est à noter que ceci reste souvent vrai pour une molécule polyatomique.

4.2. La structure r_g

Les molécules sont réparties statistiquement suivant la loi de Boltzmann entre les différents états de vibration. Cette répartition dépend de la température et la diffraction électronique en phase gazeuse [73 Sim], en déterminant directement la position instantanée des noyaux, donne une distance internucléaire moyenne à l'équilibre thermique, distance notée r_g.

bibliographie p. 41

De la distance r_g, on peut déduire, si l'on connait le champ de force harmonique, la distance r_α qui est la distance entre les positions moyennes des noyaux à l'équilibre thermique. Lorsqu'on extrapole la distance r_α à la température T = 0K, on obtient la distance r_α^0 ($\equiv r_z$) qui est la distance entre les positions moyennes des noyaux dans l'état fondamental de vibration.

Ces différentes "distances" ont été comparées tout d'abord pour des molécules simples comme CH_4, CS_2, H_2Se [62 Mor], puis plus complexes comme le butadiène, l'acroleïne et le glyoxal [69 Kuc].

La connaissance du champ de force anharmonique permet d'en déduire la structure r_e.

Lorsque deux distances sont très voisines, la diffraction électronique ne permet pas de les distinguer. Il est alors intéressant de combiner les données de la diffraction électronique et de la spectroscopie de rotation. Kuchitsu a ainsi analysé les variations des distances interatomiques lors de substitutions successives pour les molécules suivantes : C_2H_6, B_2H_6 [68 Kuc], OCS, HCN, SO_2 et H_2O [77 Kuc]. On peut trouver une liste des molécules dont la structure a été déterminée de cette manière dans [88 Kuc].

Cette technique permet en outre d'éviter les erreurs de calibration, qui sont l'une des difficultés de la diffraction électronique.

bibliographie p. 41

BIBLIOGRAPHIE

[53 Kra] J. KRAITCHMAN
Am. J. Phys. 1953, 21, 17-24

[58 Cos] C. C. COSTAIN
J. Chem. Phys. 1958, 29, 864-874

[59 Pie] L. PIERCE
J. Mol. Spectrosc. 1959, 3, 575-580

[60 Oka] T. OKA
J. Phys. Soc. Japan. 1960, 15, 2274-2279

[62 Her] D. R. HERSCHBACH & V. W. LAURIE
J Chem Phys 1962, 37, 1668-1686

[62 Lau] V. W. LAURIE & D. R. HERSCHBACH
J. Chem. Phys. 1962, 37, 1687-1693

[62 Mor] Y. MORINO, K. KUCHITSU & T. OKA
J. Chem. Phys. 1962, 36, 1108-1109

[62 Oka] T. OKA & Y. MORINO
J. Mol. Spectrosc. 1962, 8, 300-314

[64 Chu] A. CHUTJIAN
J. Mol. Spectrosc. 1964, 14, 361-370

[66 Cos] C. C. COSTAIN
Trans. Amer. Crystallogr. Assoc. 1966, 2, 157-164

[68 Kuc] K. KUCHITSU
J. Chem. Phys. 1968, 49, 4456-4462

[69 Kuc] K. KUCHITSU, T. KUKUYAMA & Y. MORINO
J. Mol. Struct. 1969, 4, 41-50

[72 Hoy] A. R. HOY, I. M. MILLS & G. STREY
Mol. Phys. 1972, 24, 1265-1290

[73 Hoy] A.R. HOY, M. BERTRAM & I. M. MILLS
J. Mol. Spectrosc. 1973, 46, 429-447

[73 Sim] G. A. SIM & L. E. SUTTON EDS
"Molecular Structure by diffraction Methods"
Chemical Society, London 1973

[73 Wat] J. K. G. WATSON
J. Mol. Spectrosc. 1973, 48, 479-502

[76 Str] G. STREY & I. M. MILLS
J. Mol. Spectrosc. 1976, 59, 103-115

[77 Kuc] K. KUCHITSU & K. OYANAGI
Faraday discuss. Chem. Soc. 1977, 62, 20-28

[77 Wat] J. K. G. WATSON
"In Vibrational Spectra and Structure"
J. R. Durig Ed, New York 1977

[78 Smi] J. G. SMITH & J. K. G. WATSON
J. Mol. Spectrosc. 1978, 69, 47-52

[79 Dem 1] J. DEMAISON & L. NEMES
J. Mol. Struct. 1979, 55, 295-299

[79 Dem 2] J. DEMAISON, A. DUBRULLE, D. BOUCHER, J. BURIE & V. TYPKE
J. Mol. Spectrosc. 1979, 76, 1-16

[80 Kir] C. KIRBY & H. W. KROTO
J. Mol. Spectrosc. 1980, 83, 130-147

[80 Nak 1] M. NAKATA, K. KOHATA, T. FUKUYAMA & K. KUCHITSU
J. Mol. Spectrosc. 1980, 83, 105-117

[80 Nak 2] M. NAKATA, T. FUKUYAMA, K. KUCHITSU, H. TAKEO & C. MATSUMURA
J. Mol. Spectrosc. 1980, 83, 118-129

[81 Nak] M. NAKATA, M. SUGIE, H. TAKEO, C. MATSUMURA, T. FUKUYAMA
& K. KUCHITSU
J. Mol. Spectrosc. 1981, 86, 241-249

[82 Van] B.P. VAN EIJCK
J. Mol. Spectrosc. 1982, 91, 348-362

[83 Nak] M. NAKATA, S. YAMAMOTO, T. FUKUYAMA & K. KUCHITSU
J. Mol. Struct. 1983, 100, 143-159

[84 Gor] W. GORDY & R. L. COOK
"Microwave Molecular Spectra"
Wiley, New York 1984

[84 Kon 1] S. KONDO, Y. KOGA & T. NAKANAGA
J. Chem. Phys. 1984, 81, 1951-1959

[84 Kon 2] S. KONDO
J. Chem. Phys. 1984, 81, 5945-5951

[84 Nak] M. NAKATA, K. KUCHITSU & I. M. MILLS
J. Phys. Chem. 1984, 88, 344-348

[86 Gaw] J. F. GAW, Y. YAMAGUCHI, H. F. SCHAFFER III & N. C. HANDY
J. Chem. Phys. 1986, 85, 5132-5142

[86 Har] M. D. HARMONY & W. H. TAYLOR
J. Mol. Spectrosc. 1986, 118, 163-173

[88 Ber] R. J. BERRY & M. D. HARMONY
J. Mol. Spectrosc. 1988, 128, 176-194

[88 Cla] D. A. CLABO JR, W. D. ALLEN, R. B. REMINGTON, Y. YAMAGUCHI & H. F. SCHAFFER III
Chem. Phys., 1988, 123, 127-239

[88 Gra] G. GRANER, J. DEMAISON, G. WLODARCZAK, R. ANTTILA, J. J. HILLMAN & D.E. JENNINGS
Mol. Phys. 1988, 64, 921-932

[88 Kuc] K. KUCHITSU, M. NAKATA & S. YAMAMOTO
"Stereochemical Application of Gas-phase Electron Diffraction"
Ed. I. Hargittai & M. Hargittai, VCH Publishers, New York 1988

[89 Ber] R. J. BERRY & M. D. HARMONY
Struct. chem. 1989, 1, 49-59

[89 Gra] G. GRANER, V. M. HORNEMAN, G. BLANQUET, J. WALRAND, M. TAKAMI & L. JÖRISSEN
J. Mol. Spectrosc. 1989, 135, 32-44

[89 Tef] J. L. TEFFO & A. CHEDIN
J. Mol. Spectrosc. 1989, 135, 389-409

[90 Ant] R. ANTTILA, V. M. HORNEMAN & S. ALANKO
Mol. Phys. 1990, 70, 991-1000

[90 Dem] J. DEMAISON, G. WLODARCZAK, J. BURIE & H. BÜRGER
J. Mol. Spectrosc. 1990, 140, 322-339

[91 Bot] P. BOTSCHWINA
"12ème Colloque sur la Spectroscopie Moléculaire à Haute Résolution"
Septembre 1991, posters D-1, F-1, H-1, J-1 et L-1, Dijon (France)

[91 Bur] K. BURZYCK, H. BÜRGER, M. LE GUENNEC, G. WLODARCZAK & J. DEMAISON
J. Mol. Spectrosc. 1991, 148, 65-79

[91 Coo] T. A. COOPER, S. FIRTH & H. W. KROTO
J. Chem. Soc. Farad. Trans. 1991, 87, 1-7

[91 LeG] M. LE GUENNEC, W. CHEN, G. WLODARCZAK, J. DEMAISON, R. EUJEN & H. BÜRGER
J. Mol. Spectrosc. 1991, 150, 493-510

[92 Rud] H. D. RUDOLPH
Struct. Chem. 1991, 2, 581-588

CHAPITRE C

ASPECTS EXPERIMENTAUX

1°) Obtention des molécules - Synthèses -

A l'exception du bromure de cyanogène (BrCN) qui a été acheté chez JANSEN CHIMICA à Geel (Belgique), aucune autre molécule, étudiée dans ce travail, n'est commerciale.

Certaines d'entre elles (OCSe, GeH_3F et $FClO_3$) nous ont été fournies par le Pr. Bürger de l'université de Wuppertal (Allemagne).

Nous avons synthétisé les molécules monodeutérées (acétonitrile et propynes) au laboratoire de chimie structurale de l'université de Rennes (France).

En ce qui concerne les molécules phosphorées, elles ont été synthétisées juste avant leur analyse, à l'entrée du spectromètre, selon des procédés mis au point par l'équipe de J. M. Denis de l'université de Rennes.

Nous allons donc voir successivement les méthodes de synthèses utilisées pour l'obtention des différentes molécules citées ci dessus.

1.1. Le séléniure de carbonyle : OCSe

* OCSe en abondance naturelle :

Le séléniure de carbonyle est synthétisé selon la méthode Finn et King [75 Fin], par chauffage de l'hydrure de sélénium avec du p-bromophénylisocyanate. La réaction procède par addition de H_2Se sur le carbone de l'isocyanate, suivie de l'élimination de OCSe.

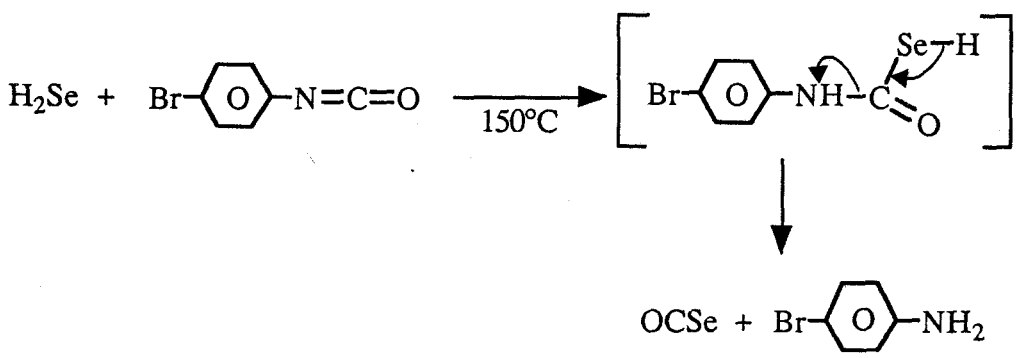

L'hydrure de sélénium, quant à lui, est obtenu par hydrolyse en milieu acide du complexe $[SeAl]_n$ formé par chauffage du mélange sélénium-aluminium à 750°C.

bibliographie p. 59

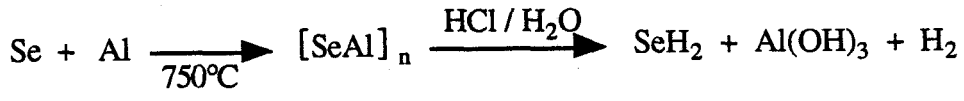

Le séléniure de carbonyle sera conservé dans une ampoule scellée à la température de l'azote liquide jusqu'à son analyse.

* <u>OCSe enrichi en oxygène 18</u> :

Le séléniure de carbonyle enrichi en oxygène 18 est, quant à lui, synthétisé selon la méthode de Kondo et collaborateurs [79 Kon]. Elle consiste à décarboxyler en milieu acide le sel d'ammonium de l'acide sélénocarboxylique préalablement formé par condensation du sélénium et du monoxyde de carbone sur la diéthylamine dans du tétrahydrofurane (THF).

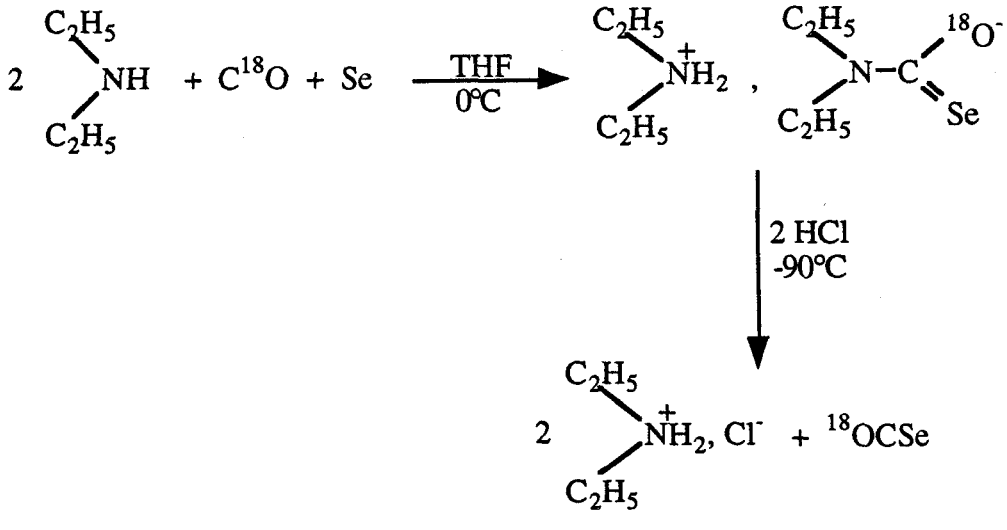

Le séléniure de carbonyle sera conservé dans une ampoule scellée et à la température de l'azote liquide jusqu'à son analyse.

1.2. <u>Le fluorure de germyle : GeH_3F</u>

Le fluorure de germyle a été préparé selon la méthode décrite par Cradock [84 Cra] en suivant la séquence suivante : le germane formé par réduction du dioxyde de germanium en milieu basique réduit partiellement le tétrachlorure d'étain ; le chlorogermane ainsi obtenu conduit au fluorogermane par échange d'halogène. Chaque réaction est réalisée sur une ligne de vide et les composés sont purifiés par condensation fractionnée à chaque étape.

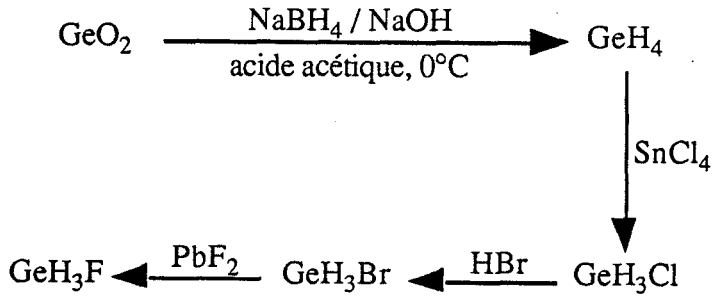

Du fait de son instabilité, le fluorure de germyle est conservé jusqu'à son analyse dans une ampoule scellée plongée dans de l'azote liquide.

1.3. Le fluorure de perchloryle : $FClO_3$

Le fluorure de perchloryle est synthétisé par action du perchlorate de potassium sur l'acide fluorosulfonique [91 Bur], puis distillé sur une ligne de vide classique.

$$KClO_4 + HSO_3F \longrightarrow FClO_3 + KHSO_4$$

Il est conservé à température ambiante dans une ampoule scellée.

1.4. L'acétonitrile monodeutéré : CH_2DCN

La réaction de base utilisée a été décrite en 1960 par Smiley et Arnold [60 Smi]. L'acétonitrile monodeutéré est préparé par traitement du cyanure de potassium sur de l'iodométhane monodeutéré (acheté chez CAMBRIDGE ISOTOPE LABORATORIES à Woburn (Mass., USA)) dans du diméthylsulfoxyde à 20°C.

$$CH_2DI + KCN \xrightarrow[20°C]{DMSO} CH_2DCN + KI$$

Dans un tricol de 50 ml muni d'un thermomètre, d'un réfrigérant surmonté d'une entrée d'azote et d'une ampoule à addition, 15 ml de diméthylsulfoxide (DMSO) fraichement distillé et 3,34 g ($5,1.10^{-2}$ moles) de KCN anhydre sont introduits et chauffés à environ 90°C jusqu'à dissolution totale du cyanure de potassium. On laisse revenir à la température ambiante avant d'ajouter, sous forte agitation, 5 g ($3,5.10^{-2}$ moles) d'iodure de méthyle monodeutéré dissouts dans 5 ml de DMSO. L'agitation est maintenue pendant environ 1h1/2.

Après distillation sous vide, l'acétonitrile monodeutéré pur est obtenu avec un excellent rendement.

bibliographie p. 59

1.5. Les propynes monodeuterés : CH_2DCCH et CH_3CCD

a) propyne-3D [74 Spe]

Le propyne-3D est obtenu par action, dans l'ammoniac liquide à -50°C, de l'acétylure de sodium sur de l'iodométhane monodeutéré.

$$CH_2DI + HCCNa \xrightarrow[-50°C \text{ à } +10°C]{NH_3 \text{ liquide}} CH_2DCCH + NaH$$

Le montage utilisé est décrit ci-dessous (figure CI). Il comprend un ballon tricol réactionnel relié à deux flacons laveurs, contenant respectivement de l'acide sulfurique 2,5N et du chlorure de calcium, et un ballon de condensation.

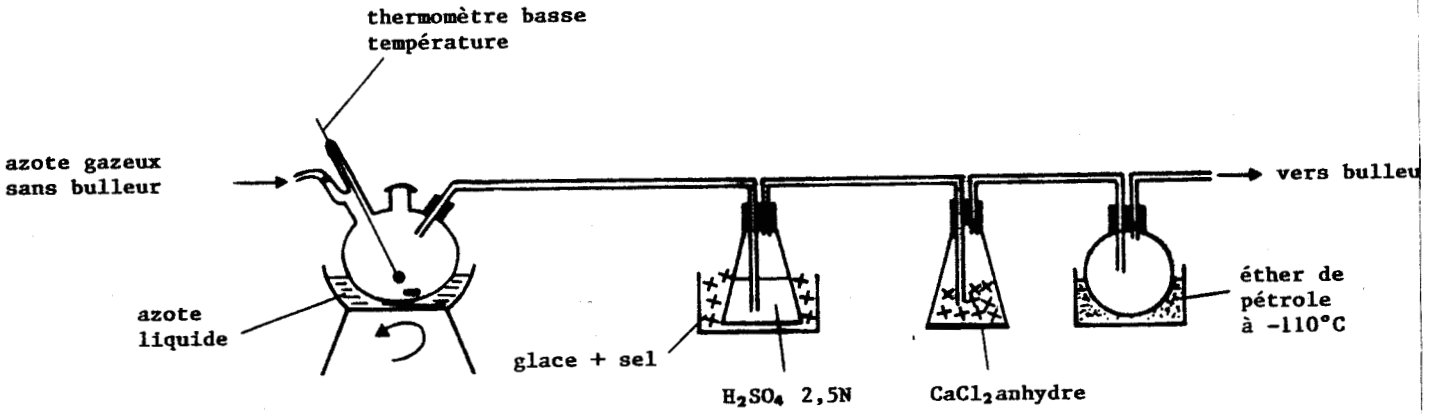

Figure CI : Montage utilisé pour la synthèse des propynes

Sous courant d'azote, on introduit dans le tricol contenant environ 15 ml d'ammoniac liquide refroidis à -50°C, 11,5 ml d'une solution d'acétylure de sodium à 18% dans le xylène (soit $4{,}3.10^{-2}$ moles). on additionne ensuite goutte à goutte 5 g ($3{,}5.10^{-2}$ moles) d'iodure de méthyle monodeutéré.

Le bain froid est retiré et les produits volatils sont neutralisés puis sèchés avant d'être condensés dans le ballon collecteur refroidi à -110°C.

Le propyne-3D ainsi obtenu est suffisamment pur pour être ensuite analysé.

bibliographie p. 59

b) propyne-1D [85 McD]

Le propyne-1D est préparé par hydrolyse de l'acétylure de lithium correspondant avec l'eau lourde D_2O.

$$CH_3CCLi + D_2O \xrightarrow[0°C]{} CH_3CCD + LiOD$$

Le montage utilisé est analogue au précédent.

Un large excès d'eau lourde (environ 7 ml) est introduit sous courant d'azote puis refroidi par un bain de glace. Sous bonne agitation, 1,6 g ($3{,}5.10^{-2}$ moles) de propyne lithium sont ensuite ajoutés par petites quantités par l'intermédiaire d'une ampoule à solide. Le propyne qui se forme instantanément est entraîné par le flux d'azote, sèché sur du chlorure de calcium et condensé dans le ballon collecteur.

Il est suffisamment pur pour être ensuite analysé.

1.6. Les molécules phosphorées

a) Cl-C≡P

Le chlorophosphaalcyne est synthétisé en deux étapes à partir du trichlorophosphonate d'éthyle [91 Gui 1]. La trichlorométhylphosphine, obtenue par réduction du trichlorophosphonate d'éthyle dans l'éther avec un réducteur électrophile, le dichloroalane, subit une bideshydrochloration sur un banc de chaux chauffé à 250°C.

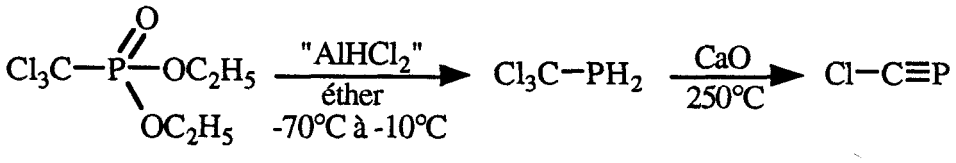

- Préparation de la trichlorométhylphosphine :

Dans un tricol de 250 ml muni d'une agitation mécanique sont agités 3 g ($7{,}9.10^{-2}$ moles) de $LiAlH_4$ et 150 ml d'éther éthylique fraîchement distillé sur sodium/benzophénone. L'ensemble est refroidi rapidement à -70°C à l'aide d'un bain d'air liquide avant d'ajouter 15 g ($11{,}2.10^{-2}$ moles) d'$AlCl_3$ en une seule fois. L'ensemble est réchauffé jusqu'à +10°C puis refroidi à nouveau à -80°C pour additionner goutte à goutte une solution de phosphonate ($5{,}5.10^{-2}$ moles) dans l'éther éthylique.La température interne du milieu réactionnel doit constamment rester inférieure à -70°C. Lorsque l'addition est terminée, le bain froid est retiré et on laisse la solution se réchauffer lentement jusqu'à -10°C.

bibliographie p. 59

L'agitation est alors arrêtée. Après quelques minutes, la phase liquide est transférée dans un ballon de 250 ml préalablement purgé sous azote. La solution est alors distillée puis concentrée sur une ligne de vide.

La phosphine ainsi obtenue avec un rendement de l'ordre de 50%, peut être conservée indéfiniment au congélateur.

- Préparation du chlorophosphaalcène :

La bideshydrochloration de la trichlorophosphine est réalisée sur base solide (CaO) dans des conditions VGSR (Vacuum Gas Solid Reaction) [89 Pel] à 250°C.

b) $H_2C = CH(PH_2)$

La vinylphosphine est obtenue par réduction du vinylphosphonate d'éthyle avec le dichloroalane dans la tétraglyme selon le protocole décrit par Cabioch [89 Cab 1].

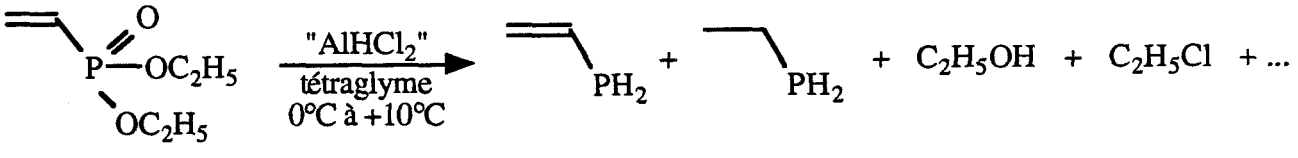

- préparation du milieu réducteur :

Dans un ballon bicol contenant 30 ml de tétraglyme distillée sur sodium/benzophénone on introduit 300 mg ($7{,}9.10^{-3}$ moles) de $LiAlH_4$. Lorsque l'ensemble, refroidi par un bain de glace, est à 0°C, 3 g ($22{,}5.10^{-3}$ moles) d'$AlCl_3$ sont ajoutés par petites quantités sous circulation d'azote et forte agitation. Le bicol est alors placé sur une ligne de vide et la suspension dégazée pendant environ 1/2 h tout en laissant la température remonter lentement.

- préparation de la phosphine :

Le milieu réducteur préalablement formé est ensuite refroidi à O°C puis on introduit goutte à goutte au travers d'un septum 300 µl ($1{,}9.10^{-3}$ moles) de vinylphosphonate d'éthyle. La vinylphosphine est évacuée du milieu dès sa formation et condensée dans un piège refroidi à la température de l'azote liquide. Tout en laissant la température du milieu réactionnel remonter lentement, on maintient le pompage pendant environ 3/4 h.

Le rendement en vinylphosphine ainsi obtenue est de l'ordre de 50%.

c) $(CH_3)CH = PH$

La synthèse du C-méthylphosphaalcène a été décrite par Cabioch [89 Cab 2]. Elle consiste à réduire l'α-chloroéthylphosphonate d'éthyle avec le dichloroalane dans les conditions

bibliographie p. 59

précédemment décrites. Le méthylphosphaalcène est ensuite obtenu par deshydrochloration sur carbonate de potassium solide chauffé à 250°C.

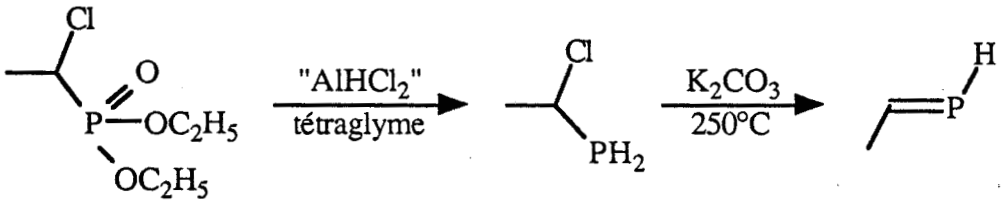

Les protocoles sont identiques aux synthèses précédentes.

d) Synthèse et isomérisation de l'yne phosphine

Le C-méthylphosphaalcène est obtenu par réarrangement de l'yne phosphine sur un banc de carbonate de potassium chauffé à 100°C via un phosphaallène intermédiaire. Sa préparation comprend deux parties : la synthèse de l'yne phosphine [91 Gui 2] et son réarrangement basocatalysé [92 Gui].

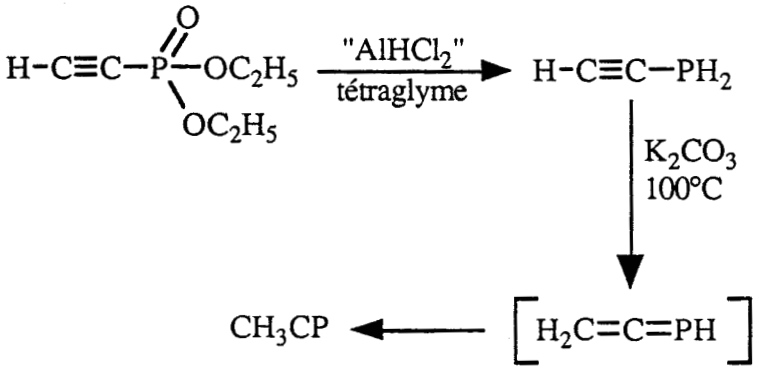

- Préparation de l'yne phosphine :

L'yne phosphine a été synthétisée par réduction de l'yne phosphonate avec le dichloroalane dans la tétraglyme selon le protocole décrit précédemment.

- isomérisation de l'yne phosphine :

L'yne phosphine passe ensuite en flux continu sur un banc de K_2CO_3 chauffé à 100°C.

Elle est alors obtenue avec un rendement de l'ordre de 60%.

e) Schéma du montage utilisé pour la mise en évidence des dérivés de basse coordinence du phosphore non stabilisés (figure CII)

Les dérivés de basse coordinence du phosphore sont des entités très réactives et sont en conséquence préparées par l'intermédiaire d'une ligne de vide branchée directement sur la cellule d'absorption.

bibliographie p. 59

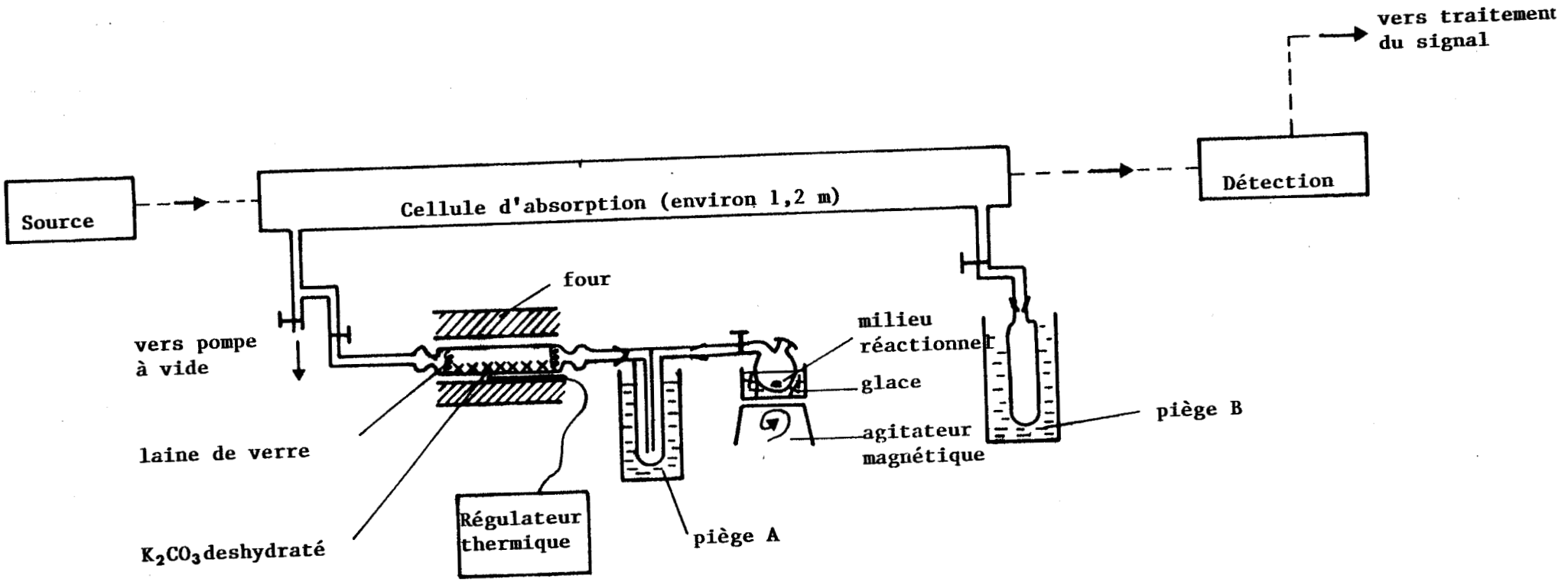

Figure CII : Montage utilisé pour la synthèse et l'analyse des composés de basse coordinence du phosphore

Cette ligne de vide comprend :

- un ballon réactionnel,
- un piège A dont la température est fonction du précurseur considéré (celle de l'azote liquide lorsque l'on souhaite tout piéger, -100°C lors de la réalisation du flux continu dans l'analyse du phosphaallène),
- un réacteur qui permet de réaliser les réactions gaz-solide sous vide (VGSR) [89 Pel].

De plus, la cellule d'absorption est prolongée dans le cas de l'analyse du phosphaallène, d'un piège B, refroidi à l'azote liquide, qui permet d'assurer, par condensation des produits formés, un flux continu dans la cellule.

Les précurseurs des phosphaalcènes et phosphaalcynes sont des phosphines qui possèdent en position α un ou deux groupes partants. Pour obtenir de bonnes conditions de deshydrochloration, la température du banc de chaux ou de carbonate de potassium constitue un point critique.

Nous avons choisi pour chaque espèce étudiée la température qui avait été donnée dans la littérature.

Les conditions expérimentales que nous utilisons (pression, débit de la pompe, longueur du banc, durée de séjour de l'espèce sur le banc, distance entre le four et la cellule, etc), sont toutefois très différentes de celles décrites. Nous ne sommes donc probablement pas dans des conditions optimales et on peut s'attendre à former des espèces secondaires non détectées dans les manipulations décrites.

Dans les cas difficiles, nous avons essayé de faire varier la température dans l'espoir d'obtenir de meilleurs spectres.

2°) Les spectromètres utilisés :

Tout au long de ce travail, nous avons utilisé différents spectromètres, au nombre de quatre (voir tableau CI), qui diffèrent par :

- la source utilisée qui fixe le domaine de fréquence étudié (centimétrique, millimétrique, submillimétrique),
- le type de détection utilisé,
- la présence ou non d'une modulation.

A l'exception du spectromètre centimétrique [88 Lop] du laboratoire de chimie physique de l'université de Valladolid (Espagne), tous les autres spectromètres ont été mis au point par

bibliographie p. 59

	Spectromètre centimétrique à modulation Stark (Valladolid)	Spectromètre millimétrique à détection superhétérodyne	Spectromètre submillimétrique à détection bolométrique	Spectromètre.submillimétrique à bandes latérales
Domaine usuel de fréquences	8 - 50 GHz ($0,4 - 1,5\ cm^{-1}$)	90 - 300 GHz ($3 - 10\ cm^{-1}$)	345 - 470 GHz ($11,5 - 15,5\ cm^{-1}$)	600 - 1500 GHz ($20 - 50\ cm^{-1}$)
Source	carcinotrons	klystrons multipliés en fréquence	carcinotrons	laser moléculaire optiquement pompé par un laser CO_2 plus générateur de bandes latérales
Détecteur	diode à l'arséniure de gallium	détection superhétérodyne	bolomètres au Ge ou à l'InSb refroidis à l'hélium liquide	détection superhétérodyne
Sensibilité maximale	$10^{-10}\ cm^{-1}$	$10^{-6}\ cm^{-1}$	$10^{-7}\ cm^{-1}$	$10^{-5}\ cm^{-1}$
Précision	< 50 kHz	< 50 kHz	< 50 kHz	environ 1 MHz
Balayage en fréquence	oui	oui	oui	non
Résolution	limitée par la fréquence de modulation	limitée par l'effet Doppler	limitée par l'effet Doppler	limitée par l'effet Doppler

Tableau CI : Comparaison entre les différents spectromètres

l'équipe de D. Boucher dans notre laboratoire et ont fait l'objet de différentes thèses de doctorat et publications ; à noter par exemple [82 Bur 1], [86 Boc] et [91 Che].

3°) Le traitement du signal par le logiciel LabVIEW

Que la détection du signal se fasse directement en sortie de cellule (utilisation d'un bolomètre) ou qu'elle se fasse indirectement (hétérodynage), ce signal est traité par la même chaîne d'acquisition et de traitement.

Au laboratoire, nous nous servons d'un logiciel d'instrumentation récent de chez National Instruments, le logiciel LabVIEW (Laboratory Virtual Instrument Engineering Workbench). Le programme que nous utilisons actuellement pour piloter la source hyperfréquence du spectromètre, acquérir et extraire le signal du bruit, soustraire la ligne de base, lisser puis mesurer les fréquences des raies d'absorption des molécules étudiées, a été réalisé par J. Burie [92 Bur].

4°) Les calculs "ab initio" avec GAUSSIAN 82

Les calculs "ab initio" à l'aide du programme GAUSSIAN sont possibles depuis 1970. Cette version, limitée par un maximum de 70 fonctions de base, 35 atomes et l'absence d'orbitales d (seulement s et p), a par la suite connu plusieurs améliorations [85 Cla] en 1976, 1980, 1982, et plus récemment en 1990.

La version utilisée, GAUSSIAN 82 [82 Gau], qui utilise la méthode des orbitales moléculaires LCAO (Linear Combinaison of Atomic Orbitals) tient compte des orbitales s, p, sp, d et f des atomes. Elle contient aussi une procédure d'optimisation qui permet de trouver la géométrie optimale des molécules en cherchant leur énergie minimale.

Ce type de programme fonctionne sur de gros ordinateurs tels que VAX, IBM, CRAY, et son utilisation est relativement coûteuse.

Les calculs effectués dans le cadre de ce travail ont été réalisés dans la base 3.21 G*. C'est une des bases les plus simples après STO.nG (n = 2 à 6), la plus performante étant la 6.31 G** (avec Gaussian 82).

On détermine ainsi, avec une précision relativement correcte, pour une molécule donnée :
- les coordonnées cartésiennes de ses atomes,
- les longueurs de liaisons, angles de valence, angles dièdres,

bibliographie p. 59

- les constantes de rotation A, B, C,
- les constantes de force harmonique,
- les composantes du moment dipolaire,
- l'énergie de la molécule, etc.

Avec la base utilisée, on remarque à partir des valeurs expérimentales des constantes de rotation A, B, C, dans le tableau CII, que les valeurs calculées sont en moyenne erronées de 3% pour A et de 1 à 2% pour B et C. En ce qui concerne le moment dipolaire, les valeurs calculées sont bien moins précises puisqu'elles sont souvent supérieures aux valeurs expérimentales d'environ 50%.

Molécule	constante	valeur observée	valeur calculée (base 3.21G*)	exp. - calc. (%)	références
H_2C=CH-CH_2-CH_2F					
Skew-gauche 1	A (MHz)	10026,32	9752	-2,7	[91 Gui 3]
	B (MHz)	3027,04	3123	+3,2	
	C (MHz)	2601,34	2650	+1,9	
	μ_a (D)	0,332	0,20	-39,7	
	μ_b (D)	1,873	2,20	+17,5	
	μ_c (D)	0,09	0,22	+144,4	
Skew-gauche 2	A (MHz)	13048,22	12350	-5,3	[91 Gui 3]
	B (MHz)	2625,57	2786	+6,1	
	C (MHz)	2406,32	2477	+2,9	
	μ_a (D)	0,841	0,64	-23,9	
	μ_b (D)	1,458	1,93	+32,4	
	μ_c (D)	0,73	0,55	-24,7	
H-C≡P	B (MHz)	19973,67	19917	-0,28	[82 Bur 2], [82 Fra]
H_2C=NH	A (MHz)	196211,046	208606	-5,9	[81 Dux],
	B (MHz)	34642,7273	35158	-1,5	[89 Kra],
	C (MHz)	29350,5211	30087	-2,5	[87 Rig]
	μ (D)	2,024	2,22	-8,8	
H_2C=PH	A (MHz)	138503,20	140366	-1,3	[81 Kro],
	B (MHz)	16418,105	16174	+1,5	[82 Fra]
	C (MHz)	14649,084	14503	+1,0	
H_2C=CH(PH_2)	A (MHz)	40306	41615	-3,1	travail présenté
	B (MHz)	5458,098	5511	-1,0	
	C (MHz)	4975,211	5074	-1,0	
	μ_a (D)	0,61	0,83	-21,4	
	μ_b (D)	0,51	0,82	-37,8	

Tableau CII : validité des calculs "ab initio"

bibliographie p. 59

BIBLIOGRAPHIE

[60 Smi] R. A. SMILEY & C. ARNOLD
J. Org. Chem. 1960, 25, 257-258

[74 Spe] G. K. SPEIRS & J. L. DUNCAN
J. Mol. Spectrosc. 1974, 51, 277-287

[75 Fin] E. J. FINN & G. W. KING
J. Mol. Spectrosc. 1975, 56, 39-51

[79 Kon] K. KONDO, S. YOKOYAMA, N. MIYOSHI, S. MURAI & N. SONODA
Angew. Chem. Int. Ed. Engl. 1979, 18, 691-691

[81 Dux] G. DUXBURRY, H. KATO & M. L. LE LERRE
Farad. Disc. Chem. Soc. 1981, 71, 97-110

[81 Kro] H. W. KROTO, J. F. NIXON & K. OHNO
J. Mol. Spectrosc. 1981, 90, 367-373

[82 Bur 1] J. BURIE, D. BOUCHER, J. DEMAISON & A. DUBRULLE
J. Phys. (Paris) 1982, 43, 1319-1325

[82 Bur 2] J. C. T. R. BURCKETT, ST LAURENT, T. A. COOPER, H. W. KROTO,
J. F. NIXON & K. OHNO
J. Mol. Struct. 1982, 79, 215-220

[82 Fra] M. M. FRANCL, W. J. PIETRO, W. J. HEHRE, J. S. GORDON, D. J. DEFREES
& J. A. POPLE
J. Chem. Phys. 1982, 77, 3654-3665

[82 Gau] J. S. BINKLEY, R. A. WHITESIDE, R. SEEGAR, D. J. DEFREES, H. B. SCHEGEL,
S. TOPIOL, L. R. KALIM, M. J. FRISH, E. M. FUOER & J. A. POPLE
"GAUSSIAN 82"
Carnegie-Mellon University, Pittsburg PA.

[84 Cra] S. CRADOCK
Mol. Phys. 1984, 51, 697-714

[85 Cla] T. CLARK
A handbook of Computational Chemistry ; A Practical Guide to chemical Structure and Energy Calculations
Wiley-Interscience, New York 1985, chap 3 et 5

[85 McD] C. MC DADE & J. E. BERCAW
J. Organomet. Chem. 1985, 279, 281-315

[86 Boc] R. BOCQUET
Thèse de Doctorat 3ème cycle, Décembre 1986, Université de Lille (France)

[87 Rig] N. V. RIGGS & L. RADOM
Int. J. Quant. Chem. 1987, 31, 393-403

[88 Lop] J. C. LOPEZ, J. L. ALONSO & F. J. PELAEZ
J. Mol. Spectrosc. 1988, 131, 9-20

[89 Cab 1] J. L. CABIOCH & J. M. DENIS
J. Organomet. Chem. 1989, 377, 227-233

[89 Cab 2] J. L. CABIOCH
Thèse de Doctorat, Avril 1989, Université de Rennes (France)

[89 Kra] H. KRAUSE, D. H. SUTTER & M. H. PALMER
Z. Naturforsch. 1989, A44, 1063-1078

[89 Pel] B. PELLERIN
Thèse de Doctorat, Avril 1989, Université de Rennes (France)

[91 Bur] K. BURCZYK, H. BÜRGER, M. LE GUENNEC, G. WLODARCZAK & J. DEMAISON
J. Mol. Spectrosc. 1991, 148, 65-79

[91 Che] W. D. CHEN
Thèse de Doctorat, Octobre 1991, Université de Lille (France)

[91 Gui 1] J. C. GUILLEMIN, T. JANATI, P. GUENOT, P. SAVIGNAC & J. M. DENIS
Angew. Chem. Int. Ed. Engl. 1991, 30, 196-198

[91 Gui 2] J. C. GUILLEMIN, P. SAVIGNAC & J. M. DENIS
Inorg. Chem. 1991, 30, 2170-2173

[91 Gui 3] G. A. GUIRGIS, K. M. MARSTOKK & H. MØLLENDAL
Acta Chem. Scand. 1991, 45, 482-490

[92 Bur] J. BURIE
Habilitation, Janvier 1992, Université de Lille (France)

[92 Gui] J. C. GUILLEMIN, T. JANATI & J. M. DENIS
J. Chem. Soc., Chem. Comm. 1992, sous presse
J. C. GUILLEMIN, T. JANATI, P. GUENOT & J. M. DENIS
J. Chem. Soc., Chem. Comm. 1992, sous presse

CHAPITRE D

ANALYSE DES SPECTRES ET STRUCTURES GEOMETRIQUES

1°) Molécules linéaires

1.1. Etat fondamental et structures géométriques du bromure de cyanogène

Publication soumise à "Journal of Molecular Spectroscopy" :

Les spectres de rotation de BrCN dans l'état fondamental ont été analysés dans les domaines millimétrique et submillimétrique pour les six isotopes majoritaires. La grande précision des constantes moléculaires obtenues a permis de déterminer et comparer les structures r_0, $r_{\varepsilon,I}$, r_s et r_m^{ρ} de cette molécule.

L'analyse des états excités de vibration $v_2 = 1, 2$ et $v_3 = 1$ a permis d'obtenir une nouvelle structure à l'équilibre.

Finalement nous montrons qu'une méthode semi-empirique dérivée de la méthode $r_{\varepsilon,I}$ permet de calculer une structure très proche de la structure r_e.

Rotational Spectrum and Equilibrium Structure of Cyanogen Bromide

M. LE GUENNEC, G. WLODARCZAK, W.D. CHEN, R. BOCQUET, AND J. DEMAISON

ABSTRACT

The rotational spectrum of BrCN has been measured in the millimeterwave and submillimeterwave ranges. r_0, r_s, $r_{\varepsilon,I}$, r_m^{ρ} and r_e structures have been calculated and compared. The value of the $r_e(C{\equiv}N)$ bond length is discussed and compared with those of similar molecules.

INTRODUCTION

The microwave spectrum of cyanogen bromide (BrCN) was first investigated in 1947 by Townes and coll. (1) and was the subject of a number of subsequent papers. A review of the work prior to 1976 may be found in (2). Cazzoli and coll. (3) determined the α_1 vibration-rotation constant for ^{79}BrCN and ^{81}BrCN by increasing the population of the $v_1 = 1$ excited vibrational state by vibrational energy transfer from active nitrogen N_2^*. Later, the same group (4) observed direct l-doublet transitions in the $v_2 = 1^1$ state and determined accurately the l-type doubling constant and the asymmetry parameter of the bromine nuclear quadrupole coupling. Blackman and coll. (5) analyzed the rotational Zeeman effect and derived the magnetic g-factor. Accurate bromine and ^{14}N quadrupole coupling parameters were given by Cogley and Kukolich (6). An experimental anharmonic force field was calculated by Whiffen (7). Maki and Gott (8) analyzed the high resolution infrared spectrum in 1962 and determined an equilibrium structure.

In fact that structure was not accurate and the r_e(C≡N) bond length was found to be shorter than in the structurally similar molecules ClCN (3) and ICN (9), a result which is quite unexpected. To shed some light on this problem we have decided to reanalyze the rotational spectra of BrCN, its isotopic species and its excited states, the ultimate goal being to be able to calculate an accurate structure for BrCN and to compare it to those of ClCN and ICN.

EXPERIMENTAL DETAILS

The sample of BrCN was obtained commercially (Jansen Chimica, Geel, Belgium) and was used without further purification. Rotational spectra under 300 GHz were measured with a computer-controlled millimeter-wave spectrometer using superheterodyne detection (10). The transitions between 340 and 470 GHz were measured with a source-modulated spectrometer using phase-stabilized submillimeter BWOs (Thomson-CSF) as sources and a He-cooled bolometer as detector.

Above 470 GHz a new FIR laser sidebands spectrometer was used. It is a considerably modified and improved version of the spectrometer described in Ref. (11). The FIR laser is 2.40 m long and 38 mm bore. It is pumped by a commercial CO_2 laser (PL6 model from Edinburgh Instruments) which can deliver a maximum output power of 200 W. A FIR power of 10 mW or more is obtained with about 35 laser lines. The FIR radiation is mixed with a tunable microwave radiation (2-20 GHz) on a Schottky diode to produce tunable sidebands. After the absorption cell an heterodyne detection of the sidebands is used. The FIR molecular laser lines used for the measurements are (in MHz): HCOOH emissions at

692951.4, 716156.8, 761608.3, 991777.8 and CH_2F_2 at 1035552.7, and 1042150.4. The frequencies are taken from Ref. (12). The accuracy of the measurements is about 1 MHz, partly due to the knowledge of the frequency of the FIR molecular lines.

All spectra were measured at room temperature and all isotopic species were studied in natural abundance.

ANALYSIS OF THE SPECTRA

The measured transitions of the ground vibrational states of all isotopomers are listed in Table I. Their assignment was straightforward because approximate constants were already available (2). The low J transitions are split by the quadrupole interaction. The frequencies given in Tables I and III were corrected for this effect using the hyperfine constants of Refs. (2, 6). A weighted least-squares program was used to fit the experimental frequencies to the parameters of the following equation:

$$\nu = 2B(J + 1) - 4D(J + 1)^3 \qquad (1)$$

The derived constants are listed in Table II. For the two most abundant isotopic species (79-12-14 and 81-12-14), it was possible to determine with accuracy the sextic centrifugal distortion constant H. For the 79-12-14 species, H was previously calculated from the anharmonic force field (7). The calculated value: -0.12 mHz is in very good agreement with the experimental value: -0.126(3) mHz. For the less abundant isotopic species, we have made two fits: one with H fixed at the parent species value and the other with H fixed at zero. In all cases the variation of the rotational constant was no more than two standard deviations.

For the two parent species (79-12-14 and 81-12-14) the rotational spectra were also measured for the vibrational states $v_2 = 1^1, 2^0, 2^2$ and $v_3 = 1$. The measured frequencies are listed in Table III. To determine the constants of the non degenerate state $v_3 = 1$, Eq. (1) was used. For the rotational transitions of the $v_2 = 1$ and 2 states the following expression was employed (13):

$$\nu = 2B(J + 1) - 4D[(J + 1)^3 - (J + 1)l^2] + \Delta \qquad (2)$$

For the $v_2 = 1^1$ state, the l-type doubling term is:

$$\Delta = \pm(J + 1)[q^0 - 2q^1(J + 1)^2] \qquad (3)$$

For the $\psi^+ \rightarrow \psi^+$ transition of the $v_2 = 2^2$ doublet, the expression of Δ is (13):

$$\Delta = -(J + 1)[(J + 1)^2 - 1]\delta \qquad (4a)$$

with $\delta = \frac{q^2}{2(B - x_{||})}$ (4b)

and for the $\psi^- \rightarrow \psi^-$ transition: $\Delta = 0$.

As the value of $x_{||}$ was not yet unambiguously determined, the sign of δ is not known. So it is not possible to know which component of the doublet is the ψ^+ transition and which one is the ψ^-. Furthermore the standard deviation of the fit does not (and cannot) depend on the assignment made. Fortunately the value of the centrifugal distortion constant is sensitive to the choice made. If the upper component is assigned to ψ^+ : D(^{79}BrCN) = 0.99345(19) kHz, and if the reverse assignment is made: D(^{79}BrCN) = 0.92621(16) kHz. As the states $v_2 = 1^1$ and 2^2 are not perturbed, the D centrifugal distortion constant is expected to vary smoothly with v_2. See Fig. 1 where D is plotted in fonction of v_2. It appears clearly that the right assignment is ψ^+ to the lower component of the doublet. To confirm this assignment, we have also determined a preliminary value of the D constant for the $v_2 = 3^3$ state, its value is also represented on Fig. 1.

Finally to fit the state $v_2 = 2^0$, eq.(3) was used with:

$$\Delta = (J + 1)[(J + 1)^2 - 1]\delta \qquad (5)$$

where δ was fixed at the value found for the state $v_2 = 2^2$.

The constants of the excited states are gathered in Table IV. The values of the l-type doubling constants are in good agreement with the results of Cazzoli and coll. (4). The determination of δ allows us to calculate $x_{||} = -1.76$ cm^{-1}. This value is not in good agreement with the results of Wang and Overend: $x_{||} = -0.36$ cm^{-1} (14).

Finally, from the rotational constants in the states $v_2 = 0$, 1^1, and 2^2, it is possible to determine $\gamma_{22} + \gamma_{||}$ using the formula:

$$B_v = B_e - \sum_i \alpha_i \left(v_i + \frac{d_i}{2}\right) + \sum_{i,\,j} \gamma_{ij} \left(v_i + \frac{d_i}{2}\right)\left(v_j + \frac{d_j}{2}\right) + \gamma_{||} l^2 \qquad (6)$$

The values found (see Table IV) are much greater than the experimental accuracy of the rotational constants, but they are nearly identical for the two isotopic species.

STRUCTURES

Least-squares structures :

We have at our disposal six moment of inertia (Table V) to determine two independent molecular parameters: the C-Br and C≡N distances. It is possible to use the least

squares method to calculate the effective structure (or r_o structure). The basic assumption of this method is that the Gauss-Markov conditions are met. In other words it is assumed that the vibrational correction $\varepsilon = I_o - I_e$ behaves like a random variable of zero mean. The result of the fit is given in the first column of Table VI. This fit is not satisfactory because its standard deviation: s = 0.0015 uÅ^2 is about 300 times greater than the mean standard deviation of the moments of inertia ($0.47 \cdot 10^{-4}$ uÅ^2). This result is not surprising because it is known that ε is generally a positive quantity increasing with the moment of inertia (15). As the range of variation of the moments of inertia is quite small (4.8 %), it is a reasonable approximation to assume that ε is a constant (it is also the basic assumption of the substitution structure) and to determine it by least squares together with the interatomic distances. Rudolph (16) has named this structure $r_{\varepsilon,I}$ (the I are fitted to determine ε). For diatomic molecules, the $r_{\varepsilon,I}$ structure is identical to the r_s structure derived from Kraitchman's equations. But as stated by Rudolph, for polyatomic molecules with large and complete collections of isotopomers, the $r_{\varepsilon,I}$ structure is preferable to a true Kraitchman-type method, particularly when near-axis atoms are present. We report in Table VII the $r_{\varepsilon,I}$ structure for some triatomic linear molecules. In this list, N_2O and CO_2 have an atom near the center of mass, nevertheless it was possible to derive a $r_{\varepsilon,I}$ structure without any difficulty. Furthermore, the $r_{\varepsilon,I}$ structure may be applied even to molecules which have one atom without isotope (or difficult to substitute): Table VII shows the examples of FCN and ICN. Inspection of Table VII also shows that the $r_{\varepsilon,I}$ structure is generally at least as good as the r_s structure. The rotational constants used to determine the $r_{\varepsilon,I}$ structure of OCS are of different origins, they are gathered in Table VIII. The result of the fit for BrCN is given in Table VI. All the parameters are well determined, particularly ε = 0.090(7) uÅ^2 has the expected order of magnitude (15) and the standard deviation of the fit drops to $0.23 \cdot 10^{-3}$ uÅ^2, i.e. about one order of magnitude less than for the r_o structure. Although the $r_{\varepsilon,I}$ structure is better (i.e. nearer the r_e structure) than the r_o structure, it often remains significantly different from the r_e structure. To still improve the fit (and the structure), it would be necessary to take into account the variations of ε with the isotopic substitutions. It is known that ε varies like I^n with the exponent n near 0.5-0.6 (15, 17). But this relationship is a statistical one: it is satisfactory when comparing the ε of quite different molecules, but it can behave poorly when the ε of different isotopomers are compared. So, it has first to be checked for each different type of molecule (18). In the particular case of BrCN the situation is quite favourable because the anharmonic force field of this molecule has been determined (7) and it is therefore possible to investigate the behaviour of ε. In Fig. 2 ε is plotted versus the ground state moment of inertia I_o of different isotopomers of BrCN and for ClCN, where the data for the latter have been taken from Ref. (19). These figures clearly show that the relationship:

$$\varepsilon = k I_o^n \qquad (7)$$

is indeed valid for the structurally similar molecules ClCN and BrCN. The problem is that the exponent n is not directly determinable because the range of variation of I_o is too small. Fig. 3 represents the variations of the interatomic distances and of the calculated equilibrium moments of inertia versus n. As the experimental equilibrium moments of inertia of $^{79}Br^{12}C^{14}N$ and $^{81}Br^{12}C^{14}N$ have been determined (see following section), it is possible to estimate the value of n. As expected it is near 0.5, the exact value being 0.52 (see Fig. 3). The result of the fit with n = 0.52 is also given in Table VI (quasi r_e structure). Although the model still is an approximate one, the derived structure should be very near the true equilibrium structure.

Substitution structures:

Each atom of BrCN has two isotopes whose natural abundance is sufficient to permit the measurement of the rotational spectrum of the corresponding isotopic species. A true substitution structure (r_s) may be calculated using Kraitchman's equations (20). The results are gathered in Table IX, the different r_s structures have been obtained by use of different choices for the parent species along with the appropriate isotopic species required for calculation of the coordinates in each case. The uncertainty of each coordinate was first calculated by the law of propagation of errors, but it gives extremely small errors ($\sim 0.2 \cdot 10^{-4}$ Å), so, the empirical rule of Costain (21) was used:

$$\sigma(z) = \frac{K}{|z|} \qquad (8)$$

where z is the cartesian coordinate of the substituted atom relative to the center of mass of the parent species and K = 0.0005 $Å^2$ as proposed by Van Eijck (22). The resulting error is still quite small suggesting that the r_s structure should be very accurate. Indeed the r_s parameters are essentially independent of the isotopic species used in the calculation of the structure. In fact this pleasing result was not unexpected because three conditions have to be met in order to obtain a reliable r_s structure:

- the cartesian substitution coordinate should be large
- the change of mass upon isotopic substitution should be small
- the mass of the substituted atom and the total mass of the molecule should be large

These three conditions are met for BrCN.

If the lightest isotopomer (79-12-14) is chosen as parent molecule, all $\Delta\varepsilon = \varepsilon$(isotopic species) - ε(parent species) are positive as shown by Fig. 2. It results from the Kraitchman's equation:

$$z_s = \sqrt{\frac{\Delta I_e + \Delta \varepsilon}{\mu}} \qquad (9)$$

that: $|z_s| > |z_e|$ (10a)

and consequently:

$$r_s(C\text{-}Br) = |z_s(C)| + |z_s(Br)| > r_e(C\text{-}Br) \qquad (10b)$$

$$r_s(Br\text{-}N) = |z_s(Br)| + |z_s(N)| > r_e(Br\text{-}N) \qquad (10c)$$

For the C≡N bond length it is not so easy to conclude, but the two errors should at least partially cancel each other, so the r_s length should be near the r_e value. Furthermore, if we use the ε calculated by Whiffen (7) it is possible to estimate the error:

$$r_s(C\equiv N) \approx r_e(C\equiv N) + \frac{1}{2}\left\{|z(N)|\,\frac{\Delta\varepsilon(15\text{-}14)}{\Delta I(15\text{-}14)} - |z(C)|\,\frac{\Delta\varepsilon(13\text{-}12)}{\Delta I(13\text{-}12)}\right\} \qquad (11)$$

with:

$$\Delta\varepsilon(15\text{-}14) = \varepsilon(79\text{-}12\text{-}14) - \varepsilon(79\text{-}12\text{-}15) \qquad (12)$$

$\Delta\varepsilon/\Delta I$ is nearly constant, and as $|z_s(N)| > |z_s(C)|$, the error should be positive. Indeed the calculation gives (in Å):

$$r_s(C\equiv N) \approx r_e(C\equiv N) + 0.0006 \qquad (13)$$

The r_s distance is also slightly larger than the r_e distance. Comparison of the r_s and $r_{\varepsilon,I}$ structures shows that they are nearly identical.

It is still possible to improve -at least slightly- these results by using the double substitution method of Pierce (23). Inspection of Eq. (9) indicates that the atom for which z_s-z_e is the largest is nitrogen. The double substitution coordinate of nitrogen was calculated using 79-12-14 as parent species and 79-12-14, 81-12-14 and 81-12-15 as isotopic species. It gives: $z_{ss}(N)$ = 2.3482 Å, i.e. 0.0016 Å shorter than the substitution coordinate. This correction is of the right order of magnitude, although a little too large.

It is also possible to calculate the bond lengths directly, without recourse to cartesian coordinates by using an alternative method due to Kirby and Kroto (24). The double substitution bond length is calculated from the following equation:

$$\Delta m_1 \Delta m_2 r_{ss}^2 = MI - M_1^* I_1^* - M_2^* I_2^* + M_{12}^{**} I_{12}^{**} \qquad (14)$$

where M and I are the total mass and moment of inertia, respectively of the parent molecule, subscripts refer to species substituted at the number positions and Δm_i is the change in mass on substituting the ith atom. The number of asterisks indicates the number of substitutions. The results are presented in Table VI where it can be seen that the r_{ss} values are slightly smaller than the r_s values. So, in the case of BrCN, the r_s structure is a very good approximation of the r_e structure, and the r_{ss} still a better one.

r_m and r_m^ρ structures:

It is possible to determine the I_m moment of inertia (25) for the two species 79-12-14 and 81-12-14 because a complete substitution structure has been determined for these two species. The results are given in Table V. Although the I_m values are very near the I_e values (determined in the next section and also listed in Table V), they are significantly different. Because the system of equations is ill-conditionned, this small difference is sufficient to render the calculation of a meaningful r_m structure impossible.

On the other hand it is quite easy to calculate an r_m^ρ structure (26) which is an approximation of the r_m structure (and therefore of the r_e structure). According to Harmony and Taylor (26) an I_m^ρ moment of inertia is defined for b = N + 1 isotopic species by:

$$\left[I_m^\rho\right]_\alpha = (2\rho - 1)\,[I_0]_\alpha \qquad \alpha = 1, \ldots b \qquad (15)$$

with $$\rho = \frac{[I_s]_1}{[I_0]_1}$$

N is the number of atoms, $[I_0]_1$ is the ground state moment of inertia of the parent species and $[I_s]_1$ is the corresponding substitution moment computed from the substitution coordinates. The basic assumption of this method is that ρ remains nearly constant by isotopic substitution. This assumption was checked for several molecules, either by comparing the r_m^ρ structure with the experimental r_e structure (26) or by computing the vibration-rotation parameters from the anharmonic force field (27). By convention the r_m^ρ computations use a minimal substitution data set (SDS) where the parent species ($^{79}Br^{12}C^{14}N$) consists of all the light isotopes (28). The I_s and $I_m^\rho = I_m$ values for $^{79}Br^{12}C^{14}N$ are computed according to Watson's method (25). The remaining I_m^ρ were computed according to Eq. (15) using $\rho = 0.99919071$. They are listed in Table V together with the I_0 and the I_e. The b = 4 moments of inertia I_m^ρ are used for a least-squares determination of the structure. The results are listed in Table VI.

Equilibrium structure (r_e):

There are enough data from rotational spectroscopy to determine the rotation-vibration interaction constants α with an accuracy sufficient to calculate the equilibrium rotational constants of $^{79}Br^{12}C^{14}N$ and $^{81}Br^{12}C^{14}N$. To cancel the effects of the Fermi

resonance between the $v_3 = 1$ and $v_2 = 2^0$ levels, the equilibrium rotational constants were calculated by the following formula (29):

$$B_e = \frac{1}{2} (5B_{000} - B_{100} - B_{001} - B_{02^00}) \qquad (16)$$

The equilibrium moment of inertia are listed in Table V and the derived structure in Table VI. The uncertainty on the distances was calculated using the law of propagation of errors. Although the moments of inertia are accurate, the calculated standard deviations are rather large due to the fact that the system of equations is ill-conditionned. To improve it, it would be useful to determine the equilibrium rotational constant of the ^{15}N or ^{13}C isotopic species. Despite its low accuracy, the r_e structure should be considered as reliable because it is in very good agreement with the r_m^ρ and the quasi-r_e structures. Furthermore it is fully compatible with the substitution structures.

The coefficients $\gamma_{22} + \gamma_{ll}$ were neglected in the calculation of B_e (Eq. 16). Although they are not negligible (see Table IV), they have no sizable influence on the structure because their values are the same for the two isotopomers. The magnetic correction to the rotational constants has also been neglected. It is possible to estimate it because the rotational g factor of BrCN has been measured (5). In fact this correction increases the rotational constants by about 70 kHz, which is much greater than the accuracy of the rotational constants. However there is only a difference of a few kHz between the two isotopomers, so it has a negligible effect on the structure.

COMPARISON OF THE C≡N BOND LENGTHS

The r_e(C≡N) distance has been determined for several simple molecules. The values are gathered in Table X together with the nuclear quadrupole coupling constant of the ^{14}N atom. The r_e(C≡N) distance in BrCN is expected to be near the values found for ClCN (3) and ICN (9). Furthermore it has been argued that a correlation should exist between r_e(C≡N) and eqQ(^{14}N) (30). Fig. 4 shows that these two assertions are clearly not verified. The conclusion of the preceding section was that our r_e structure is very likely reliable. This is further strengthened by the fact that BrCN and CNCN have nearly identical r_e(C≡N) distances and eqQ(^{14}N) values (Table X). To try to clarify this problem, we have redetermined the r_s(C≡N) distance in ClCN and ICN and we have estimated the $r_s - r_e$ values with the help of Eq. (11) and the data of Whiffen (7, 19). The results are listed in Table XI. The large value of $z_s - z_e$ for the C atom in ICN is at first sight surprising. But, in this particular case, we can use the experimental values of Cazzoli and coll. (9) instead of the calculated values of Whiffen (7) and we obtain the same result. The quasi-r_e structure of ClCN may also be

calculated using the same method as for BrCN. It gives r_e(C≡N) = 1.1589 Å, in very good agreement with the value of Table XI.

In conclusion, for ClCN, r_e(C≡N) = 1.1590 Å is more accurate than the preceding value of 1.1606(28) Å (3). This is not surprising because the r_e structure of ClCN was calculated using the equilibrium rotational constants of ^{35}ClCN and ^{37}ClCN. As for BrCN, they give a system of equations which is not well conditionned. The situation is quite different for ICN, the experimental r_e structure: 1.1604(3) Å is very accurate and in good agreement with our estimation: 1.1594(10) Å. The "corrected" values are also represented on Fig. 5. To see the correlation between r_e(C≡N) and eqQ(^{14}N) more easily, it is better to plot eqQ(^{14}N) versus $1/r^3$: as far as similar bonds are concerned a linear correlation should be obtained (30). See Fig. 5. There is clearly one outlier: FCN. It could be explained by the fact that the CN bond as a greater triple-bond character in FCN than in the other molecules (31). The abnormal behaviour of ICN could similarly be explained by a smaller triple-bond character of the CN bond.

REFERENCES

1. C.H. TOWNES, A.N. HOLDEN, AND F.R. MERRIT, Phys.Rev. 71, 64-64 (1947).
2. F.J. LOVAS, J. Phys. Chem. Ref. Data 7, 1445-1750 (1978).
3. G. CAZZOLI, P.G. FAVERO, AND C. DEGLI ESPOSTI, Chem. Phys. Lett. 50, 336-338 (1977).
4. G. CAZZOLI, R. CERVELLATI, D.G. LISTER, D. DAMIANI, AND C. DEGLI ESPOSTI, J. Mol. Spectrosc. 101, 94-103 (1983).
5. G.L. BLACKMAN, R.D. BROWN, AND F.R. BURDEN, J. Chem. Phys. 59, 3760-3761 (1973).
6. C.D. COGLEY and S.G. KUKOLICH J. Mol. Spectrosc. 97, 220-223 (1983).
7. D.H. WHIFFEN, Spectrochim. Acta A 34, 1183-1192 (1978).
8. A.G. MAKI AND C.T. GOTT, J. Chem. Phys. 36, 2282-2285 (1962).
9. G. CAZZOLI, C. DEGLI ESPOSTI, AND P.G. FAVERO, J. Mol. Struct. 48, 1-8 (1978).
10. J. BURIE, D. BOUCHER, J. DEMAISON, AND A. DUBRULLE, J. Phys. (Paris) 43, 1319-1325 (1982).
11. G. PIAU, F.X. BROWN, D. DANGOISSE, AND P. GLORIEUX, IEEE J. Quantum Electronics **QE-23**, 1388-1391 (1987).
12. N.G. DOUGLAS, "Millimetre and Submillimetre Wavelength Lasers", Springer, Berlin, 1989.
13. G. AMAT, H.H. NIELSEN, AND G. TARRAGO, "Rotation-Vibration of Polyatomic Molecules", Marcel Dekker, New York, 1971.

14. V.K. WANG AND J. OVEREND, Spectrochim. Acta A **29**, 1623-1633 (1973).
15. J. DEMAISON AND L. NEMES, J. Mol. Struct. **55**, 295-299 (1979).
16. H. D. RUDOLPH, Struct. Chem. **2**, 581-588 (1991).
17. K. BURCZYK, H. BÜRGER, M. LE GUENNEC, G. WLODARCZAK, AND J. DEMAISON, J. Mol. Spectrosc. **148**, 65-79 (1991).
18. M. LE GUENNEC, W.D. CHEN, G. WLODARCZAK, J. DEMAISON, R. EUJEN, AND H. BÜRGER, J. Mol. Spectrosc. **150**, 000-000 (1991).
19. D.H. WHIFFEN, Spectrochim. Acta A **34**, 1173-1182 (1978).
20. C.C. COSTAIN, J. Chem. Phys. **29**, 864-874 (1958).
21. C.C. COSTAIN, Trans. Amer. Crystallogr. Assoc. **2**, 157-164 (1966).
22. B.P. VAN EIJCK, J. Mol. Spectrosc. **91**, 348-362 (1982).
23. L. PIERCE, J. Mol. Spectrosc. **3**, 575-580 (1959).
24. C. KIRBY AND H.W. KROTO, J. Mol. Spectrosc. **83**, 130-147 (1980).
25. J.K.G. WATSON, J. Mol. Spectrosc. **48**, 479-502 (1973).
26. M.D. HARMONY AND W.H. TAYLOR, J. Mol. Spectrosc. **118**, 163-173 (1986).
27. M.D. HARMONY, R. BERRY, AND W.H. TAYLOR, J. Mol. Spectrosc. **127**, 324-336 (1988).
28. R. BERRY AND M.D. HARMONY, Struct. Chem. **1**, 49-59 (1989).
29. Y. MORINO AND C. MATSUMURA, Bull. Chem. Soc. Japan, **40**, 1095-1100 (1967).
30. A. WEISS AND S. WIGAND, Z. Naturforsch. A **45**, 195-212 (1990).
31. P. PULAY, A. RUOFF, AND W. SAWODNY, Mol. Phys. **30**, 1123-1131 (1975).
32. M. LE GUENNEC, G. WLODARCZAK, J. DEMAISON, H. BÜRGER, M. LITZ, AND H. WILLNER, to be published.
33. J.L. TEFFO AND A. CHEDIN, J. Mol. Spectrosc. **135**, 389-409 (1989).
34. G. GRANER, C. ROSSETTI, AND D. BAILLY, Mol. Phys. **58**, 627-636 (1986).
35. C. DEGLI ESPOSTI, P.G. FAVERO, S. SERENELLINI, AND G. CAZZOLI, J. Mol. Struct. **82**, 221-236 (1982).
36. H. JONES AND J. LINDENMAYER, J. Mol. Spectrosc. **113**, 339-354 (1985).
37. C.D. COGLEY, H.A. FRY, AND S.G. KUKOLICH, J. Mol. Spectrosc. **75**, 447-453 (1979).
38. Y. KAWASHIMA, K. KAWAGUCHI, Y. ENDO, AND E. HIROTA, J. Chem. Phys. **87**, 2006-2009 (1987).
39. K. KAWAGUCHI, Y. ENDO, AND E. HIROTA, J. Mol. Spectrosc. **93**, 381-388 (1982).
40. T.A. COOPER, S. FIRTH, AND H. KROTO, J. Chem. Soc. Faraday Trans. **87**, 1-7 (1991).
41. J.G. LAHAYE, R. VANDENHAUTE, AND A. FAYT, J. Mol. Spectrosc. **123**, 48-83 (1987).

42. J. GRIPP, H. DREIZLER, J. GADHI, G. WLODARCZAK, J. LEGRAND, J. BURIE, AND J. DEMAISON, J. Mol. Spectrosc. **129**, 381-387 (1988).
43. J. GRIPP AND H. DREIZLER, Z. Naturforsch. A **43**, 133-137 (1988).
44. A. FAYT, R. VANDENHAUTE, AND J.G. LAHAYE, J. Mol. Spectrosc. **119**, 233-266 (1986).
45. A. DUBRULLE, J. DEMAISON, J. BURIE, AND D. BOUCHER, Z. Naturforsch. A **35**, 471-474 (1980)
46. A.V. BURENIN, E.N. KARYAKIN, A.F. KRUPNOV, S.M. SHAPIN, AND S.M. VAL'DOV, J. Mol. Spectrosc. **85**, 1-7 (1981).
47. R.C. WOODS, Philos. Trans. R. Soc. London, Ser. A **324**, 141-146 (1988).
48. P. BOTCHWINA AND J. FLÜGGE, Chem. Phys. Lett. **180**, 589-593 (1991).
49. M. LE GUENNEC, G. WLODARCZAK, AND J. DEMAISON, to be published.
50. W.L. EBENSTEIN AND J.S. MUENTER, J. Chem. Phys. **80**, 3989-3991 (1984).
51. J. SHERIDAN, J.K. TYLER, E.E. AYNSLEY, R.E. DODD, AND R. LITTLE, Nature **185**, 96-96 (1960).
52. J.M.L.J. REINARTZ, W.L. MEERTS, AND A. DYMANUS, Chem. Phys. **45**, 387-392 (1980).
53. M.C.L. GERRY, F. STROH, AND M. WINNEWISSER, J. Mol. Spectrosc. **140**, 147-161 (1990).
54. D. BOUCHER, J. BURIE, J. DEMAISON, A. DUBRULLE, J. LEGRAND, AND B. SEGARD, J. Mol. Spectrosc. **64**, 290-294 (1977).

J	Freq.	e.-c.	Acc.	Ref.
	79-12-14			
0	8240.437	-0.006	10	a
1	16480.866	0.002	6	a
2	24721.069	-0.174	200	b
3	32961.787	0.229	200	b
5	49441.605	-0.307	200	b
8	74160.760	-0.675	1000	b
9	82405.000	4.078	10000	b
11	98879.190	-0.047	200	b
14	123594.720	-0.026	250	b
17	148307.416	0.029	50	c
18	156544.198	0.000	50	c
20	173016.450	-0.137	150	b
23	197721.779	0.007	50	c
24	205955.853	0.011	50	c
26	222422.340	-0.028	50	c
29	247117.750	-0.051	100	b
32	271807.590	0.094	100	b
35	296490.860	-0.019	50	b
38	321167.100	-0.274	300	b
41	345837.000	0.592	600	b
52	436216.381	-0.004	50	c
53	444426.418	0.011	50	c
55	460842.989	0.007	50	c
83	690096.390	-0.069	1000	c
84	698260.565	-0.329	1000	c
87	722743.478	0.254	1000	c
91	755359.582	-0.340	1000	c
94	779801.600	-0.283	1000	c
95	787944.500	-0.671	1000	c
121	998887.380	0.528	1000	c
125	1031191.703	-0.224	1000	c
126	1039261.260	-0.225	1000	c
127	1047328.550	0.235	1000	c
	79-12-15			
0	7889.810	0.124	200	b
1	15779.400	0.046	200	b
5	47337.710	0.267	200	b
18	149882.038	0.004	50	c
19	157768.033	-0.019	50	c
24	197191.961	-0.005	50	c
25	205075.374	-0.004	50	c
55	441257.640	0.094	50	c
56	449116.413	-0.007	50	c
57	456974.116	-0.077	50	c
	79-13-14			
3	32586.870	-0.041	100	b
5	48879.700	-0.248	200	b
17	146621.736	-0.001	50	c
18	154764.930	-0.004	50	c
23	195474.541	0.015	50	c
24	203615.014	-0.006	50	c
25	211754.980	-0.009	50	c
53	439376.404	0.045	50	c
54	447492.053	0.032	50	c
55	455606.459	-0.070	50	c

J	Freq.	e.-c.	Acc.	Ref.
	81-12-14			
0	8193.606	-0.012	12	a
1	16387.220	0.005	12	a
2	24580.520	-0.249	200	b
3	32774.380	0.119	100	b
5	49160.780	-0.192	100	b
8	73739.510	-0.529	500	b
9	81936.000	3.289	5000	b
11	98317.370	-0.035	200	b
14	122892.500	-0.001	250	b
17	147464.756	-0.005	50	c
18	155654.780	-0.005	50	c
20	172033.530	-0.086	100	b
23	196598.487	-0.012	50	c
24	204785.822	0.010	50	c
26	221158.860	0.018	50	c
29	245714.320	0.244	300	b
32	270263.950	0.315	300	b
35	294807.520	0.571	600	b
38	319345.520	2.070	2000	b
41	343873.000	0.432	500	b
47	392907.000	0.619	700	b
51	425575.900	0.230	300	b
53	441903.768	-0.063	50	c
54	450066.237	0.019	50	c
55	458227.474	0.028	50	c
83	686185.688	-0.041	1000	c
86	710535.758	0.147	1000	c
87	718648.394	-0.198	1000	c
92	759184.984	-0.207	1000	c
93	767286.183	-0.517	1000	c
120	985206.580	0.421	1000	c
127	1041415.200	-0.164	1000	c
	81-12-15			
0	7843.570	0.042	200	b
1	15687.010	-0.026	200	b
5	47060.460	-0.037	200	b
18	149005.265	0.003	50	c
19	156845.151	-0.011	50	c
24	196038.558	0.001	50	c
55	438679.055	0.053	50	c
56	446492.032	-0.032	50	c
57	454304.020	-0.017	50	c
	81-13-14			
3	32396.860	-0.006	100	b
5	48594.584	-0.301	200	b
17	145766.739	-0.010	50	c
18	153862.484	0.010	50	c
23	194334.757	-0.020	50	c
24	202427.834	0.006	50	c
25	210520.374	0.012	50	c
53	436816.832	0.013	50	c
54	444885.339	0.025	50	c
55	452952.658	-0.010	50	c
56	461018.839	-0.024	50	c

Acc. = Accuracy in kHz . [a]) ref. (6) . [b]) ref. (2) . [c]) this work.

Table I.: Measured Rotational Frequencies (MHz) of BrCN in the Ground Vibrational State.

	79-12-14				81-12-14			
B (MHz)	4120.22307 (31)	1.000			4096.81066 (47)	1.000		
D (kHz)	0.884865 (75)	0.893	1.000		0.87543 (11)	0.903	1.000	
H (mHz)	-0.1262 (35)	0.724	0.886	1.000	-0.1192 (56)	0.663	0.840	1.000
lines	33				32			
	79-13-14				**81-13-14**			
B (MHz)	4073.39183 (48)	1.000			4049.63590 (35)	1.000		
D (kHz)	0.873149 (89)	0.933	1.000		0.863463 (63)	0.939	1.000	
lines	10				11			
	79-12-15				**81-12-15**			
B (MHz)	3944.84485 (68)	1.000			3921.76535 (40)	1.000		
D (kHz)	0.80442 (11)	0.938	1.000		0.795368 (65)	0.954	1.000	
lines	10				9			

Table II : Ground State Rotational Constants of BrCN.

$v_2 = 1$				$v_2 = 2$				$v_3 = 1$		
J	l	Freq.	e.-c.	J	l	Freq.	e.-c.	J	Freq.	e.-c.
		79-12-14				**79-12-14**			**79-12-14**	
17	-1	148652.564	0.005	17	0	148990.725	0.037	0[a]	8217.719	0.074
18	-1	156908.470	-0.026	18	0	157265.708	0.048	1[a]	16435.476	0.209
23	-1	198181.558	-0.010	23	0	198634.516	-0.043	2[a]	24652.604	-0.241
24	-1	206434.737	0.028	24	0	206906.985	-0.025	5[a]	49304.896	-0.190
52	-1	437223.489	-0.014	52	0	438265.949	-0.023	17	147895.936	0.024
53	-1	445452.158	0.025	53	0	446516.344	0.016	18	156109.738	0.010
54	-1	453679.582	-0.012	54	0	454765.637	0.008	23	197171.975	-0.004
17	1	148793.371	0.012	17	-2	149135.415	0.038	24	205382.901	-0.006
18	1	157057.075	-0.028	18	-2	157417.927	0.045	52	434979.778	-0.014
23	1	198369.201	0.028	23	-2	198823.224	0.089	53	443165.412	0.016
24	1	206630.088	-0.017	24	-2	207102.726	0.161	54	451349.787	-0.003
52	1	437635.305	0.007	52	-2	438597.536	0.076			
53	1	445871.595	0.019	53	-2	446849.913	-0.010			
54	1	454106.653	-0.024	54	-2	455100.965	-0.133			
				17	2	149136.859	-0.082			
				18	2	157419.645	-0.077			
				23	2	198826.720	-0.127			
				24	2	207106.694	-0.067			
				52	2	438637.505	0.016			
				53	2	446892.255	-0.006			
				54	2	455145.847	0.014			
		81-12-14				**81-12-14**			**81-12-14**	
17	-1	147808.222	-0.020	17	0	148147.236	0.027	0[a]	8171.162	0.316
18	-1	156017.340	0.041	18	0	156375.370	0.027	5[a]	49024.235	-0.069
23	-1	197056.047	0.005	23	0	197510.100	-0.011	17	147053.811	0.010
24	-1	205262.310	-0.023	24	0	205735.724	-0.025	18	155220.944	0.079
53	-1	442924.510	-0.007	52	0	435786.524	-0.032	23	196049.418	-0.022
54	-1	451105.405	0.007	53	0	443990.296	-0.017	24	204213.604	-0.047
17	1	147947.463	0.006	54	0	452193.072	0.046	53	440645.402	-0.031
18	1	156164.211	-0.023	17	-2	148287.822	0.022	54	448783.441	0.007
23	1	197241.553	0.010	18	-2	156523.268	0.022	55	456920.243	0.024
24	1	205455.540	0.001	23	-2	197693.402	0.121			
53	1	443339.415	0.014	24	-2	205925.819	0.136			
54	1	451527.866	0.019	52	-2	436107.311	0.099			
55	1	459714.982	-0.125	53	-2	444312.904	-0.022			
				54	-2	452517.262	-0.104			
				17	2	148289.279	-0.081			
				18	2	156524.997	-0.084			
				23	2	197696.915	-0.068			
				24	2	205929.777	-0.091			
				52	2	436147.143	0.007			
				53	2	444355.155	0.002			
				54	2	452561.996	0.013			

a) ref. (2)

Table III : Measured Rotational Frequencies (MHz) of BrCN in Excited Vibrational States.

		^{79}BrCN	^{81}BrCN	Ref.
$v_1 = 1$	B (MHz)	4099.824 (30)	4076.550 (30)	a
	D (kHz)	0.853 (8)	0.870 (8)	a
$v_2 = 1^1$	B (MHz)	4131.77833 (23)	4108.29680 (29)	b
	D (kHz)	0.905605 (43)	0.895902 (55)	b
	$q^{(0)}$ (Hz)	3.91452 (46)	3.87029 (58)	b
	$q^{(1)}$ (mHz)	5.279 (86)	4.93 (11)	b
$v_2 = 2^0$	B (MHz)	4139.15784 (52)	4115.72275 (47)	b
	D (kHz)	0.881245 (98)	0.873170 (88)	b
	δ (Hz)	0.26897 *	0.26826 *	b
$v_2 = 2^2$	B (MHz)	4119.73522 (77)	4143.32856 (82)	b
	D (kHz)	0.91615 (15)	0.92621 (16)	b
	δ (Hz)	0.26897 (49)	0.26826 (53)	b
$v_3 = 1$	B (MHz)	4108.82434 (89)	4085.4250 (10)	b
	D (kHz)	0.93296 (17)	0.92159 (18)	b
$\gamma_{22} + \gamma_{11}$ (MHz)		-0.02395	-0.02386	b

*) fixed at $v_2 = 2^2$ value. [a]) ref. (3). [b]) this work.

Table IV : Molecular Constants of BrCN in Excited States.

	I_0	I_s	I_m	I_m^ρ	I_e
79-12-14	122.658165 (9)	122.5589 (23)	122.4596 (46)	122.45964	122.46700 (45)
79-12-15	128.111249 (22)	-	-	127.90399	-
79-13-14	124.068349 (15)	-	-	123.86761	-
81-12-14	123.359130 (14)	123.2542 (23)	123.1493 (46)	123.15947	123.16771 (45)
81-12-15	128.865181 (13)	-	-	-	-
81-13-14	124.79616 (11)	-	-	-	-

Conversion factor : BI = 505379 uÅ^2

Table V : Moments Inertia (uÅ^2) of BrCN.

	r_o	$r_{\varepsilon,I}$	quasi-r_e	r_s	r_{ss}	r_m^ρ	r_e
r(C-Br)	1.7905(3)	1.7892(1)	1.7885	1.7891(9)	1.7887	1.7891(4)	1.7888(48)
r(C≡N)	1.1581(5)	1.1586(1)	1.1581	1.1586(5)		1.1571(6)	1.1577(69)
r(Br N)	2.9486(3)	2.9478(1)	2.9466	2.9477(8)	2.9473	2.9462(4)	2.9465(21)

Table VI. Structure (Å) of BrCN.

Molecule	Bond	r_o	r_s	$r_{\varepsilon,I}$	r^{ρ}_m	r_e	Ref.
OCS	OC	1.1567	1.1602	1.1581		1.1562	a
	CS	1.5646	1.5601	1.5618		1.5614	
OCSe	OC	1.1536	1.1564	1.1561	1.1523(22)	1.1534(1)	32
	CSe	1.7130	1.7093	1.7093	1.7106(13)	1.70981(6)	
N_2O	NN	1.1304	1.1297	1.1288		1.1273	33
	NO	1.1877	1.1857	1.1874		1.1851	
CO_2	CO	1.1620	1.1613	1.1613		1.1600	34
FCN	FC	1.2686	1.2632	1.2626		1.2640(7)	35,36
	CN	1.1557	1.1588	1.1591		1.1568(8)	
ClCN	ClC	1.6329	1.631	1.6309		1.6290(24)	3,37
	CN	1.1587	1.159	1.1594		1.1606(28)	
BrCN	BrC	1.7905	1.7891	1.7892	1.7877	1.7888	this work
	CN	1.1581	1.1586	1.1586	1.1576	1.1577	
ICN	IC	1.9943	1.9944	1.9944		1.9921(2)	b
	CN	1.1584	1.1584	1.1584		1.1604(3)	
FBO	FB	1.2848		1.2707			38
	BO	1.2063		1.2153			
ClBO	ClB	1.6855		1.6828	1.6835(13)		39
	BO	1.2044		1.2061	1.2037(19)		
ClBS	ClB	1.6823	1.681	1.6817	1.6803(33)		24
	BS	1.6058	1.606	1.6055	1.6050(35)		
BrBS	BrB	1.8345	1.8312	1.8313	1.8341(29)		40
	BS	1.6058	1.6084	1.6079	1.6049(32)		

a) The r_e structure is from Ref. (41) and the rotational constants are listed in Table VIII.

b) The r_e structure is from Ref. (9) and the rotational constants from Refs. (42, 43).

Table VII. Comparison of the r_o, $r_{\varepsilon,I}$, r_s, r^{ρ}_m and r_e Structures (Å) for Heavy Atom Linear Triatomic Molecules.

Species			B_0(MHz)	Ref.
16	12	32	6081.492121 (16)	44
16	12	33	6004.91536 (57)	45
16	12	34	5932.833838 (68)	41
16	12	36	5799.69204 (37)	46
16	13	32	6061.924003(240)	41
16	13	33	5984.56325 (48)	46
16	13	34	5911.73314 (21)	46
17	12	32	5883.67237 (26)	46
18	12	32	5704.856854(125)	41
18	12	34	5559.96722 (46)	46
18	13	32	5691.069 (5)	46
18	13	34	5544.864 (20)	46

Table VIII. Ground State Rotational Constants (MHz) for OCS.

Parent Molecule	z(Br)[a]	z(C)[a]	z(N)[a]	$\Sigma m_i z_i$ [b]	r(CBr)	r(CN)	r(BrN)
79-12-14	0.597 9 (8)	1.191 2 (4)	2.349 8 (2)	0.010 6	1.789 1 (9)	1.158 6 (5)	2.947 7 (9)
79-13-14	0.609 2 (8)	1.179 9 (4)	-	-	1.789 1 (9)	-	-
79-12-15	0.620 0 (8)	-	2.327 6 (2)	-	-	-	2.947 7 (8)
81-12-14	0.586 7 (9)	1.202 4 (4)	2.360 9 (2)	0.014 6	1.789 1 (9)	1.158 6 (5)	2.947 6 (9)
81-13-14	0.597 9 (8)	1.191 2 (4)	-	-	1.789 1 (9)	-	-
81-12-15	0.608 6 (8)	-	2.339 1 (2)	-	-	-	2.947 7 (8)
Average					1.789 1	1.158 6	2.947 7
Range					7.10^{-5}	5.10^{-6}	6.10^{-5}

a) The uncertainties on the coordinates were calculated using the empirical relation of Costain $\sigma(z) = \frac{K}{z}$ (21) with K = 0.0005 uÅ^2 as suggested by Van Eijck (22).
b) in uÅ.

Table IX : Substitution structure (Å) for BrCN.

Molecule	r_e(C≡N)	Ref.	eqQ(^{14}N)	Ref.
HCN	1.15321(5)	47	-4.70783(6)	50
FCN	1.1568(8)	35	-2.67 (5)	51
ClCN	1.1606(28)	3	-3.6228 (9)	52
BrCN	1.1577(69)	a	-3.78 (2)	6
ICN	1.1604(3)	9	-4.0816(15)	42
CNCN	1.1581(5)	48	-3.7811 (3)	53
CH_3CN	1.1558	49	-4.2253 (7)	54

a) This work.

Table X. r_e(C≡N) Bond Lengths (Å) and ^{14}N Nuclear Quadrupole Coupling Constants (MHz) in some Nitriles.

species	B_0(parent)	B_0(^{13}C)	B_0(^{15}N)	r_s(CN)	r_s-r_e g	r_e(CN)
^{35}ClCN	5970.820(10)[a]	5939.775(30)[b]	5748.061(30)[b]	1.1591(7)	-0.0001	1.1592
^{79}BrCN	4120.22307(59)[c]	4073.3897(22)[c]	3944.8420(30)[c]	1.1586(4)	0.0006	1.5180
ICN	3225.548495(30)[d]	3177.0419(16)[e]	3082.67943(13)[f]	1.1584(3)	-0.0010	1.1594

Rotational constants in MHz.
a) Ref. (37). b) Ref. (3). c) This work. d) Ref. (42). e) Ref. (9). f) Ref. (43).
g) Calculated with Eq. (11).

Table XI. Corrected r_s Structure (Å) of ClCN, BrCN, and ICN.

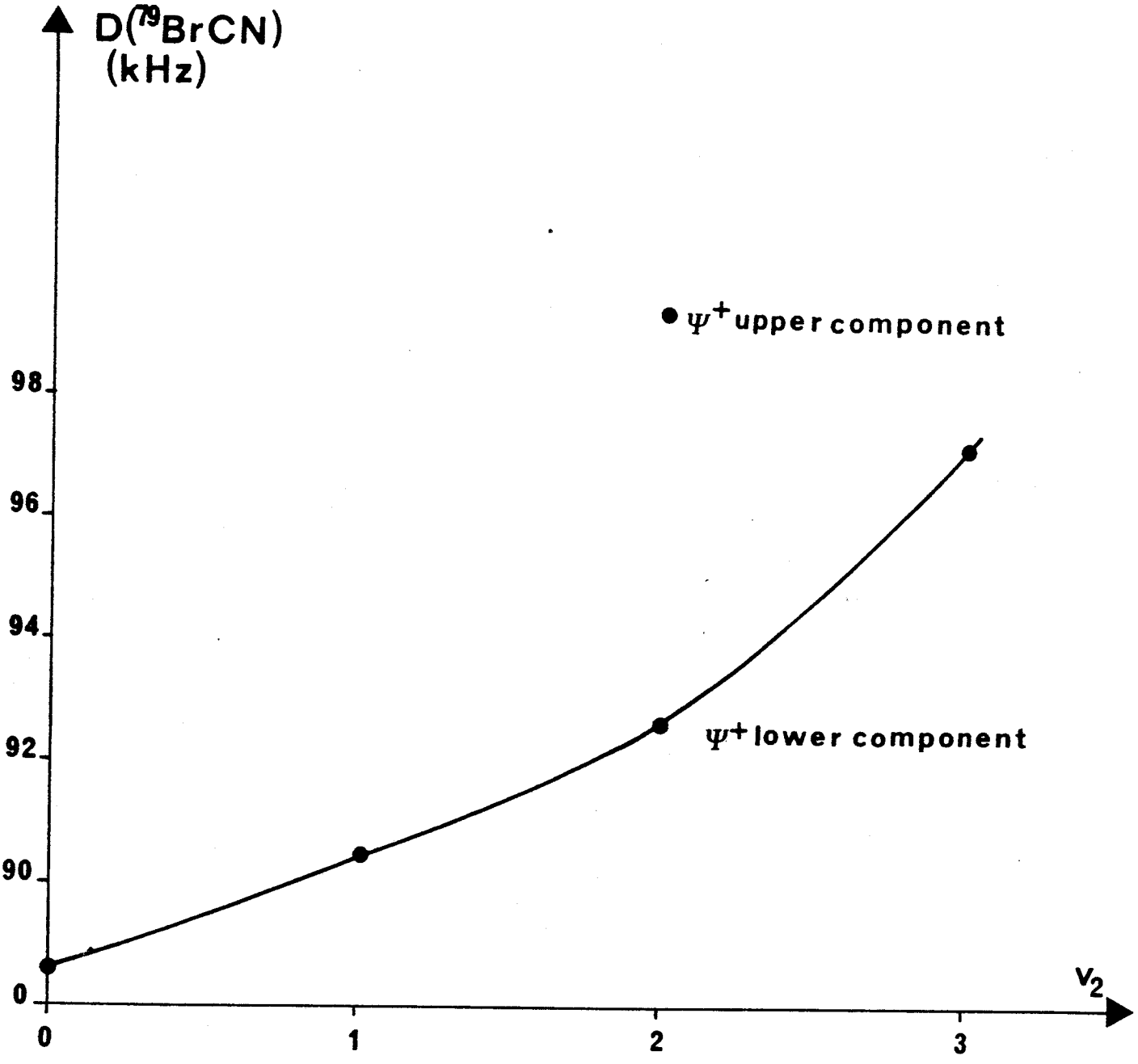

Fig. 1 Plot of D(^{79}BrCN) versus the vibrational quantum number v_2.

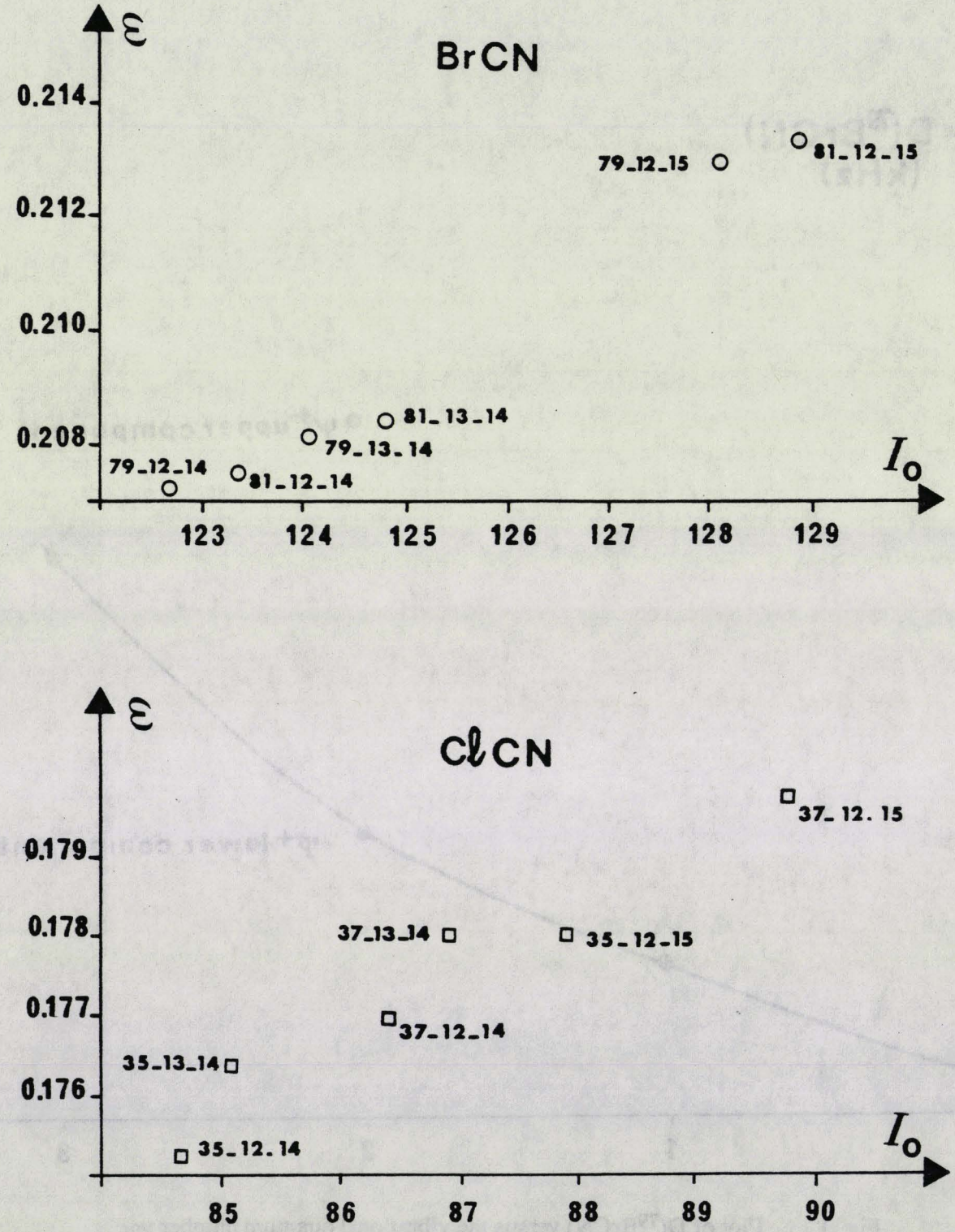

Fig. 2 Plot of $\varepsilon = I_o - I_e$ versus I_o for BrCN and for ClCN (ε and I in uÅ^2).

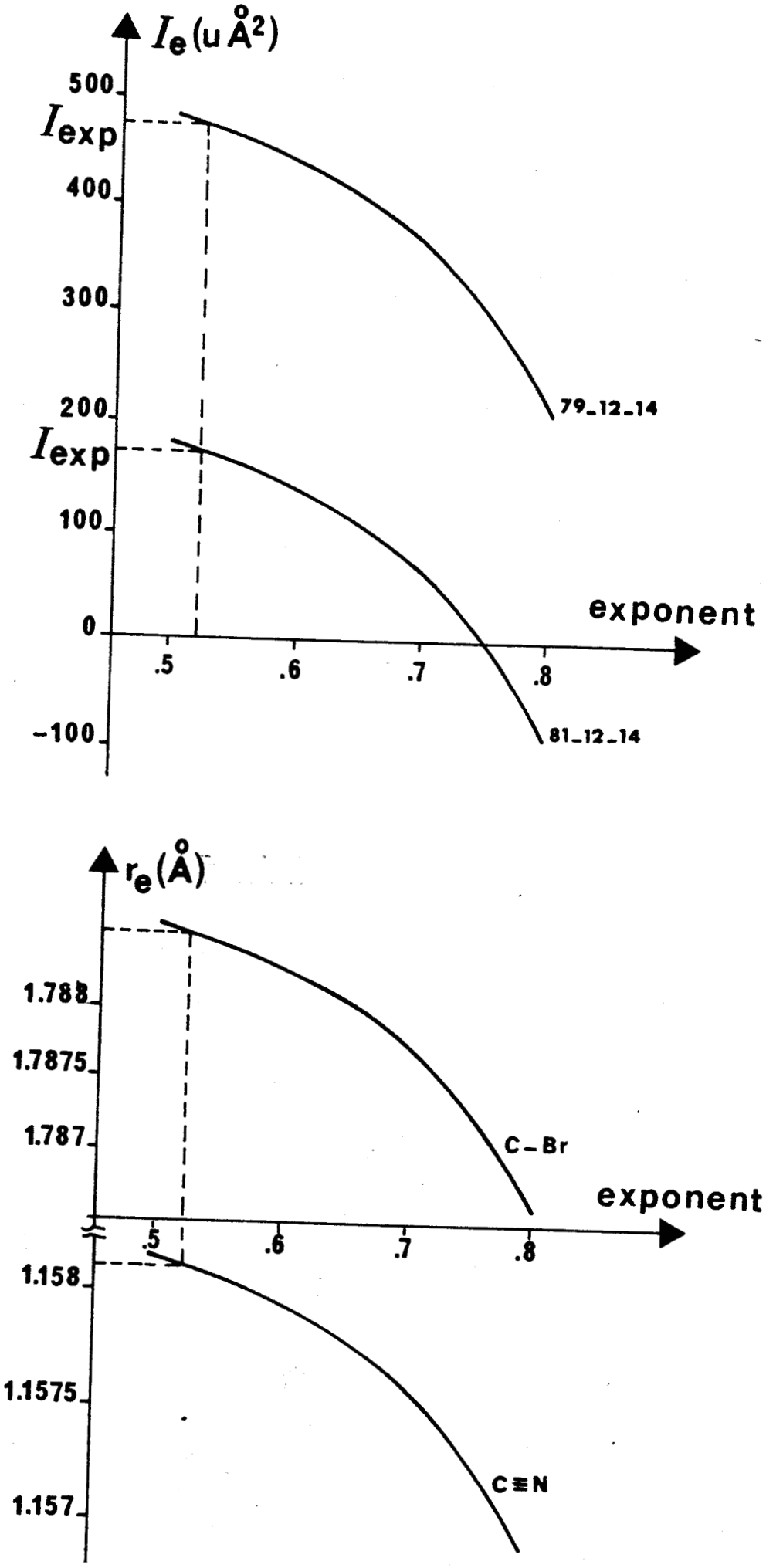

Fig. 3 Plot of I_e, r(C≡N) and r(C-Br) versus n, the exponent in $\varepsilon = kI_o^n$.

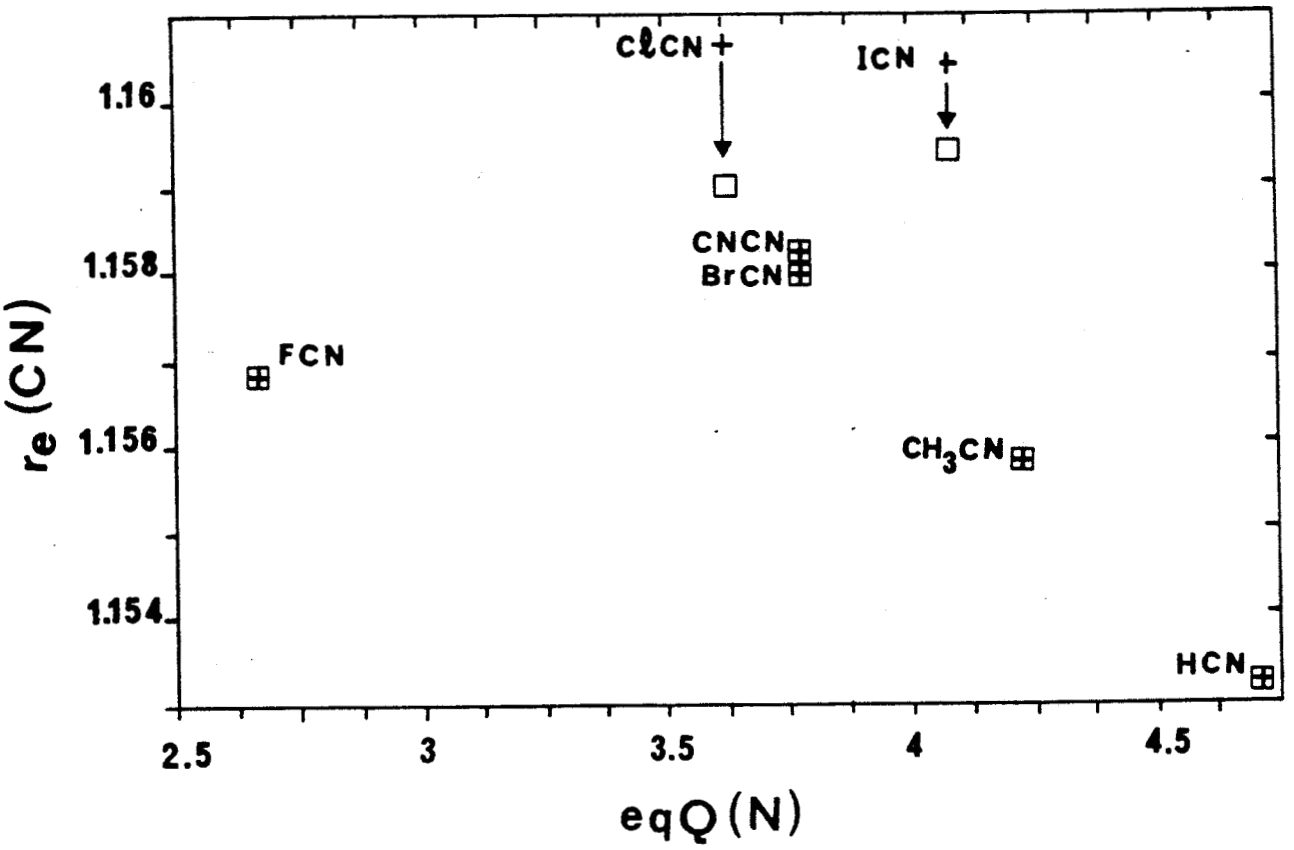

Fig. 4 Plot of r_e(C≡N) (Å) versus eqQ(^{14}N) (MHz).

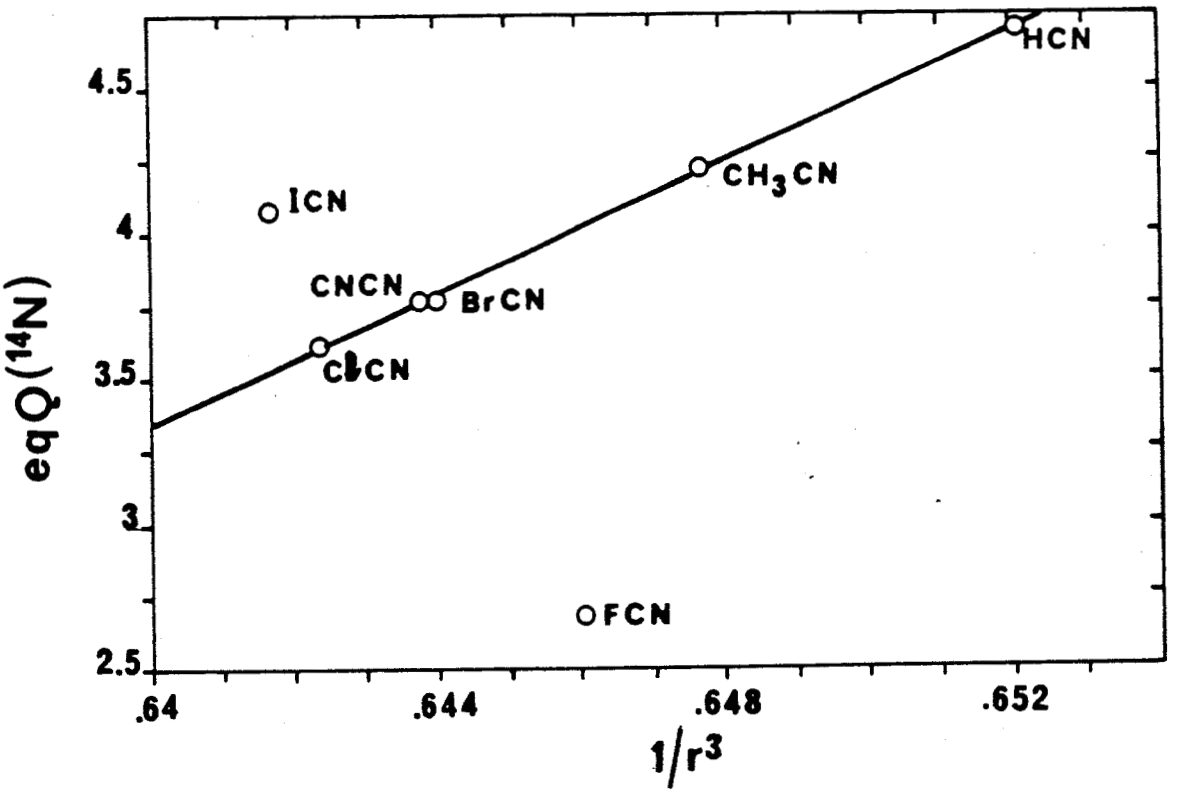

Fig. 5 Plot of eqQ(^{14}N) (MHz) versus $1/r^3_{C\equiv N}$ (Å^{-3}).

1.2. Etat fondamental et structures géométriques du séléniure de carbonyle

Projet de publication :

Nous avons déterminé la constante de rotation B et la constante de distorsion centrifuge D de 27 isotopomères dans leur état fondamental afin de calculer les distances r_0, $r_{\varepsilon,I}$, r_s, r_{ss} et r_m^{ρ}.

Le grand nombre d'isotopomères étudiés nous a permis de faire une étude critique de chaque structure et de déterminer une structure très proche de la structure r_e.

ABSTRACT

The rotational spectrum of OCSe has been measured in the millimeterwave and submillimeterwave ranges. The ground state rotational constants of 27 isotopomers have been accurately determined. r_0, r_s, $r_{\varepsilon,I}$, r_m^{ρ} and r_e structures have been calculated and compared.

INTRODUCTION

The rotational spectrum of OCSe (carbonyl selenide) has been relatively little studied, probably because it is an unstable molecule. However it is a very interesting molecule from the point of view of structure determination because it is a linear heavy-atom triatomic molecule which has many isotopic species. The determination of its equilibrium structure is a tractable problem and it is an ideal probe to test various procedures of structure determination.

The microwave spectrum of OCSe was first studied by Strandberg and coll. (**49Str**) and later by Morino and Matsumura (**67Mor**). The equilibrium structure was calculated by Maki and coll. (**77Mak**) who could determine the equilibrium rotational constant of OCSe enriched in ^{18}O. Recently we have reported preliminary values of the rotational constants of OCSe which were used to analyze the vibrational fundamentals ν_2 and ν_3 from high resolution Fourier Transform spectra (**91Bur**). Other analyzes of the high resolution infrared spectra have been limited to the ν_1 fundamental and the $\nu_1 + \nu_3$ combination bands (**77Mak**, **88Sue**, **87Sug**).

This paper deals mainly with the analysis of the ground state rotational spectra of many isotopic species, the ultimate goal being to obtain a reliable structure using only ground state rotational constants. Ground state constants are indeed much easier to obtain than excited state constants. Furthermore, even when it is possible to determine all the needed excited state constants, the derived r_e structure is not always accurate because some interactions have not been properly taken into account. The recent case of HCO^+ (**91Bot**) is a striking example. A forthcoming paper will report the analysis of the high resolution infrared spectra and of the rotational spectra in excited vibrational states and the derivation of a new equilibrium structure.

ANALYSIS OF THE SPECTRA

The measured transitions are listed in Table I. For the least abundant isotopic species the assignment was not straightforward because the spectrum is very crowdy due to the low lying excited states and to the numerous isotopic species. However the rotational constants of unknown isotopic species could be accurately predicted and the assignment could be confirmed thanks to the structure calculation. The method is detailled in the section devoted to the structure determination. A weighted least-squares program was used to fit the experimental frequencies to the parameters of the following equation:

$$\nu = 2B(J + 1) - 4D(J + 1)^3 \qquad (1)$$

The derived constants are listed in Table II. The previously measured transitions which are gathered in Ref. (**78Lov**) has also been included into the fit. It may be noted that the measurements of Ref. (**56Bur**) are affected by a systematic deviation . However they have no significant influence on the fit because their weight is very low. It has been sometimes noticed that the constants determined by different analyses do not agree within 3σ (standard deviations). If there is no error, neither in the assignment of the spectra, nor in the measurements of the frequencies, the most probable cause of error is due to the neglect of higher order terms in the rotational Hamiltonian. To check this point, we have used our submillimeter-wave superheterodyne spectrometer (**89Bou**) to measure an high-J line for the two isotopic species: $OC^{76}Se$ and $OC^{80}Se$. This allows us to determine the sextic centrifugal distortion constant H, see Table III. We see that the inclusion of the sextic term may alter the rotational constant B of more than 5σ. In conclusion, the systematic error due to the neglect of higher order terms is significantly greater than the standard deviation. However this systematic deviation is nearly constant for all isotopomers (insofar as the same J values have been used in the least-squares fits), so it almost vanishes when differences of constants are used (in the calculation of the r_s structure for instance).

As the quartic centrifugal distortion constant D has been accurately determined for many isotopic species, it may be interesting to see if this constant complies with a simple law of variation. It is expected that D should vary roughly like B^2 (**76Dem**). Indeed a plot of D in function of B^2 nearly gives a straight line with a very high correlation coefficient: ρ = 0.998. A linear least-squares fit gives:

$$D = -55.0(84) + 44.99(55)B^2 \qquad (2)$$

with D in Hz and B in GHz. The standard deviation of the fit, 3 Hz is much greater than the experimental accuracy which is never worse than 0.5 Hz. Nevertheless Eq. (2) is very useful to help, first in the prediction of the spectra and then, in their assignment. It is also interesting to use as independent variables the masses of the three atoms forming the molecule. The result of the fit is:

$$D(Hz) = 1876(14) - 51.52(35)m_O - 5.62(66)m_C - 3.94(13)m_{Se} \qquad (3)$$

where m_O, m_C and m_{Se} are the atomic masses of O, C and Se respectively, expressed in u. The standard deviation of the fit is slightly better: 1.6 Hz, but still worse than the experimental accuracy, indicating that Eq. (3) is only an approximation. Of course, it is easy to improve the fit by more terms (like m_O^2, $m_O m_C$, ...) into Eq. (3), but this equation then becomes too complicated to remain useful.

Structure of OCSe

r_e structure

The equilibrium structure is the reference structure which is used for testing all approximate methods of structure determination. The r_e structure of OCSe has been previously determined by Maki and coll. (**77Mak**). As we have at our disposal more accurate rotational constants, as well for the ground state (Table II) as for the excited states (**88Sue**, **91Bur**) it is possible to slightly refine this r_e structure. The results are given in Table IV. They are in very good agreement with those of Maki and coll. (**77Mak**).

r_0 and $r_{\varepsilon,I}$ structures

We have accurately determined 27 different ground state moments of inertia for OCSe (Table II). It is possible to calculate an effective structure (r_0) by using a non-linear least-squares method. The assumption of this method is the basic least-squares one, i.e. the rotation-vibration parameters $\varepsilon = I_0 - I_e$ behave like a random variable and have a mean of zero. The same weight is assigned to all moments of inertia because the main cause of error does not come from the uncertainty of the rotational constants but from ε which is significantly different from zero. The result of the calculation is given in Table IV. The standard deviations of the parameters are rather small ($< 10^{-3}$ Å). However the reduced standard deviation of the fit σ = 0.00455 uÅ^2 is much too high compared to the experimental uncertainty of the moments of inertia ($0.1 \cdot 10^{-4}$ to $0.8 \cdot 10^{-4}$ uÅ^2) and an analysis of the residuals shows that the chosen model is indeed incorrect: there is a strong correlation between the residuals and either the moment of inertia or the masses of the atoms. See Figs. 1 and 2. This unsatisfactory result was of course expected because it is well known that when the ε are neglected, it introduces a systematic error which is many orders of magnitude greater than the experimental errors (**74Schw**).

For a heavy-atom molecule like OCSe, it is easy to significantly improve this method by supposing that rotation-vibration parameter ε is a constant independent of the particular isotopomer. This gives what Rudolph has named the $r_{\varepsilon,I}$ structure (**91Ru**, **92Leg**). For instance, for OCSe, there are now three independent variables in the least-squares fit: r(CO), r(CSe) and ε. For diatomic molecules, the $r_{\varepsilon,I}$ structure is identical to the r_s structure derived from Kraitchman's equations. But as stated by Rudolph, for polyatomic molecules with large and complete collections of isotopomers, the $r_{\varepsilon,I}$ structure is preferable to a true Kraitchman-type method, particularly when near-axis atoms are present. It has already been shown (**92Leg**) that this method gives good results for triatomic linear molecules, even when an atom is near the center of mass (like N_2O and CO_2) or when an atom has no isotope (for instance FCN and ICN), or is difficult to substitute. The derived $r_{\varepsilon,I}$ structure for OCSe is also given in Table IV. The value found for ε is: ε =

0.1826(77) uÅ^2. When ε is determined by the empirical formula of Demaison and Nemes (**79Dem**):

$$\log \varepsilon = 1.247 \log I_0 - 2.651 \qquad (4)$$

it gives $\varepsilon \approx 0.12$, which is indeed of the same order of magnitude. The standard deviation drops to 0.00094 uÅ^2 (instead of 0.00455 uÅ^2), which is much better, but still too high. This too was expected because the analysis of the residuals (Fig. 1) shows that a linear term is still missing in the model. Ideally one should have to fit the I_0 to an expression of the type:

$$I_0 = Ie + \varepsilon_0 + \sum_i \frac{\partial \varepsilon}{\partial m_i} \Delta m_i + \ldots \qquad (5)$$

where i = O, C, Se

This expression should give a very good approximation of the r_e structure because the Δm_i are only a small fraction of the corresponding atomic masses. However, in the particular case of OCSe, this method fails because the normal least-squares equations are ill conditioned and it is not possible to independantly determine the three $\partial\varepsilon/\partial m_i$. If $\partial\varepsilon/\partial m_C$ is kept fixed at zero, a very good fit is obtained but the derived structure is affected by an unknown systematic error, and, in fact, it happens to be far from the r_e sructure. It is however possible to solve this problem by taking into account a constraining relation between the derivatives. As noticed by Watson (**73Wat**) ε is an homogeneous fonction of degree 1/2 of the masses. Application of Euler's theorem gives:

$$\sum_i m_i \frac{\partial \varepsilon}{\partial m_i} = \frac{\varepsilon}{2} \qquad (6)$$

The number of independent parameters is reduced to five and the least-squares problem becomes again soluble. The derived structure is given in Table IV and the derivatives in Table V. It is important to note that $\partial\varepsilon/\partial m_{Se}$ is much smaller than the other two derivatives and that $\partial\varepsilon/\partial m_C$ is negative. The standard deviation of the fit drops to 0.00018 uÅ^2, i.e. nearly an order of magnitude less than for the $r_{\varepsilon,I}$ structure (0.00094 uÅ^2). However the standard deviations of the bond lengths are relatively high: about 0.002 Å. It is due to the fact that five parameters have to be determined and that the problem is still not well conditioned, particularly the correlations between the parameters are extremely high. It is worth to note that the rotational constants of the $^{18}O^{13}CSe$ species are necessary to be able to determine these five parameters. To obtain a better fit, it would be necessary to reduce the number of parameters or to have a broader variety of data, but neither way is easy.

It was possible to obtain a near-equilibrium structure for ClCN and BrCN by assuming that ε varies like I^n with $n \approx 0.5$ (**92Leg**). It is tempting to try that method on OCSe. But the resulting fit is not satisfactory: the standard deviation of the fit is not smaller

than that of the $r_{\varepsilon,I}$ structure and the derived parameters (r(CO) = 1.1553(14) Å, r(CSe) = 1.7082(22) Å and ε = 0.358(15) uÅ^2 with $^{16}O^{12}C^{80}Se$ as parent species) are not significantly nearer from the r_e structure. This failure is easy to understand if we plot ε versus I. Although ε increases with I when O or Se are substituted, it decreases with I when the central atom C is susbstituted, see Fig. 1. Similar results are obtained for the similar molecules OCS, N_2O and CO_2. It is due to the fact that $\partial\varepsilon/\partial m_C < 0$ (C = central atom) for these molecules. However the ε of these XYZ molecules shows a very interesting behaviour. If we plot ε versus $m_X m_Z/M$ (m_X = mass of atom X, m_Z = mass of atom Z, and M = total mass of the molecule), we obtain a straight line, see Fig. 3. So, for OCSe (and the similar molecules OCS, N_2O and CO_2), it is possible to accurately calculate the structure using the following relation:

$$I_o(\text{exp.}) = I_e[r(CO),\ r(CSe)] + \varepsilon_o + k\,\frac{m_X m_Z}{M} \qquad (7)$$

This is equivalent to relax the condition: r(OSe) = r(OC) + r(CSe) in the calculation of the moment of inertia. The derived distances are listed in Table IV and the values of the two remaining parameters are: ε_o = 0.17397(86) uÅ^2 and k = 0.02757(62) uÅ^2. The standard deviation of the fit is still lower: 0.000103 uÅ^2. The system is better conditioned and there is only one correlation coefficient greater than 0.9 instead of six with Eqs. (5) and (6). Eq. (7) was found very powerful to predict with accuracy the moments of inertia of isotopic species and to check the assignment.

Substitution structure (r_s)

It is interesting to compare the $r_{\varepsilon,I}$ structure with the r_s structure derived from Kraitchman's equations (**58Cos**). As the rotational constant B has been determined accurately for 27 different isotopic species, it is possible to calculate the substitution coordinates in many different ways. The atomic cartesian coordinates for the different $OC^{80}Se$ species are given in Table VI. The derived interatomic distances are also given in this Table and their arithmetic mean, standard deviation and range (greatest value minus lowest value) are listed in Table IV. The standard deviation of the mean is extremely low: 10^{-5} Å. It is to be noted that it is in good agreement with the value calculated from the standard deviations of the rotational constants using the law of propagation of errors: $0.5\cdot10^{-5}$ Å. However the range, which is here about five times the standard deviation, is probably a better indicator of the internal consistancy of the r_s structure.

The least accurate coordinate is that of C because it is near the center of mass and it is the lightest atom (it has also the smallest change of mass upon isotopic substitution). If we use the proposition of Van Eijck (**66Cos**, **82Van**) to estimate the error for z(C):

$$\sigma(z) = \frac{0.0005}{|z|} \qquad (8)$$

we find $\sigma(z_C) = 5 \cdot 10^{-4}$ Å. It is still an order of magnitude higher than the range, but it is an upper limit and shows that the r_s structure of OCSe is very accurate. It may also be noted that $r_s(OSe) = 2.86567$ Å is in very good agreement with the sum $r_s(CO) + r_s(CSe) = 2.86569$ Å. If we compare the r_s and $r_{\varepsilon,I}$ structures, we see that they are compatible within 2σ:

$$r_s(CO) - r_{\varepsilon,I}(CO) = 0.00038(22) \text{ Å}$$
$$r_s(CSe) - r_{\varepsilon,I}(CSe) = -0.00015(23) \text{ Å}$$

It is possible to estimate the accuracy of the r_s structure by using the first-moment equation: $\Sigma m_i z_i$ which should be equal to zero for equilibrium coordinates and whose value remains near 0.025 uÅ for all the isotopomers studied. This value is rather low, but of the right order of magnitude when compared to other similar molecules (for instance: 0.033 uÅ for OCS (**84Gor**)). The error in the coordinates may be estimated by the following formula:

$$\delta z_j = \sum_i \frac{m_i z_i}{m_j} \qquad (9)$$

It is smaller than $2 \cdot 10^{-3}$ Å.

A basic assumption of the r_s structure is that the interatomic distances remain constant by isotopic substitution. In fact it is well known that this assumption is not exactly fulfilled., and OCSe is a propitious molecule to check it because it has many isotopomers. Indeed it seems that the coordinate $z_s(Se)$ decreases as $\Delta m = m_{Se}(\text{daughter}) - m_{Se}(\text{parent})$ increases. See Fig. 4 where $z_s^2(Se)$ is plotted in function of $\Delta m(Se)$ for the different parent species containing ^{80}Se. Similar patterns are obtained when the other species are used as parents. This decrease is of same order of magnitude as the standard deviation $\sigma(z_{Se}) \approx 0.5 \cdot 10^{-5}$ Å, calculated using the law of propagation of errors with the standard deviations of the rotational constants as input data. It seems nevertheless to be real because it occurs for nearly all species. The $^{16}O^{12}C^{74}Se$ species is clearly an outlier. It could probably be explained by the fact that this species is the least abundant one, so its lines are weak and the derived rotational constants are not as accurate as for the other species. In fact it is enough to increase $B(^{16}O^{12}C^{74}Se)$ by 1.1 kHz to obtain a consistent result The case of the ^{78}Se species is more puzzling, because its representative point (on Fig. 4) is always too high. It is difficult to admit that the rotational constants of all the different ^{78}Se species have all been determined with a similar systematic error. Moreover we have tried to determine the rotational constants using different selection of lines and, in all cases, we have found

compatible results. A possible explanation could be that m(^{78}Se) is affected by a small error (about $0.5 \cdot 10^{-6}$ u). But the hypothesis of a small error on B cannot be excluded.

On the other hand the variation of z_s^2(Se) with Δm may be interpreted easily using the theory of the r_m structure of Watson (**73Wat**). Retaining Watson's notations, it is easy to show that (**90Dem**, **91Leg**):

$$[z_s(i)]^2 = [z_e(i)]^2 + \frac{\partial \varepsilon}{\partial m_i} + \left[\frac{1}{2}\frac{\partial^2 \varepsilon}{\partial m_i^2} + M^{-1}\frac{\partial \varepsilon}{\partial m_i}\right]\Delta m_i \qquad (10)$$

A linear least-squares fit allows us to determine for each isotopomer k the value:

$$p_k = \left[\frac{1}{2}\frac{\partial^2 \varepsilon}{\partial m_i^2} + \frac{1}{M_k}\frac{\partial \varepsilon}{\partial m_i}\right] \qquad (11)$$

Although the M^{-1} dependence of p_k may be pointed out, the values of p_k are not accurate enough to determine separately $\partial\varepsilon/\partial m_i$ and $\partial^2\varepsilon/\partial m_i^2$ Instead we have calculated a mean value of $p_k = -1.64(51) \cdot 10^{-6}$ u^{-1}Å^2, and we have used the $\partial\varepsilon/\partial m_i$ (i = Se) value of Table V to calculate $\partial^2\varepsilon/\partial m_i^2 \approx -9.4 \cdot 10^{-6}$ u^{-1}Å^2. Although this result is very inaccurate, it is interesting to note that: $(\partial\varepsilon/\partial m_i)/(\partial^2\varepsilon/\partial m_i^2) \approx -70$, i.e. about the value of m_{Se}. Differentiation of the empirical Eq. (7) gives a ratio of -54. This indicates that at least the orders of magnitude of the parameters are correct.

Inspection of Table VI does not reveal any trend for $z_s(O)^2$, although $\partial\varepsilon/\partial m_O$ is very large and $\partial^2\varepsilon/\partial m_O^2$ is also expected to be large. It could be explained by the fact that both terms compensate each other in Eq. (11). If that assumption is true, the order of magnitude of $\partial^2\varepsilon/\partial m_O^2$ may be easily estimated: -0.0002 u^{-1}Å^2. It gives: $(\partial\varepsilon/\partial m_O)/(\partial^2\varepsilon/\partial m_O^2) \approx -54$ in perfect agreement with the differentiation of empirical Eq. (7).

To first order the relation between the cartesian substitution and equilibrium coordinates is (**73Wat**) :

$$z_s^2(i) \approx z_e^2(i) + \frac{\partial \varepsilon}{\partial m_i} \qquad (12)$$

The equilibrium structure being known, it is possible to estimate independently the $\partial\varepsilon/\partial m_i$ thanks to Eq. (12). The results are given in Table VI. They are in satisfactory agreement with the values obtained from the least-squares fit of Eq. (5). The value of ε calculated by application of Euler's theorem (Eq. (6)): 0.337 uÅ is also in fair agreement.

As the derivatives $\partial\varepsilon/\partial m_i$ have been determined, it is possible to discuss more extensively the r_s structure. Eq. (12) leads to:

$$r_s(OC) = r_e(OC) + \frac{1}{2|z_O|}\frac{\partial \varepsilon}{\partial m_O} - \frac{1}{2|z_C|}\frac{\partial \varepsilon}{\partial m_C} \qquad (13a)$$

$$r_s(CSe) = r_e(CSe) + \frac{1}{2|z_C|}\frac{\partial\varepsilon}{\partial m_C} + \frac{1}{2|z_{Se}|}\frac{\partial\varepsilon}{\partial m_{Se}} \qquad (13b)$$

$$r_s(OSe) = r_e(OSe) + \frac{1}{2|z_O|}\frac{\partial\varepsilon}{\partial m_O} + \frac{1}{2|z_{Se}|}\frac{\partial\varepsilon}{\partial m_{Se}} \qquad (13c)$$

From the sign of the derivatives, it may be deduced immediately that: $r_s(OC) > r_e(OC)$ and $r_s(OSe) > r_e(OSe)$. It is even possible to calculate the correction terms in Eqs. (13). Using the values of Table V (first column), one obtains:

$r_s(OC) - r_e(OC) = 0.0048$ Å (experimentally: 0.0031 Å) (14a)
$r_s(CSe) - r_e(CSe) = -0.0017$ Å ((experimentally: -0.005 Å) (14b)
$r_s(OSe) - r_e(OSe) = 0.0030$ Å (experimentally: 0.0030 Å) (14c)

The corrections are indeed of the right order of magnitude although they a little bit too high (in absolute value). It may be due, either to the inaccuracy of the r_e structure, or to the neglect of higher order terms in Eq. (12), which are known to be often non negligible (**78Smi**, **90Dem**, **91Leg**). Starting from Eq. (12) it is also possible to interpret the non-zero value of the first-moment relation:

$$\sum_i m_i z_s(i) = \frac{m_O}{2|z_O|}\frac{\partial\varepsilon}{\partial m_O} + \frac{m_C}{2|z_C|}\frac{\partial\varepsilon}{\partial m_C} - \frac{m_{Se}}{2|z_{Se}|}\frac{\partial\varepsilon}{\partial m_{Se}} \qquad (15)$$

Using the values listed in Table V, it gives S = 0.030(9) uÅ, a result compatible with the experimental value 0.025(3) uÅ. It may be tempting to use Eq. (15) as constraint (together with Eq. (6)) to obtain a better conditioned least-squares fit by the determination of the parameters of Eq. (7). But, as the higher order terms in the expansion of ε (Eq. (5)) have been neglected, it induces a large systematic error.

Examination of Table VI shows that the substitution distances are significantly different for the ^{16}O and the ^{18}O species. This behaviour may also, at least semi-quantitatively, be explained by using Eq. (13). It gives:

$\Delta r_s(OC)_{\{16\text{-}12\text{-}80 - 18\text{-}12\text{-}80\}} = -0.00014$ Å (experimentally: -0.00029 Å) (16)
$\Delta r_s(CSe)_{\{16\text{-}12\text{-}80 - 18\text{-}12\text{-}80\}} = 0.00012$ Å (experimentally: 0.00030 Å) (17)

This variation with the parent species is explained only by the variation of the cartesian coordinates by the substitution $^{16}O \rightarrow {}^{18}O$ (the center of mass is nearer O -and so farther Se- for the $^{18}OCSe$ species). The above discussion remains valid to explain the differences between the calculated and the experimental values (Eqs. (17) and (18)). Two important conclusions may be drawn from this discussion:

i) although O is the farthest atom from the center of mass, its substitution coordinate is the less accurate (because $\partial\varepsilon/\partial m_O$ is the largest derivative), in contradiction with Eq. (8).
ii) the substitution coordinates calculated with ^{16}OCSe as parent species are more accurate than those calculated with ^{18}OCSe as parent species, although this latter species is heavier.

Double substitution structure

OCSe is also a good molecule to test the double substitution structure because we have accurately determined the rotational constants of many doubly substituted isotopic species. It is possible to calculate the bond lengths directly, without recourse to cartesian coordinates by using a method due to Watson and first worked out by Kirby and Kroto (**80Kir**). The double substitution bond length is calculated from the following equation:

$$\Delta m_1 \Delta m_2 r_{ss}^2 = MI - M_1^{**} I_1^{**} - M_2^{**} I_2^{**} + M_{12}^{****} I_{12}^{****} \qquad (18)$$

where M and I are the total mass and moment of inertia, respectively of the parent molecule, subscripts refer to species substituted at the number positions and Δm_i is the change in mass on substituting the ith atom. The number of asterisks indicates the number of substitutions. The results are presented in Table IV. Although the range of the r_{ss}(C=Se) and r_{ss}(O=Se) lengths is rather large, they are in better agreement with the r_e values than the r_s values. On the other hand, the r_{ss}(C=O) value is clearly unacceptable because it is very different from the other values. This result, at first sight surprising, may be easily explained by the fact that Eq. (18) is not well conditioned. Indeed $\partial r(CO)/\partial B \approx 0.7$ mÅ/Hz, and a very small cross-term like $\partial^2\varepsilon/\partial m_O \partial m_C$ is enough to explain the discrepancy. Starting from Eqs. (5) and (18) we find:

$$r_{ss}(12) \approx r_e(12) + \frac{1}{2r_e(12)}\left(\frac{\partial\varepsilon}{\partial m_1} + \frac{\partial\varepsilon}{\partial m_2} + M_{12}^{**}\frac{\partial^2\varepsilon}{\partial m_1 \partial m_2}\right) \qquad (19)$$

Using the $\partial\varepsilon/\partial m_O$ and $\partial\varepsilon/\partial m_C$ derived previously (Table V) and the difference r_{ss}(OC) - r_e(OC) = -0.0112 Å, we find $\partial^2\varepsilon/\partial m_O \partial m_C \approx -0.0003$ u^{-1}Å^2, i.e. 38 times smaller than $\partial\varepsilon/\partial m_O$, which is plausible. r_{ss}(CSe) and r_{ss}(OSe) are nearer the equilibrium structure because the cross-terms $\partial^2\varepsilon/\partial m_C \partial m_{Se}$ and $\partial^2\varepsilon/\partial m_O \partial m_{Se}$ are much smaller (differentiation of Eq. (7) can give a rough indication of their value).

Using the double substitution method as described by Pierce (**59Pie**) should give better results because the first order derivatives $\partial\varepsilon/\partial m_i$ disappear and the cross-term $\partial^2\varepsilon/\partial m_i^2$ is not multiplied by M. Indeed the double difference of the moments of inertia may be written:

$$\Delta\Delta I_o = I - I_1^{*} - I_2^{*} + I_{12}^{**} = \Delta\Delta I_e + \frac{\partial^2\varepsilon}{\partial m_1 \partial m_2}\Delta m_1 \Delta m_2 \qquad (20)$$

Application of this latter method gives a much more reasonable value for $r_{ss}(CO)$ = 1.15422 Å. The difference between this value and the r_e value allows us to estimate the cross-term: $\partial^2\varepsilon/\partial m_O \partial m_C \approx$ -0.000015 $u^{-1}Å^2$. This latter value is an order of magnitude smaller than that found by using Eq. (19). It shows the limits of the method and the importance of the approximations made.

r^{ρ}_{m} structure

It is quite easy to calculate an r^{ρ}_{m} structure (**86Har**, **88Har**) which is an approximation of the r_m structure (and therefore of the r_e structure). According to Harmony and Taylor (**86Har**) an I^{ρ}_{m} moment of inertia is defined for b isotopic species by:

$$\left[I^{\rho}_{m}\right]_{\alpha} = (2\rho - 1)\,[I_0]_{\alpha} \qquad \alpha = 1 \ldots b \qquad (21)$$

with $$\rho = \frac{[I_s]_1}{[I_0]_1}$$

$[I_0]_1$ is the ground state moment of inertia of the parent species and $[I_s]_1$ is the corresponding substitution moment computed from the substitution coordinates. The basic assumption of this method is that ρ remains nearly constant by isotopic substitution. This assumption was checked for several molecules, either by comparing the r^{ρ}_{m} structure with the experimental r_e structure (**86Har**) or by computing the vibration-rotation parameters from the anharmonic force field (**88Har**). OCSe is ideally suited for further testing this assumption. We have calculated ρ for different isotopic forms of OCSe, see Table VII. At first sight the total range of variation of ρ seems rather large: 0.0001. But closer inspection of the values of ρ shows that they are not constant. A simple sign test indicates that the following inequalities hold:

$$\rho(^{16}O^{13}CSe) < \rho(^{16}O^{12}CSe) < \rho(^{18}OCSe) \qquad (22)$$

the difference being the biggest for $\rho(^{18}OCSe)$, see Table VII. On the other hand, the variations within each set (or parent species) are small. For instance the range of variation for the different $^{16}O^{12}CSe$ species is only 0.00002. Furthermore, for $^{16}O^{12}CSe$, there is no significant difference between the two substitution schemes $^{16}O \rightarrow {}^{17}O$ and $^{16}O \rightarrow {}^{18}O$. If the r_e and r^{ρ}_{m} structures are really equivalent, it follows from Eq. (21) that:

$$\rho = 1 - \frac{1}{2}\frac{\varepsilon}{I_o} \qquad (23)$$

so ρ is constant if ε varies like I_o. But Fig. 2 shows that it is not true and Eq. (7) may be used to explain the small variations of ρ.

By convention the r_m^ρ computations use a minimal substitution data set (SDS) where the parent species consists of all the light isotopes (**89Ber**). The I_s and $I_m^\rho = I_m$ moments of inertia are computed according to Watson's method (**73Wat**). The remaining I_m^ρ were computed according to eq. (21). A representative selection of the least-squares derived structures are also given in Table VII. Different combinations have been tried and the results confirm the recommendations of Berry and Harmony (**89Ber**): to obtain reliable results, it is important that all Δm_i (isotopic changes of mass of the atoms) have the same sign (either positive or negative). The Δm_i should also not be too great. It is striking that the r_m^ρ structure is in very good agreement with the r_e structure when the isotopic substitution $^{16}O \rightarrow {}^{17}O$ is used for the calculation of the I_s. On the other hand, the isotopic substitution $^{16}O \rightarrow {}^{18}O$ gives results which are definitely worse, because that substitution induces a so large variation of ε that the assumption ρ = constant does not remain valid. The standard deviations of the derived parameters are rather high (0.002 Å), furthermore the standard deviation of the fit: $\sigma \approx 0.004$ uÅ^2 is very high, especially if we take into account the fact that there are only four input data to calculate two parameters. This indicates that the fit is not very satisfactory. It is probably due to the fact that ε does not vary like kI.

CONCLUSION

The r_0 structure appears to be the worst approximation of the r_e structure, as expected. All the other structures give an accurate value for the r(CSe) distance, but only the r_m^ρ structure is near the r_e structure for the r(CO) distance.

The superiority of the r_m^ρ structure over the pseudo-r_m and near-r_e structures lies in the fact that the r_m^ρ method eliminates the vibrational contribution before calculating the structure. On the other hand the pseudo-r_m and near-r_e methods also determinate, at least approximately, the vibrational contribution. Inspection of the correlation coefficients shows that the r(CO) distance is highly correlated with the vibrational term(s). For instance ρ(r(CO), k) = -0.987. So a small variation of the vibrational correction is sufficient to explain the change of the r(CO) distance.

In conclusion, the best approximation for the r_e structure is the r_m^ρ structure.

REFERENCES

49Str M.P.W. STRANDBERG, T. WENTINK, AND A.G. HILL, Phys.Rev. **75**, 827-832 (1949).

56Bur C.A. BURRUS AND W. GORDY, Phys. Rev. **101**, 599-602 (1956).

58Cos C.C. COSTAIN, J. Chem. Phys. **29**, 864-874 (1958).

59Pie L. PIERCE, J. Mol. Spectrosc. **3**, 575-580 (1959).

66Cos C.C. COSTAIN, Trans. Amer. Crystallogr. Assoc. **2**, 157-164 (1966).

67Mor Y. MORINO AND C. MATSUMURA, Bull. Chem. Soc. Japan **40**, 1101-1104 (1967).

73Wat J.K.G. WATSON, J. Mol. Spectrosc. **48**, 479-502 (1973).

74Schw R.H. SCHWENDEMAN, "Structural Parameters from Rotational Spectra", in *Critical Evaluation of Chemical and Physical Structural Information*, D.R. Lide and M.A. Paul, Eds., National Academy of Science, Washington, D.C., 1974.

75Fin E.J. FINN AND G.W. KING, J. Mol. Spectrosc. **56**, 39-51 (1975).

76Dem J. DEMAISON, J. Mol. Struct. **31**, 233-236 (1976).

77Mak A.G. MAKI, R.L. SAMS, AND R. PEARSON, J. Mol. Spectrosc. **64**, 452-459 (1977).

78Lov F.J. LOVAS, J. Phys. Chem. Ref. Data **7**, 1445-1750 (1978).

78Smi J.G. SMITH AND J.K.G. WATSON, J. Mol. Spectrosc. **69**, 47-52 (1978).

79Dem J. DEMAISON AND L. NEMES, J. Mol. Struct. **55**, 295-299 (1979).

79Kon K. KONDO, S. YOKOYAMA, N. MIYOSHI, S. MURAI, AND N. SONODA, Angew. Chem. (int. ed.) **18**, 691-691 (1979).

80Kir C. KIRBY AND H.W. KROTO, J. Mol. Spectrosc. **83**, 130-147 (1980).

82Van B.P. VAN EIJCK, J. Mol. Spectrosc. **91**, 348-362 (1982).

84Gor W. GORDY AND R.L. COOK, "Microwave Molecular Spectra", Chap. XIII, p. 693, Wiley, New York, 1984.

86Har M.D. HARMONY AND W.H. TAYLOR, J. Mol. Spectrosc. **118**, 163-173 (1986).

87Sug H. SUGURO, T. KONNO, K. SUEOKA, Y. HAMADA, AND H. UEHARA, J. Mol. Spectrosc. **124**, 46-52 (1987).

88Har M.D. HARMONY, R. BERRY, AND W.H. TAYLOR, J. Mol. Spectrosc. **127**, 324-336 (1988).

88Sue K. SUEOKA, Y. HAMADA, AND H. UEHARA, J. Mol. Spectrosc. **127**, 370-381 (1988).

89Ber R. BERRY AND M.D. HARMONY, Struct. Chem. **1**, 49-59 (1989).

89Bou D. BOUCHER, J. BURIE, J. DEMAISON, J. GADHI, E. MARIAGE, AND G. WLODARCZAK, J. Phys. France **50**, 397-404 (1989).

90Dem J. DEMAISON, G. WLODARCZAK, J. BURIE, AND H. BÜRGER, J. Mol. Spectrosc. **140**, 322-339 (1990).

91Bot P. BOTSCHWINA, 12th Colloquium on High Resolution Molecular Spectroscopy, Dijon, paper H1, 1991.

91Bur H. BÜRGER, M. LITZ, H. WILLNER, M. LE GUENNEC, G. WLODARCZAK, AND J. DEMAISON, J. Mol. Spectrosc. **146**, 220-223 (1991).

91Leg M. LE GUENNEC, W.D. CHEN, G. WLODARCZAK, J. DEMAISON, R. EUJEN, AND H. BÜRGER, J. Mol. Spectrosc. **150**, 493-510 (1991).

91Ru H.D. RUDOLPH, Struct. Chem. **2**, 581-588 (1991).

92Leg M. LE GUENNEC, G. WLODARCZAK, W.D. CHEN, R. BOCQUET, AND J. DEMAISON, J. Mol. Spectrosc. submitted.

J	Freq.	e.- c.	J	Freq.	e.- c.	J	Freq.	e.- c.
	16-12-74		23	194613.750	-0.168	6	56246.470	0.267
2	24574.760	-0.132	24	202719.449	-0.039	11	96418.950	-0.060
17	147433.566	-0.012	26	218929.210	-0.173	14	120520.400	-0.110
24	204747.912	-0.013	42	348533.867	0.005	17	144619.810	-0.031
42	352020.026	0.003	43	356628.861	0.009	18	152652.419	0.025
43	360195.914	0.027	44	364723.134	0.012	20	168716.410	-0.158
44	368370.993	-0.023	45	372816.668	0.013	23	192810.170	-0.089
45	376545.379	-0.015	46	380909.448	0.014	24	200840.775	0.036
46	384719.015	0.010	47	389001.470	0.026	26	216900.380	-0.098
47	392891.826	-0.005	48	397092.692	0.024	29	240986.620	-0.170
48	401063.880	0.024	53	437536.433	0.012	32	265068.600	-0.161
53	441911.425	0.046	54	445622.573	-0.011	35	289145.500	-0.455
55	458244.134	-0.062	55	453707.863	0.016	38	313217.570	-0.367
54	450078.266	0.020	56	461792.152	-0.040	43	353325.103	-0.037
56	466409.201	-0.010	57	469875.577	-0.027	42	345305.048	-0.003
						44	361344.507	-0.013
	16-12-76			**16-12-78**		45	369363.177	0.002
0	8136.900	0.019	2	24254.430	0.002	46	377381.069	-0.021
2	24410.480	-0.097	5	48508.880	0.464	47	385398.234	-0.013
11	97637.780	-0.082	6	56593.160	0.255	48	393414.603	-0.029
14	122043.900	-0.093	11	97013.240	-0.075	49	401430.256	0.029
17	146447.900	-0.002	14	121263.280	-0.068	54	441495.796	0.002
18	154581.966	-0.001	17	145511.080	-0.103	55	449506.324	0.011
20	170849.060	-0.083	18	153593.199	-0.031	56	457515.941	0.013
23	195247.170	-0.101	20	169756.270	-0.111	57	465524.648	0.024
24	203379.249	0.037	23	193998.340	-0.162	85	689328.633	-0.052
26	219641.790	-0.052	24	202078.416	-0.033			
29	244032.330	-0.080	26	218236.970	-0.137		**16-12-82**	
42	349667.736	-0.014	29	242471.470	-0.286	2	23964.330	0.005
43	357789.074	0.029	32	266701.930	-0.080	6	55916.190	0.174
44	365909.601	-0.015	42	347432.123	-0.015	11	95852.940	-0.064
45	374029.421	-0.023	43	355501.577	0.007	14	119812.890	-0.144
46	382148.511	-0.002	44	363570.306	0.021	17	143770.820	-0.095
47	390266.794	-0.014	45	371638.301	0.033	18	151756.297	-0.027
48	398384.307	-0.004	46	379705.511	0.009	20	167726.080	-0.140
53	438959.364	-0.007	47	387771.986	0.015	23	191678.340	-0.177
54	447071.804	0.028	48	395837.655	-0.003	25	207644.818	-0.014
55	455183.274	0.000	49	403902.572	0.024	26	215627.180	-0.198
56	463293.854	0.006	53	436153.824	0.019	29	239572.080	-0.292
84	689947.206	-0.017	54	444214.450	-0.013	32	263512.900	-0.171
			55	452274.224	-0.001	43	351251.966	0.026
	16-12-77		56	460333.062	-0.014	44	359224.346	0.027
2	24331.380	-0.003	57	468390.962	-0.036	45	367195.978	-0.004
11	97321.070	-0.039				46	375166.920	0.007
14	121647.980	-0.090		**16-12-80**		47	383137.115	0.018
17	145972.740	-0.080	0	8035.300	0.000	48	391106.531	0.015
18	154080.469	-0.033	2	24105.850	0.013	49	399075.127	-0.029
20	170294.800	-0.117	5	48211.460	0.220	54	438906.112	0.006

Table I : Rotational Frequencies (MHz) of OCSe in the Ground Vibrational State.

J	Freq.	e.- c.	J	Freq.	e.- c.	J	Freq.	e.- c.
55	446869.736	0.002	48	393455.915	0.018	47	379493.659	0.026
56	454832.426	-0.046	49	401472.279	0.034	48	387387.285	-0.006
57	462794.317	0.015	54	441541.533	0.022	49	395280.234	0.057
			55	449552.729	-0.027	50	403172.292	0.015
	16-13-74		56	457563.084	-0.010	55	442620.410	-0.021
18	154232.072	-0.056	57	465572.469	-0.039	56	450507.434	-0.049
25	211031.885	-0.056				57	458393.621	-0.016
42	348875.626	0.138		**16-13-78**		58	466278.871	-0.009
43	356978.390	0.058	2	24030.580	0.075			
44	365080.442	-0.007	18	152175.215	-0.037		**17-12-76**	
45	373181.821	-0.001	25	208217.774	-0.065	44	351945.270	-0.023
46	381282.521	0.085	43	352219.895	0.032	45	359755.610	-0.132
47	389382.306	0.033	44	360214.140	0.028	46	367565.547	0.053
48	397481.320	0.003	45	368207.643	0.007	47	375374.557	0.021
53	437964.049	-0.016	46	376200.439	0.020	48	383182.802	-0.049
54	446057.977	-0.027	47	384192.444	-0.001	50	398797.237	-0.004
55	454151.001	-0.034	48	392183.736	0.037	57	453422.472	-0.029
56	462243.148	0.007	49	400174.161	-0.002	58	461222.769	0.049
			54	440114.076	-0.010	59	469022.027	-0.018
	16-13-76		55	448099.479	0.001			
3	32251.300	-0.354	56	456083.967	-0.001		**17-12-77**	
18	153177.551	0.007	57	464067.494	-0.047	44	350773.295	0.012
24	201531.423	-0.043				45	358557.985	0.236
25	209589.085	-0.037		**16-13-80**		48	381906.892	-0.040
42	346491.133	0.020	2	23879.891	0.010	49	389688.424	-0.115
43	354538.646	0.001	3	31839.760	-0.007	50	397469.327	-0.066
44	362585.502	0.043	18	151221.484	-0.030	55	436361.871	0.017
45	370631.549	0.009	25	206912.974	-0.014	57	451913.025	-0.022
46	378676.862	-0.008	43	350013.439	-0.001	58	459687.421	0.080
47	386721.425	-0.010	44	357957.693	0.022	59	467460.730	-0.018
48	394765.234	0.017	45	365901.161	-0.026			
53	434971.807	-0.011	46	373843.985	0.015		**17-12-78**	
49	402808.227	0.027	47	381786.029	0.023	44	349634.388	0.044
54	443010.537	-0.025	48	389727.309	0.030	46	365152.070	-0.031
55	451048.442	0.032	49	397667.814	0.042	47	372909.892	-0.041
56	459085.339	-0.006	54	437357.990	0.004	48	380667.035	-0.013
57	467121.313	-0.037	55	445293.478	0.011	49	388423.369	-0.061
			56	453228.003	-0.055	50	396179.101	0.036
	16-13-77		57	461161.719	-0.022	51	403933.983	0.046
3	32144.800	0.195				55	434945.482	-0.021
18	152669.164	-0.014		**16-13-82**		56	442696.326	-0.013
24	200862.618	-0.060	3	31648.200	-0.261	58	458195.417	-0.023
42	345341.724	0.016	18	150312.951	-0.057	59	465943.705	0.031
43	353362.544	-0.031	25	205669.932	-0.082			
44	361382.711	-0.019	43	347911.628	0.017		**17-12-80**	
45	369402.194	0.039	44	355808.247	0.053	45	355145.880	-0.020
46	377420.883	0.047	45	363704.094	0.025	46	362855.748	0.039
47	385438.751	-0.004	46	371599.216	-0.005	47	370564.819	-0.005

Table I : Rotational Frequencies (MHz) of OCSe in the Ground Vibrational State.

J	Freq.	e.- c.	J	Freq.	e.- c.	J	Freq.	e.- c.
48	378273.198	-0.032	45	345639.946	-0.014			
49	385980.893	-0.020	46	353143.795	0.034		**18-12-82**	
50	393687.878	0.020	47	360646.975	0.065	19	147967.588	-0.039
51	401394.086	0.036	48	368149.461	0.069	27	207130.494	-0.060
56	439913.189	-0.011	49	375651.228	0.033	46	347533.154	-0.002
57	447614.562	-0.003	50	383152.289	-0.014	47	354917.303	0.055
58	455315.034	-0.039	51	390652.649	-0.055	48	362300.695	0.002
59	463014.747	0.036	52	398152.363	-0.020	49	369683.531	0.053
			57	435639.502	0.036	50	377065.590	0.000
	17-12-82		58	443134.511	-0.012	51	384447.031	0.015
45	353004.957	-0.051	59	450628.784	0.023	52	391827.771	0.030
47	368331.124	0.037	60	458122.097	-0.070	53	399207.704	-0.049
48	375993.099	0.016	61	465614.723	-0.003	58	436096.680	0.040
51	398974.716	0.000				59	443472.049	-0.039
56	437262.018	-0.038		**18-12-78**		60	450846.715	-0.014
57	444917.096	0.012	3	29974.700	-0.151	61	458220.504	-0.044
58	452571.346	0.080	19	149856.563	-0.035	62	465593.547	0.014
59	460224.573	-0.014	27	209774.448	-0.071			
60	467876.988	-0.043	46	351967.573	0.032		**18-12-76**	
			47	359445.729	0.001	19	149699.380	-0.002
	18-12-74		48	366923.257	0.003	20	157182.360	-0.006
18	144347.706	-0.010	49	374400.133	0.029	25	194592.668	0.017
19	151943.094	-0.030	50	381876.283	0.019	26	202073.691	0.007
25	197509.152	0.026	51	389351.716	-0.004	27	209554.326	-0.017
26	205102.258	0.004	52	396826.499	0.039			
57	440229.411	0.055	53	404300.486	0.018		**18-13-78**	
59	455376.207	-0.054	58	441659.055	-0.005	19	148669.805	0.013
			59	449128.391	-0.001	20	156101.302	-0.017
	18-12-76		60	456596.884	-0.012	25	193254.391	0.017
27	211197.581	-0.039	61	464064.508	-0.051	26	200683.959	-0.013
45	346824.866	0.022				27	208113.203	0.001
46	354354.352	0.015		**18-12-80**				
47	361883.172	0.000	2	22336.032	-0.003		**18-13-80**	
48	369411.356	0.018	3	29781.312	-0.005	19	147690.047	0.014
49	376938.828	0.010	4	37226.535	-0.009	20	155072.586	-0.017
50	384465.602	0.002	19	148889.105	-0.044	25	191980.949	0.005
51	391991.657	-0.013	26	200980.160	-0.025	26	199361.620	0.003
52	399516.996	-0.017	46	349696.508	0.032	27	206741.921	-0.004
57	437132.344	0.003	47	357126.488	0.014			
58	444653.026	-0.006	48	364555.825	0.007		**18-13-82**	
59	452172.916	0.018	49	371984.505	0.010	19	146756.739	0.051
60	459691.904	-0.022	50	379412.538	0.047	20	154092.556	-0.061
61	467210.100	-0.002	51	386839.799	0.007	25	190767.834	0.027
			52	394266.383	-0.002	26	198101.844	-0.018
	18-12-77		53	401692.261	0.006	27	205435.561	0.002
19	150357.602	-0.031	58	438810.303	0.000			
26	202962.177	-0.079	59	446231.539	-0.018			
27	210475.849	0.034	60	453651.948	-0.044			

Table I : Rotational Frequencies (MHz) of OCSe in the Ground Vibrational State.

isotopomer	B (MHz)	D (kHz)	ρ(B, D)	n[a]
16-12-74	4095.82780(38)	0.695435(73)	0.971	14
16-12-76	4068.44316(26)	0.686645(51)	0.970	22
16-12-77	4055.24272(25)	0.682367(47)	0.969	21
16-12-78	4042.41682(27)	0.678268(51)	0.972	26
16-12-80	4017.65371(27)	0.670334(52)	0.968	28
16-12-82	3994.06611(27)	0.662909(51)	0.970	23
16-13-74	4059.23718(55)	0.68833(11)	0.971	13
16-13-76	4031.47843(29)	0.679287(55)	0.967	17
16-13-77	4018.09727(38)	0.674965(73)	0.970	15
16-13-78	4005.09632(38)	0.670939(72)	0.971	14
16-13-80	3979.99214(32)	0.662884(60)	0.965	15
16-13-82	3956.07864(47)	0.655374(87)	0.971	15
17-12-76	3913.05696(62)	0.63054(11)	0.979	9
17-12-77	3900.0198(12)	0.62689(20)	0.991	9
17-12-78	3887.34872(58)	0.622884(91)	0.983	11
17-12-80	3862.88461(47)	0.615095(81)	0.983	11
17-12-82	3839.58620(78)	0.60852(12)	0.984	9
18-12-74	3799.05008(37)	0.589986(78)	0.793	6
18-12-76	3772.29886(21)	0.582136(34)	0.975	14
18-12-77	3759.40347(49)	0.578305(80)	0.971	16
18-12-78	3746.87476(37)	0.574744(60)	0.973	15
18-12-80	3722.68279(28)	0.567567(48)	0.966	16
18-12-82	3699.63943(42)	0.560930(67)	0.972	15
18-13-76	3742.94571(63)	0.57645(48)	0.976	5
18-13-78	3717.20067(74)	0.56983(56)	0.976	5
18-13-80	3692.69951(56)	0.56085(42)	0.976	5
18-13-82	3669.36001(21)	0.5535(16)	0.976	5

[a]) number of lines.

Table II : Rotational Constants of OCSe in the Ground Vibrational State.

Species		16-12-76	
Jmax	56	84[b]	Variation
B (MHz)	4068.44316(26)	4068.44180(32)	0.00136(41)
D (Hz)	686.645(51)	685.947(93)	0.698(106)
H (Hz)	n.d.[a]	-0.1072(84)X10^{-3}	
Species		16-12-80	
Jmax	57	85[c]	Variation
B (MHz)	4017.65371(27)	4017.65150(37)	0.00221(46)
D (Hz)	670.334(52)	669.22(11)	1.12(12)
H (Hz)	n.d.[a]	-0.1677(95)X10^{-3}	

[a] Not determined. [b] ν = 689 947.21 MHz. [c] ν = 689 328.63 MHz

Table III. Influence of the Sextic Constant H on the other Constants.

	r(CO)	r(CSe)	σ [a]
r_e	1.15344(10)	1.709808(61)	
r_o	1.15364(59)	1.71299(44)	0.00455
$r_{\varepsilon,I}$	1.15613(16)	1.70934(18)	0.00094
pseudo-r_m [b]	1.1516(21)	1.7110(15)	0.00018
near-r_e [c]	1.1512(11)	1.7097(2)	0.000103
r_m^{ρ}	1.1537(16)	1.7095(12)	0.00321

	r(CO)			r(CSe)			r(OSe)		
	value	range	n[d]	value	range	n[d]	value	range	n[d]
r_s	1.15651(15)	0.00039	27	1.70919(14)	0.00036	92	2.86567(3)	0.00014	181
r_{ss}	1.14217(75)	0.00180	4	1.70959(38)	0.0015	42	2.86557(57)	0.0034	72

a) Standard deviation of the least-squares fit. b) Calculated with Eq. (5).
c) Calculated with Eq. (7). d) Number of data.

Table IV. Structures (in Å) of OCSe.

	from fit to Eq. (5)	from Eq. (12)
$\frac{\partial\varepsilon}{\partial m_O}$ (Å^2)	0.01130(28)	0.00874
$\frac{\partial\varepsilon}{\partial m_{Se}}$ (Å^2)	0.00066(11)	0.00065
$\frac{\partial\varepsilon}{\partial m_C}$ (Å^2)	-0.00493(83)	-0.00193
ε (uÅ^2)	0.3481(30)	0.337 [a]
$\sum_i m_i z_i$ [b]	0.030(9)	0.022

[a] From Eq. (6). [b] From Eq. (15).

Table V. Values of the Derivatives $\partial\varepsilon/\partial m_i$.

parent	daughter	$\|z_s(O)\|$	$\|z_s(C)\|$	$\|z_s(Se)\|$	$\Sigma m_i z_i$	$\Sigma m_i z_i$	C=O	C=Se	O-Se	O-Se
16-12-80	16-12-74	-	-	0.615054	0.0233	0.0234	-	1.709295	2.865696	2.865687
	16-12-76	-	-	0.615056	0.0234	0.0235	-	1.709296	2.865698	2.865688
	16-12-77	-	-	0.615055	0.0233	0.0235	-	1.709295	2.865697	2.865687
	16-12-78	-	-	0.615055	0.0233	0.0235	-	1.709295	2.865697	2.865688
	16-12-82	-	-	0.615048	0.0228	0.0230	-	1.709289	2.865690	2.865681
	16-13-80	-	1.094241	-	-	-	-	-	-	-
	17-12-80	2.250642	-	-	-	-	1.156401	-	-	-
	18-12-80	2.250633	-	-	-	-	1.156392	-	-	-
16-13-80	16-13-74	-	-	0.625143	0.0252	-	-	1.709303	2.865628	-
	16-13-76	-	-	0.625140	0.0250	-	-	1.709301	2.865625	-
	16-13-77	-	-	0.625137	0.0247	-	-	1.709298	2.865622	-
	16-13-78	-	-	0.625146	0.0254	-	-	1.709306	2.865630	-
	16-13-82	-	-	0.625134	0.0244	-	-	1.709294	2.865618	-
	16-12-80	-	1.084160	-	-	-	-	-	-	-
	18-13-80	2.240485	-	-	-	-	1.156324	-	-	-
17-12-80	17-12-76	-	-	0.635804	-	-	-	-	2.865695	2.865676
	17-12-77	-	-	0.635827	-	-	-	-	2.865718	2.865699
	17-12-78	-	-	0.635825	-	-	-	-	2.865716	2.865698
	17-12-82	-	-	0.635755	-	-	-	-	2.865646	2.865627
	16-12-80	2.229891	-	-	-	-	-	-	-	-
	18-12-80	2.229872	-	-	-	-	-	-	-	-
18-12-80	18-12-74	-	-	0.656085	0.0262	0.0263	-	1.709002	2.865679	2.865669
	18-12-76	-	-	0.656085	0.0262	0.0264	-	1.709002	2.865679	2.865670
	18-12-77	-	-	0.656083	0.0260	0.0262	-	1.709000	2.865677	2.865668
	18-12-78	-	-	0.656093	0.0269	0.0270	-	1.709010	2.865687	2.865678
	18-12-82	-	-	0.656076	0.0255	0.0257	-	1.708993	2.865670	2.865661
	18-13-80	-	1.052917	-	-	-	-	-	-	-
	16-12-80	2.209594	-	-	-	-	1.156677	-	-	-
	17-12-80	2.209584	-	-	-	-	1.156668	-	-	-
18-13-80	18-13-76	-	-	0.665621	0.0284	-	-	1.709014	2.865622	-
	18-13-78	-	-	0.665645	0.0302	-	-	1.709037	2.865645	-
	18-13-82	-	-	0.665630	0.0290	-	-	1.709022	2.865630	-
	18-12-80	-	1.043392	-	-	-	-	-	-	-
	16-13-80	2.200000	-	-	-	-	1.156608	-	-	-

Table VI : Structure r_s of OCSe (in Å).

species	$\rho = I_s/I_0$	range
$^{16}O^{12}CSe$ ($^{16}O \rightarrow {}^{17}O$)	0.9986467(59)	0.000020
$^{16}O^{12}CSe$ ($^{16}O \rightarrow {}^{18}O$)	0.9986480(35)	0.000016
$^{16}O^{13}CSe$	0.9986300(81)	0.000032
$^{18}O^{12}CSe$	0.9987002(96)	0.000036
$^{18}O^{13}CSe$	0.9986888(182)	0.000055
mean	0.998659(27)	0.000104

$\rho(^{18}O^{12}CSe) - \rho(^{16}O^{12}CSe) = 5.11(75)\cdot10^{-5}$

$\rho(^{16}O^{13}CSe) - \rho(^{16}O^{12}CSe) = -1.82(58)\cdot10^{-5}$

parent	Δm_O	Δm_C	Δm_{Se}	r(OC)	r(CS)	σ (uÅ^2)[a]
$^{16}O^{12}C^{76}Se$	1	1	1	1.1537(17)	1.7095(12)	0.00332
$^{16}O^{12}C^{76}Se$	1	1	2	1.1537(16)	1.7095(12)	0.00321
$^{16}O^{12}C^{77}Se$	1	1	1	1.1537(17)	1.7095(12)	0.00337
$^{16}O^{12}C^{78}Se$	1	1	2	1.1537(16)	1.7095(12)	0.00327
$^{16}O^{12}C^{80}Se$	1	1	2	1.1537(16)	1.7095(12)	0.00328
$^{16}O^{12}C^{82}Se$	1	1	-2	1.1538(19)	1.7094(14)	0.00381
$^{16}O^{12}C^{82}Se$	1	1	-6	1.1540(21)	1.7093(15)	0.00439
$^{16}O^{12}C^{76}Se$	2	1	1	1.1521(15)	1.7107(11)	0.00438
$^{16}O^{12}C^{77}Se$	2	1	1	1.1521(15)	1.7107(11)	0.00440
$^{16}O^{12}C^{78}Se$	2	1	2	1.1521(14)	1.7107(10)	0.00431
$^{16}O^{12}C^{80}Se$	2	1	2	1.1521(14)	1.7107(10)	0.00435
$^{18}O^{13}C^{78}Se$	-2	-1	-2	1.1521(14)	1.7106(11)	0.00434
$^{18}O^{13}C^{80}Se$	-2	-1	-2	1.1522(14)	1.7107(11)	0.00440
$^{18}O^{13}C^{82}Se$	-2	-1	-2	1.1522(14)	1.7107(11)	0.00440

[a] Standard deviation of the fit.

Table VII. Structure r_m^ρ (in Å) of OCSe.

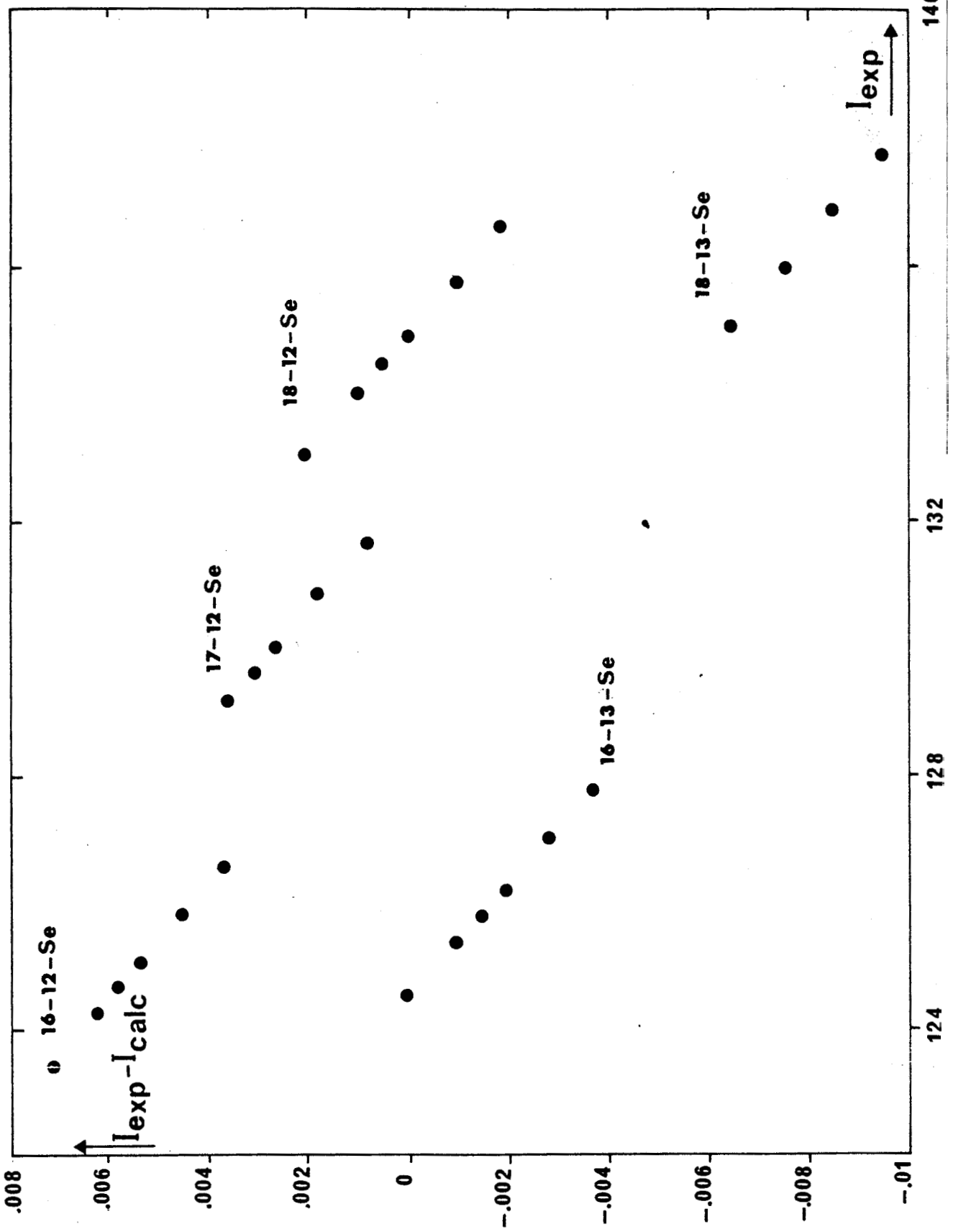

Fig. 1 Plot of $I_{exp.} - I_{calc.}$ versus $I_{exp.}$ for OCSe.

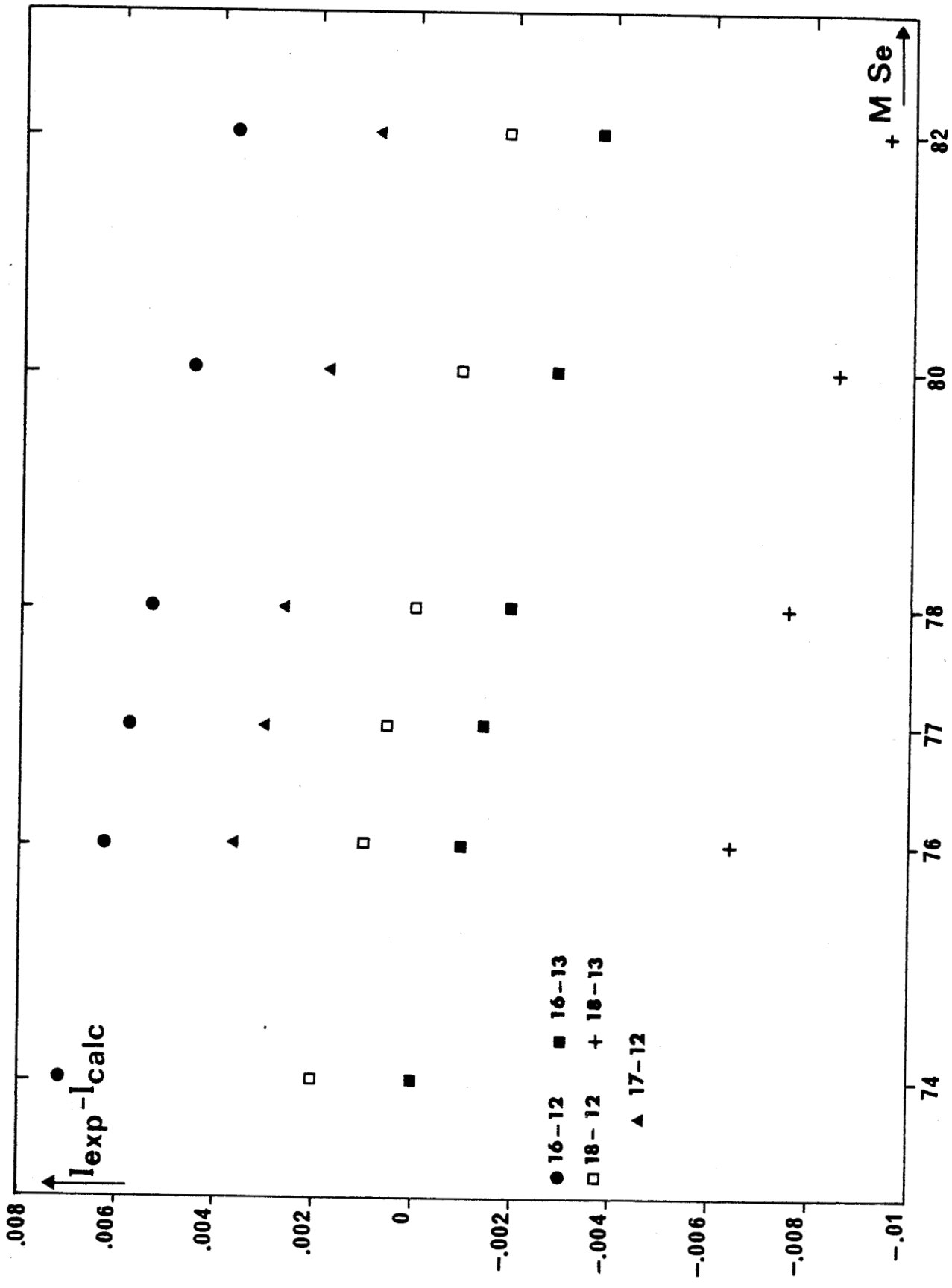

Fig. 2 Plot of $I_{exp.} - I_{calc.}$ versus M_{Se} for OCSe.

OCS

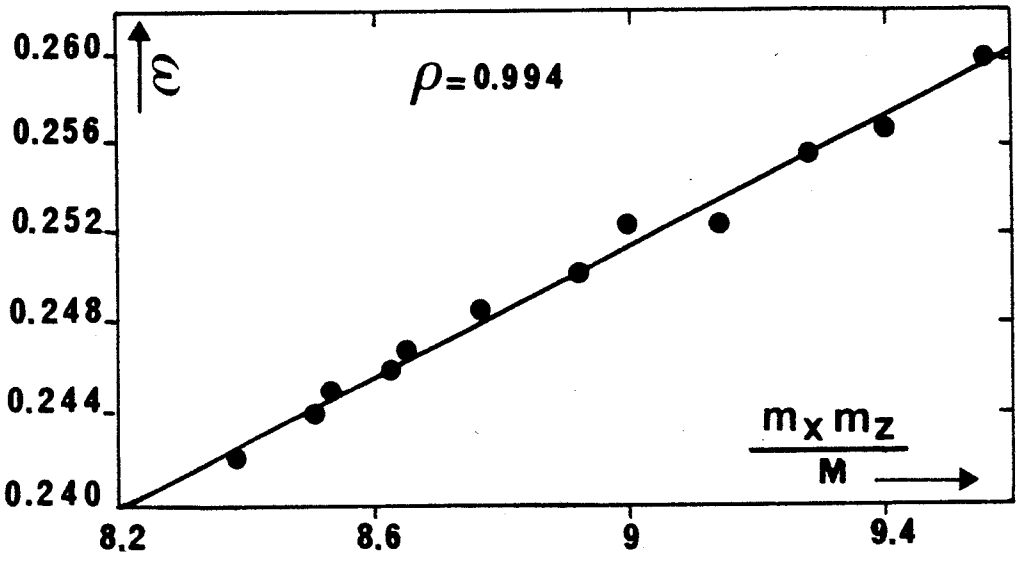

Fig. 3a Plot $\varepsilon = I_o - I_e$ versus I or versus mm_S/M for OCS.

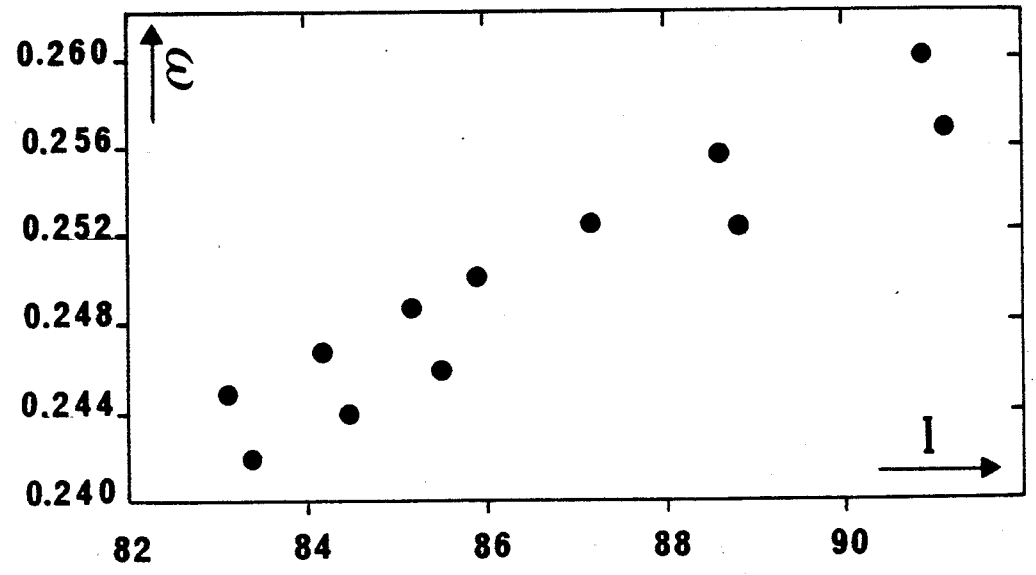

N_2O

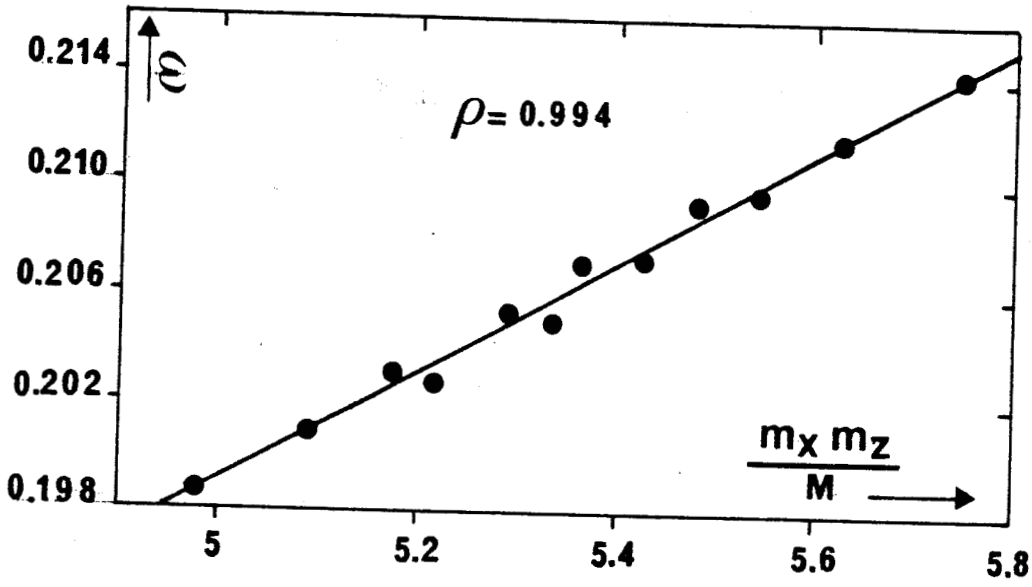

Fig. 3b Plot $\varepsilon = I_o - I_e$ versus I or versus $m_N m_O/M$ for N_2O.

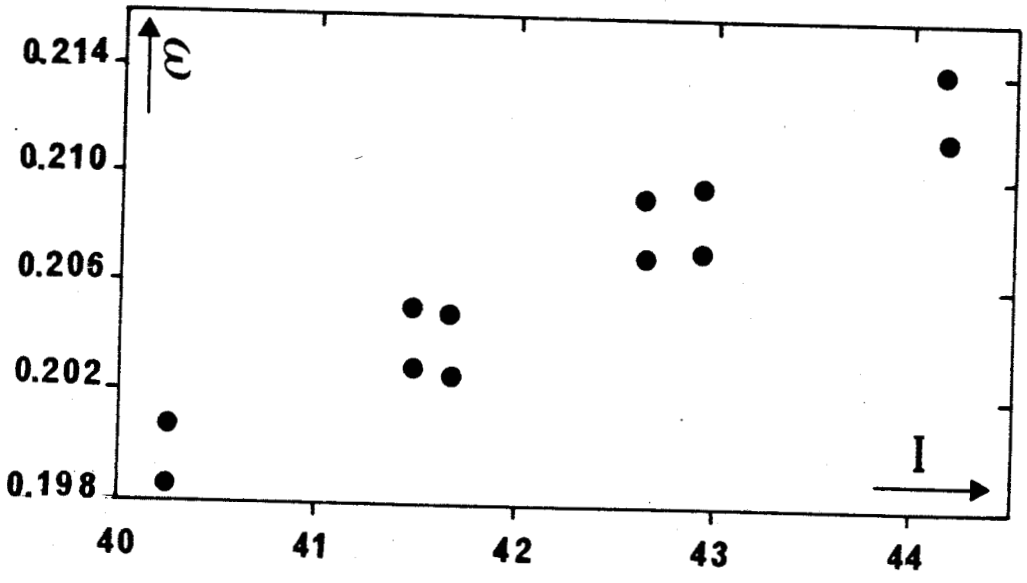

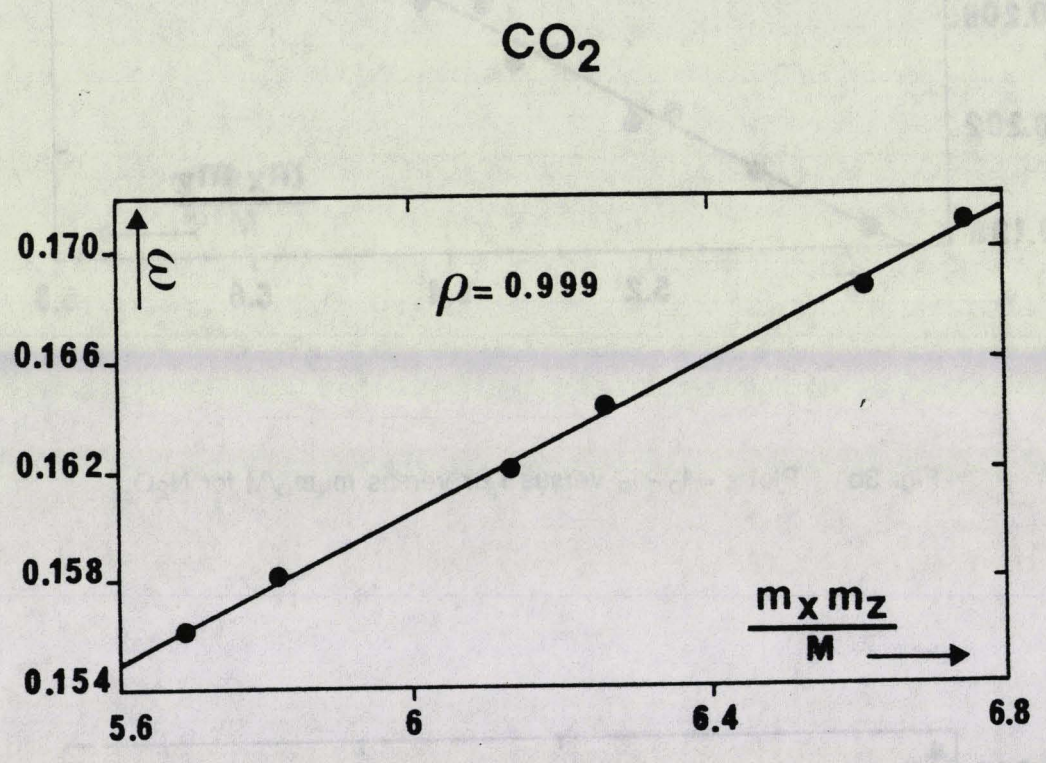

Fig. 3c Plot $\varepsilon = I_o - I_e$ versus $m_o m_o/M$ for CO_2.

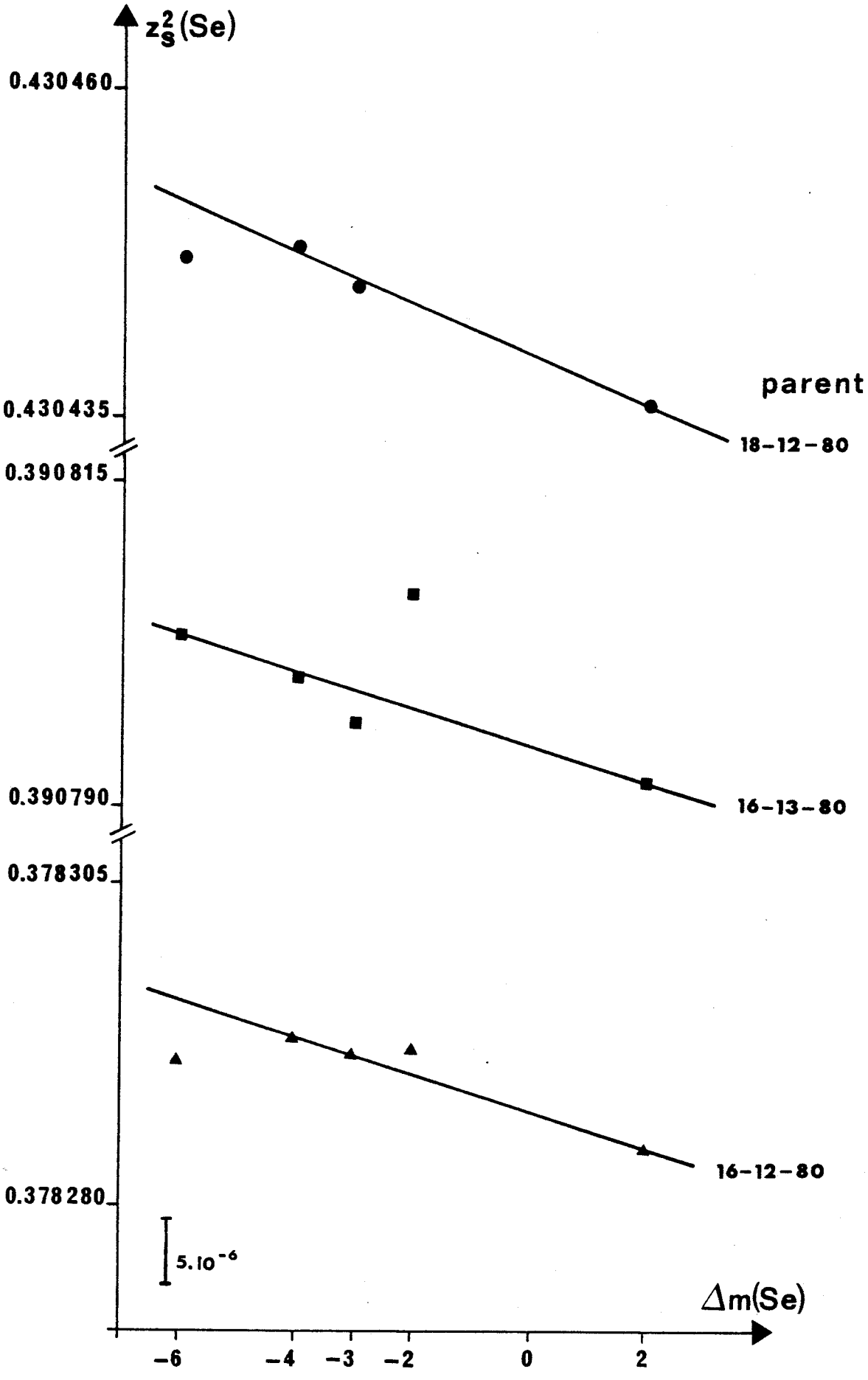

Fig. 4 Plot of z_s^2(Se) versus Δm_{Se}

2°) Molécules symétriques

2.1. Le fluorure de perchloryle

La publication qui suit réunit les résultats obtenus en infra-rouge par l'équipe du Pr. Bürger en ce qui concerne les états excités $v_2 = 1$, $v_3 = 1$, $v_5 = 1$ et $v_6 = 1$ de $F^{35}ClO_3$, et ceux des états fondamentaux de $F^{35/37}ClO_3$ que nous avons obtenus en spectroscopie de rotation.

Le but de ce travail était de déterminer une structure r_e et d'analyser, pour une molécule lourde, la variation de la correction vibrationnelle avec les substitutions isotopiques.

JOURNAL OF MOLECULAR SPECTROSCOPY 148, 65–79 (1991)

High-Resolution FTIR and Millimeter-Wave Study of $FClO_3$: Ground State Rotational Constants Including A_0, Structure, and the ν_2, ν_3, ν_5, and ν_6 Excited States

K. BURCZYK AND H. BÜRGER

Anorganische Chemie, FB 9, Universität-Gesamthochschule, D-5600 Wuppertal 1, Germany

AND

M. LE GUENNEC, G. WLODARCZAK, AND J. DEMAISON

Laboratoire de Spectroscopie Hertzienne associé au CNRS, P5, Université de Lille I, F-59655 Villeneuve d'Ascq Cedex, France

The millimeter-wave spectrum of natural $FClO_3$ has been recorded in the 350–400 GHz range, and transitions with $33 \leqq J \leqq 37$ and $0 \leqq K \leqq 30$ have been measured. The infrared spectrum of monoisotopic $F^{35}ClO_3$ has been investigated in the 350–800 cm^{-1} region with a resolution of $3–4 \times 10^{-3}$ cm^{-1}, and the fundamentals ν_2, ν_3, ν_5, and ν_6 were rotationally resolved. The ground state constants B_0, D_J^0, and D_{JK}^0 were obtained by combining microwave and millimeter-wave data and ground state combination differences determined from the ν_2 and ν_5 infrared bands. The axial rotational constant A_0 of $F^{35}ClO_3$ has been accurately determined from $\Delta K = \pm 3$ resonance effects detected in the ν_5 band. Equilibrium rotational constants of $F^{35}ClO_3$ were deduced with the help of vibrational corrections $\alpha_i^{A,B}$, $i = 1–6$, and the r_s, r_0, and r_e structure of $FClO_3$ determined.

I. INTRODUCTION

Perchloryl fluoride $FClO_3$ is a nearly spherical prolate symmetric top molecule. Its microwave spectrum was first studied in 1965 by Lide (*1*), who determined reasonably accurate B_0 values, while D_J^0 and D_{JK}^0 were derived only with poor significance. More recently improved B_0 and D_J^0 constants were deduced from a precise microwave FT spectrum (*2*), which also provided quadrupole coupling and spin–rotation coupling constants and the dipole moment, $\mu = 0.02700(4)$ D (*2*). The axial rotational constant A_0 required for a structure determination has been inaccessible up to now, a calculated value, $A = 0.1847$ cm^{-1}, obtained from the geometry of $FClO_3$ determined by gas phase electron diffraction (*3*), being the best estimate (*4*).

The vibrational spectrum of gaseous $FClO_3$ has been studied with low resolution and in a matrix (*5*), and the vibrational fundamentals ν_1–ν_6 of the ^{35}Cl species were located at 1063(a_1), 717(a_1), 550(a_1), 1318(e), 590(e), and 405 cm^{-1} (e). Gas phase FTIR spectra of monoisotopic $F^{35}ClO_3$ and of natural material recorded with a resolution of 0.04 cm^{-1} enabled, for the first time, the J structure of all parallel bands ν_1, ν_2, ν_3 and of some of their overtones, combination bands, and associated hot bands (*4*) to be resolved. Although some K structure was indicated as well, this remained

0022-2852/91 $3.00

mostly unresolved in spite of the absence of any transitions involving $K'' \neq 3p$, $p = 0$, 1, 2 · · · states (e symmetry) due to spin statistics obeyed by the three ^{16}O nuclei ($I = 0$).

The goals of the present study are

(i) the measurement, by millimeter-wave spectroscopy, of the entire K manifolds of high-J rotational transitions in order to determine B_0 and centrifugal distortion constants with significantly higher accuracy than previously;

(ii) to search for possibilities to determine the normally inaccessible axial rotational constant A_0 from high-resolution IR spectra revealing either normally forbidden, but perturbation allowed lines, or perturbation induced shifts sensitive to A_0 (6);

(iii) the elucidation of vibration–rotation interaction parameters required for vibrational corrections to ground state rotational constants in order to obtain equilibrium values;

(iv) to determine the accurate structure of $FClO_3$ in the ground state and at equilibrium.

TABLE I

Ground State Rotational Transitions of Perchloryl Fluoride (MHz)

$F^{35}ClO_3$				$F^{37}ClO_3$			
J	K	$F_{exp.}$	(exp.-calc.)	J	K	$F_{exp.}$	(exp.-calc.)
0	0	10 517.377[a]	-0.001	0	0	10 512.294[a]	-0.008
1	0	21 034.719[a]	-0.001	1	0	21 024.565[a]	-0.003
2	0	31 552.000[a]	0.009	2	0	31 536.767[a]	0.005
4	3	52 585.970[b]	-0.051	4	3	52 560.400[b]	-0.239
6	3	73 619.400[b]	-0.022	6	3	73 583.910[b]	0.021
6	6	73 618.720[b]	-0.068	33	0	357 183.262	0.061
33	0	357 355.608	0.151	33	3	357 182.124	-0.046
33	3	357 354.456	0.026	33	6	357 179.068	-0.010
33	6	357 351.431	0.080	33	9	357 173.927	0.003
33	9	357 346.321	0.102	33	12	357 166.730	0.022
33	12	357 338.993	-0.041	33	15	357 157.383	-0.048
33	15	357 329.830	0.034	33	18	357 146.112	0.020
34	0	367 851.425	-0.010	33	21	357 132.661	-0.031
34	3	367 850.345	-0.033	33	24	357 117.160	-0.070
34	6	367 847.237	0.029	34	0	367 674.190	0.057
34	9	367 841.898	-0.027	34	3	367 673.051	-0.021
34	12	367 834.438	-0.091	34	6	367 669.850	-0.039
34	15	367 824.968	-0.051	34	9	367 664.575	-0.008
34	18	367 813.377	-0.019	34	12	367 657.157	0.001
34	21	367 799.642	-0.017	34	15	367 647.584	-0.022
34	24	367 783.779	-0.031	34	18	367 635.939	0.005
37	0	399 331.647	-0.025	34	21	367 622.149	0.010
37	3	399 330.544	0.019	35	9	378 153.987	0.001
37	6	399 326.972	-0.111	37	0	399 139.271	0.025
37	9	399 321.395	0.048	37	3	399 138.105	0.011
37	12	399 313.283	-0.034	37	6	399 134.659	0.021
37	15	399 302.973	-0.019	37	9	399 128.852	-0.026
37	18	399 290.422	0.049	37	12	399 120.813	0.000
37	21	399 275.427	-0.032	37	15	399 110.454	0.009
37	24	399 258.224	-0.027	37	18	399 097.750	-0.022
37	27	399 238.767	0.019	37	21	399 082.807	0.012
37	30	399 217.182	0.231	37	24	399 065.496	-0.018
				37	27	399 045.936	0.007
				37	30	399 024.104	0.064

[a] Ref. (2).

[b] Ref. (1).

II. EXPERIMENTAL DETAILS

(a) Material

$FClO_3$ was prepared from $KClO_4$ and HSO_3F and handled on a standard vacuum line. Monoisotopic $F^{35}ClO_3$, 99.4% ^{35}Cl, was obtained from $Na^{35}ClO_4$ which was generated by anodic oxidation of $Na^{35}Cl$.

(b) Millimeter-Wave Spectra

The rotational spectra were measured with a source-modulated millimeter-wave spectrometer. The sources are phase locked submillimeter BWOs (Thomson). The

TABLE II

Rotational Constants, Centrifugal Distortion Constants, and Correlation Matrix for the Ground State of Perchloryl Fluoride

		$F^{35}ClO_3$		
From v_5 = 1 excited state rotational analysis:				
A (MHz)	5 608.72(21)	D_K (kHz)	-2.28 (assumed)	
From rotational data:				
B (MHz)	5 258.692 10(73)	1.000		
D_J (kHz)	1.498 611(30)	0.943	1.000	
D_{JK} (kHz)	1.677 209(86)	-0.074	-0.303	1.000
From ground state combination differences:				
B (MHz)	5 258.692 7(17)	1.000		
D_J (kHz)	1.498 318(19)	0.833	1.000	
D_{JK} (kHz)	1.659 165(85)	0.134	-0.275	1.000
From rotational data and ground state combination differences[a]:				
B (MHz)	5 258.687 00(38)	1.000		
D_J (kHz)	1.497 109(13)	0.823	1.000	
D_{JK} (kHz)	1.667 775(64)	-0.163	-0.499	1.000
		$F^{37}ClO_3$		
From rotational data:				
B (MHz)	5 256.153 87(44)	1.000		
D_J (kHz)	1.496 428(18)	0.953	1.000	
D_{JK} (kHz)	1.684 295(42)	-0.069	-0.279	1.000

[a]Weight of the rotational data: 20000.

submillimeter power is optically focused through a free space absorption cell (length 1 m) and detected by a He-cooled Ge bolometer. After phase-sensitive detection, the signal is processed by a microcomputer which calculates the line frequency after averaging and digital filtering. The measured transitions are summarized in Table I.

(c) Infrared Spectra

High-resolution FTIR spectra of $F^{35}ClO_3$ in the 800–350 cm^{-1} region were recorded at room temperature with a Bruker 120 HR interferometer (*7*) employing a He-cooled Cu:Ge detector. A KBr/Ge beam splitter was used to study the ν_2 and ν_5 bands with a resolution (FWHM) of 3×10^{-3} cm^{-1}. A pressure of $\simeq$2 mbar was adjusted in a 19-cm cell equipped with KBr windows, and 75 scans were coadded. The ν_3 and ν_6 bands were investigated employing a 3.5-μm Mylar beam splitter, with 270 scans coadded. The pressure was 20 mbar in a 26-cm cell fitted with CsBr windows, and the resolution (FWHM) was close to 4×10^{-3} cm^{-1}. Calibration was with H_2O lines reported in Ref. (*8*). Wavenumber accuracy relative to these is assumed to be better than 2×10^{-4} cm^{-1} for ν_2 and ν_5 and better than 5×10^{-4} cm^{-1} for ν_3 and ν_6.

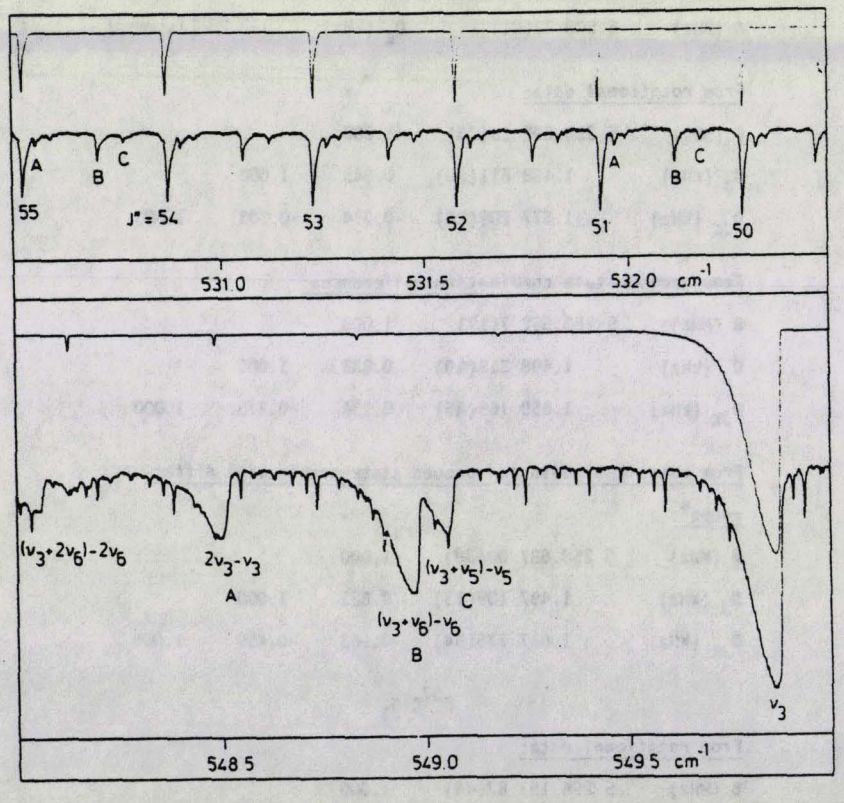

FIG. 1. Spectrum of $F^{35}ClO_3$ in the ν_3 region. (Above) Detail of the *P* branch, with *J"* values of the unresolved ${}^{Q}P_K(J")$ clusters indicated. Upper trace: Simulated spectrum, ν_3 band only. Lower trace: Experimental spectrum. Peaks labeled A, B, and C refer to the hot bands assigned in the lower part of the figure. (Below) *Q*-branch range. Upper trace: Simulated spectrum, ν_3 band only. Lower trace: Experimental spectrum, with some assignments indicated. Additional lines belong to ${}^{P}P$ lines of the very intense ν_5 band.

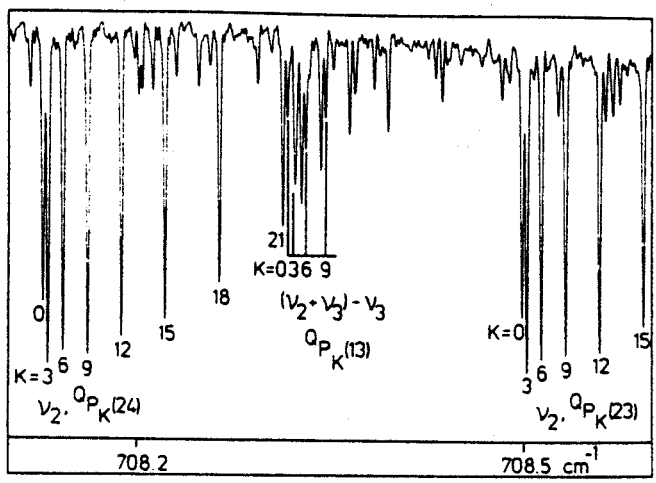

FIG. 2. Detail of the ν_2 band of $F^{35}ClO_3$. Assignments of the $^QP_K(24)$ cluster, the $^QP_K(23)$ cluster in part, and the $^QP_K(13)$ cluster of the hot band $(\nu_2 + \nu_3) - \nu_3$ are indicated.

III. GROUND STATE

(a) Analysis of the Rotational Spectra

Although the lines are very weak, their assignment was easy because the spectrum is sparse and rather good rotational constants were already known (*1*). The frequency of a rotational transition $J + 1, K \leftarrow J, K$ in the ground vibrational state may be written as

$$\nu = 2B(J + 1) - 4D_J(J + 1)^3 - 2D_{JK}(J + 1)K^2. \quad (1)$$

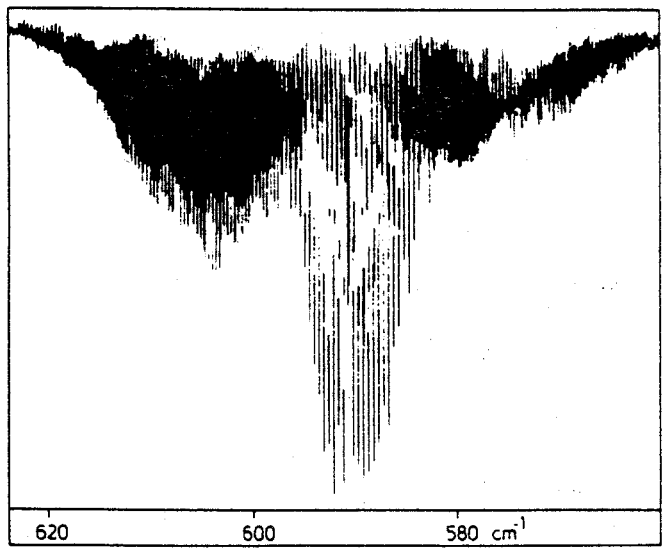

FIG. 3. Survey spectrum of the ν_5 band of $F^{35}ClO_3$; resolution 0.04 cm^{-1}.

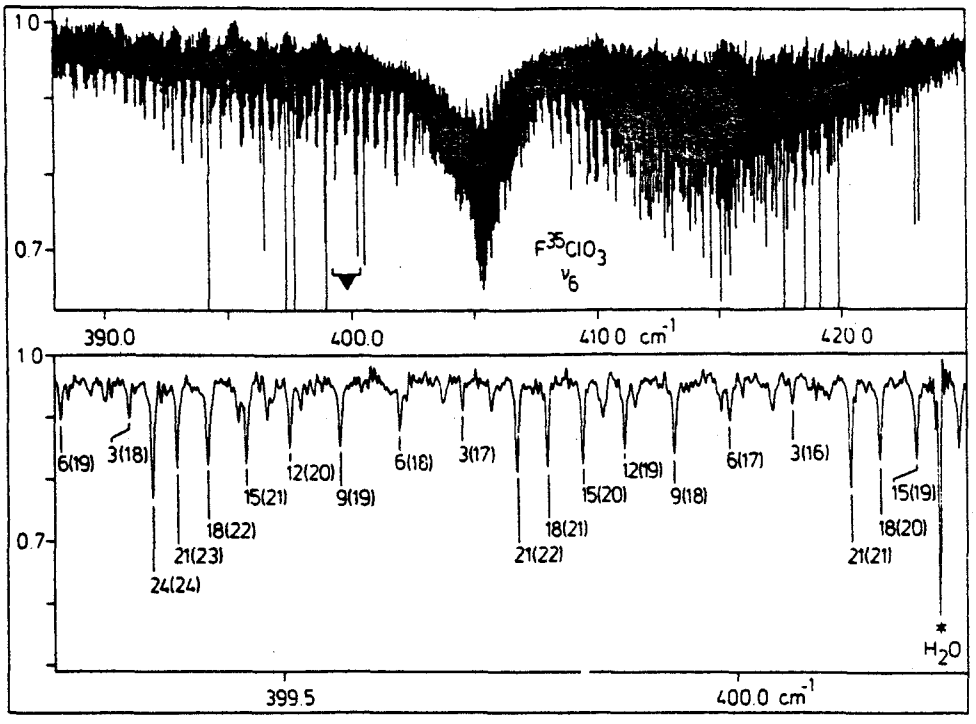

FIG. 4. The ν_6 band of $F^{35}ClO_3$, 26-cm cell, 20 mbar. (Above) Survey spectrum. Strong lines are due to residual H_2O in the instrument. (Below) Detail showing ^PP lines. Assignments are indicated by $K(J)$.

A weighted least-squares method was used to fit the experimental frequencies of Table I to the parameters of Eq. (1). The weight of each transition was taken equal to the inverse square of the measurement accuracy: 100 kHz for the millimeter-wave measurements, 10 kHz for the microwave FT measurements of Ref. (*2*), and 50 kHz for the microwave measurements of Ref. (*1*), except for the $J = 4$, $K = 3$ transition of $F^{37}ClO_3$ whose accuracy was estimated to be only 300 kHz. The derived parameters are listed in Table II, together with their standard deviations and their correlation coefficients. It was checked that the sextic centrifugal distortion constants are not determinable.

(b) Ground State Combination Differences

Additional information on the J-dependent rotational constants of $F^{35}ClO_3$ was gathered from the high-resolution infrared spectra in the ν_2 and ν_5 regions. Ground state combination differences (GSCD) were formed from $R(J-1)$, $Q(J)$, and $P(J+1)$ transitions reaching the same upper states, only unblended and unit-weighted lines being used for this purpose. Of the 2149 differences available, 1308 belonged to ν_2, with J'_{max} and $K'_{max} = 77$ and 57, respectively, while the others were from ν_5 transitions, $J'_{max} = 70$ and $K'_{max} = 45$. These were fitted, $\sigma = 1.8 \times 10^{-4}$ cm^{-1}, to yield the ground state parameters set out in Table II. The σ value gives credit to the estimated relative accuracy of an individual line, $\leqslant 2 \times 10^{-4}$ cm^{-1}, which should be $\sigma/\sqrt{2}$. No systematic differences between observed and calculated GSCD were detected.

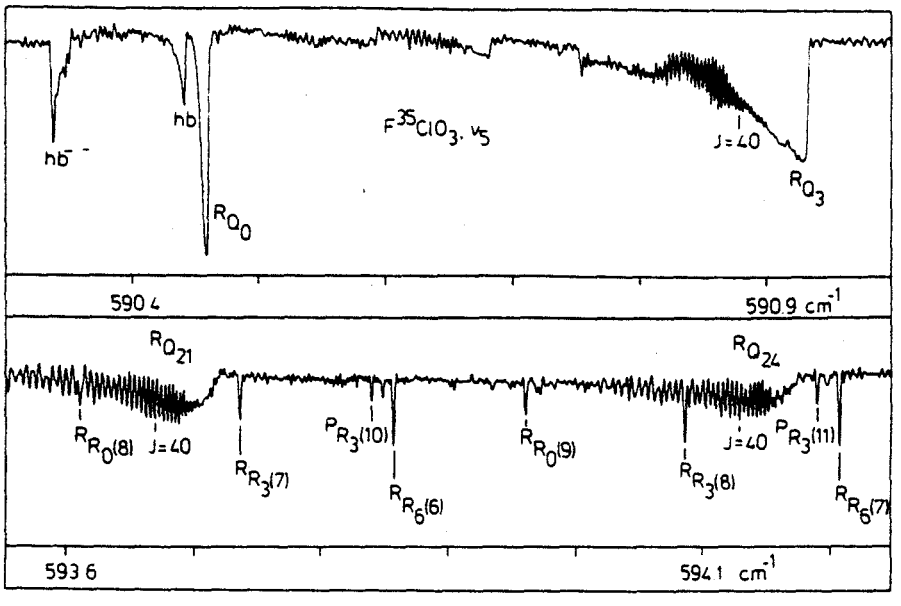

FIG. 5. Detail of the ν_5 band of $F^{35}ClO_3$. (Above) Display of $^RQ_0$ and $^RQ_3$, illustrating the effect of the $q_t^{(+)}$ resonance. (Below) Detail of the spectrum, with some assignments indicated.

To obtain the best constants, the GSCD and the rotational frequencies were fitted together, the weight of the latter being 20 000 times greater. The results are also listed in Table II. It is to be noted that the derived constants are not compatible with the simple weighted mean of the rotational and GSCD results. This shows the influence of the correlations. To check the validity of the combined fit, we have also determined the constants by a merged least-squares fit of the rotational and GSCD constants (*9*). This merged fit gives results in perfect agreement with those of the combined fit.

IV. INFRARED SPECTRA

(a) Parallel Bands

The infrared spectrum of $FClO_3$ comprises, aside from combination bands and overtones, six fundamental bands for each of the $^{35,37}Cl$ isotopic species. Of these, ν_1–$\nu_3(a_1)$ reveal apparently unperturbed parallel band structure, and the resolved J structure of their P and R branches has been analyzed in a previous investigation based on FT spectra recorded with a resolution of ca. 0.04 cm^{-1} (*4*). K structure, however, was only indicated in the wings of J clusters of ν_1 and ν_2, and (A_v-A_0) values were deduced from band contour simulations (*4*).

While the ν_1 and ν_2 bands are strong and isolated, the ν_3 band at 550 cm^{-1} is weak, and its R branch becomes more and more obscured by strong ν_5 features as J increases. Furthermore, in the previous study (*4*) both the Q branch and $\Delta J = \pm 1$ clusters appeared to be very sharp. Indeed no details could be resolved even at a resolution of 4×10^{-3} cm^{-1}, although now some broadening becomes discernible in high-J clusters of the P branch; Fig. 1. In conjunction with the envelope of the Q branch these high wavenumber wings give some information on (A_3-A_0) by means of a contour simulation; Fig. 1.

TABLE III

Excited State Parameters of $F^{35}ClO_3$ (cm^{-1})

	$v_2 = 1$	$v_3 = 1$	$v_5 = 1$	$v_6 = 1$
ν_0	716.809 727(8)[a]	549.878 85(6)	590.314 776(20)	405.605 07(4)
$(A'-A_0)\times10^4$	-0.603 83(11)	-0.25[b]	-1.223 84(28)	0.072 5(10)
$(B'-B_0)\times10^4$	-4.823 25(5)	-0.266 6(7)	-0.323 64(21)	-4.834 6(4)
$(D_J'-D_J^0)\times10^8$	-0.112 90(7)	0.175 8(13)	0.037 8(5)	
$(D_{JK}'-D_{JK}^0)\times10^8$	0.330 57(24)	0.0	0.081 6(13)	0.048(4)
$(D_K'-D_K^0)\times10^8$	-0.212 4(4)	0.0	-0.172 6(10)	
$A\zeta_v^z\times10^2$			-6.732 5(6)	5.936 37(10)
$\eta_{vJ}\times10^6$			-0.244 9(11)	-0.970 9(18)
$\eta_{vK}\times10^6$			-0.114 1(11)	1.435 3(18)
$\eta_{vJJ}\times10^{12}$			-4.80(22)	
$\eta_{vJK}\times10^{12}$			12.1(4)	
$\eta_{vKK}\times10^{12}$			-8.14(24)	
$q_t^{(+)}\times10^4$			0.646 4(13)	-3.530 5(15)
$q_t^{(+)J}\times10^{10}$			3.8(5)	
$W_v^{K\pm3}\times10^8$			1.608 0(28)	
No. of data	2372	106	2490	1017
$\sigma\times10^4$	1.3	3.5	3.3	5.5

[a]One standard deviation given in parentheses.

[b]Constrained.

The ν_2 band centered at 717 cm^{-1} is very strong, with a Q branch degraded to low wavenumber and J clusters in the P and R branches degraded to high wavenumber. Its general appearance is consistent with that illustrated in Ref. (*4*). Figure 2 which displays the $^QP_K(24)$ cluster shows a small portion of the present spectrum. This cluster was completely resolved into its K components, starting with $K = 0$, and the assignments for ν_2 and the $(\nu_2 + \nu_3) - \nu_3$ hot band are given. Clearly additional hot band features are discernible, which above all belong to $(\nu_2 + \nu_6) - \nu_6$.

A medium-resolution spectrum of the ν_1 band has been studied previously (*4*), and the reported ν_1 parameters are quite consistent with more recent ones based on a spectrum recorded with a resolution of 4×10^{-3} cm^{-1}. The latter are quoted in this communication and used for vibrational corrections of A and B; they will be discussed in greater detail in a forthcoming contribution dealing with ν_1, ν_4, and $\nu_2 + \nu_5$ (*10*).

(b) Perpendicular Bands

Since $FClO_3$ is a nearly spherical top the $^{(P,R)}Q_K$ branches of the perpendicular bands are gathered in the band centers, and the $(A\zeta^z)_v$ values determine whether successive ^PQ (^RQ) branches extend with increasing K to high or low wavenumber.

While ν_4 and ν_5 are very strong, ν_6 is by far the weakest of all fundamentals, and as a consequence of the required pressure using a 26-cm cell, lines were slightly broadened in our spectra.

Contrary to the prominence Q branches of ν_5 reveal (Fig. 3) those of ν_6 are rather spread and obscured by $\Delta J = \pm 1$ lines, and assignments require extensive use of GSCD. On the other hand, ν_4 is strongly perturbed by interaction with the combination level ($\nu_2 + \nu_5$, E). Since however ν_5 itself is perturbed by an essential resonance (vide infra), which will also affect ($\nu_2 + \nu_5$), we have postponed the $\nu_4/(\nu_2 + \nu_5)$ analysis until the work on ν_5 has been completed, and for ν_4 we refer to preliminary results in the present paper.

The ν_6 band is illustrated in Fig. 4. In the band center near 405 cm^{-1} ^PQ branches extend to high wavenumber while ^RQ branches appear to low wavenumber, both revealing J degradation to low wavenumber. ^PP and ^RR lines form well-resolved clusters constituted of components with $(K - 3p)$ and $(J - p)$, $p = 0, 1, 2 \cdots$ and $K \leqq J$, the ^PP lines developing cluster heads for high K values; Fig. 4. The data refinement clearly indicates the presence of an essential $l(2, 2)$ resonance; see Section V. Lines were assigned for J and K up to 54.

The band center of ν_5 is dominated by condensed Q branches (Fig. 3) which extend to high and low wavenumber for $\Delta K = +1$ and -1, respectively. The $^{\backslash R}Q_0$ branch, typically affected by $l(2, 2)$ resonance, is extremely sharp and unresolved, while all other Q branches reveal resolved J structure; Fig. 5. Assignments are therefore

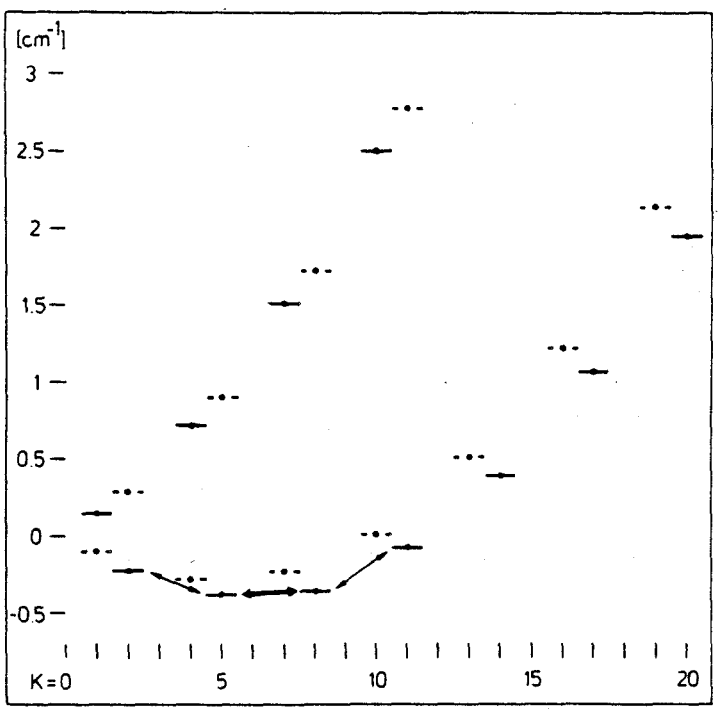

FIG. 6. Reduced relative $J = 0$ upper state energies for $F^{35}ClO_3$ for the $v_5 = 1$ state (full lines) and $v_6 = 1$ state (broken lines). Arrows indicate where $\Delta K = \pm 3$ perturbations are significant. Note that sublevels reached by $\Delta K = +1$ transitions are *above* those with $\Delta K = -1$ for ν_5, but *below* for ν_6.

straightforward and easily proved by GSCD. Lines were followed up to $J = 80$ and $K = 75$. Many hot band features are clearly indicated, although their assignment is at present ambiguous and postponed until attached combination (overtone) levels will have been analyzed.

V. EXCITED STATES

Excited state energies of levels with a_1 vibrational symmetry ($v_2 = 1$; $v_3 = 1, 2$; $v_2 = v_3 = 1$) are given by

$$E(v, J, K) = \nu_0 + (A_v - B_v)K^2 + B_vJ(J+1) - D_J^vJ^2(J+1)^2 - D_{JK}^vJ(J+1)K^2 - D_K^vK^4 \qquad (K = |k|) \quad (2)$$

while those associated with degenerate vibrational states ($v_5 = 1$; $v_6 = 1$; e symmetry) were taken as

$$E(v, l, J, k) = \nu_0 + (A_v - B_v)k^2 + B_vJ(J+1) - D_J^vJ^2(J+1)^2 - D_{JK}^vJ(J+1)k^2 - D_K^vk^4 - [2A\zeta_v^z - \eta_{vJ}J(J+1) - \eta_{vK}k^2 - \eta_{vJJ}J^2(J+1)^2 - \eta_{vJK}J(J+1)k^2 - \eta_{vKK}k^4]kl. \quad (3)$$

Two kinds of essential resonances were found to be of importance: the $\Delta l = \Delta k = \pm 2$ resonance within v_5 and v_6 with the following matrix elements (sign convention of Ref. (*11*))

$$\langle v_t = 1, l_t = \pm 1, J, k \pm 1 | \mathbf{H} | v_t = 1, l_t = \mp 1, J, k \mp 1 \rangle = -\tfrac{1}{2}[q_t^{(+)} + q_t^{(+)J}J(J+1)][J(J+1) - k(k \pm 1)]^{1/2}[J(J+1) - k(k \mp 1)]^{1/2} \quad (4)$$

TABLE IV

Hot Band Parameters of $F^{35}ClO_3$ (cm^{-1})

	$2\nu_3 - \nu_3$[a]	$(\nu_2 + \nu_3) - \nu_3$[a]
ν_0	548.514 52(12)[b]	712.953 69(4)
$(A'-A'')\times10^4$	-0.25[c]	-0.606 1(4)
$(B'-B'')\times10^4$	-0.349 1(18)	-4.831 9(5)
$(D_J'-D_J'')\times10^8$	0.175(4)	-0.133[c]
$(D_{JK}'-D_{JK}'')\times10^8$		0.331[c]
$(D_K'-D_K'')\times10^8$		-0.212[c]
No. of data	57	448
$\sigma\times10^4$	4.8	3.7
x_{ij} (cm^{-1})	x_{33} -0.682 17(9)	x_{23} -3.856 04(4)

[a] Lower state parameters fixed to values of Table III.

[b] One standard deviation in parentheses.

[c] Constrained.

and $\Delta l = 0$, $\Delta k = \pm 3$ resonance within ν_5 given by (*12*)

$$\langle v_5 = 1, l_5 = \pm 1, J, k | \mathbf{H} | v_5 = 1, l_5 = \pm 1, J, k \pm 3 \rangle$$
$$= W_5^{k\pm 3}(2k \pm 3)[J(J+1) - k(k \pm 1)]^{1/2} \times [J(J+1) - (k \pm 1)(k \pm 2)]^{1/2}$$
$$\times [J(J+1) - (k \pm 2)(k \pm 3)]^{1/2}. \quad (5)$$

Except for ν_5, observed line positions were fitted to excited state parameters, with ground state parameters fixed to the values listed in Table II, by means of a computer program described in Ref. (*13*). Since no perturbations with $(\Delta k - \Delta l) \neq 0$ affect the ν_2, ν_3, and ν_6 levels the respective fits are insensitive to the adopted A_0 value. The results of the refinement are collected in Table III. The σ values of the fits with regard to the quality of the data are throughout satisfactory, no systematic deviations between observed and calculated line positions being evident. Since J clusters of ν_3 and $2\nu_3 - \nu_3$ could not be resolved, the peaks were associated with hypothetical K_{max} values obtained from a band contour simulation.

When the ν_5 data were treated in the same fashion, systematic displacements of observed $^PP_6$ lines from their calculated positions to low wavenumber and of $^PP_9$ and (to a lesser extent) $^PP_3$ and $^PP_{12}$ lines to high wavenumber were noticed. The displacements are J dependent, and they increase with high power of $(J - K)$. Such strong J-

TABLE V

Vibrational Corrections for $F^{35}ClO_3$ and Structure of $FClO_3$

	A (MHz)	B (MHz)
α_1	17.172	9.738[a]
α_2	1.810	14.459[b]
α_3	0.749	0.799[b]
α_4	19.756	10.115[a]
α_5	3.687	0.970[b]
α_6	-0.217	14.494[b]
A_0	5 608.718	B_0 5 258.687
A_e	5 641.993	B_e 5 296.788

	r_a[c]	r_0	r_e
θ(OClO) (°)	116.5(5)	115.3	115.3
r(ClO) (Å)	1.404(2)	1.405	1.400
r(ClF) (Å)	1.619(4)	1.604	1.598

[a] Ref. (10).

[b] This work.

[c] Ref. (3).

TABLE VI

Vibration–Rotation Interaction Constants for Heavy-Atom Molecules (μ Å^2)

Parent Species	Axis	I_e	$\epsilon_{exp.}$	Daughter Species	I_e	$\epsilon_{exp.}$	$\epsilon_{calc.}$	$\Delta\epsilon/\epsilon$ (%)	Ref.
OCS		82.905 0	0.245 4	$OC^{34}S$	84.984 6	0.249 4	0.248 5	0.36	22
				$O^{13}CS$	83.176 1	0.242 8	0.245 8	-1.24	
				^{18}OCS	88.383 7	0.256 3	0.253 4	1.15	
NF_3		46.987 8	0.355 9	$^{15}NF_3$	47.212 8	0.360 6	0.356 7	1.08	23
$^{70}GeF_2$	A	32.353 8	-0.103 5	$^{72}GeF_2$	32.674 2	-0.105 1	-0.104 0	1.05	24
	B	64.127 3	0.300 1		64.128 8	0.298 4	0.300 1	-0.57	
	C	96.474 5	0.477 0		96.795 5	0.475 5	0.477 8	-0.48	
$^{78}SeO_2$	A	17.474 0	-0.059 5	$^{80}SeO_2$	17.602 8	-0.060 5	-0.059 7	1.35	25
	B	58.070 4	0.210 9		58.071 4	0.209 7	0.210 9	-0.57	
	C	75 533 8	0.358 6		75.665 8	0.354 6	0.358 9	-1.21	
S_2O	A	12.091 1	-0.026 8	$S_2{}^{18}O$	12.663 4	-0.028 1	-0.027 5	2.41	26
	B	99.637 1	0.317 3		104.434 3	0.329 5	0.324 9	1.42	
	C	111.720 7	0.473 9		117.089 9	0.489 0	0.485 1	0.79	
ClNO	B	87.960 1	0.171 3	$Cl^{15}NO$	88.644 4	0.171 6	0.172 0	-0.21	27
	C	93.757 8	0.300 4		94.712 9	0.292 4	0.301 9	-3.28	
	B			$^{37}ClNO$	90.111 2	0.167 3	0.173 4	-3.62	
	C				95.904 4	0.307 7	0.303 9	1.26	
FCN		47.770 8	0.141 8	$F^{13}CN$	47.799 5	0.142 4	0.141 9	0.41	28
				$FC^{15}N$	49.500 3	0.142 8	0.144 3	-1.07	
ICN		156.597 7	0.175 3	$I^{13}CN$	158.984 9	0.181 8	0.176 6	2.83	29
ClCN		84.519 4	0.172 3	$^{37}ClCN$	86.307 2	0.174 3	0.174 2	0.11	30
N_2O		40.054 2	0.201 8	$^{14}N^{15}N^{16}O$	40.059 2	0.199 6	0.201 8	-1.12	31
				$^{15}N^{14}N^{16}O$	41.457 3	0.206 0	0.205 3	0.36	
				$^{15}N^{15}N^{16}O$	41.459 4	0.203 7	0.205 3	-0.79	
				$^{14}N^{14}N^{17}O$	41.271 2	0.206 1	0.204 8	0.64	
				$^{14}N^{15}N^{17}O$	41.280 4	0.203 9	0.204 8	-0.48	
				$^{15}N^{14}N^{17}O$	42.733 8	0.210 6	0.208 4	1.03	
				$^{15}N^{15}N^{17}O$	42.738 7	0.208 2	0.208 4	-0.13	
				$^{14}N^{14}N^{18}O$	42.430 4	0.210 3	0.207 7	1.24	
				$^{14}N^{15}N^{18}O$	42.444 6	0.207 9	0.207 7	0.12	
				$^{15}N^{14}N^{18}O$	43.950 8	0.214 9	0.211 4	1.63	
				$^{15}N^{15}N^{18}O$	43.959 5	0.212 4	0.211 4	0.49	
FNO	B	42.504 4	0.189 5	$FN^{18}O$	44.733 3	0.199 9	0.194 4	2.78	32
	C	47.828 7	0.293 7		50.202 5	0.305 8	0.300 9	1.59	
OCSe		125.520 2	0.344 1	$^{18}OCSe$	135.475 8	0.361 5	0.357 5	1.10	33
				$O^{13}CSe$	126.713 6	0.341 5	0.345 7	-1.24	
CO_2		43.068 1	0.158 0	$^{16}O^{12}C^{18}O$	45.648 8	0.164 2	0.162 6	0.95	34
				$^{16}O^{13}C^{18}O$	45.651 2	0.162 0	0.162 6	-0.36	
				$^{18}O^{12}C^{18}O$	48.464 6	0.170 9	0.167 5	1.97	
				$^{16}O^{13}C^{16}O$	43.068 1	0.156 0	0.158 0	-1.27	
				$^{18}O^{13}C^{18}O$	48.464 5	0.168 6	0.167 5	0.63	

dependence is consistent with a $\Delta k = \pm 3$ resonance, and introduction of the off-diagonal element Eq. (5) accounted for the observed shifts after the relative energies of the $(kl) = -2, -5, -8$, and -11 sublevels had been properly adjusted. This enabled

the determination of A_0 with high accuracy; Table II. Inspection of Fig. 6 proves that the $kl = -5$ and -8 sublevels of the $v_5 = 1$ state are indeed very close, with the former slightly below the latter, and strong interactions represented by the bold arrow are likely to occur. Weaker interactions shifting the $kl = -2$ and -11 sublevels to higher energy are also indicated.

An untruncated computer program kindly provided by L. Halonen and related to that previously described (*14*) was used for this purpose. The constant D_K^0 was not determined with significance by the experimental data. The results were confirmed with the program MILLI (*13*) truncated to $K - 9$, $K - 6$, $K - 3$, K, $K + 3$, $K + 6$, and $K + 9$ levels with A_0 fixed, and the results are quoted in Table III.

The $kl > 0$ sublevels of the $v_6 = 1$ state marked by broken lines, in particular those reached by $^R(P, Q, R)_3$ and $^R(P, Q, R)_6$ transitions, might in principle be similarly involved in $\Delta k = \pm 3$ perturbations and thereby sensitive to A_0. Our v_6 spectrum, however, did not give any evidence at all for such a perturbation, and we consider three reasons which may hide perturbation effects. First, the product $W_6^{K\pm3} \times (2k \pm 3)$ is likely to be significantly smaller than for v_5; second, the mostly affected (kl) sublevels are much closer in v_5 ($\Delta\nu = 0.021$ cm^{-1}) than in v_6 ($\Delta\nu = 0.046$ cm^{-1} at zeroth order); third, we have measured lines of v_5 more accurately and up to considerably higher J values than for v_6, keeping in mind the strong J dependence of the $\Delta k = \pm 3$ resonance.

Some information related to the hot bands $(2v_3 - v_3)$ and $(v_2 + v_3) - v_3$ which is confirmed by the previously investigated $2v_3$ and $v_2 + v_3$ state parameters is collected in Table IV. We note that the $(B' - B'')$ values of v_3 and $2v_3 - v_3$, $-0.267(1)$ and $-0.349(2) \times 10^{-4}$ cm^{-1}, are significantly different, their sum, $-0.616(3) \times 10^{-4}$ cm^{-1}, being quite close to that reported for $2v_3$, $-0.542(16) \times 10^{-4}$ cm^{-1} (*4*). We suppose that the values determined for the hot band reflect some anharmonic perturbation of $2v_3$ (1098 cm^{-1}) by v_1 (1063 cm^{-1}), the effective $(B_1 - B_0)$ value being -3.248×10^{-4} cm^{-1} (*4*).

Lists of observed and calculated wavenumbers have been deposited as supplementary material.[1]

VI. STRUCTURE

The B_0 rotational constant has been determined for the two isotopomers $F^{35}ClO_3$ and $F^{37}ClO_3$, so, using Kraitchman's equations (*15*, *16*), it is possible to determine the distance of the Cl atom from the center of mass of the molecule (i.e., the substitution coordinate of Cl). The result relative to the center of mass of $F^{35}ClO_3$ is $z_s(Cl) = 0.1538(78)$ Å. The error limit was estimated by the empirical rule proposed by Costain (*17*):

$$\sigma(z) = \frac{0.0012}{z_s}.$$

[1] Lists of observed and calculated wavenumbers (119 pp.) have been deposited in the Editorial Office of the *Journal of Molecular Spectroscopy* and may be obtained from Fachinformationszentrum Karlsruhe, D-7514 Eggenstein-Leopoldshafen, Germany, on submission of the names of the authors, the literature reference, and the registry number IRD-10043.

This error is very large, but, as shown by Van Eijck (*18*), it is an upper limit, and when the substitution of a heavy atom (like Cl) is involved, the error should be smaller (by a factor of 2 or more). Nevertheless the error remains large due to the fact that the Cl atom is near the center of mass. Furthermore, as only the ^{37}Cl isotopomer was studied, it is not possible to calculate the substitution coordinates of the F and O atoms.

On the other hand, we know three rotational constants, namely A_0 and B_0 for $F^{35}ClO_3$ and B_0 for $F^{37}ClO_3$. So we may calculate an r_0 structure. The results are collected in Table V. It may be noted that the values for the angle $\measuredangle$(OClO) and the Cl–O distance are in good agreement with the r_a structure determined by electron diffraction (*3*). These values agree also with those found by electron diffraction for the structurally related molecule Cl_2O_7, r(Cl–O) = 1.405(2) Å and $\measuredangle$(OClO) = 115.2(2)° (*19*). But the agreement is not as good for the r_0 and r_a(Cl–F) distances. It may be argued that the system of equations giving the r_0 structure is not well conditioned because the B_0 values of $F^{35}ClO_3$ and $F^{37}ClO_3$ give nearly the same equation. However, if we do not take into account $B_0(F^{37}ClO_3)$ and keep r_0(Cl–O) constant at 1.405 Å, we find the same value r_0(Cl–F) = 1.604 Å. Error limits cannot be given for the r_0 structure because we do not have enough data.

The axial rotational constant A_0 has been determined with high accuracy in the present work for the main isotopic species from $\Delta k = \pm 3$ perturbations within ν_5. Furthermore the rotation–vibration interaction constants α_v^A and α_v^B (Table V) are known from the present study, or from preliminary investigations of ν_1 and ν_4 (*10*), with an accuracy sufficient to calculate the equilibrium rotational constants A_e and B_e (Table V). If it were possible to estimate B_e for $F^{37}ClO_3$, an r_e structure could, in principle, be calculated. $FClO_3$ is a heavy-atom molecule and, in that case, the vibration–rotation contribution $\epsilon = I_0 - I_e$ to $I_0^B(F^{37}ClO_3)$ may be approximately estimated. For a diatomic molecule, ϵ is proportional to $I_e^{1/2}$ (*20*), and for a polyatomic molecule this proportionality remains approximately valid (*21*). So, we can write

$$\frac{\epsilon(\text{daughter})}{\epsilon(\text{parent})} \approx \sqrt{\frac{I_0(\text{daughter})}{I_0(\text{parent})}}.$$

We have checked this relation for some heavy-atom molecules for which the experimental ϵ values are known; see Table VI. It may be concluded that ϵ of a daughter molecule (or isotopomer) may be calculated with a relative accuracy of about 1%. This is often the same order of magnitude as the experimental uncertainty. In other words, this approximation is very good. Using $\epsilon(^{35}Cl) = 0.69124\mu$ Å^2, we find $\epsilon(^{37}Cl) = 0.69108\mu$ Å^2 and $I_e^B = 95.45872\mu$ Å^2. The resulting r_e structure is given in Table V. The θ_0 and θ_e angles are in good agreement. We have also $r_e < r_0$ with $r_o - r_e \leqq 6 \times 10^{-3}$ Å. This result seems at first sight satisfactory, but such a good agreement could be accidental because a variation of 1% for $\epsilon(^{37}Cl)$ induces changes of 0.6° for θ_e(OClO), 0.005 Å for r_e(Cl–O), and 0.017 Å for r_e(Cl–F). So it may be concluded that the derived r_e structure is not very accurate, with an error limit which can be as much as 0.02 Å for r_e(Cl–F). To improve the accuracy of the r_e structure, it would be necessary to study an isotopomer with at least one substituted oxygen.

ACKNOWLEDGMENTS

We thank Dr. G. Pawelke for the synthesis of various $FClO_3$ samples, K. Lattner for assistance in obtaining FT spectra, and Dr. L. Halonen for a computer program. Financial support by the Deutsche Forschungsgemeinschaft is gratefully acknowledged.

RECEIVED; February 11, 1991

REFERENCES

1. D. R. LIDE, JR., *J. Chem. Phys.* **43,** 3767–3768 (1965).
2. C. HELDMANN AND H. DREIZLER, *Z. Naturforsch. A; Phys.; Phys. Chem.; Kosmophys.* **45,** 811–813 (1990).
3. A. H. CLARK, B. BEAGLEY, D. W. J. CRUICKSHANK, AND T. E. HEWITT, *J. Chem. Soc. A* 872–875 (1970).
4. K. BURCZYK AND H. BÜRGER, *J. Mol. Spectrosc.* **118,** 288–297 (1986).
5. K. O. CHRISTE, E. C. CURTIS, W. SAWODNY, H. HÄRTNER, AND E. FOGARASI, *Spectrochim. Acta Part A* **37,** 549–556 (1981).
6. H. BÜRGER AND A. RAHNER, *in* "Vibrational Spectra and Structure" (J. R. Durig, Ed.), Vol. 18, p. 217, Elsevier, Amsterdam, 1990.
7. M. BIRK, M. WINNEWISSER, AND E. A. COHEN, *J. Mol. Spectrosc.* **136,** 402–445 (1989).
8. G. GUELACHVILI AND K. NARAHARI RAO, "Handbook of Infrared Standards," Academic Press, San Diego, 1986.
9. D. L. ALBRITTON, A. L. SCHMELTEKOPF, AND R. N. ZARE, *J. Mol. Spectrosc.* **67,** 132–156 (1977).
10. K. BURCZYK AND H. BÜRGER, unpublished results.
11. G. J. CARTWRIGHT AND I. M. MILLS, *J. Mol. Spectrosc.* **34,** 415–439 (1970).
12. Y. T. CHEN AND T. OKA, *J. Mol. Spectrosc.* **133,** 148–156 (1989).
13. C. BETRENCOURT-STIRNEMANN, G. GRANER, D. E. JENNINGS, AND W. E. BLASS, *J. Mol. Spectrosc.* **69,** 179–198 (1978).
14. G. L. CALDOW AND L. HALONEN, *Mol. Phys.* **46,** 223–237 (1982).
15. J. KRAITCHMAN, *Am. J. Phys.* **21,** 17–24 (1953).
16. C. C. COSTAIN, *J. Chem. Phys.* **29,** 864–874 (1958).
17. C. C. COSTAIN, *Trans. Am. Crystallogr. Assoc.* **2,** 157–164 (1966).
18. B. P. VAN EIJCK, *J. Mol. Spectrosc.* **91,** 348–362 (1982).
19. B. BEAGLEY, *J. Chem. Soc. Faraday Trans.* **60,** 1821–1830 (1965).
20. W. GORDY AND R. L. COOK, "Microwave Molecular Spectra," Chap. XIII, Wiley, New York, 1984.
21. J. DEMAISON AND L. NEMES, *J. Mol. Struct.* **55,** 295–299 (1979).
22. J. G. LAHAYE, R. VANDENHAUTE, AND A. FAYT, *J. Mol. Spectrosc.* **123,** 48–83 (1987).
23. M. OTAKE, C. MATSUMURA, AND Y. MORINO, *J. Mol. Spectrosc.* **28,** 316–324 (1968).
24. H. TAKEO AND R. F. CURL, *J. Mol. Spectrosc.* **43,** 21–30 (1972).
25. H. TAKEO, E. HIROTA, AND Y. MORINO, *J. Mol. Spectrosc.* **37,** 370–382 (1970).
26. J. LINDENMAYER, H. D. RUDOLPH, AND H. JONES, *J. Mol. Spectrosc.* **119,** 56–67 (1986).
27. G. CAZZOLI, C. DEGLI ESPOSTI, P. PALMIERI, AND S. SIMEONE, *J. Mol. Spectrosc.* **97,** 165–185 (1983).
28. C. DEGLI ESPOSTI, P. G. FAVERO, AND S. SERENELLINI, *J. Mol. Struct.* **82,** 221–236 (1982).
29. G. CAZZOLI, C. DEGLI ESPOSTI, AND P. G. FAVERO, *J. Mol. Struct.* **48,** 1–8 (1978).
30. G. CAZZOLI, P. G. FAVERO, AND C. DEGLI ESPOSTI, *Chem. Phys. Lett.* **50,** 336–338 (1977).
31. J. L. TEFFO AND A. CHEDIN, *J. Mol. Spectrosc.* **135,** 389–409 (1989).
32. C. DEGLI ESPOSTI, G. CAZZOLI, AND P. G. FAVERO, *J. Mol. Struct.* **109,** 229–238 (1985).
33. M. LE GUENNEC, G. WLODARCZAK, J. DEMAISON, H. BÜRGER, M. LITZ, AND H. WILLNER, to be published.
34. G. GRANER, C. ROSSETTI, AND D. BAILLY, *Mol. Phys.* **58,** 627–636 (1986).

2.2. Le fluorure de germyle

Nous avons analysé les spectres de rotation de l'état fondamental des cinq espèces isotopiques $^{70/72/73/74/76}GeH_3F$, dans les domaines millimétrique et submillimétrique jusque 1273 GHz.

La grande précision des constantes de rotation obtenues a permis de visualiser la variation de la coordonnée cartésienne de substitution du germanium en fonction de sa masse.

La structure à l'équilibre a également été déterminée après avoir analysé la variation de la correction vibrationnelle pour des molécules du type CH_3X et GeH_3X (X = F, Cl, Br, I).

JOURNAL OF MOLECULAR SPECTROSCOPY 150, 493–510 (1991)

The Millimeterwave Spectrum of Germyl Fluoride: Determination and Comparison of the Effective, Substitution, and Equilibrium Structures

M. LE GUENNEC, W. CHEN, G. WLODARCZAK, AND J. DEMAISON[1]

Laboratoire de Spectroscopie Hertzienne, UA CNRS 249, P5, Université de Lille I, 59655 Villeneuve d'Ascq Cedex, France

AND

R. EUJEN AND H. BÜRGER

FB9 Anorganische Chemie, Universität-Gesamthochschule Wuppertal, D-5600 Wuppertal, Federal Republic of Germany

The ground state rotational spectrum of germyl fluoride was measured up to 1273 GHz ($J \leq 63$). The rotational constants and quartic and sextic centrifugal distortion constants have been determined accurately for five isotopic species in natural abundance ($^{70/72/73/74/76}$Ge). The high accuracy of the rotational constants of these five isotopomers allowed us to study the mass dependence of the substitution coordinate of Ge. Equilibrium rotational constants of $^{74}GeH_3F$ were deduced with the help of the axial rotational constant and the rotation–vibration interaction constants determined by high resolution infrared spectroscopy. The r_0, $r_{s,I}$, and r_e structures of GeH_3F were determined. © 1991 Academic Press, Inc.

I. INTRODUCTION

The ground state rotational spectrum of germyl fluoride (GeH_3F) was first studied in the microwave range by Krisher *et al.* (*1*) who measured the $J = 1 \leftarrow 0$ transition for GeH_3F and GeD_3F. They also determined the dipole moment: $\mu = 2.33(6)$ D and an approximate r_0 structure. Later Cradock *et al.* (*2*) measured the microwave spectra of GeD_3F and $GeHD_2F$ and analyzed the infrared spectra in the GeH stretching region of the asymmetric species. The resulting A_0 and B_0 values have been combined with existing data on GeH_3F to give a r_0 and a r_z structure. More recently Cradock and Smith (*3*) have measured the ground state millimeterwave spectrum of the $^{74}GeH_3F$ isotopomer up to 300 GHz ($J \leq 14$). They could determine accurate quartic centrifugal distortion constants and approximate values for the sextic constants. The same authors have also analyzed the $v_3 = 1$, $v_6 = 1$, $v_2 = 1$ and $v_5 = 1$ excited states of $^{74}GeH_3F$ (*4*). Strong Coriolis x, y type perturbations between v_3 and v_6 and between v_2 and v_5 were analyzed. The infrared spectrum of monoisotopic $^{74}GeH_3F$ was also recently recorded with a high resolution Fourier transform (FTIR) spectrometer (*5, 6*). The

[1] To whom correspondence should be addressed.

0022-2852/91 $3.00

TABLE I

Measured Rotational Frequencies (MHz) of Germyl Fluoride in the Ground Vibrational State

J	K	freq.	e.-c.	J	K	freq.	e.-c.	J	K	freq.	e.-c.
	^{70}Ge			22	13	463252.35	-0.03	18	12	381161.41	-0.01
				22	12	463404.83	-0.01	18	9	381477.59	-0.02
0	0	20204.63	-0.10	22	9	463789.92	-0.06	18	6	381704.14	-0.01
17	17	362101.63	0.04	22	6	464065.91	-0.03	18	3	381840.35	-0.01
17	16	362258.28	0.07	22	3	464231.75	-0.10	18	1	381880.74	0.00
17	15	362405.65	0.03	22	2	464262.54	-0.06	18	0	381885.78	-0.02
17	14	362543.78	0.03	22	1	464280.99	-0.06	19	17	400434.54	0.03
17	13	362672.53	-0.02	22	0	464287.20	-0.01	19	16	400607.21	-0.01
17	12	362792.00	0.00	37	7	765379.7	-0.35	19	15	400769.75	-0.01
17	9	363093.76	0.00	37	6	765510.8	-0.43	19	14	400922.06	-0.01
17	7	363247.46	0.02	37	5	765622.8	0.50	19	13	401064.06	-0.05
17	6	363309.98	0.01	37	4	765713.4	0.17	19	12	401195.83	0.00
17	3	363440.00	0.05	37	3	765784.0	0.01	19	11	401317.17	-0.01
17	2	363464.07	0.02	37	2	765834.3	-0.25	19	10	401428.08	-0.02
17	1	363478.55	0.05	37	1	765864.9	0.01	19	9	401528.57	-0.01
17	0	363483.38	0.06	37	0	765874.6	-0.40	19	8	401618.58	0.00
18	18	382019.28	0.03	51	8	1044881.7	0.73	19	7	401698.04	-0.02
18	17	382194.17	-0.06	51	7	1045086.6	0.08	19	6	401766.99	-0.01
18	15	382515.10	0.01	51	6	1045265.2	0.40	19	5	401825.40	0.03
18	12	382922.84	-0.02	51	5	1045416.6	0.84	19	4	401873.14	-0.02
18	9	383241.31	-0.01	51	4	1045539.7	0.36	19	1	401952.86	0.00
18	6	383469.48	0.00	51	3	1045636.3	0.79	19	0	401958.19	0.03
18	3	383606.66	0.00	51	2	1045704.8	0.58	22	21	459489.16	-0.20
18	1	383647.37	0.03	51	1	1045745.6	0.15	22	18	460188.55	-0.03
18	0	383652.46	0.02	51	0	1045759.6	0.40	22	17	460398.70	0.03
19	19	401904.55	0.00	62	6	1263604.7	0.69	22	16	460597.14	-0.01
19	18	402098.83	0.02	62	5	1263785.7	0.06	22	15	460783.94	0.01
19	17	402282.94	-0.01	62	4	1263933.9	-0.44	22	14	460959.02	0.04
19	16	402456.94	0.03	62	3	1264049.6	-0.44	22	12	461122.20	0.00
19	15	402620.62	-0.01	62	2	1264132.3	-0.41	22	12	461273.60	0.04
19	14	402774.04	0.00	62	1	1264182.4	0.07	22	9	461655.97	0.01
19	13	402917.05	-0.06	62	0	1264197.9	-0.97	22	6	461929.95	0.01
19	12	403049.81	0.03					22	2	462125.23	0.04
19	11	403171.99	0.01					22	1	462143.52	0.00
19	10	403283.71	-0.01		^{72}Ge			22	0	462149.67	0.05
19	9	403384.91	-0.02					35	12	721046.8	-0.24
19	8	403475.57	0.01	0	0	20111.62	-0.04	35	10	721463.0	-0.05
19	7	403555.62	0.01	17	17	360437.66	0.03	35	9	721643.0	-0.02
19	6	403625.06	0.02	17	16	360593.16	0.03	35	8	721804.0	-0.21
19	5	403683.83	-0.01	17	15	360739.48	0.00	35	7	721946.4	-0.16
19	4	403731.98	0.02	17	14	360876.63	0.01	35	6	722070.2	0.17
19	1	403812.27	0.03	17	13	361004.53	0.02	35	5	722174.2	-0.38
19	0	403817.60	0.02	17	12	361123.10	-0.01	35	4	722260.0	-0.17
22	21	461607.72	0.03	17	9	361422.69	-0.02	35	3	722326.3	-0.47
22	20	461853.89	-0.07	17	6	361637.36	-0.02	35	2	722374.1	-0.26
22	19	462088.73	-0.02	17	3	361766.41	-0.03	35	1	722402.4	-0.52
22	18	462312.00	0.00	17	2	361790.32	-0.03	35	0	722412.0	-0.44
22	17	462523.60	-0.01	17	1	361804.73	0.02	51	10	1039596.3	-0.03
22	16	462723.52	0.00	17	0	361809.53	0.03	51	9	1039854.5	0.26
22	15	462911.66	-0.01	18	17	380437.97	-0.04	51	8	1040085.2	-0.04
22	14	463087.97	0.01	18	15	380756.57	0.01	51	7	1040289.2	-0.05

ν_2/ν_5 and ν_3/ν_6 systems were analyzed and J-dependent rotational constants were obtained from ground state combination differences. A_0 and D_K^0 were determined with the help of perturbation-allowed lines. In order to derive the equilibrium rotational constants A_e and B_e, the ν_1/ν_4 band, which is strongly perturbed, was also studied to some extent.

Despite this body of work, accurate rotational constants were not known for the other isotopomers of GeH_3F (^{70}Ge, ^{72}Ge, ^{73}Ge, and ^{76}Ge). And so, no accurate experimental structure could be determined. From the point of view of structure determination, it is interesting to study a molecule with many isotopomers because it permits one to calculate a more accurate structure or, at least, to estimate the accuracy of the derived structure. Germyl fluoride is particularly interesting because Ge has five isotopes whose natural abundance is greater than 7%. It is thus possible to measure

TABLE I—*Continued*

J	K	freq.	e.-c.	J	K	freq.	e.-c.	J	K	freq.	e.-c.
51	6	1040466.2	-0.01	19	1	401056.44	-0.03	11	6	240105.80	0.19
51	5	1040616.1	0.06	19	0	401061.73	-0.04	11	5	240140.60	0.16
51	4	1040738.9	0.20	22	12	460245.97	0.07	11	4	240168.90	-0.05
51	3	1040834.1	-0.05	22	11	460385.03	0.06	11	3	240191.20	0.06
51	2	1040902.3	-0.05	22	10	460512.02	-0.05	11	2	240207.10	0.10
51	1	1040943.3	0.02	22	9	460627.16	-0.03	11	1	240216.50	-0.01
51	0	1040956.9	-0.02	22	8	460730.24	-0.04	11	0	240219.70	0.02
59	6	1198682.2	-0.32	22	7	460821.25	-0.06	14	9	299912.39	-0.39
59	5	1198855.0	0.46	22	6	460900.24	-0.02	14	6	300090.07	-0.47
59	4	1198994.6	-0.76	22	5	460967.09	-0.02	14	4	300169.04	-0.65
59	3	1199105.5	0.56	22	4	461021.84	0.02	14	2	300217.03	-0.19
59	2	1199183.8	0.56	22	3	461064.40	0.01	14	1	300228.85	-0.26
59	1	1199229.9	-0.33	22	2	461094.83	0.02	17	17	358856.27	0.07
59	0	1199245.7	-0.19	22	1	461113.08	0.02	17	16	359010.73	0.06
				22	0	461119.16	0.01	17	12	359537.07	0.01
								17	9	359834.61	-0.02
	^{73}Ge							17	6	360047.81	-0.01
					^{74}Ge			17	3	360176.02	0.03
0	0	20066.46	-0.33					17	2	360199.78	0.02
17	9	360616.68	-0.08	0	0	20023.21	0.02	17	1	360214.00	-0.01
17	8	360697.59	-0.02	4	4	100090.82	0.10	17	0	360218.74	-0.02
17	7	360768.99	-0.01	4	3	100100.10	0.13	18	18	378596.43	0.06
17	6	360830.99	0.08	5	5	120092.30	-0.04	18	15	379085.35	0.02
17	5	360883.35	0.02	5	4	120106.60	-0.01	18	12	379487.43	-0.03
17	4	360926.28	0.04	5	3	120117.70	-0.01	18	9	379801.44	-0.05
17	3	360959.60	-0.02	5	2	120125.70	0.06	18	6	380026.47	-0.01
17	2	360983.44	-0.03	5	1	120130.40	0.00	18	4	380126.66	0.01
17	1	360997.76	-0.03	5	0	120132.00	0.01	18	1	380201.86	-0.01
17	0	361002.55	-0.01	8	7	180067.62	-0.07	18	0	380206.89	0.01
18	11	380426.62	0.02	8	6	180098.57	0.01	19	18	398496.25	0.06
18	10	380531.69	-0.10	8	5	180124.72	0.03	19	17	398677.77	-0.02
18	9	380626.95	-0.10	8	4	180146.16	0.08	19	16	398849.37	0.04
18	8	380712.38	0.03	8	3	180162.72	-0.01	19	15	399010.81	0.03
18	7	380787.72	0.04	8	2	180174.59	-0.04	19	14	399162.09	0.02
18	6	380853.05	0.05	8	1	180181.74	-0.02	19	13	399303.12	-0.04
18	5	380908.31	0.00	8	0	180184.10	-0.04	19	12	399433.95	-0.02
18	4	380953.59	0.01	9	9	199984.50	0.07	19	11	399554.48	-0.01
18	3	380988.82	0.00	9	8	200029.16	-0.04	19	10	399664.65	-0.02
18	2	381013.93	-0.05	9	7	200068.58	-0.15	19	9	399764.44	-0.02
18	1	381029.07	-0.01	9	6	200103.00	-0.02	19	8	399853.84	0.00
18	0	381034.08	-0.04	9	5	200132.12	0.06	19	7	399932.80	0.02
19	11	400422.68	0.15	9	4	200155.83	0.01	19	6	400001.21	-0.03
19	10	400533.26	0.06	9	3	200174.14	-0.18	19	5	400059.16	-0.05
19	9	400633.49	0.06	9	2	200187.51	-0.03	19	4	400106.65	-0.02
19	8	400723.24	0.05	9	1	200195.58	0.12	19	3	400143.61	0.01
19	7	400802.52	0.07	9	0	200198.22	0.11	19	2	400169.99	0.00
19	6	400871.25	0.06	11	11	239837.00	-0.17	19	1	400185.81	-0.01
19	5	400929.40	0.01	11	10	239903.30	-0.07	19	0	400191.08	-0.02
19	4	400977.05	0.03	11	9	239963.30	-0.04	22	22	457221.88	-0.01
19	3	401014.10	0.01	11	8	240017.00	-0.04	22	21	457476.01	0.02
19	2	401040.58	0.01	11	7	240064.70	0.23	22	20	457718.88	0.02

their rotational spectra in natural abunda .ce without too much difficulty. Another reason to determine the structure of germyl fluoride is that the equilibrium structures of germane, GeH_4 (*7*), and germyl chloride, GeH_3Cl (*8*), have been recently determined. Particularly the substitution coordinate of Ge in GeH_3Cl could be accurately determined and its variation with mass change analyzed. It would be very interesting to try such an analysis for the similar molecule GeH_3F.

The goals of the present study are:

(i) measurement of the millimeterwave spectra of natural GeH_3F in order to determine accurate ground state rotational and centrifugal distortion constants;

(ii) determination of the substitution coordinate of Ge and analysis of its mass dependence;

TABLE I—*Continued*

J	K	freq.	e.-c.	J	K	freq.	e.-c.	J	K	freq.	e.-c.
22	19	457950.43	0.01	63	1	1272487.9	0.26	19	5	398378.72	0.00
22	18	458170.24	-0.33	63	0	1272504.2	0.02	19	4	398425.87	0.00
22	17	458379.11	-0.14					19	3	398462.56	0.00
22	16	458576.41	0.02					19	2	398488.78	0.01
22	15	458761.91	-0.01			^{76}Ge		19	1	398504.53	0.03
22	14	458935.74	-0.04					19	0	398509.78	0.03
22	13	459097.86	-0.04	0	0	19939.14	0.11	22	21	455560.36	-0.19
22	12	459248.19	-0.04	17	17	357351.66	0.03	22	19	456031.79	-0.03
22	9	459628.00	-0.02	17	16	357505.10	0.03	22	18	456250.51	-0.01
22	6	459900.07	-0.05	17	15	357649.47	0.00	22	17	456457.83	0.01
22	3	460063.70	-0.01	17	14	357784.77	-0.02	22	16	456653.70	0.04
22	2	460094.03	-0.01	17	13	357910.98	0.01	22	15	456838.00	0.03
22	1	460112.24	0.00	17	12	358027.98	-0.01	22	14	457010.70	0.02
22	0	460118.30	-0.01	17	9	358323.56	-0.04	22	13	457171.74	0.00
37	10	758010.9	-0.37	17	6	358535.39	0.00	22	12	457321.08	-0.01
37	9	758199.8	0.03	17	3	358662.73	0.00	22	9	457698.39	0.01
37	8	758368.5	-0.10	17	2	358686.33	0.00	22	6	457968.73	0.02
37	7	758518.1	0.39	17	1	358700.50	0.00	22	3	458131.16	-0.07
37	6	758647.5	0.47	17	0	358705.24	0.02	22	2	458161.33	-0.02
37	5	758757.4	0.86	18	18	377009.49	-0.02	22	1	458179.45	0.02
37	4	758846.7	0.52	18	16	377342.86	0.01	22	0	458185.47	0.01
37	3	758916.4	0.46	18	15	377495.24	0.00	37	3	755731.2	-0.41
37	2	758966.3	0.52	18	12	377894.72	0.01	37	0	755821.3	0.55
37	1	758995.9	0.21	18	9	378206.66	-0.02	51	8	1031192.4	0.10
37	0	759006.1	0.44	18	6	378430.18	-0.02	51	7	1031393.4	-0.22
51	10	1035043.7	0.64	18	3	378564.58	0.00	51	6	1031568.1	-0.14
51	9	1035299.3	0.12	18	2	378589.50	0.01	51	5	1031716.1	0.01
51	8	1035528.7	0.12	18	1	378604.46	0.02	51	4	1031837.0	-0.13
51	7	1035732.0	0.83	18	0	378609.45	0.03	51	3	1031931.4	0.09
51	6	1035907.7	0.80	19	17	397006.01	-0.37	51	2	1031998.4	-0.21
51	5	1036056.3	0.62	19	16	397176.37	-0.43	51	1	1032039.2	0.20
51	4	1036177.7	0.21	19	15	397337.17	-0.01	51	0	1032052.6	0.14
51	3	1036272.6	0.33	19	14	397487.46	-0.01	59	6	1188443.2	0.02
51	2	1036339.9	-0.10	19	13	397627.60	-0.02	59	5	1188612.8	-0.13
51	1	1036380.4	-0.24	19	12	397757.58	-0.01	59	4	1188751.9	0.00
51	0	1036393.7	-0.49	19	11	397877.30	-0.01	59	3	1188860.2	0.17
63	6	1271909.2	0.05	19	10	397986.76	0.00	59	2	1188937.4	0.10
63	5	1272090.7	-0.14	19	9	398085.89	-0.02	59	1	1188983.5	-0.17
63	4	1272239.6	0.03	19	8	398174.70	0.00	59	0	1188999.2	0.07
63	3	1272355.0	-0.31	19	7	398253.10	-0.02				
63	2	1272437.0	-1.01	19	6	398321.11	-0.02				

(iii) estimation of the vibration–rotation interaction constants in order to be able to calculate equilibrium rotational constants;

(iv) determination of the effective, substitution, and equilibrium structures of germyl fluoride and comparison with those of GeH_4 and GeH_3Cl.

II. EXPERIMENTAL DETAILS

The sample of germyl fluoride was prepared as described previously (*9*).

Between 340 and 470 GHz a submillimeterwave source modulated spectrometer was used. The sources are two phase locked submillimeter BWOs (Thomson-CSF). The submillimeter power is optically focused through a free space absorption cell (length 1 m) and detected by a He-cooled InSb detector. After phase-sensitive detection, the signal is processed in the usual way by a microcomputer, which calculates the line frequency after averaging. The accuracy of the measurements is better than 50 kHz for the lines that are not significantly broadened by the nonresolved quadrupole hyperfine structure (due to the ^{73}Ge nucleus).

Above 470 GHz a new FIR laser sidebands spectrometer was used. It is a considerably modified and improved version of the spectrometer described in Ref. (*10*). The FIR laser is 2.40 m long and 38 mm bore. It is pumped by a commercial CO_2 laser (PL6 model from Edinburgh Instruments) which can deliver a maximum output power of 200 W. A FIR power of 10 mW or more is obtained with about 35 laser lines. The FIR radiation is mixed with a tunable microwave radiation (2–20 GHz) on a Schottky diode to produce tunable sidebands. After the absorption cell a heterodyne detection of the sidebands is used. The noise temperature of the receiver is about 100 000 K. The FIR molecular laser lines used for the measurements are (in MHz): HCOOH emissions at 716156.8, 761608.3; CH_2F_2 at 1035552.7, 1042150.4, 1267081.5; and CH_3OH at 1193727.3. The frequencies are taken from Ref. (*11*). The accuracy of the measurements is about 1 MHz, partly due to the knowledge of the frequency of the FIR molecular lines. It is possible to improve the accuracy of the measured frequencies by repeating the measurements several times after detuning and retuning the spectrometer. The measured frequencies are listed in Table I. The $J = 1 \leftarrow 0$ transitions were taken from Ref. (*1*), and for $^{74}GeH_3F$, the measurements between 100 and 300 GHz were taken from Ref. (*3*).

III. ANALYSIS OF THE SPECTRA

The assignment was relatively straightforward because the spectra are strong and not too dense. Moreover, good starting values of the rotational constants were already known (*1, 3*). The frequency of a rotational transition $J+1, K \leftarrow J$, K in the ground vibrational state of a C_{3v} symmetric top molecule may be written as

$$\nu_0 = 2B(J+1) - 4D_J(J+1)^3 - 2D_{JK}(J+1)K^2 + H_J(J+1)^3 \times [(J+2)^3 - J^3] + 4H_{JK}(J+1)^3K^2 + 2H_{KJ}(J+1)K^4. \quad (1)$$

A weighted least-squares program was used to fit the experimental frequencies of Table I to the parameters of Eq. (1). To check the internal consistency of the derived parameters, we have plotted B, D_J, and D_{JK} versus the mass of the atom Ge. This simple method was found powerful to eliminate transitions affected by a systematic deviation. The accuracy of the sextic constants is not good enough to point out an isotopic dependence. The derived parameters are listed in Table II. For $^{74}GeH_3F$, they are in rather satisfactory agreement with the GSCD (Ground state combination differences) constants from FTIR spectroscopy (*5*) although the difference between the two B_0 values is 14 kHz (see Table III), which is much greater than the standard deviation, 2 kHz, of the FTIR value. But this standard deviation is obtained from the least-squares fit and it does not take into account either the error of calibration (about 3 kHz with regard to B) or the uncertainty in the wavenumbers of N_2O and OCS (contributions: about 1 kHz on B). So a conservative estimate of the uncertainty of the FTIR value of B is about 6 kHz. We have finally determined the constants of $^{74}GeH_3F$ by a merged least-squares fit of the rotational and GSCD constants. The results are reported in Table III. For $^{73}GeH_3F$, it was not possible to measure transitions at frequencies higher than 500 GHz, so the constant H_J could not be determined and was fixed at the mean value of the other isotopomers. It was checked that a fit with

TABLE II

Ground State Molecular Constants of Germyl Fluoride

Species	$^{70}GeH_3F$	$^{72}GeH_3F$	$^{73}GeH_3F$	$^{74}GeH_3F$	$^{76}GeH_3F$
Abundance %	20.5	27.4	7.8	36.5	7.8
B/MHz	10 102.38154 (67)	10 055.84597 (55)	10 033.40978 (143)	10 011.61437 (51)	9 969.53309 (46)
D_J/kHz	8.67481 (81)	8.61293 (69)	8.57988 (167)	8.54396 (69)	8.48498 (59)
D_{JK}/kHz	134.1333 (47)	133.1853 (43)	132.9909 (288)	132.2718 (48)	131.4019 (32)
H_J/mHz	-4.159 (128)	-3.012 (118)	-3.5[a]	-3.642 (109)	-2.961 (101)
H_{JK}/Hz	0.3598 (48)	0.3666 (35)	0.6594 (319)	0.3673 (55)	0.3579 (31)
H_{KJ}/Hz	3.7770 (92)	3.7633 (110)	3.2100 (147)	3.6968 (75)	3.6922 (75)
No. Data	81	80	48	126	74
$\rho(D_J, H_J)$	0.98	0.98	–	0.96	0.98

The uncertainties shown in parentheses are in units of the last digit and are standard deviations.
[a]) Fixed at the mean value of the other isotopomers, see text.

H_J fixed at zero gives practically identical results. The constant H_{JK} is very different from that of the other isotopomers. In fact, a fit with H_{JK} fixed at the value (0.3673 Hz) of the $^{74}GeH_3F$ species is only slightly worse, the calculated values of the high K lines being affected by a small systematic deviation. In that case, the derived value for H_{KJ} is 3.568 Hz, in better agreement with the values found for the other isotopomers. H_{JK} is mainly determined by these high K transitions, which are broadened by the nonresolved quadrupole hyperfine structure due to the ^{73}Ge nucleus. This broadening induces a small asymmetry in the line profile (see Fig. 1) and, therefore, the frequencies are affected by a small systematic error which takes effect on H_{JK} and H_{KJ}. So, these two parameters should be considered only as fitting parameters. It was checked that this effect has no significant influence on the value of B. This surprisingly substantial value of a frequency shift due to the nonresolved quadrupole structure may in fact be explained by the high value of the ^{73}Ge nuclear spin ($I = 9/2$), which implies many components of about the same intensity.

IV. EFFECTIVE STRUCTURE

In addition to the five B rotational constants determined in this work, the axial rotational constant A was determined by FTIR spectroscopy (*5*) for the main isotopic

TABLE III

Rotational Constants, Centrifugal Distortion Constants, and Correlation Matrix for the Ground State of $^{74}GeH_3F$

	MW[a]	FTIR[b]	merged fit						
B/MHz	10011.61437 (51)	10011.6288 (18)	10011.61240 (42)	1.000					
D_J/kHz	8.54396 (69)	8.54783 (11)	8.54003 (49)	0.822	1.000				
D_{JK}/kHz	132.2718 (48)	132.170 (33)	132.2752 (44)	0.541	0.322	1.000			
H_J/mHz	-3.64 (11)	-2.86 (19)	-4.212 (84)	0.725	0.945	0.178	1.000		
H_{JK}/Hz	0.3673 (55)	0.3398 (82)	0.3663 (43)	0.403	0.480	0.708	0.316	1.000	
H_{KJ}/Hz	3.6968 (75)	3.83 (11)	3.6987 (68)	0.149	-0.163	0.357	-0.125	-0.125	1.000

[a]) from rotational transitions, this work.
[b]) from ground state combination differences, Ref. (5).

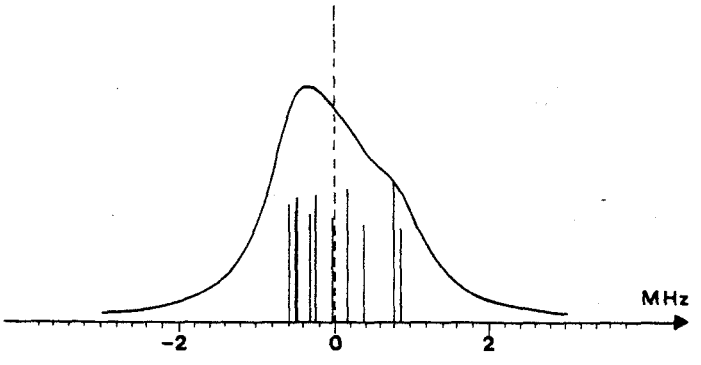

FIG. 1. Simulated line profile of the $J = 22$, $K = 12$ transition of $^{73}GeH_3F$. The dashed line represents the unperturbed frequency. The quadrupole hyperfine structure was calculated with $eQq(^{73}Ge) = -93$ MHz.

species $^{74}GeH_3F$. B rotational constants are also known for GeD_3F and approximate values of A, B, and C have been obtained for $GeHD_2F$ (*3*). These data are summarized in Table IV. Cradock *et al.* (*2*) estimate that the accuracy of $A(GeHD_2F)$ is about 50 MHz. In fact if we compare his proposed values for $A(GeH_3F)$ and $A(GeH_3Cl)$ with those determined from high resolution spectroscopy, we find a deviation of about 150 MHz. Furthermore, Mallinson (*12*) has found for CH_2DI and CHD_2Cl that the A constant derived from microwave spectroscopy is about 90 MHz higher than the

TABLE IV

Ground State Rotational Constants of Germyl Fluoride Used in the Structural Calculations

Isotopomer		Value (MHz)	Estimated accuracy	Ref.
$^{74}GeH_3F$	A	78149.6	0.15	a
	B	10011.61437	0.00051	b
$^{70}GeH_3F$	B	10102.38154	0.00067	b
$^{72}GeH_3F$	B	10055.84597	0.00055	b
$^{73}GeH_3F$	B	10033.40978	0.00143	b
$^{76}GeH_3F$	B	9969.53309	0.00046	b
$^{70}GeHD_2F$	A	47164	300	c
	B	9680.81	0.2	c
	C	9284.8	0.2	c
$^{72}GeHD_2F$	A	47164	300	c
	B	9641.93	0.2	c
	C	9249.23	0.2	c
$^{74}GeHD_2F$	A	47164	300	c
	B	9604.93	0.2	c
	C	9215.33	0.2	c
$^{70}GeD_3F$	B	9199.47	0.1	c
$^{72}GeD_3F$	B	9166.04	0.1	c
$^{74}GeD_3F$	B	9134.23	0.1	c
$^{76}GeD_3F$	B	9103.9	0.1	c

[a]) Ref. (**6**). [b]) This work. [c]) Ref. (**2**).

TABLE V

Numerical Values Used in Converting Rotational Constants into Distances

B * I	505379 uÅ2
^{70}Ge	69.9242498
^{72}Ge	71.92208
^{73}Ge	72.9234639
^{74}Ge	73.9211788
^{76}Ge	75.92114027
H	1.007825037
D	2.014101787
F	18.99840325

From Ref. (27).

infrared value. A similar difference (87 MHz) is found for CHD_2CN if we compare the infrared value (*13*) and the microwave value (*14*) of the *A* constant. This difference is explained by the neglect of the centrifugal distortion in the infrared analysis and by the use of *Q*-branch maxima rather than *Q*-branch origin (*12*). This explanation remains very probably valid for $GeHD_2F$. So, we choose 300 MHz as a conservative estimate of the uncertainty on $A(GeHD_2F)$. There are 19 experimental moments of inertia to determine two independent interatomic distances and one angle. A weighted least-squares fit was used (program Ru 111, author: H. D. Rudolph). The fundamental constants and atomic masses used are given in Table V and the results are reported in Table VI. The weight assigned to each moment of inertia was the inverse of its experimental variance. As a consequence, the residuals corresponding to the GeH_3F

TABLE VI

Structure of GeH_3F

	r_0	$r_{e,I}$	r_e	ab initio[a]
r(Ge-F)	1.734026(67)	1.73008(12)	1.730945(40)	1.697
r(Ge-H)	1.52427(23)	1.52529(51)	1.51453(13)	1.529
∠(F-Ge-H)	106.370(28)	105.466(35)	106.071(17)	107.8
ε_A		-1.0671(68)		
ε_B		0.2801(69)		
σ[b]	60	2.5	0.5	

a) Ref. (24)
b) Standard deviation of unit weight.

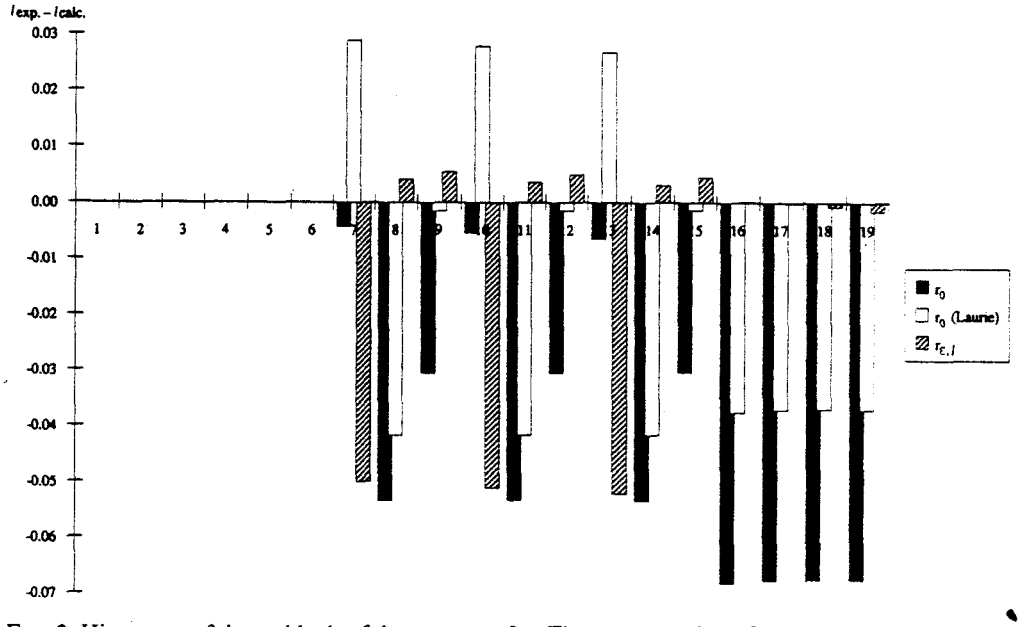

FIG. 2. Histogram of the residuals of the structure fits. The numerotation of the data corresponds to that of Table VII.

species are much smaller because the corresponding experimental moments of inertia are much more accurate (See Table VII and Fig. 2). The derived r_0 parameters seem very accurate as shown by their small standard deviation. But, in fact, the standard deviation of unit weight is high: $\sigma = 60$. This indicates that the fit is not satisfactory and that the experimental data are probably affected by a systematic deviation (or that the model is not correct), which is confirmed by the examination of the residuals of the fit, see Table VII and Fig. 2. This is not surprising because it is well known that when the vibrational contribution to the moment of inertia is neglected, a systematic error is introduced which is many orders of magnitude greater than the experimental error (*15*). One well established consequence of these vibration–rotation interactions is that the effective structure is mass dependent. Large variations in bond distances X–H can occur when D is substituted for H. The following empirical relation (*16*) has been suggested to take this effect into account:

$$r_0(X - H) = r_0(X - D) + \eta \quad \text{with } 0.003 \leqslant \eta \leqslant 0.005\text{Å}. \tag{2}$$

This effect has been particularly studied for the C–H bond, and recently a bond elongation parameter of 0.0028 Å has been proposed for this bond in order to determine r_m^ρ structures (*17*). This bond shortening on deuteration also occurs for the Ge–H bond. Comparison of the effective structures of GeH_4 and GeD_4 (*7*) shows that r_0(Ge–H)-r_0(Ge–D) = 0.003 Å. Introduction of this constraint into the least-squares fit lowers somewhat the standard deviation of unit weight, $\sigma = 34$, as well as the residuals (Fig. 2). The derived parameters are not significantly modified but their corresponding standard deviations are lowered by a factor of two. However, this constraint is clearly not sufficient to obtain a good fit. It is, however, easy to significantly improve the

TABLE VII

Residuals of the Structure Calculations

				$I_{exp.} - I_{calc.}$			
Isotopomer	axis	N°	$I_{exp.}$	r_0	r_0[a]	$r_{\epsilon,I}$	r_c
$^{74}GeH_3F$	A	1	6.466 815	0.000 080	0.000 042	0.000 000	0.000 000
	B	2	50.479 272	-0.000 015	-0.000 006	0.000 005	-0.000 001
$^{70}GeH_3F$	B	3	50.025 729	0.000 158	0.000 091	0.000 010	0.000 490
$^{72}GeH_3F$	B	4	50.257 234	0.000 051	0.000 023	-0.000 012	0.000 199
$^{73}GeH_3F$	B	5	50.369 616	0.000 009	-0.000 001	-0.000 012	0.000 132
$^{76}GeH_3F$	B	6	50.692 344	-0.000 098	-0.000 053	0.000 001	-0.000 246
$^{70}GeHD_2F$	A	7	10.715 355	-0.004 456	0.028 867	-0.050 143	0.017 984
	B	8	52.204 206	-0.053 615	-0.041 881	0.004 111	-0.015 896
	C	9	54.430 790	-0.030 755	-0.001 604	0.005 478	0.023 787
$^{72}GeHD_2F$	A	10	10.715 355	-0.005 578	0.027 755	-0.051 262	0.016 880
	B	11	52.414 714	-0.053 525	-0.041 782	0.003 649	-0.016519
	C	12	54.640 116	-0.030 725	-0.001 574	0.004 953	0.023 299
$^{74}GeHD_2F$	A	13	10.715 355	-0.006 645	0.026 697	-0.052 325	0.015 831
	B	14	52.616 625	-0.053 574	-0.041 822	0.003 070	-0.016 758
	C	15	54.841 118	-0.030 616	-0.001 466	0.004 528	0.022 801
$^{70}GeD_3F$	B	16	54.935 665	-0.068 315	-0.037 771	0.000 121	-0.000 409
$^{72}GeD_3F$	B	17	55.136 024	-0.067 780	-0.037 245	-0.000 176	-0.000 164
$^{74}GeD_3F$	B	18	55.328 035	-0.067 643	-0.037 118	-0.000 838	-0.000 703
$^{76}GeD_3F$	B	19	55.512 363	-0.067 694	-0.037 177	-0.001 657	-0.001 468

[a] r_0 structure with Laurie correction, eq. (2) of text.

results of the calculation by supposing that the vibration–rotation constant ϵ_g is independent of the particular isotopomer for a given axis g. Rudolph (*15*) has labeled the derived structure $r_{\epsilon,I}$ and has shown that it is at least as good as (and often better than) the r_s structure. The results are also reported in Table VI and the residuals in Table VII and Fig. 2. The standard deviation of unit weight is this time much lower: $\sigma = 2.4$. There remain only three big residuals which correspond to the A rotational constants of the three $GeHD_2F$ species. These high residuals may be explained by the fact that the accuracy of A is rather poor and by the fact that A is very sensitive to the hydrogen coordinates, which are not expected to be determined accurately by this method (the assumption ϵ_A = constant is not a good one when D is substituted for H).

V. SUBSTITUTION STRUCTURE

It is not possible to determine a complete substitution structure using Kraitchman's equations (*18*) because fluorine is monoisotopic. This does not matter, because it was shown by Rudolph (*15*) that the $r_{\epsilon,I}$ structure (preceding section) is equivalent to the r_s structure. Nevertheless it is interesting to determine the substitution coordinate of Ge because it can be done in many different ways. The atomic cartesian coordinates of Ge are given in Table VIII. Examination of this table shows that the coordinate increases with the mass of germanium; see also Fig. 3 where $[z_s(i)]^2$ is plotted versus

TABLE VIII

Substitution Coordinates of Ge in GeH_3F (in Å)

Substituted atom	Parent 70	72	73	74	76
70		-0.336 69	-0.333 11	-0.329 61	-0.322 82
72	-0.344 17		-0.333 22	-0.329 70	-0.322 90
73	-0.344 22	-0.336 85		-0.329 73	-0.322 94
74	-0.344 26	-0.336 87	-0.333 27		-0.322 98
76	-0.344 34	-0.336 95	-0.333 35	-0.329 86	
70		-0.329 37	-0.329 54	-0.329 61	-0.329 55
72	0.000 99		-0.329 64	-0.329 70	-0.329 64
73	0.000 94	0.000 33		-0.329 73	-0.329 67
74	0.000 90	-0.002 34	0.000 17		-0.329 72
76	0.000 82	-0.007 09	0.000 08	0.000 00	

Upper part: origin at the center of mass of the parent species.
Lower right triangle: z_s with origin at the center of mass of $^{74}GeH_3F$.
Lower left triangle: difference $z_s - z_s(74 \rightarrow 76)$.

Δm_i, the change in mass of atom i. This effect may be analyzed using the theory of the r_m structure of Watson (*19*). Retaining Watson's notations, the substitution coordinate of atom i may be written as

$$[z_s(i)]^2 = \frac{I'_0 - I_0}{\mu_i}, \tag{3}$$

where μ_i is the reduced mass. As $I_0 = I_e + \epsilon$, the equilibrium coordinate may be written

$$[z_e(i)]^2 = \frac{I'_e - I_e}{\mu_i} = [z_s(i)]^2 + \frac{\epsilon' - \epsilon}{\mu_i}. \tag{4}$$

If we assume that $\epsilon' - \epsilon$ can be expanded in a Taylor series, we obtain

$$[z_s(i)]^2 = [z_e(i)]^2 + \frac{\partial \epsilon}{\partial m_i} + \left[\frac{1}{2}\frac{\partial^2 \epsilon}{\partial m_i^2} + M^{-1}\frac{\partial \epsilon}{\partial m_i}\right]\Delta m_i. \tag{5}$$

A linear least-squares fit allows us to determine for each isotopomer k the value:

$$p_k = \left[\frac{1}{2}\frac{\partial^2 \epsilon}{\partial m_i^2} + \frac{1}{M_k}\frac{\partial \epsilon}{\partial m_i}\right] \tag{6}$$

see Table IX. The M^{-1} dependence of p_k is apparent on Fig. 4 where p_k is plotted versus M^{-1}. So it is possible to determine separately $\partial\epsilon/\partial m_i$ and $\partial^2\epsilon/\partial m_i^2$. Although the results are not accurate, it appears that $(\partial^2\epsilon/\partial m_i^2) = -3.4 \times 10^{-5}$ and M^{-1}

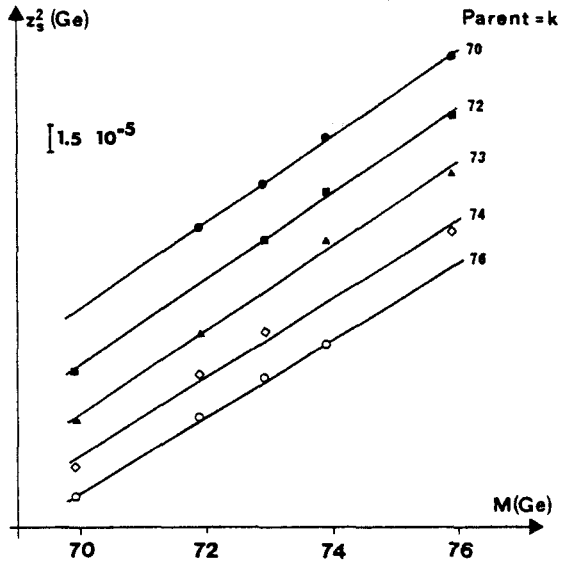

FIG. 3. Substitution coordinate z_s^2 of Ge vs. mass of isotopic species for different parent molecules.

$(\partial\epsilon/\partial m_i) = 4.5 \times 10^{-5}$ are of the same order of magnitude, but in that particular case of opposite sign. It is also possible to calculate

$$z_s - z_e \approx \frac{1}{2z_e}\frac{\partial\epsilon}{\partial m_i} = 0.005(1)\text{Å}. \tag{7}$$

This value seems to be very large, but it is due mainly to the fact that z_e is small. In fact values of the same order of magnitude are obtained for OCS (see Table X) and many other molecules. It confirms the empirical rule of Costain (*20*) which shows that the error for the substitution coordinate is inversely proportional to z:

TABLE IX

Coefficients of the Equation $[z_s(i)]^2 = a_k + p_k \Delta m_i^a$

parent = k	$z_e^2 + \partial\epsilon/\partial m_i$ (Å2)	$p_k * 10^5$ (u^{-1}Å2)
70	0.116281(51)	3.008(69)
72	0.111295(67)	2.966(93)
73	0.108933(96)	2.906(132)
74	0.106756(115)	2.700(160)
76	0.102343(55)	2.678(84)

derived parameters:

$\frac{\partial^2\epsilon}{\partial m_i^2} = -1.7(11)\cdot 10^{-5}$

$\frac{\partial\epsilon}{\partial m_i} = 0.00333(84)$

[a] $p_k = \left[\frac{1}{2}\frac{\partial^2\epsilon}{\partial m_i^2} + \frac{1}{M_k}\frac{\partial\epsilon}{\partial m_i}\right]$

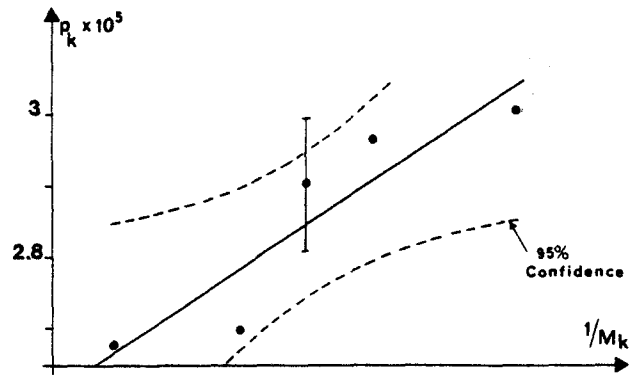

FIG. 4. Plot of $p_k = [\frac{1}{2}(\partial^2\epsilon/\partial m_i^2) + (1/M_k)(\partial\epsilon/\partial m_i)]$ vs. $(1/M_k)$. Data from Table IX.

$$\sigma(z) = \frac{K}{z}. \tag{8}$$

For GeH_3Cl a plot of $[z_s(i)]^2$ versus Δm_i did not give a straight line (*8*), which is very surprising. But a careful examination of the data of Ref. (*8*) shows that if we eliminate the ^{76}Ge data, a straight line is also obtained. Trying to explain the abnormal behavior of $^{76}GeH_3Cl$, we have made a new fit of the experimental frequencies and we have searched for possible outliers, but we could not find any, although the fit of the $^{76}GeH_3Cl$ species is definitely worse than that of the other species. To explain this discrepancy, it would probably be necessary to perform new measurements. For both GeH_3F and GeH_3Cl, $(\partial^2\epsilon/\partial m_i^2)$ and M^{-1} $(\partial\epsilon/\partial m_i)$ are of the same order of magnitude, but for GeH_3F $[z_s(i)]^2$ increases with the germanium mass because

$$\frac{1}{M}\frac{\partial\epsilon}{\partial m_i} > \frac{1}{2}\left|\frac{\partial^2\epsilon}{\partial m_i^2}\right|,$$

whereas the contrary is true for GeH_3Cl. This may be simply explained by the fact that the molecular mass M of GeH_3Cl is greater than that of GeH_3F.

TABLE X

Values of $\partial\epsilon/\partial m$ and $|z_s| - |z_e|$ for Some Molecules

		$\partial\epsilon/\partial m$	$\lvert z_s\rvert$	$\lvert z_s\rvert - \lvert z_e\rvert$	Ref.
OCS	O	0.0056	1.682	0.0017	28
	C	-0.0026	0.521	-0.0025	
	S	0.0020	1.038	0.0010	
OCSe	O	0.0086	2.251	0.0019	29
	C	-0.0031	1.094	-0.0014	
	Se	0.0006	0.6151	0.0005	
FCN	N	0.0022	1.332	0.0008	30
	C	-0.0012	0.173	-0.0036	
HNC	H	-0.0246	1.470	-0.0084	31
	N	0.0024	0.484	0.0024	
	C	0.0015	0.688	0.0011	
GeH_3Cl	Cl	0.0062	1.489	0.0021	8
	Ge	0.0013	0.659	0.0010	

TABLE XI

Vibrational Corrections for GeH_3F

	A(MHz)		B(MHz)
α_1	710.84(21)		4.05(1)
α_2	-293.128(21)		17.301(2)
α_3	32.4795(90)		68.8920(6)
α_4	513.12(24)		-0.31(1)
α_5	341.587(12)		-16.671(1)
α_6	-311.3465(60)		20.2585(12)
Ao	78149.60(15)	Bo	10011.6144(18)
Ae	78918.06(30)	Be	10060.013(16)

VI. EQUILIBRIUM STRUCTURE

For $^{74}GeH_3F$, the axial rotational constant A and the vibrational corrections α^A and α^B have been determined by FTIR spectroscopy (*6*). The corresponding equilibrium rotational constants may be derived, see Table XI. However, there are only two data to determine three geometrical parameters. It is known that for diatomic molecules (*21*)

$$\epsilon = I_0 - I_e \text{ varies like } I^{1/2}. \tag{9}$$

This behavior was shown to remain statistically valid for polyatomic molecules (*22*). But its validity is only a statistical one and it has to be checked for each type of molecule. It was recently shown that Eq. (9), rewritten under the more convenient form (10),

$$\epsilon' = \epsilon \sqrt{\frac{I'}{I}}, \tag{10}$$

may be used to calculate the vibrational correction ϵ' of isotopomers of heavy atom molecules (molecules without hydrogen) with an accuracy better than 4% (*23*). It is worth noting that ϵ is itself only a small (3 to 5%) correction to I. This approximation was used to determine the structure of $FClO_3$ which, like GeH_3F, had only two equilibrium rotational constants known. To check if Eq. (10) may also be used for GeH_3F, we have used it for CH_3X (X = F, Cl, Br, I) molecules and for GeH_3Cl, see Table XII. It appears that it also works correctly for that type of molecules. So, it seems that it can be applied with confidence in the case of GeH_3F. Using Eq. (10), the vibrational corrections were calculated for the isotopomers of GeH_3F, and the results are summarized in Table XIII. Then a weighted least-squares method was used to calculate the r_e structure of GeH_3F (Table VI). The weight assigned to each moment of inertia was the inverse of the square of the uncertainty, whose main contribution comes from the inadequacy of Eq. (10).

TABLE XII

Vibration–Rotation Interaction Constants (in MHz) for Some XH_3Y Molecules

Molecule	Axis	α exp.	α calc.[a]	Δα/α	Ref.
CH_3F	A	2517			32
	B	243			
CH_2DF	A	1704	1702	0.12	
	B	209	222	-6.22	
	C	223	208	6.73	
CD_3F	A	933	897	3.86	
	B	179	174	2.79	
CH_3Cl	A	1863			33
	B	119			
CHD_2Cl	A	894	891	0.34	
	B	89	98	-10.11	
	C	92	94	-2.17	
CD_3Cl	A	670	663	1.04	
	B	80	88	-10.00	
CH_3Br	A	1988			34
	B	83			
CD_3Br	A	747	707	5.35	
	B	58	60	-3.45	
CH_3I	A	1756			b
	B	63			
CHD_2I	A	1239	1179	4.84	
	B	53	56	-5.66	
	C	55	55	0.00	
CD_3I	A	703	656	6.69	
	B	42	45	-7.14	
$^{74}GeH_3Cl$	A	744			8
	B	17.62			
$^{74}GeHD_2Cl$	A	429[c]	348	18.88	
	B	15	17	-13.33	
	C	16	16	0.00	
$^{74}GeD_3Cl$	B	14	16	-14.29	
$^{70}GeH_3Cl$	B	17.97	18	-0.17	
$^{72}GeH_3Cl$	B	17.81	17.8	0.06	
$^{73}GeH_3Cl$	B	17.71	17.7	0.06	
$^{76}GeH_3Cl$	B	17.5	17.4	0.57	

[a]) Calculated with eq. (10).
[b]) New value determined in this work.
[c]) The uncertainty on this value is about 150 MHz.

In this work, higher-order effects have been neglected. However, it is well established that some of these effects are not necessarily negligible (*35*). In particular, the electrons of each bonded atom must not be concentrated at the nucleus. This effect could be important essentially for the axial rotational constant A. The constant which should be used for a structure determination may be expressed as (*35*):

$$A = A_{\text{eff}}\left(1 - \frac{g_{aa}}{1836}\right) \tag{11}$$

where A_{eff} is the experimental constant of rotation and g_{aa} the corresponding molecular rotational g factor, which may be determined by Zeeman spectroscopy. The rotational Zeeman spectrum of GeH_3F was not yet investigated. But it has been observed that the g_{aa} factor remains approximately constant for the C_{3v} molecules CH_3X (X = H,

TABLE XIII

Equilibrium Rotational Constants of Germyl Fluoride Used in the Structural Calculations (All Values in MHz)

Isotopomer		Value	Estimated accuracy	exp. - calc.
$^{74}GeH_3F$	A	78918.06	0.15	0.0006
	B	10060.013	0.016	0.0001
$^{70}GeH_3F$	B	10151.44	0.5	-0.0100
$^{72}GeH_3F$	B	10104.57	0.5	-0.0403
$^{73}GeH_3F$	B	10081.96	0.5	-0.0266
$^{76}GeH_3F$	B	10017.63	0.5	0.0489
$^{70}GeHD_2F$	A	47524	300	-81
	B	9726.83	3	2.97
	C	9328.03	3	-4.10
$^{72}GeHD_2F$	A	47524	300	-76
	B	9687.67	3	3.07
	C	9292.21	3	-3.98
$^{74}GeHD_2F$	A	47524	300	-71
	B	9650.41	3	3.09
	C	9258.07	3	-3.87
$^{70}GeD_3F$	B	9242.10	2	0.07
$^{72}GeD_3F$	B	9208.44	2	0.03
$^{74}GeD_3F$	B	9176.41	2	0.12
$^{76}GeD_3F$	B	9145.87	2	0.24

F, Cl, Br, I, C ≡ CH) and SiH_3X (X = H, Br). This should remain valid for GeH_3X. In fact, the molecular beam magnetic resonance method was used to determine the rotational g factor of GeH_4 (*36*): $g = -0.10815$ nuclear magnetons. The correction to the rotational constant A is +4.6 MHz, not negligible indeed. But it has no significant effect on the derived r_e structure. The new r_e structure with this correction taken into account is: r_e(GeF) = 1.730945(40) Å, r_e(GeH) = 1.51451(13) Å, and ∠(FGeH) = 106.073(17)°.

The ab initio structure of GeH_3F was recently calculated at the Hartree–Fock level using effective core potentials and polarized double-zeta basis sets for valence electrons (*24*). The ab initio results are also given in Table VI. The calculated Ge–H bond length is slightly too long, by 0.01 Å. The computed angle is within 2° of the r_e value. Comparison of the experimental structures of Table VI shows that the $r_{\epsilon,I}$ distance of Ge–F is closer to the r_e value than to r_0, whereas the contrary is true for the Ge–H distance. This result is not surprising because it is a well established fact that the substitution coordinates (r_s as well as $r_{\epsilon,I}$) of H atoms are often less accurate than the r_0 ones (*21*). The value of $r_0 - r_e$ is 0.0031 Å for Ge–F and 0.0048 Å for Ge–Cl (*8*). For the Ge–H distance, the $r_0 - r_e$ value is 0.0093 Å in GeH_3F and 0.0087 Å in GeH_4 (*7*). Furthermore the r_e (Ge–H) distance is very close to that found for GeH_4, 1.51635(17) Å, and for GeH_3Cl, 1.51559(63) Å. The small variation of the Ge–H bond length in GeH_3X (X = H, Cl, F) may be simply explained by the electronegativity

change of the X substituent. Indeed it has been observed that substitution by electronegative atoms often shortens the neighboring bonds (*25*). The bond shortening in the series X = H, F, Cl is paralleled by an electronegativity increase of X: $\chi(H) = 2.2 < \chi(Cl) = 2.8 < \chi(F) = 4.1$. A (small) increase in the HGeH angle with the electronegativity of the substituent is also observed as expected (*26*). The FGeH angle is also smaller than the ClGeH angle, in good agreement with the correlation found between the XGeH angles and the Ge–H stretching frequencies (*3*). In conclusion, these comparisons show that the r_e structure of GeH_3F determined in this work seems to be reliable. This is further confirmed by the inspection of the residuals of the least-squares fits, which are very small except for the $GeHD_2F$ species, see Table XIII. But the rotational constants of $GeHD_2F$ are not accurate (the experimental A constant is about 80 MHz too low; this is probably due to a systematic error in its determination, (see discussion Section IV) and it was checked that they have not a great influence on the results of the fit. It seems also possible that the empirical relation (10) is worse when the symmetry of the molecule changes. But this point should be further investigated.

ACKNOWLEDGMENTS

We appreciate financial support by the Deutsche Forschungsgemeinschaft, the CNRS, and the Région Nord/Pas-de-Calais.

RECEIVED: July 23, 1991

REFERENCES

1. L. C. KRISHER, J. A. MORRISON, AND W. A. WATSON, *J. Chem. Phys.* **57**, 1357–1358 (1972).
2. S. CRADOCK, D. C. MCKEAN, AND M. W. MCKENZIE, *J. Mol. Struct.* **74**, 265–276 (1981).
3. S. CRADOCK AND J. G. SMITH, *J. Mol. Spectrosc.* **98**, 502–504 (1978).
4. S. CRADOCK AND J. G. SMITH, *J. Mol. Spectrosc.* **102**, 184–192 (1983).
5. H. BÜRGER, R. EUJEN, M. LITZ, AND S. CRADOCK, *J. Mol. Spectrosc.* **138**, 332–345 (1989).
6. S. CRADOCK, H. BÜRGER, R. EUJEN, M. LITZ, AND A. RAHNER, *J. Mol. Spectrosc.* **142**, 10–23 (1990).
7. H. BÜRGER AND A. RAHNER, *in* "Vibrational Spectra and Structure" (J. R. Durig, Ed.), Vol. 18, p. 217, Elsevier, Amsterdam, 1990.
8. J. DEMAISON, G. WLODARCZAK, J. BURIE, AND H. BÜRGER, *J. Mol. Spectrosc.* **140**, 322–339 (1990).
9. S. CRADOCK, *Mol. Phys.* **51**, 697–714 (1984).
10. G. PIAU, F. X. BROWN, D. DANGOISSE, AND P. GLORIEUX, *IEEE J. Quantum Electron.* **QE-23**, 1388–1391 (1987).
11. N. G. DOUGLAS, "Millimetre and Submillimetre Wavelength Lasers," Springer, Berlin, 1989.
12. P. D. MALLINSON, *J. Mol. Spectrosc.* **68**, 68–76 (1977).
13. J. L. DUNCAN, D. C. MCKEAN, AND N. D. MICHIE, *J. Mol. Struct.* **21**, 405–410 (1974).
14. L. HALONEN AND I. M. MILLS, *J. Mol. Spectrosc.* **73**, 494–502 (1978).
15. H. D. RUDOLPH, *Struct. Chem.*, in press.
16. V. W. LAURIE AND D. R. HERSCHBACH, *J. Chem. Phys.* **37**, 1687–1692 (1962).
17. R. J. BERRY AND M. D. HARMONY, *Struct. Chem.* **1**, 49–59 (1989).
18. C. C. COSTAIN, *J. Chem. Phys.* **29**, 864–874 (1958).
19. J. K. G. WATSON, *J. Mol. Spectrosc.* **48**, 479–502 (1973).
20. C. C. COSTAIN, *Trans. Amer. Cristallogr. Assoc.* **2**, 157–164 (1966).
21. W. GORDY AND R. L. COOK, "Microwave Molecular Spectra," Chap. XIII, Wiley, New York, 1984.
22. J. DEMAISON AND L. NEMES, *J. Mol. Struct.* **55**, 295–299 (1979).

23. K. BURCZYK, H. BÜRGER, M. LE GUENNEC, G. WLODARCZAK, AND J. DEMAISON, *J. Mol. Spectrosc.* **148,** 65–79 (1991).
24. W. SCHNEIDER AND W. THIEL, *J. Chem. Phys.* **86,** 923–936 (1987).
25. H. HAYD, H. SAVIN, A. STOLL, H. PREUSS, AND G. BECKER, *J. Mol. Struct. (Theochem.)* **165,** 87–97 (1988).
26. R. J. GILLESPIE AND I. HARGITTAI, "The VSEPR Model of Molecular Geometry," Allyn and Bacon, Needham Heights, NJ, 1991.
27. P. DEBIEVRE, M. GALLET, N. E. HOLDEN, AND I. L. BARNES, *J. Phys. Chem. Ref. Data Suppl.* **13,** 809–891 (1984).
28. J. G. LAHAYE, R. VANDENHAUTE, AND A. FAYT, *J. Mol. Spectrosc.* **123,** 48–83 (1987).
29. M. LE GUENNEC, G. WLODARCZAK, J. DEMAISON, H. BÜRGER, M. LITZ, AND H. WILLNER, to be published.
30. C. DEGLI ESPOSTI, P. G. FAVERO, AND S. SERENELLINI, *J. Mol. Struct.* **82,** 221–236 (1982).
31. R. C. WOODS, *Philos. Trans. R. Soc. London A* **324,** 141–146 (1988).
32. T. EGAWA, S. YAMAMOTO, M. NAKATA, AND K. KUCHITSU, *J. Mol. Struct.* **156,** 213–228 (1987).
33. P. JENSEN, S. BRODERSEN, AND G. GUELACHVILI, *J. Mol. Spectrosc.* **88,** 378–393 (1981).
34. G. GRANER, *J. Mol. Spectrosc.* **90,** 394–438 (1981).
35. W. GORDY AND R. L. COOK, "Microwave Molecular Spectra," Chap. XI, Wiley, New York, 1984.
36. I. OZIER, S. S. LEE, AND N. F. RAMSEY, *J. Chem. Phys.* **65,** 3985–3993 (1976).

2.3. L'acétonitrile

Publication soumise à "Journal of Molecular Spectroscopy" :

Le spectre de rotation de CH_2DCN et de ses isotopomères ^{13}C et ^{15}N ont été analysés dans les domaines millimétrique et submillimétrique (exemple figure DI). Le grand nombre de constantes de rotation disponibles a permis de faire une étude comparative des différentes structures r_0, $r_{\varepsilon,I}$, r_s et $r^{\rho}_{m,}$ ainsi que de calculer une structure vraissemblablement proche de la structure r_e.

CH_2DCN était une molécule potentiellement interstellaire et notre travail a effectivement permis sa détection.

Pour la même raison, nous avons analysé les spectres de rotation de $CH_2DC{\equiv}CH$ et $CH_3C{\equiv}CD$. Le propyne $CH_2DC{\equiv}CH$ a ensuite été détecté dans TMC1. Nous n'avons pas entrepris la détermination de la structure du propyne car cette molécule contient plus d'atomes que l'acétonitrile (et en particulier un hydrogène de plus). En outre elle possède deux vibrations de grande amplitude (ν_9 et ν_{10}) qui rendent le calcul d'une structure r^{ρ}_{m} dénué de sens. Les spectres de $CH_2DC{\equiv}CH$ et $CH_3C{\equiv}CD$ et les constantes dérivées sont reportées dans l'annexe.

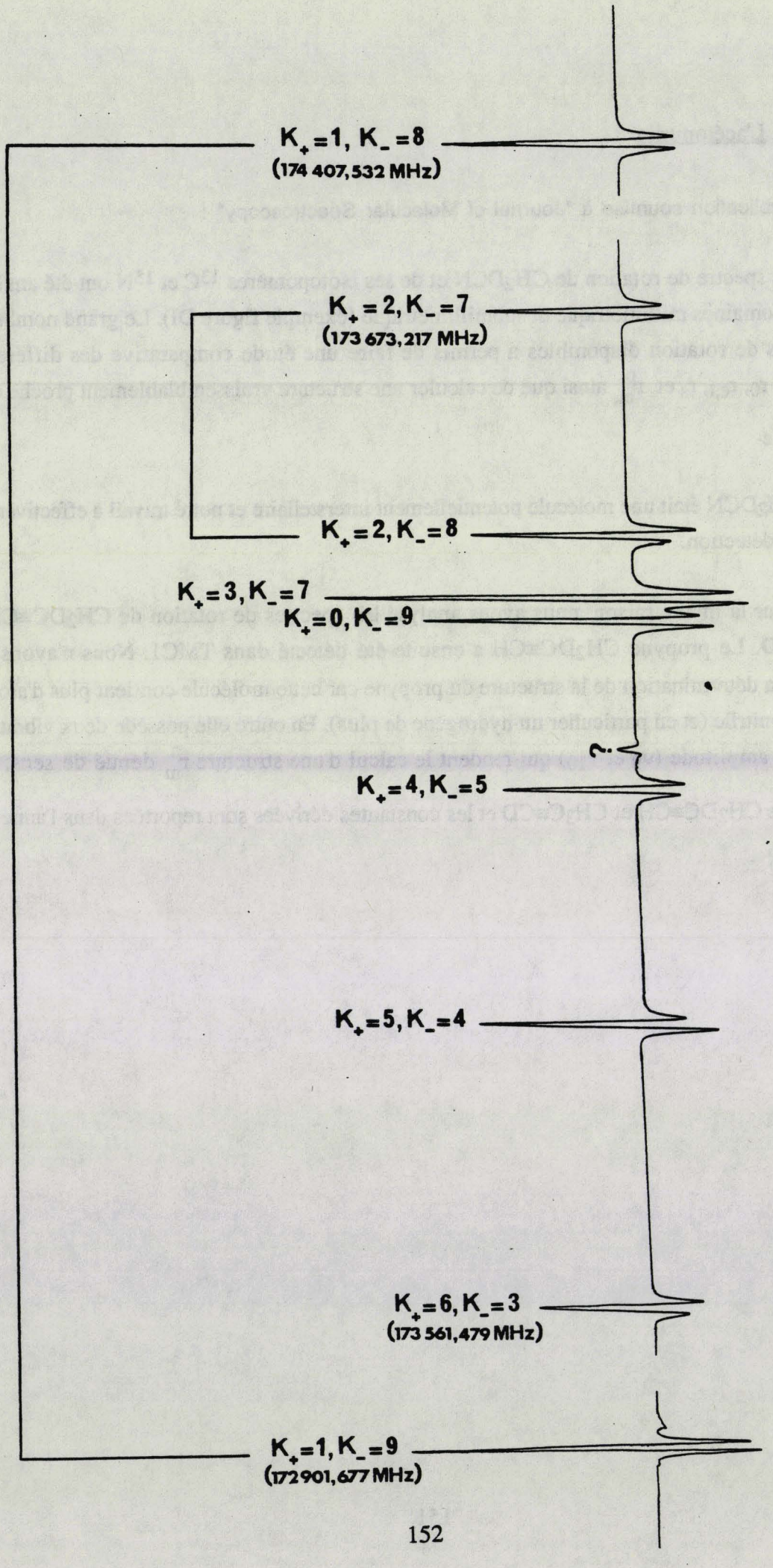

Figure DII : Transition $10_{K+,K-+1} \leftarrow 9_{K+,K-}$ de CH_2DCN

Rotational Spectrum of CH_2DCN and Structure of Methyl Cyanide.

M. LE GUENNEC, G. WLODARCZAK, J. BURIE, AND J. DEMAISON

ABSTRACT

The ground state rotational spectra of CH_2DCN (main species and ^{13}C and ^{15}N substituted species) have been measured from 120 to 470 GHz. Accurate rotational and centrifugal distortion constants have been determined. r_o, r_s, $r_{\varepsilon,I}$ and r_m^{ρ} structures of methyl cyanide have been calculated and compared. A near-equilibrium structure has been estimated to be: r(C≡N) = 1.156(2), r(C-C) = 1.457(2), r(C-H) = 1.087(3) Å and ∠(HCC) = 110.1(3)°.

INTRODUCTION

The rotational constants of CH_3CN, CD_3CN and their ^{13}C and ^{15}N isotopic species are accurately known (1-11). This is due to the fact that methyl cyanide is a light molecule with a large dipole moment. Therefore its submillimeterwave spectrum is strong and well suited to test new spectrometers (3-7). For the same reason, CH_3CN has been easily detected in several interstellar molecular clouds, even in the $v_8 = 1$ excited state (see Ref. (3) for a list of references) and it is actually an ideal observational probe of the kinetic temperature and density of interstellar clouds. Its interstellar importance has therefore prompted the detailed study of its ground state as well as its $v_8 = 1$ excited state. Another reason for these many studies is the fact that CH_3CN produces far infrared continuous emissions when pumped by CO_2 lasers (see Ref. (12) for a review).

The microwave spectrum of CHD_2CN has also been measured between 18 and 40 GHz and accurate rotational constants and centrifugal distortion constants have been determined for this isotopic species (13). This study has been undertaken, mainly to determine the quartic centrifugal distortion constants (particularly D_K) and the axial rotational constant A of an asymmetric species and to subsequently refine the harmonic force field and the average structure.

On the other hand very little is known about the rotational spectrum of the other asymmetric isotopomer: CH_2DCN. Only the three $J = 2 \leftarrow 1$ ^aR branch transitions have been measured by Thomas and coll. (14) and, therefore, only approximate values of the rotational constants B and C can be deduced. However as CH_3CN is very abundant in interstellar space and as its rotational spectrum is very strong, its monodeuterated isotopomer could also be detected. This alone justifies the measurement of the rotational spectrum of CH_2DCN. Another interest in this study lies in the accurate determination of new rotational constants which may be used to refine the structure.

In fact the structure of methyl cyanide has been often investigated. In 1958 Costain has determined its r_s structure (15) which was later refined by Matsumura and coll. (16). Duncan and coll. (17) have determined a r_o structure using $A(CHD_2CN)$ obtained from the analysis of the rovibrational spectrum of this molecule. The r_g and r_z structures have also been determined by gas electron diffraction (18). And finally two spectroscopic r_z structures have appeared almost simultaneously (1, 13). These three r_z structures are in rather good agreement within each other although they were calculated with different force fields. On the other hand the r_g(C-C) bond length is about 0.01 Å longer than the r_o or r_s distances and the r_s(C-H) =1.103 Å is considerably longer than r_o(C-H) = 1.094 Å although the reverse should be the case. The reason of this latter discrepancy has already been investigated (17) and it was shown that the Kraitchman relations used to determine the

off-axis hydrogen coordinates give abnormally long CH bonds when the experimental A constants are not known.

The goals of the present study are:

i) the measurement, by millimeterwave spectroscopy, of the ground state rotational spectra of CH_2DCN and its ^{13}C and ^{15}N isotopomers in order to accurately determine the rotational and centrifugal distortion constants. This will allow us to predict an accurate rotational spectrum which can be used by radioastronomers to detect the presence of CH_2DCN in interstellar space.

ii) the determination of a reliable structure for methyl cyanide.

EXPERIMENTAL DETAILS

CH_2DCN was prepared by reaction of CH_2DI on KCN dissolved in dimethylsulfoxide following the procedure described in Ref. (19). After 1h1/2, the product was distilled on a vacuum line. The ^{13}C and ^{15}N isotopic species were measured in natural abundance. Rotational spectra under 300 GHz were measured with a computer-controlled millimeter-wave spectrometer using superheterodyne detection (20). The transitions between 340 and 470 GHz were measured with a source-modulated spectrometer using phase-stabilized submillimeter BWOs (Thomson-CSF) as sources and a He-cooled bolometer as detector. The accuracy of the measurements is better than 50 kHz.

ANALYSIS

The assignment was easy because the spectrum is intense and not dense. The identified transitions are listed in Table I. They were fitted to the asymmetric top (A) reduction of the rotational Hamiltonian in the I^r representation (21). The symmetric top (S) reduction was also tried but did not give a significant better fit. In the least-squares fit, a low weight was assigned to the high K transitions, because an octic centrifugal distortion constant seems necessary for these transitions. However it was not possible to determine it with an acceptable accuracy. The resulting parameters are given in Table II together with their standard deviations and their correlation matrix. The measured lines are mainly ^aR transitions, but, for the parent species CH_2DCN, it was possible to assign some μ_b transitions (10 ^bQ with $10 \leq J \leq 38$, 2 ^bR with J = 12, 15 and one ^bP with J = 10) and two ^aQ (J = 44, 45) transitions. So, all rotational constants, including A, and all quartic centrifugal distortion constants, including Δ_K, are well determined. Two sextic constants (Φ_{JK} and Φ_{KJ}) could also be determined. The ^{13}C and ^{15}N isotopomers were measured in

natural abundance, so it was only possible to assign ^aR transitions. Consequently Δ_K was determined using the method of predicate observables. As input value: Δ_K = 1826.6(350) kHz was used. Of course the resulting value of Δ_K is not expected to be accurate. For the same reason the A rotational constants could not be accurately determined. A plot of D_J (symmetric reduction) versus n, the number of deuterium atoms ($0 \leq n \leq 3$) gives a straight line. See Fig. 1. However such a linear relationship does not hold any more either for D_{JK} or D_K (or T_{aa}).

The rotational constants of an asymmetric top obtained from a fit using the Hamiltonian of Watson (21) are affected by a small centrifugal distortion contribution which depends on the choice of the reduction and of the representation. Watson (21) has shown that the following linear combinations can be determined from the analysis of the spectra:

$$A = A^{(A)} + 2\Delta_J \qquad (1a)$$

$$B = B^{(A)} + 2\Delta_J + \Delta_{JK} + 2\delta_J - 2\delta_K \qquad (1b)$$

$$C = C^{(A)} + 2\Delta_J + \Delta_{JK} + 2\delta_J + 2\delta_K \qquad (1c)$$

$A^{(A)}$, $B^{(A)}$, and $C^{(A)}$ are the experimental constants in the A reduction and A, B, C are the determinable constants. These latter constants are still contaminated by the centrifugal distortion. As shown by Kivelson and Wilson (22), the true rigid rotor constants A', B', and C' are given by:

$$A' = A + \frac{1}{2}(\tau_{bbcc} + \tau_{abab} + \tau_{acac}) + \frac{1}{4}\tau_{bcbc} \qquad (2a)$$

$$B' = B + \frac{1}{2}(\tau_{aacc} + \tau_{abab} + \tau_{bcbc}) + \frac{1}{4}\tau_{acac} \qquad (2b)$$

$$C' = C + \frac{1}{2}(\tau_{aabb} + \tau_{acac} + \tau_{bcbc}) + \frac{1}{4}\tau_{abab} \qquad (2c)$$

These formulas are written such that the τ constants have units of MHz. The problem is that the τ constants are not experimentally determinable for a non planar molecule. However they can be calculated from the harmonic force field which has already been accurately determined for methyl cyanide (13). Results of such a calculation are summarized in Table III. Three conclusions may be drawn from inspection of Table III:

i) the centrifugal distortion correction is indeed much greater than the accuracy of the rotational constants.

ii) the main contribution to the corrections in Eq. (2) comes from the term τ_{abab}, τ_{bcbc} being completely negligible. So, if the harmonic force field had not been known, it would have been possible to estimate the three $\tau_{\alpha\alpha\beta\beta}$ from the $T_{\alpha\alpha}$ by means of the planarity relations of Dowling (23) and then τ_{abab} and τ_{acac} from T_1 and T_2. This method gives satisfactory results when all the heavy atoms lie on the symmetry plane and was already applied to dimethylallene (24) and to dimethylsulfide (25).

iii) the accuracy of the corrections is rather low. In fact it determines the accuracy of the rotational constants of a light asymmetric top.

Before to use the rigid rotor constants for a structure determination, it is still necessary to correct them for electronic contribution. It is due to the fact that the distribution of electrons contributes to the moments of inertia. The electronic contribution is related to the molecular g factor by the following relation (26):

$$\delta B_{\alpha\alpha} = B_{\alpha\alpha} \frac{g_{\alpha\alpha}}{1836} \qquad (3)$$

where $g_{\alpha\alpha}$ is expressed in units of the nuclear magneton. $g_{bb} = g_{\perp}$ has been determined by rotational Zeeman effect for CH_3CN, CD_3CN and $CH_3C^{15}N$ (27). Its value is about -0.032 which corresponds to a correction of 0.17 MHz and 0.13 MHz for the B rotational constants of CH_3CN and CD_3CN respectively. $g_{aa} = g_{||}$ has not been determined, but it has been demonstrated by Vanderhart and Flygare (28) that the sign and magnitude of the rotational g-factor associated with the rotation of a methyl group about its symmetry axis ($g_{||}$ for all methyl halides) is approximately $g_{||}(CH_3\text{-}) = +0.31$. For CH_3CN, the correction on A is -27 MHz, and -7 MHz for CD_3CN. The known rotational constants of the different isotopomers of methyl cyanide are summarized in Table IV. The centrifugal and magnetic corrections, although often much greater than the experimental uncertainty, are small compared to the vibrational corrections. But, if they are neglected, they may contribute to a systematic error. And more interesting, as it is not possible to calculate them accurately (about 10%), its gives an upper limit of the accuracy of the true vibrationally averaged rotational constants. This so calculated uncertainty is much larger than the standard deviation derived from the least-squares fits, see Table IV.

$A(CH_3CN)$ has been determined from high resolution infrared spectroscopy with a great precision: 158099.2(6) MHz (29, 30). However the quoted standard deviation does not fully take into account all the assumptions made for calculating A. When different determinations are compared, they often differ by 10 to 25 standard deviations. See, for instance, Ref. (31) for CH_3Cl, Ref. (32) for CH_3Br, Ref. (33) for CH_3I and Ref. (34) for CD_3I. Furthermore, the A rotational constant has the largest vibrational contribution. So, an uncertainty of about 30 MHz for $A(CH_3CN)$ seems more realistic. The A rotational constants of the asymmetric species CH_2DCN and CHD_2CN are also very sensitive to the number and variety of transitions used to determine them. The uncertainties given in Table IV take this effect into account.

EFFECTIVE STRUCTURE

The rotational constants of seventeen isotopomers of methyl cyanide are known. This is more than sufficient to determine the four independent parameters: three distances and one angle. A weighted least-squares program (Program Ru 111, author H.D. Rudolph) was used to fit the experimental moments of inertia. The weight assigned to each data was, as usual, the inverse of the square of its uncertainty (see Table IV). A first fit showed that the residuals are much greater than the experimental uncertainty. Particularly the axial rotational constant of CD_3CN seems much too low $\Delta A \approx 500$ MHz. It is possible to estimate its value by using the changes in P_c^o (planar moment of inertia) for the normal and deuterated species, as suggested by Laurie (35, 36):

$$2P_c^o = I_a^o + I_b^o - I_c^o \qquad (4)$$

$$\delta P_c^o = P_c^o(CD_2\text{-}) - P_c^o(CH_2\text{-}) \approx P_c^e \qquad (5)$$

$$I_a^o(CD_3CN) = P_c^o(CH_2DCN) + P_c^o(CHD_2CN) - I_a^o(CH_3CN) \qquad (6)$$

Using the values of Table IV, it gives $I_a^o(CD_3CN) = 6.3657$ uÅ^2 or $A_o = 79391$ MHz to be compared with the experimental value: 78845 MHz (37). Halonen and Mills (13) have also estimated $A_o(CD_3CN)$. They have first calculated I_a^z according to the relation:

$$I_a^z(CD_3\text{-}) = (I_a^z + I_b^z - I_c^z)(CHD_2\text{-}) \qquad (7)$$

Then they have corrected A_z for the harmonic contribution to the α's and have obtained $A_o = 79339$ MHz, in good agreement with our estimation. In conclusion, the experimental value of $A_o(CD_3CN)$ seems to be about 500 MHz too low. It may be noted that the axial rotational constant of CH_3CN was determined in the same work (37) and was later found to be about 1 GHz too low (29, 30). Finally, for $A(CD_3CN)$, we have adopted the estimated value of Halonen and Mills (13) with a conservative uncertainty of 100 MHz . Another point worth to be discussed is that the residuals for the B and C rotational constants of the asymmetric species are very large and of opposite sign. A similar behaviour was previously observed for similar molecules and, quite recently, for GeH_3F (38). It could be explained by the fact that α^B and α^C are rather different although B and C are very near. What supports this assumption is the fact that the harmonic contributions to the α's are themselves different and that these differences are of the right order of magnitude to explain the large residuals. When only the harmonic contributions are taken into account we find for CH_2DCN: $\alpha^B - \alpha^C = -3.8$ MHz, and, for CHD_2CN: $\alpha^B - \alpha^C = -3.35$ MHz (1, 13). To take this fact into account, an uncertainty of 5 MHz was assigned to the B and C rotational constants of the asymmetric

species. This weighting scheme was found to have a great influence on the quality of the results. The results of the final fit are listed in Table V. The derived r_o parameters seem precise. They are also in good agreement with the previous r_o structure also given in Table V. But inspection of the residuals shows that they are greater than the experimental uncertainty. Particularly the standard deviation of unit weight is much too high: $\sigma = 13.5$. This is not surprising because the ground state moment of inertia have been used instead of the equilibrium ones, and it is well known that the vibrational correction $\varepsilon_g = I_g^o - I_g^e$ is

many orders of magnitude greater than the experimental error (**39**, **40**). It is however possible to improve the results by supposing that ε_g is independent of the particular isotopomer for a given axis g. One may eliminate the ε_g by forming differences of moments of inertia. This method gives the r_s structure (**15**, **41**). Alternatively one may determine the ε_g together with the structural parameters by least-squares fitting the moment of inertia. Rudolph (**39**) has labelled the derived structure $r_{\varepsilon,I}$ and has shown that it is at least as good as the r_s structure. The $r_{\varepsilon,I}$ structure is discussed in the next section together with the r_s structure.

SUBSTITUTION STRUCTURE

Three completely different substitution structures of methyl cyanide may be calculated by means of Kraitchman equations (**15**) with CH_3CN, CH_2DCN or CD_3CN as parent species. The substitution coordinates are listed in Table VI. To estimate the errors on the coordinates, the empirical rule of Costain has been used (**42**):

$$\sigma(z) = \frac{K}{|z|} \qquad (8)$$

where z is the cartesian coordinate of the substituted atom in the principal axes system of the parent species. For an H coordinate, the value $K = 0.0012$ Å^2 has been used, as proposed by Costain (**42**). But for the C and N heavy atom coordinates, we have preferred the value suggested by Van Eijck: $K = 0.0005$ Å^2 (**43**). The determination of the coordinates of H (or D) is not straightforward. If we use the Kraitchman's equations for the location of an atom off the symmetry axis (see eqs. (13.56) and (13.57) of Ref.(**26**)), we obtain a value of r(C-H) which is much too large. This fact has been explained by Duncan (**44**). These equations do not use the experimental value of $I_a(CH_3\text{-})$, instead they calculate it from the relation:

$$I_a^o(CH_3\text{-}) = (I_a^o + I_b^o - I_c^o)(CH_2D\text{-}) \qquad (9)$$

which is only a rough approximation for ground state moments of inertia. For the case of parent species CH_3CN (or CD_3CN), the substitution coordinates of the off-axis H (or D) atom were calculated by:

$$|y| = \left[\frac{(I_y' - I_z)(I_z' - I_z)}{\mu(I_y - I_z)}\right]^{1/2} \qquad (10a)$$

$$|z| = \left[\frac{(I_y' - I_y)(I_z' - I_y)}{\mu(I_z - I_y)}\right]^{1/2} \qquad (10b)$$

where μ is the reduced mass as usual. These coordinates may be also calculated using the multi-substitution method ($CH_3- \rightarrow CD_3-$) of Chutjian (**45**) or the disubstitution method of Rudolph (**46**) and Nygaard (**47**). The results are also given in Table VI. The C-C and C≡N distances are practically identical in the different isotopic species. They are also slightly smaller than the r_o structure. Their accuracy is limited by the fact that the central carbon atom is near the center of mass: z(C) = 0.1666 Å (for CH_3CN). On the other hand the range of r_s(C-H) is relatively large: Δr = 0.0049 Å. Nevertheless, in the particular case of methyl cyanide, r_s(C-H) is a better approximation of r_e(C-H) than r_o(C-H). It appears that, for a given parent species, the value of r_s(C-H) increases with the mass of the substituted species. But this trend should be considered with caution because the coordinates have been calculated by different formulas which do not reduce the effects of the zero-point vibrations in the same way. It is worth noting that Chutjian's equations give satisfactory results. A(CD_3CN) is not accurately known (see preceding discussion), but its accuracy is certainly better than 100 MHz and if A increases of 100 MHz, r_s(C-H) decreases of only 0.001 Å. Chutjian's equations have been rarely used up to now for symmetric tops because the axial rotational constant cannot be determined from the pure rotational spectrum. But, recently, it has been possible to accurately determine the A rotational constant of all methyl halides thanks to high resolution infrared spectroscopy. See Table VII which shows the structure of methyl halides calculated with Kraitchman's and Chutjian's equations. Table VIII lists the rotational constants used for these calculations. In all cases, the Kraitchman method gives r_s values which are only slightly higher (by 0.0006 Å) than the r_e values. The Chutjian method gives larger values: $r_s - r_e$ = 0.0026 Å. It is easy to explain because the substitution method assumes that the vibrational contribution ε remains constant by isotopic substitution whereas it is known that ε increases with the moment of inertia I (**40**). When one goes from CH_3- to CD_3-, I_a doubles and ε^A is expected to vary quite a lot. The y coordinate is the most affected:

$$y_s(H) = \left[\frac{I_a^e(CD_3-) - I_a^e(CH_3-) + \varepsilon^A(CD_3-) - \varepsilon^A(CH_3-)}{3\Delta m}\right]^{1/2} \qquad (11)$$

The z coordinate, which depends mainly on ΔI_b, is much less affected by the vibrational contribution because $I_b(CH_3\text{-})$ and $I_b(CD_3\text{-})$ are not very different. It has been checked that for methyl halides ε^A varies roughly like $I_a^{1/2}$ (38). In that particular case, it is possible to eliminate the vibrational contribution and a better approximation of y is:

$$y = \frac{\sqrt{I_a(CD_3\text{-})} - \sqrt{I_a(CH_3\text{-})}}{\sqrt{3m_D} - \sqrt{3m_H}} \qquad (12)$$

The structure calculated with eq. (12) is also given in Table VII under the name Chutjian-r_e. It is in very good agreement with the r_e structure.

The results of the $r_{\varepsilon,I}$ structure calculation are given in Table V. The standard deviation of unit weight is only 0.8, indicating a good fit. The vibrational contributions ε^A and ε^B are well determined and are of the expected order of magnitude (40):

$$\varepsilon^A = 0.02542(16)\ u\text{Å}^2$$

$$\varepsilon^B = 0.1037(90)\ u\text{Å}^2$$

An attempt to fit separately ε^B and ε^C failed because the two parameters are strongly correlated: $\rho(\varepsilon^B, \varepsilon^C) = 0.999$. This is the reason why the same weights were chosen as for the r_0 structure calculation (i.e. an uncertainty of 5 MHz for the B and C rotational constants of the asymmetric substituted species). The choice of the weighting scheme appears to be very important: if we affect the same weight to the B and C rotational constants of all isotopic species, the resulting fit is bad. The standard deviation of unit weight raises to 34. ε^A is no more well determined and it has furthermore the wrong sign: $\varepsilon^A = -0.020(9)\ u\text{Å}^2$. As a consequence the residuals of the A constants are greater than in the r_0 fit and the derived r(C-H) distance is inacceptable (see following discussion). This indicates that the B and C rotational constants of an asymmetrically substituted isotopic species should be used with caution in a structure determination. It is interesting to note that Van Eijck (43) has shown that the substitution $CH_3\text{-} \rightarrow CH_2D\text{-}$ also gives a poor substitution coordinate in asymmetric tops.

In this method it is assumed that ε^A remains constant when D is substituted for H. It is well known that it is not a good assumption and that ε^A varies a great deal when one goes from CH_3X to CD_3X going through CH_2DX (see for instance Table XII of Ref. (38)). For this reason we have tried to exclude from the fit all the A rotational constants except the four ones of the CH_2DCN species. But as a result ε^A is fully correlated with r(C-H). Fortunately there is another way to solve this problem. It is the topic of the next section.

NEAR EQUILIBRIUM STRUCTURE

It is known that ε varies roughly like $I^{1/2}$ (**40**). It has been recently checked that for CH_3X (X = F, Cl, Br, I) and GeH_3Y molecules (Y = F, Cl) (**38**) and for ZCN molecules (Z = Cl, Br) (**48**), the variations of the vibrational contribution are well explained by an equation of the form:

$$\varepsilon^g = C_g I_g^{1/2} \qquad \text{with } g = a, b, c \qquad (13)$$

So, instead of directly fitting the "constants" ε^A and ε^B, we may fit the parameters C_A and C_B of Eq. (13). This method should give a structure nearer the equilibrium structure than the $r_{\varepsilon,I}$ structure. Using the same data with the same weights as in the $r_{\varepsilon,I}$ fit, we obtain:

$$C_A = 10.96(62)\ u^{1/2}\text{Å}$$
$$C_B = 12.051(99)\ u^{1/2}\text{Å}$$

The derived geometrical parameters are listed in Table V. The standard deviation of unit weight is only 0.7 which indicates a good fit. This is confirmed by the examination of the residuals which are in good agreement with the expected uncertainty of the rotational constants (see Table IV for the uncertainties). The parameters C_A and C_B are also well determined and of the expected order of magnitude (**38**, **40**).

In fact, the value n = 0.5 of the exponent in Eq.(13) is a "theoretical" value. Experimentally, it is found that n is often slightly greater than 0.5 (**38**, **48**). To check the influence of this uncertainty, we have repeated the calculation with n = 0.7. This value is very likely too high but the fit is only slightly worse. The results are also listed in Table V. It appears that the variation of the C-C and C≡N distances is less than $2 \cdot 10^{-3}$ Å and that of C-H less than $3 \cdot 10^{-3}$ Å. These numbers are very likely a good estimate of the accuracy of the structure.

There is still another way to obtain an estimate of the r_e structure. Recently Harmony and coll. (**49**-**54**) have proposed a new procedure for obtaining near-equilibrium structures using only ground state data. The ground state moments of inertia I_o are first scaled by a factor 2ρ - 1:

$$I_m^{\rho} = (2\rho - 1) I_o \qquad \text{with } \rho = \frac{I_s}{I_o} \qquad (14)$$

I_s is the moment of inertia calculated from the substitution coordinates. Then the data of the deuterated isotopic species are corrected to account for overscaling. This correction is equivalent to an elongation of the C-D bond by an amount δr = 0.0028 Å. For instance for the a-axis:

$$(I^{\rho}_{m})^{D}_{corr} = (I^{\rho}_{m})^{D} + 2m_D \sum_i (b_i \delta b_i + c_i \delta c_i) \qquad (15)$$

and analogously for the b and c axes by cyclic permutation of a, b, and c. a_i, b_i and c_i are the cartesian coordinates of the D atoms and δa_i, δb_i, δc_i the components of $\delta\vec{r}$. The derived structural parameters are symbolised by r^{ρ}_{m}. Although this method has already been applied to several molecules containing hydrogen (**51**-**56**), it has not yet been tested on methyl halides. Before to use it for methyl cyanide, we have applied it to methyl chloride (CH_3Cl) and methyl bromide (CH_3Br) whose equilibrium structure is accurately known and for which it is possible to calculate a full substitution structure. In both cases the Chutjian's equations have been used to calculate the hydrogen coordinates because the rotational constants of asymmetric methyl bromide are not known. The I^{ρ}_{m} and I_e moments of inertia are listed in Table IX and the corresponding structures in Table X. It appears that the r^{ρ}_{m} parameters are indeed very near the r_e ones, especially for the distances between the heavy atoms. For methyl cyanide, we have made two calculations with two different sets of substitution coordinates: one obtained from the substitution $CH_3- \rightarrow CH_2D-$ and the other from $CH_3- \rightarrow CD_3-$. The results for the heavy atom coordinates are very close to each other and to the near-r_e structure, on the other hand the result for H is unsatisfactory, particularly for the substitution $CH_3- \rightarrow CH_2D-$. It is known that with the r^{ρ}_{m} method, molecules containing large-amplitude low frequency bending modes (**51**, **54**) scale poorly. This is the case for CH_3CN which has a very low bending vibration: $\nu_8 = 365.05\ cm^{-1}$.

DISCUSSION

To test more completely the validity of those methods, it is interesting to comment the derived geometrical parameters.

r(C≡N) bond length:

The r_g(C≡N) bond length has already been determined by electron diffraction for CH_3CN (**18**) and for HCN (**18**) and NCCN (**57**). The r_e structure of these latter two molecules is also known. See Table XI. As noted by Kuchitsu and Oyanagi (**58**), the difference $r_g - r_e$ should remain nearly constant. This should be particularly true for a highly rigid bond like C≡N which is known to vary little (**55**). In fact, for both HCN and NCCN, we find $r_g - r_e = 0.005$ Å, so the r_e(C≡N) value of CH_3CN should be near 1.154 Å, in satisfactory agreement with our result. But such a good agreement cannot be taken as proof because two

molecules constitute a very small sample and, furthermore, the r_g distances are determined with an accuracy not better than one thousanth of an Å. So, further checks are necessary.

The equilibrium C≡N distance has been determined for a few molecules. There is a non-linear relation between the bond-stretching force constant and the bond length for carbon-nitrogen bonds (**59**). The problem is that the force constants are not known with enough accuracy to explain small variations of C≡N bond length. But it has been claimed that the force constant is approximately proportional to the nuclear quadrupole coupling constant (**60**). And it is easy to determine the latter constant with precision. This relation has been analyzed in Ref. (**48**) where the references to the original data may be found. Fig. 2 (taken from Ref. (**48**)) shows that the correlation is not perfect. Particularly FCN seems to be an exception. Nevertheless our experimental value is in very good agreement with the correlation as can be seen on Fig. 2.

Finally ab initio geometry refinements with a relatively modest basis set are known to engender accurate parameters with well characterized empirical corrections (**61**). The geometries of HCN and CH_3CN have been recently determined by SCF gradient optimization using the 4-21 G basis set (**62**). The ab initio C≡N distance is 1.1368 Å for HCN and 1.1383 Å for CH_3CN, respectively. The experimental r_e(C≡N) distance in HCN is 1.1532 Å (**63**), so the corrected ab initio bond length in CH_3CN is:

$$r_e(C{\equiv}N) = 1.1532 + 1.1383 - 1.1368 = 1.1547 \text{ Å}$$

This result is in fair agreement with the experimental value, if we take into account the limited accuracy obtainable with the 4-21 G basis set. It may be argued that the 4-21 G basis is too small to reproduce small differences in bond length. However both CH_3CN (**64**) and HCN (**65**) have been calculated with larger bases including the polarization and it was found that the offset remains nearly constant.

r(C-C) bond length:

To date the equilibrium C-C distance has been experimentally determined for only one molecule: ethane where r_e(C-C) = 1.522(2) Å (**53**, **66**). But the r_m^ρ distance (which is a better approximation of the r_e distance than the r_s distance (**54**)) has already been determined for several molecules. The r_m^ρ values are listed in Table XII together with the r_g values and the ab initio results (when they exist). The difference $r_g - r_e$ is nearly constant, its mean value being 0.011(2) Å. So, we should have: r_e(C-C)= 1.457(3) Å, in very good agreement with our experimental value. Inspection of Table XII shows that the basis-set offset r(ab initio) - r_e is not constant. This behaviour makes comparisons more difficult. Pulay (**67**) has suggested that the offset should decrease by ≈ 0.005 Å for every 0.03 Å decrease in the 4-21 G r(C-C) value. So, the offset for CH_3CN should be only 0.006 Å, which gives a calculated r_e value of 1.455 Å, in fair agreement with the experimental value:

1.457 Å. But, as the offset value is very inaccurate, this agreement could be accidental. On the other hand, if we compare the r_e distance with the substitution distances (r_S and $r_{\varepsilon,I}$ in Tables V and VI), we find a very satisfactory agreement, the substitution value being a little bit larger (0.001-0.002 Å) as expected.

HCH angle:

All the experimental values (r_O, r_e, r_S and $r_{\varepsilon,I}$, see Table V) of the HCH angle are very near each other. the range is only 0.22° if we omit the r_O value which is different from the other ones. They are also in good agreement with the ab initio values (Table V) and with the r_Z value $\angle(HCH)_Z$ = 109.09(10)° (1, 13, 18). So, it may be concluded that the $\angle$ (HCH) angle has been determined with an accuracy better than 1°.

r(C-H) bond length:

Although the C-H bond length is difficult to determine experimentally with accuracy, there are several methods which allow to estimate its value. These methods will be reviewed elsewhere (68).

Briefly, there is a relationship between the C-H bond length and the nuclear quadrupole coupling constant of deuterium (69). The problem is that it is difficult to determine eqQ(D) with accuracy and that the relation is not linear. However this relation indicates that the C-H length in CH_3CN should be near that of CHF_3 : 1.091(14) Å, smaller than that of H_2CO: 1.101 Å and greater than those of methyl halides: 1.0858 Å for CH_4. In conclusion:

$$1.0858 < r_e(C\text{-}H) < 1.101$$

A simpler and more accurate empirical relation exists between the isolated C-H stretching frequencies and the C-H bond lengths (70). This linear relation was established with r_O distances, but, in fact, it works at least as well with r_e distances (the evident advantage of r_O distances is that they are much more numerous). This relation gives for CH_3CN: $r_e(C\text{-}H)$ = 1.087 Å.

The geometry of methyl cyanide was already determined by SCF gradient optimization using the 4-21 G, 5-31 G** (62) and larger (64) basis sets (table V). Actually the 4-21 G basis set is probably the most popular one, and it gives, after corrrection: $r_e(C\text{-}H)$ = 1.088 Å. All these methods give bond lengths in good agreement with each other, indicating that our near-equlibrium structure is very likely a good approximation of the true r_e structure.

CONCLUSIONS

The rotational spectra of CH_2DCN were measured and analyzed. The newly determined molecular constants were used to predict accurate frequencies in the millimeterwave range. That work made possible the detection of CH_2DCN in the hot core of IRc2 in OMC1 and in G34.3 (71). A reliable structure of methyl cyanide could also be determined.

ACKNOWLEDGMENTS

The authors thank Dr. J.M. DENIS and Dr. J.C. GUILLEMIN for their help during the synthesis of the sample of CH_2DCN. They would also like to thank Dr. G. Graner, Prof. K. Kuchitsu and Prof. H. D. Rudolph for having read and criticized the original manuscript. This work was supported by the CNRS (GDR Physico-chimie des molécules interstellaires).

REFERENCES

1. J. DEMAISON, A. DUBRULLE, D. BOUCHER, J. BURIE, AND V. TYPKE, J. Mol. Spectrosc. **76**, 1-16 (1979).
2. D. BOUCHER, J. BURIE, A. BAUER, A. DUBRULLE, AND J. DEMAISON, J. Phys. Chem. Ref. Data **9**, 659-719 (1980).
3. R. BOCQUET, G. WLODARCZAK, A. BAUER, AND J. DEMAISON, J. Mol. Spectrosc. **127**, 382-389 (1988).
4. M. CARLOTTI, G. DI LONARDO, L. FUSINA, AND B. CARLI, J. Mol. Spectrosc. **129**, 314-325 (1988).
5. F.X. BROWN, D. DANGOISSE, AND J. DEMAISON, J. Mol. Spectrosc. **129**, 483-485 (1988).
6. F.S. PAVONE, L.R. ZINK, M. PREVEDELLI, M. INGUSCIO, AND L. FUSINA, J. Mol. Spectrosc. **144**, 45-50 (1990).
7. G. SCHWAAB, P.H.D. thesis, Bonn, 1991.
8. H.S. TAM, I. AN, AND J.A. ROBERTS, J. Mol. Spectrosc. **129**, 202-215 (1988).
9. H.S. TAM AND J.A. ROBERTS, J. Mol. Spectrosc. **134**, 281-289 (1989).
10. J. COSLEOU, G. WLODARCZAK, J. BURIE, AND J. DEMAISON, J. Mol. Spectrosc. **137**, 47-54 (1989).
11. F.X. BROWN, J. COSLEOU, D. DANGOISSE, J. DEMAISON, AND G. WLODARCZAK, J. Mol. Spectrosc. **134**, 234-236 (1989).

12. M. INGUSCIO, *in* "Reviews of Infrared and Millimeter Waves" (K.J. Button, M. Inguscio, and F. Strumia, Eds.), Vol. 2, p. 193, Plenum, New York, 1984.
13. L. HALONEN AND I.M. MILLS, J. Mol. Spectrosc. **73**, 494-502 (1978).
14. L.F. THOMAS, E.J. SHERRARD, AND J. SHERIDAN, Trans. Faraday Soc. **51**, 619-625 (1955).
15. C.C. COSTAIN, J. Chem. Phys. **29**, 864-874 (1958).
16. C. MATSUMURA, E. HIROTA, T. OKA, AND Y. MORINO, J. Mol. Spectrosc. **9**, 366-380 (1962).
17. J.L. DUNCAN, D.C. MCKEAN, AND N.D. MICHIE, J. Mol. Struct. **21**, 405-410 (1974).
18. K. KARAKIDA, T. FUKUYAMA, AND K. KUCHITSU, Bull. Chem. Soc. Japan, **47**, 299-304 (1974).
19. R.A. SMILEY AND C. ARNOLD, J. Org. Chem. **25**, 257-258 (1960).
20. J. BURIE, D. BOUCHER, J. DEMAISON, AND A. DUBRULLE, J. Phys. (Paris) **43**, 1319-1325 (1982).
21. J.K.G. WATSON, *in* "Vibrational Spectra and Structure" (J.R. Durig, Ed.), Vol. 6, p. 1, Elsevier, Amsterdam, 1977.
22. D. KIVELSON AND E.B. WILSON, J. Chem. Phys. **20**, 1575-1579 (1952).
23. J.M. DOWLING, J. Mol. Spectrosc. **6**, 550-553 (1961).
24. J. DEMAISON, D. SCHWOCH, B.T. TAN, AND H.D. RUDOLPH, J. Mol. Spectrosc. **60**, 324-331 (1976).
25. J. DEMAISON, D. SCHWOCH, B.T. TAN, AND H.D. RUDOLPH, J. Mol. Spectrosc. **83**, 391-400 (1980).
26. W. GORDY AND R.L. COOK, "Microwave Molecular Spectra", Chap. XI, p. 505, Wiley, New York, 1984.
27. J.M. POCHAN, R.L. SCHOEMAKER, R.G. STONE, AND W.H. FLYGARE, J. Chem. Phys. **52**, 2478-2484 (1970).
28. D.L. VANDERHART AND W.H. FLYGARE, Mol. Phys. **18**, 77-93 (1970).
29. J. SAKAI, private communication, quoted in P. WALLRAFF, K.M.T. YAMADA, R. SCHIEDER, AND G. WINNEWISSER, J. Mol. Spectrosc. **112**, 163-172 (1985).
30. V.M. HORNEMAN, M. KOIVUSAARI, AND R. ANTTILA, 12th Colloquium on High Resolution Molecular Spectroscopy, Dijon, paper O20, 1991.
31. N.F. HENFREY AND B.A. THRUSH, J. Mol. Struct. **146**, 71-83 (1986).
32. J. SAKAI AND M. KATAYAMA, J. Mol. Struct. **190**, 113-123 (1988).
33. R. ANTTILA, V.M. HORNEMAN, AND S. ALANKO, Mol. Phys. **70**, 991-1000 (1990).
34. C. POULSEN AND S. BRODERSEN, J. Raman Spectrosc. **14**, 77-82 (1983).
35. V.W. LAURIE, J. Chem. Phys. **28**, 704-706 (1958).
36. J. DEMAISON, G. WLODARCZAK, K. SIAM, J.D. EWBANK, AND L. SCHÄFER, Chem. Phys. **120**, 421-428 (1988).

37. F.N. MASRI, J.L. DUNCAN, AND G.K. SPIERS, J. Mol. Spectrosc. **47**, 163-178 (1973).
38. M. LE GUENNEC, W. CHEN, G. WLODARCZAK, J. DEMAISON, R. EUJEN, AND H. BÜRGER, J. Mol. Spectrosc. **150**, 493-510 (1991).
39. H.D. RUDOLPH, Struct. Chem., **2**, 581-588 (1991).
40. J. DEMAISON AND L. NEMES, J. Mol. Struct. **55**, 295-299 (1979).
41. P. NÖSBERGER, A. BAUDER, AND HS.H. GÜNTHARD, Chem. Phys. **1**, 418-425 (1973).
42. C.C. COSTAIN, Trans. Amer. Crystallogr. Assoc. **2**, 157-164 (1966).
43. B.P. VAN EIJCK, J. Mol. Spectrosc. **91**, 348-362 (1982).
44. J.L. DUNCAN, J. Mol. Struct. **22**, 225-235 (1974).
45. A. CHUTJIAN, J. Mol. Spectrosc. **14**, 361-370 (1964).
46. H.D. RUDOLPH, J. Mol. Spectrosc. **89**, 430-439 (1981).
47. L. NYGAARD, J. Mol. Spectrosc. **62**, 292-293 (1976).
48. M. LE GUENNEC, G. WLODARCZAK, W. CHEN, R. BOCQUET, AND, J. DEMAISON, J. Mol. Spectrosc., in press.
49. M.D. HARMONY AND W.H. TAYLOR, J. Mol. Spectrosc. **118**, 163-173 (1986).
50. M.D. HARMONY, R.J. BERRY, AND W.H. TAYLOR, J. Mol. Spectrosc. **127**, 324-336 (1988).
51. R.J. BERRY AND M.D. HARMONY, J. Mol. Spectrosc. **128**, 176-194 (1988).
52. R.J. BERRY AND M.D. HARMONY, Struct. Chem. **1**, 49-59 (1990).
53. M.D. HARMONY, J. Chem. Phys. **93**, 7522-7523 (1990).
54. H.S. TAM, J.I. CHOE AND M.D. HARMONY, J. Phys. Chem. **95**, 9267-9272 (1991).
55. J. RANDELL, A.P. COX, I. MERKE, AND H. DREIZLER, J. Chem. Soc. Faraday Trans. **86**, 1981-1989 (1990).
56. R.D. BROWN, P.D. GODFREY, D. MCNAUGHTON, A.P. PIERLOT, AND W.H. TAYLOR, J. Mol. Spectrosc. **140**, 340-352 (1990).
57. Y. MORINO, K. KUCHITSU, Y. HORI, AND M. TANIMOTO, Bull. Chem. Soc. Japan, **41**, 2349-2352 (1968).
58. K. KUCHITSU AND K. OYANAGI, Faraday Discussion, **62**, 20-28 (1977).
59. D.M. BYLER, H. SUSI, AND W.C. DAMERT, Spectrochim. Acta A, **43**, 861-863 (1987).
60. A. WEISS AND S. WIGAND, Z. Naturforsch. A, **45**, 195-212 (1990).
61. L. SCHÄFER, C. VAN ALSENOY, AND J.N. SCARSDALE, J. Mol. Struct. **86**, 349-364 (1982).
62. K. SIAM, M. DAKKOURI, J.D. EWBANK, AND L. SCHÄFER, J. Mol. Struct. **204**, 291-300 (1990).
63. R.C. WOODS, Philos. Trans. R. Soc. London, Ser. A **324**, 141-146 (1988).
64. M.H. PALMER, J. Mol. Struct. **200**, 1-17 (1989).

65. J.F. GAW, Y. YAMAGUCHI, H.F. SCHAEFER III, AND N.C. HANDY, J. Chem. Phys. **85**, 5132-5142 (1986).
66. J.L. DUNCAN, D.C. MCKEAN, AND A.J. BRUCE, J. Mol. Spectrosc. **74**, 361-374 (1979).
67. P. PULAY, G. FOGARASI, F. PANG, AND J. BOGGS, J. Amer. Chem. Soc. **101**, 2550-2560 (1979).
68. J. DEMAISON AND G. WLODARCZAK, to be published.
69. H. HUBER, J. Chem. Phys. **83**, 4591-4598 (1985).
70. D.C. MCKEAN, Chem. Soc. Rev. **7**, 399-422 (1978).
71. M. GERIN, F. COMBES, G. WLODARCZAK, T. JACQ, M. GUELIN, P. ENCRENAZ, AND C. LAURENT, Astron. Astrophys. in press.
72. M.M. LAW, J.L. DUNCAN, AND I.M. MILLS, 12th Colloquium on High Resolution Molecular Spectroscopy, Dijon, paper M18, 1991.
73. P. JENSEN, S. BRODERSEN, AND G. GUELACHVILI, J. Mol. Spectrosc. **88**, 378-393 (1981).
74. G. GRANER, J. Mol. Spectrosc. **90**, 394-438 (1981).
75. T. EGAWA, S. YAMAMOTO, M. NAKATA, AND K. KUCHITSU, J. Mol. Struct. **156**, 213-228 (1987).
76. F.X. BROWN, D. DANGOISSE, J. GADHI, G. WLODARCZAK, AND J. DEMAISON, J. Mol. Struct. **190**, 401-407 (1988).
77. W.W. CLARK AND F.C. DE LUCIA, J. Mol. Struct. **32**, 29-36 (1976).
78. L. HALONEN, J. KAUPPINEN, AND G.L. CALDOW, J. Chem. Phys. **81**, 2257-2269 (1984).
79. G. WLODARCZAK, D. BOUCHER, R. BOCQUET, AND J. DEMAISON, J. Mol. Spectrosc. **116**, 251-255(1986).
80. P.D. MALLINSON, J. Mol. Spectrosc. **68**, 68-76 (1977).
81. A. MITO, J. SAKAI, AND M. KATAYAMA, J. Mol. Spectrosc. **112**, 252-284 (1985).
82. O.I. BASKAKOV, B.I. POLEVOI, O.I. SUKHNO, A.S. SHEVYREV, M.N. EFIMENKO, AND S.F. DYUBKO, Zh. Prikl. Spektrosk. **44**, 419-424 (1986).
83. R. BOCQUET, D. BOUCHER, J. DEMAISON, G. WLODARCZAK, AND G. GRANER, Europhys. Lett. **2**, 275-278 (1986).
84. M.V. MOSKIENKO AND S.F. DYUBKO, J. Appl. Spectrosc. **28**, 387-389 (1978).
85. H.G. CHO AND R.H. SCHWENDEMAN, J. Mol. Spectrosc. **138**, 181-186 (1989),
86. G. WLODARCZAK, D. BOUCHER, R. BOCQUET, AND J. DEMAISON, J. Mol. Spectrosc. **124**, 53-65 (1987).
87. P.D. MALLINSON, J. Mol. Spectrosc. **55**, 94-107 (1975).
88. J. GADHI, G. WLODARCZAK, J. LEGRAND, AND J. DEMAISON, Z. Naturforsch. A **42**, 1241-1246 (1987).

89. P. BOTSCHWINA AND J. FLÜGGE, Chem. Phys. Lett. **180**, 589-593 (1991).
90. C.E. BLOM, P.J. SLINGERLAND, AND C. ALTONA, Mol. Phys. **31**, 1359-1376 (1976).
91. A. KOMORNICKI, F. PAUZAT, AND Y. ELLINGER, J. Phys. Chem. **87**, 3847-3857 (1983).
92. W.B. DE ALMEIDA AND A. HINCHLIFFE, J. Mol. Struct. **206**, 77-87 (1990).
93. M. HIROTA, T. IIJIMA, AND M. KIMURA, Bull. Chem. Soc. Japan, **51**, 1594-1598 (1978).
94. T. IIJIMA, Bull. Chem. Soc. Japan, **46**, 2311-2314 (1973).
95. I. TOKUE, T. FUKUYAMA, AND K. KUCHITSU, J. Mol. Struct. **17**, 207-213 (1973).
96. S. YAMAMOTO, M. NAKATA, T. FUKUYAMA, AND K. KUCHITSU, J. Phys. Chem. **89**, 3298-3302 (1985).
97. T. IIJIMA, Bull. Chem. Soc. Japan, **45**, 1291-1293 (1972).

J'	K'+	K'-	← J	K+	K-	Freq.	e.- c.
CH_2DCN							
2[a]	1	2	1	1	1	34584.05	-0.09
2[a]	0	2	1	0	1	34735.18	-0.03
2[a]	1	1	1	1	0	34885.50	0.06
10	1	9	10	0	10	116572.26	0.02
39	1	38	39	1	39	116636.12	0.01
11	1	10	11	0	11	117422.43	0.04
12	1	11	12	0	12	118354.96	0.04
13	0	13	12	1	12	119086.92	0.04
13	1	12	13	0	13	119371.18	0.04
28	1	27	28	0	28	145849.40	0.02
44	1	43	44	1	44	147530.50	0.01
31	1	30	31	0	31	154039.82	0.03
45	1	44	45	1	45	154111.08	0.02
32	1	31	32	0	32	157014.91	0.03
31	1	31	30	2	28	157992.57	0.01
9	2	8	10	1	9	159314.10	0.01
10	1	10	9	1	9	172901.68	0.01
10	6	4	9	6	3	173561.48	0.01
10	5	5	9	5	4	173593.31	0.04
10	4	6	9	4	5	173619.65	-0.02
10	0	10	9	0	9	173638.56	0.04
10	3	8	9	3	7	173641.17	0.04
10	2	9	9	2	8	173648.22	-0.04
10	2	8	9	2	7	173673.22	0.04
37	1	36	37	0	37	173837.52	-0.08
16	0	16	15	1	15	174131.50	0.04
10	1	9	9	1	8	174407.53	0.03
38	1	37	38	0	38	177607.78	-0.06
13	1	13	12	1	12	224754.53	0.09
13	10	4	12	10	3	225379.33	0.15
13	9	4	12	9	3	225450.04	0.05
13	8	6	12	8	5	225513.37	-0.03
13	7	7	12	7	6	225569.45	-0.01
13	6	7	12	6	6	225618.19	-0.02
13	5	9	12	5	8	225659.81	-0.02
13	2	12	12	2	11	225726.54	-0.01
13	2	11	12	2	10	225781.54	0.05
13	1	12	12	1	11	226711.29	0.01
17	1	17	16	1	16	293869.52	0.00
17	14	4	16	14	3	294231.99	-0.26
17	13	5	16	13	4	294363.61	-0.04
17	12	6	16	12	5	294485.40	0.10
17	11	7	16	11	6	294597.36	0.10
17	10	8	16	10	7	294699.57	0.06
17	9	9	16	9	8	294792.16	0.06
17	8	10	16	8	9	294875.03	-0.05
17	7	11	16	7	10	294948.46	-0.07
17	6	11	16	6	10	295012.55	-0.06
17	0	17	16	0	16	295060.16	-0.03
17	5	13	16	5	12	295067.51	-0.12
17	4	13	16	4	12	295114.36	-0.05
17	2	16	16	2	15	295144.02	-0.05
17	3	15	16	3	14	295155.02	-0.05
17	3	14	16	3	13	295156.10	-0.06
17	2	15	16	2	14	295267.06	0.03
17	1	16	16	1	15	296426.45	0.01
26	1	26	25	1	25	449251.64	0.03
26	0	26	25	0	25	450880.51	0.03
26	2	25	25	2	24	451215.41	-0.06
26	2	24	25	2	23	451651.50	0.07
26	1	25	25	1	24	453148.29	0.00
27	1	27	26	1	26	466502.92	0.01
27	14	14	26	14	13	467154.03	-0.29
27	13	15	26	13	14	467362.40	0.19
27	12	16	26	12	15	467555.12	0.34
27	11	17	26	11	16	467732.40	0.31
27	10	18	26	10	17	467894.43	0.22
27	9	19	26	9	18	468041.37	0.12
27	0	27	26	0	26	468167.56	0.01
27	8	20	26	8	19	468173.42	0.03
27	7	21	26	7	20	468290.93	-0.03
27	6	22	26	6	21	468394.49	-0.05
27	5	23	26	5	22	468485.36	-0.05
27	2	26	26	2	25	468544.02	-0.12
27	3	25	26	3	24	468643.87	-0.03
27	3	24	26	3	23	468655.04	-0.02
27	2	25	26	2	24	469031.48	0.07
27	1	26	26	1	25	470547.00	0.01
$^{13}CH_2DCN$							
7	1	7	6	1	6	117941.91	0.02
7	4	3	6	4	2	118418.06	0.16
7	3	4	6	3	3	118431.85	-0.00
7	2	6	6	2	5	118439.26	-0.01
7	0	7	6	0	6	118440.33	-0.02
7	2	5	6	2	4	118446.98	0.02
7	1	6	6	1	5	118946.70	-0.03
10	1	10	9	1	9	168478.87	-0.05
10	6	5	9	6	4	169106.66	0.03
10	5	6	9	5	5	169137.21	0.03
10	4	7	9	4	6	169162.49	-0.01
10	0	10	9	0	9	169182.09	0.02
10	2	9	9	2	8	169190.29	0.01
10	2	8	9	2	7	169212.91	0.00
10	1	9	9	1	8	169914.08	0.01
14	1	14	13	1	13	235845.55	0.00
14	5	9	13	5	8	236775.68	-0.01
14	0	14	13	0	13	236806.42	-0.01

[a]) Ref. (14).

Table I : Rotational Frequencies (MHz) of CH_2DCN in the Ground Vibrational State.

J'	K'_+	K'_-	← J	K_+	K_-	Freq.	e.- c.
14	4	10	13	4	9	236811.81	-0.03
14	2	13	13	2	12	236843.52	-0.02
14	2	12	13	2	11	236905.85	-0.01
14	1	13	13	1	12	237853.70	-0.02
26	1	26	25	1	25	437769.93	0.05
26	0	26	25	0	25	439337.48	0.03
26	2	25	25	2	24	439640.18	-0.04
26	2	24	25	2	23	440036.36	0.04
26	1	25	25	1	24	441484.84	0.04
27	1	27	26	1	26	454581.24	0.04
27	11	17	26	11	16	455740.58	0.07
27	10	18	26	10	17	455896.25	0.04
27	9	19	26	9	18	456037.37	-0.04
27	8	20	26	8	19	456164.21	-0.06
27	0	27	26	0	26	456184.52	-0.06
27	7	21	26	7	20	456276.96	-0.12
27	6	22	26	6	21	456376.29	-0.07
27	5	23	26	5	22	456463.27	-0.05
27	2	26	26	2	25	456525.13	0.05
27	3	25	26	3	24	456613.89	0.00
27	3	24	26	3	23	456623.53	-0.02
27	2	25	26	2	24	456967.96	0.00
27	1	26	26	1	25	458436.86	0.04

$CH_2D^{13}CN$

10	1	10	9	1	9	172776.59	-0.02
10	6	5	9	6	4	173436.21	-0.01
10	4	6	9	4	5	173493.93	-0.05
10	0	10	9	0	9	173512.61	0.02
10	3	7	9	3	6	173515.34	-0.03
10	2	8	9	2	7	173547.30	0.09
10	1	9	9	1	8	174280.62	-0.01
13	1	13	12	1	12	224591.87	-0.01
13	0	13	12	0	12	225531.34	-0.04
13	2	12	12	2	11	225562.87	0.01
13	1	12	12	1	11	226546.33	-0.03
26	1	26	25	1	25	448926.51	0.01
26	0	26	25	0	25	450553.78	-0.00
26	2	25	25	2	24	450888.02	-0.01
26	1	25	25	1	24	452818.54	0.03
27	1	27	26	1	26	466165.35	0.04
27	1	26	26	1	25	470204.57	0.02
27	12	16	26	12	15	467222.45	0.12
27	10	18	26	10	17	467559.49	0.15
27	9	19	26	9	18	467705.34	0.01
27	0	27	26	0	26	467828.35	0.00
27	8	20	26	8	19	467836.49	-0.04
27	7	21	26	7	20	467953.19	-0.07
27	6	22	26	6	21	468056.02	-0.09
27	5	23	26	5	22	468145.97	-0.39
27	2	26	26	2	25	468204.12	0.03
27	3	25	26	3	24	468303.92	0.05
27	3	24	26	3	23	468314.93	-0.08
27	2	25	26	2	24	468690.40	0.04

$CH_2DC^{15}N$

7	1	7	6	1	6	117401.76	0.03
7	5	2	6	5	1	117854.28	0.00
7	4	3	6	4	2	117871.66	0.03
7	3	4	6	3	3	117885.44	0.02
7	2	6	6	2	5	117892.84	0.04
7	0	7	6	0	6	117893.97	0.00
7	2	5	6	2	4	117900.30	0.02
7	1	6	6	1	5	118393.85	-0.02
10	7	4	9	7	3	168291.40	0.02
10	6	5	9	6	4	168326.94	0.01
10	5	6	9	5	5	168357.20	0.03
10	4	7	9	4	6	168382.19	-0.03
10	0	10	9	0	9	168402.02	0.03
10	2	9	9	2	8	168409.85	0.05
10	2	8	9	2	7	168431.86	0.03
10	1	9	9	1	8	169124.50	0.02
14	1	14	13	1	13	234766.08	-0.02
14	5	9	13	5	8	235683.97	-0.01
14	0	14	13	0	13	235715.43	-0.05
14	4	10	13	4	9	235719.66	-0.10
14	2	13	13	2	12	235751.33	-0.02
14	2	12	13	2	11	235812.06	0.02
14	1	13	13	1	12	236748.85	-0.01
26	1	26	25	1	25	435770.44	0.14
26	0	26	25	0	25	437322.09	0.00
26	2	25	25	2	24	437616.34	-0.08
26	2	24	25	2	23	438002.20	-0.05
26	1	25	25	1	24	439438.38	0.04
27	1	27	26	1	26	452505.26	-0.01
27	12	16	26	12	15	453477.84	-0.06
27	11	17	26	11	16	453646.43	0.05
27	10	18	26	10	17	453800.48	0.06
27	9	19	26	9	18	453940.13	0.01
27	8	20	26	8	19	454065.63	0.00
27	0	27	26	0	26	454092.87	-0.02
27	7	21	26	7	20	454177.18	-0.05
27	6	22	26	6	21	454275.40	-0.04
27	5	23	26	5	22	454361.38	-0.03
27	2	26	26	2	25	454424.11	0.06
27	3	25	26	3	24	454510.01	0.02
27	3	24	26	3	23	454519.27	0.01
27	2	25	26	2	24	454855.41	0.03
27	1	26	26	1	25	456312.27	0.01

Table I : Rotational Frequencies (MHz) of CH_2DCN in the Ground Vibrational State.

CH_2DCN											
A (MHz)	121074.490(27)	1.000									
B (MHz)	8759.2669(15)	-0.236	1.000								
C (MHz)	8608.4705(14)	0.504	-0.628	1.000							
Δ_J (kHz)	3.48000(57)	0.055	0.805	-0.126	1.000						
Δ_{JK} (kHz)	143.128(19)	0.299	0.100	0.420	0.350	1.000					
Δ_K (kHz)	1826.6(69)	0.860	-0.496	0.617	-0.148	0.146	1.000				
δ_J (kHz)	0.078968(42)	-0.555	0.738	-0.801	0.329	-0.115	-0.654	1.000			
δ_K (kHz)	35.46(60)	-0.374	0.911	-0.888	0.543	-0.172	-0.594	0.813	1.000		
H_{JK} (Hz)	0.827(13)	0.140	0.340	0.113	0.561	0.744	0.018	0.032	0.145	1.000	
H_{KJ} (Hz)	-0.848(91)	0.245	-0.054	0.353	0.081	0.810	0.119	-0.087	-0.235	0.319	1.000
n[a]	78										
$^{13}CH_2DCN$ [b]											
A (MHz)	120975.8(73)	1.000									
B (MHz)	8532.7384(46)	-0.375	1.000								
C (MHz)	8389.0576(46)	0.373	-0.974	1.000							
Δ_J (kHz)	3.31435(74)	-0.398	0.809	-0.696	1.000						
Δ_{JK} (kHz)	137.5681(69)	0.271	-0.631	0.632	-0.684	1.000					
Δ_K (kHz) [c]	1827(14)	0.004	0.002	-0.002	0.000	0.000	1.000				
δ_J (kHz)	0.07209(78)	0.080	0.437	-0.434	0.036	-0.025	0.000	1.000			
δ_K (kHz)	25.6(20)	-0.510	0.894	-0.896	0.838	-0.706	0.002	0.036	1.000		
n[a]	41										
$CH_2D^{13}CN$ [b]											
A (MHz)	121071.9(95)	1.000									
B (MHz)	8752.8635(63)	-0.232	1.000								
C (MHz)	8602.2753(63)	0.221	-0.962	1.000							
Δ_J (kHz)	3.4806(11)	-0.255	0.781	-0.633	1.000						
Δ_{JK} (kHz)	142.126(12)	0.071	-0.559	0.565	-0.617	1.000					
Δ_K (kHz) [c]	1827(19)	0.004	0.002	-0.002	0.000	0.000	1.000				
δ_J (kHz)	0.0787(11)	0.111	0.478	-0.469	0.037	-0.016	0.000	1.000			
δ_K (kHz)	28.9(27)	-0.372	0.868	-0.873	0.805	-0.648	0.002	0.030	1.000		
n[a]	30										
$CH_2DC^{15}N$											
A (MHz)	121079.9(83)	1.000									
B (MHz)	8492.7814(51)	-0.360	1.000								
C (MHz)	8350.9191(52)	0.345	-0.961	1.000							
Δ_J (kHz)	3.24652(88)	-0.372	0.744	-0.571	1.000						
Δ_{JK} (kHz)	136.167(42)	-0.006	-0.004	0.177	0.294	1.000					
Δ_K (kHz) [c]	1827(16)	0.004	0.002	-0.002	0.000	0.000	1.000				
δ_J (kHz)	0.07205(92)	0.101	0.447	-0.466	-0.031	-0.046	0.000	1.000			
δ_K (kHz)	24.7(22)	-0.511	0.884	-0.872	0.778	-0.076	0.002	0.030	1.000		
H_{JK} (Hz)	0.809(30)	0.004	0.085	0.086	0.416	0.933	0.000	-0.046	0.025	1.000	
H_{KJ} (Hz)	-0.53(12)	-0.180	0.056	-0.065	-0.071	0.050	0.000	0.011	0.069	-0.278	1.000
n[a]	43										

[a]) number of lines.

[b]) H_{JK} and H_{KJ} fixed at the values.of the parent species.

[c]) predicate observations, see text.

Table II. Constants of CH_2DCN in the Ground Vibrational State.

	CH_2DCN		CHD_2CN	
Calculated $\tau_{\alpha\alpha\beta\beta}$ and $\tau_{\alpha\beta\alpha\beta}$ Constants:				
τ_{aabb}	45.519		27.657	
τ_{bbcc}	-13.143		-11.604	
τ_{aacc}	22.767		18.587	
τ_{abab}	-240.301		-202.221	
τ_{bcbc}	-0.115		-0.085	
τ_{acac}	-90.957		-83.78	
Determinable combinations:				
	calc.	exp.	calc.	exp.
A (MHz)		121074.497 (27)		96500.196 (30)
B (MHz)		8759.34596(62)		8320.1996(25)
C (MHz)		9608.69166(64)		8164.5552(25)
T_{aa}	-2244	-1973 (69)	-1282.9	-1329.1 (15)
T_{bb}	-3.4605	-3.63794(61)	-3.056	-3.2119(16)
T_{cc}	-3.19285	-3.32207(55)	-2.909	-3.0219(16)
T_1	-151.901	-153.568 (20)	-134.383	-135.901 (45)
$T_2/(A+B+C)$	-12.8973	-12.4191 (16)	-12.0635	-12.2828(44)
Rotational Constants (MHz) Independent of Centrifugal Distortion:				
A'		121074.325		96500.047
B'		8759.21435		8320.08687
C'		8608.60878		8164.4766

Table III. Centrifugal Distortion Constants (kHz) of CH_2DCN and CHD_2CN.

Species	axis	exp. constant	unperturbed constant	σ[a]	ref.
CH_3CN	A	158099.2(6)	158072	30[c]	30
	B	9198.89938(7)	9199.069	0.02	5
$^{13}CH_3CN$	B	8933.3139(23)	8933.480	0.02	1
$CH_3{}^{13}CN$	B	9194.3490(22)	9194.517	0.02	1
$CH_3C^{15}N$	B	8922.04343(97)	8922.197	0.02	1
$^{13}CH_3{}^{13}CN$	B	8927.2369(72)	8927.400	0.02	8[d]
$^{13}CH_3C^{15}N$	B	8659.8513(93)	8660.002	0.02	9[d]
$CH_3{}^{13}C^{15}N$	B	8919.215(12)	8919.368	0.02	9[d]
$^{13}CH_3{}^{13}C^{15}N$	B	8655.897(16)	8656.041	0.02	9[d]
CD_3CN	A		79339.	100[c]	13
	B	7857.98361(28)	7858.118	0.02	11
$^{13}CD_3CN$	B	7695.30617(66)	7695.439	0.02	10
$CD_3{}^{13}CN$	B	7848.53388(109)	7848.668	0.02	10
$CD_3C^{15}N$	B	7619.30697(61)	7619.429	0.02	10

Species	axis	exp. constant	unperturbed constant	σ[a]	ref.
CH_2DCN	A	121074.490(27)	121058.67	10	b
	B	8759.269(15)	8759.373	5	
	C	8608.4704(14)	8608.763	5	
$^{13}CH_2DCN$	A	120975.8(73)	120960	20	b
	B	8532.7384(46)	8532.854	5[c]	
	C	8389.0576(46)	8389.320	5[c]	
$CH_2D^{13}CN$	A	121071.9(95)	121056	20	b
	B	8752.8635(63)	8752.981	5[c]	
	C	8602.2753(63)	8602.553	5[c]	
$CH_2DC^{15}N$	A	121079.9(83)	121064	20	b
	B	8492.7814(51)	8492.897	5[c]	
	C	8350.9191(51)	8351.178	5[c]	
CHD_2CN	A	96500.190(30)	96490.10	20	13
	B	8320.1624(25)	8320.232	5[c]	
	C	8164.3268(25)	8164.619	5[c]	

[a]) Estimated uncertainty = $\sqrt{\sigma^2 + (10\%\ \text{centrifugal correction})^2 + (10\%\ \text{magnetic correction})^2}$
[b]) This work. [c]) See text. [d]) Recalculated value.

Table IV. Rotational Constants (MHz) of Methyl Cyanide.

	r_o	$r_{\varepsilon l}$	r_s[b]	r_e		r_m^{ρ}
				n=0.5	n=0.7	
r(C≡N)	1.1583(6)	1.1569(0)	1.1564(20)	1.1557	1.1542	1.1546(11)
r(C-C)	1.4594(6)	1.4579(0)	1.4585(20)	1.4568	1.4553	1.4570(11)
r(C-H)	1.0922(3)	1.0900(2)	1.0905(16)	1.0874	1.0847	1.0892(19)
∠(CCH)	108.85(2)	110.02(1)	109.94(13)	110.09	110.16	110.15(2)
σ[c]	13.5	0.768		0.696	0.774	
			ab initio			
	4-21G[d]	5-31G**[d]	DZP[e]	TZVP[e]	r_z[f]	r_g[g]
r(C≡N)	1.1383	1.1343	1.1363	1.1286	1.1567(6)	1.159(2)
r(C-C)	1.4608	1.4663	1.4735	1.4569	1.4617(6)	1.468(2)
r(C-H)	1.0814	1.0822	1.0905	1.0810	1.0947(24)	1.107(4)
∠(CCH)	110.06	109.80	109.55	109.69	109.09(10)	109.7(2)

[a]) Previous r_o structure: r(C≡N) = 1.1572(10) ; r(C-C) = 1.4596(10) ; r(C-H) = 1.094(2) ; ∠(HCC) = 110.00(25). Ref. (17).
[b]) Mean value, see Table VI. [c]) Standard deviation of unit weight.
[d]) Ref. (62). [e]) Ref. (64). [f]) Ref. (1). [g]) Ref. (18).

Table V. Structure of Methyl Cyanide.

	parent	CH_3CN	CH_2DCN	CD_3CN	mean
	r(C-C)	1.4580(30)	1.4592(25)	1.4582(18)	1.4585
	r(CN)	1.1568(30)	1.1558(25)	1.1565(18)	1.1564
parent		CH_3CN	CH_2DCN	CHD_2CN	CD_3CN
CH_3CN	r(C-H)	...	1.0881	1.0899	1.0910
	∠(HCC)	...	109.78	110.03	109.99
	$\sum m_i a_i$ [a]	...	0.0167	0.0016	0.0027
CH_2DCN	r(C-H)	1.0877	...	1.0915	1.0926
	∠(HCC)	109.80	...	110.12	110.07
	$\sum m_i a_i$ [a]	-0.0903	...	0.1052	0.1048
CD_3CN	r(C-H)	1.0910	1.0918	1.0909	...
	∠(HCC)'	109.99	109.95	109.75	...
	$\sum m_i a_i$ [a]	0.0070	0.0093	0.0327	...
		mean	σ	range	
	r(C-H)	1.0905	0.0016	0.0049	
	∠(HCC)	109.94	0.13	0.37	

a) in uÅ.

Table VI. Substitution Coordinates (in Å or °) of Methyl Cyanide.

	Method	CH_3F	CH_3Cl	CH_3Br	CH_3I	CH_3CN	mean diff.[g]
r(C-H) Å	Kraitchman	1.0890	1.0862		1.0830	1.0877	0.0006
	Chutjian	1.0912	1.0876	1.0849	1.0844	1.0910	0.0026
	Chutjian-r_e [a]	1.0885	1.0845	1.0828	1.0807	1.0890	-0.0001
	r_e	1.088(2)[b]	1.0854(5)[c]	1.0823[d]	1.0828[e]	1.0874[f]	
∠(HCX) °	Kraitchman	108.54	108.18		107.16	109.78	-0.35
	Chutjian	108.77	108.34	107.60	107.32	109.99	-0.16
	Chutjian-r_e [a]	108.82	108.38	107.63	107.39	110.02	-0.11
	equilibrium	108.8(3)[b]	108.58(5)[c]	107.73[d]	107.6[e]	110.09[f]	

a) From Eq. (12), see text.
b) Ref. (72). c) Ref. (73). d) Ref. (74). e) Ref. (38). f) This work.
g) Mean value of $r_s - r_e$.

Table VII. Substitution Structures of Methyl Halides.

Molecule	Axis	B(MHz)	ref.	Molecule	Axis	B(MHz)	ref.
CH_3F	a	155352.72 (36)	75	$CD_3{}^{35}Cl$	a	78346.9 (16)	81
	b	25536.1498 (17)	76		b	10658.4534(13)	82
$^{13}CH_3F$	b	24862.6546 (19)	76	$CH_3{}^{79}Br$	a	155311.44 (25)	32
CH_2DF	a	119675.054 (74)	77		b	9568.19279(28)	83
	b	24043.442 (72)	77	$^{13}CH_3{}^{79}Br$	b	9119.4644(40)	84
	c	22959.373 (72)	77	$CH_3{}^{81}Br$	b	9531.83031(29)	83
CD_3F	a	78040.25 (10)	78	$CD_3{}^{79}Br$	a	77958.05	85
	b	20449.8485 (51)	78		b	7714.6501(68)	85
$CH_3{}^{35}Cl$	a	156063.3 (27)	31	CH_3I	a	155110.549 (60)	33
	b	13292.876565(40)	79		b	7501.27575(21)	86
$^{13}CH_3{}^{35}Cl$	b	12796.1817 (26)	79	$^{13}CH_3I$	b	7119.04685(28)	86
$CH_3{}^{37}Cl$	b	13088.1708 (40)	79	CH_2DI	a	118905.662 (44)	87
$CHD_2{}^{35}Cl$	a	95426.077 (61)	80		b	6980.6766(23)	87
	b	11679.7051 (79)	80		c	6883.4852(18)	87
	c	11370.0711 (80)	80	CD_3I	a	77828.5 (30)	34
					b	6040.29766(11)	88

Table VIII. Rotational Constants of Methyl Halides Used in the Substitution Structure Calculations.

	axis	I_m^ρ	I_e	$I_e - I_m^\rho$ (%)
$CH_3{}^{35}Cl$	a	3.19625[a]	3.20012(45)[b]	0.117
	b	37.70604	37.68061(22)	-0.067
$CD_3{}^{35}Cl$	a	6.40001	6.3862(17)	-0.21
	b	46.26235	46.2701(17)	0.017
$CH_3{}^{79}Br$	a	3.21343[c]	3.2128(136)[d]	-0.019
	b	52.40119	52.3664(78)	-0.066
$CD_3{}^{79}Br$	a	6.43516	6.4249(52)	-0.16
	b	65.02726	65.0187(75)	-0.013

[a]) $\rho_a = 0.993509$ and $\rho_b = 0.995887$. [b]) Ref. (73).
[c]) $\rho_a = 0.993770$ and $\rho_b = 0.996048$. [d]) Ref. (74).

Table IX. I_e and I_m^ρ Moments of Inertia for Methyl Chloride and Methyl Bromide (in uÅ^2).

		r_m^ρ	r_e
CH_3Cl	r(C-H) Å	1.0835(3)	1.0845(5)[a]
	r(C-Cl) Å	1.7777(1)	1.7760(3)
	∠(HCCl) °	108.35(2)	108.58(5)
CH_3Br	r(C-H) Å	1.0816(3)	1.0823[b]
	r(C-Br) Å	1.9353(2)	1.9340
	∠(HCBr) °	107.56(3)	107.73

a) Ref. (73). b) Ref. (74).

Table X. r_m^ρ Structure of Methyl Chloride and Methyl Bromide.

	r_g	r_e	$r_g - r_e$
HCN	1.158(3)[a]	1.1532[b]	0.005
NCCN	1.163(2)[c]	1.1578[d]	0.005
CH_3CN	1.159(2)[a]	1.1558[e]	0.003

a) Ref. (18). b) Ref. (63). c) Ref. (57).
d) Ref. (89). e) This work.

Table XI. Comparison of $r_g(C\equiv N)$ and $r_e(C\equiv N)$ Bond lengths (in Å).

			ab initio		
molecule	r_e	r_g	4-21G	4-31G	$r_g - r_e$
NCCN	1.3839(15)[a]	1.3925(20)[d]		1.372[m]	0.009
c-C_2H_4O	1.4594(4)[b]		1.475[k]	1.461[n]	
CH_3CH_2Cl	1.5096(22)[b]	1.523 (8)[e]	1.528[k]		0.013
CH_3CH_3	1.522 (2)[c]	1.5323(11)[f]	1.5406[l]	1.529[p]	0.010
$CH_3CH{=}CH_2$	1.4957(18)[b]	1.5063(30)[g]	1.512[k]	1.501[p]	0.011
c-C_3H_6	1.501 (4)[h]	1.5139(12)[h]		1.502[p]	0.013
c-C_3H_4	1.5051(3)[b]			1.512[p]	
$CH_3CH_2CH_3$	1.5209(9)[b]	1.5323[i]	1.541[k]	1.530[p]	0.011
mean					0.011(2)
CH_3CN		1.468 (2)[j]	1.4608[o]		

a) Ref. (89). b) Ref. (54). c) Ref. (53). d) Ref. (57). e) Ref. (93). f) Ref. (94). g) Ref. (95). h) Ref. (96). i) Ref. (97). j) Ref. (18). k) Ref. (61). l) Ref. (67). m) Ref. (92). n) Ref. (91). p) Ref. (90). o) Ref. (62).

Table XII. Comparison of r(C-C) Bond Lengths (in Å).

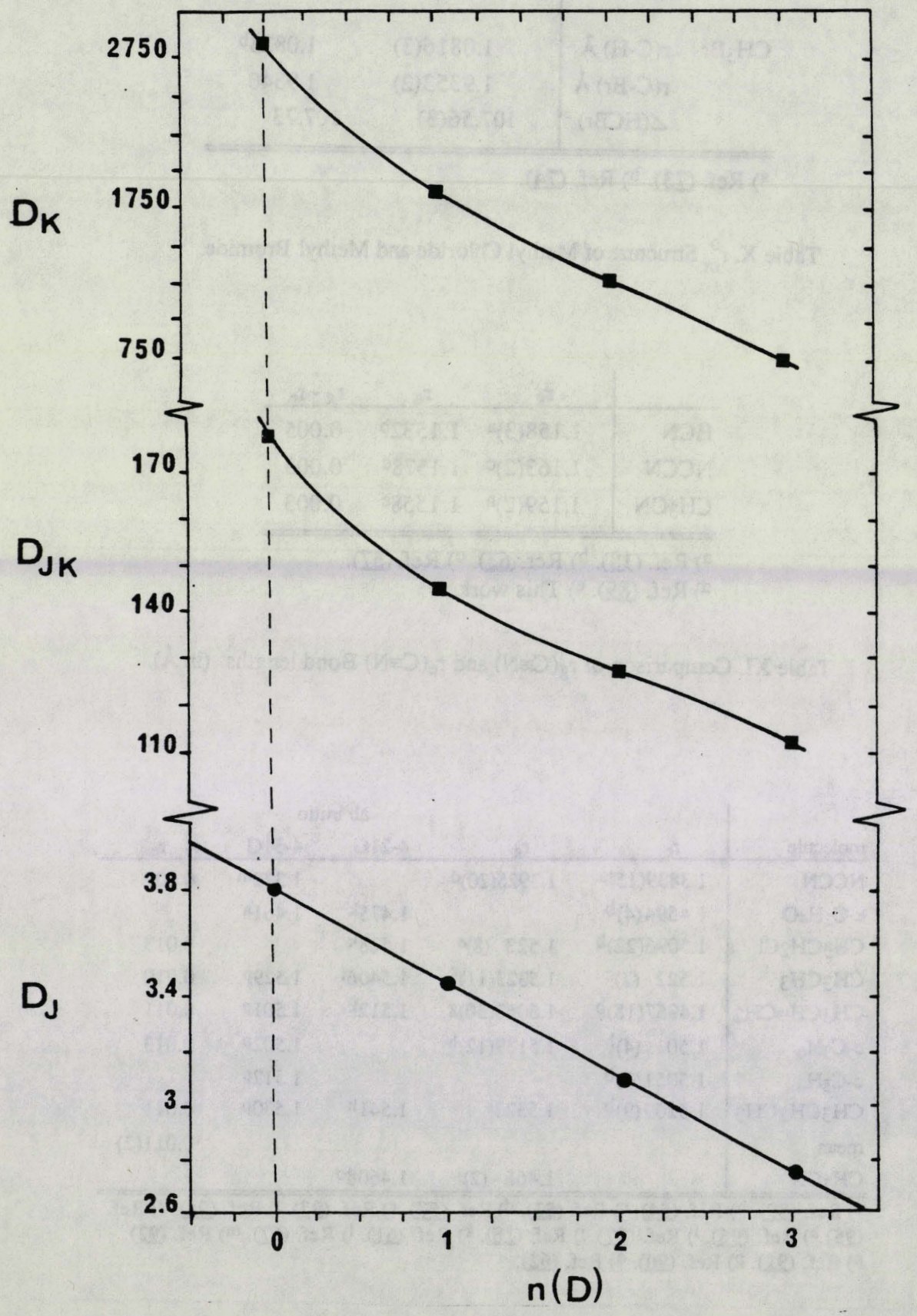

Fig. 1. Plot of D_J, D_{JK} and D_K of the deuterated isotopic species of methyl cyanide versus the number of deuterium atoms.

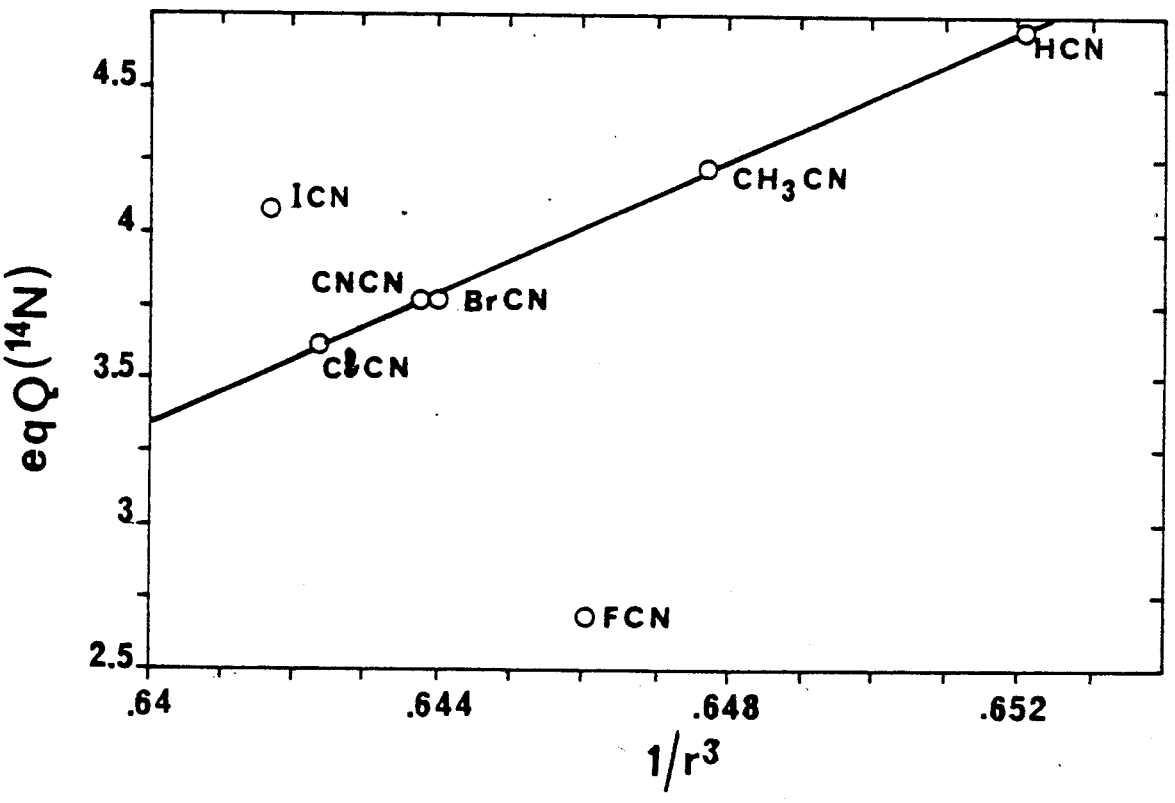

Fig. 2 Plot of $eqQ(^{14}N)$ (MHz) versus $1/r^3_{C\equiv N}$ ($Å^{-3}$).

CHAPITRE E

ANALYSE DE COMPOSES DE BASSE COORDINENCE DU PHOSPHORE NON STABILISES

Introduction :

La chimie des composés de phosphore trivalent de bas degré de coordination (phosphaalcènes et phosphaalcynes) est une chimie récente. C'est en 1961 que Gier [61 Gie] a, pour la première fois, mis en évidence, par spectroscopie infra-rouge, H-C≡P par décharge électrique entre deux électrodes de graphite dans une enceinte contenant la phosphine PH_3. Du fait de sa grande réactivité, ce composé a longtemps été considéré comme une curiosité de laboratoire.

Trois revues récentes de Nixon [88 Nix], de Regitz [90 Reg] et de Maah [90 Maa] font le point sur les différentes voies d'accès aux phosphaalcènes et phosphaalcynes stabilisés par des effets stériques ou électroniques. Quelques phosphaalcynes non stabilisés ont été, quant à eux, mis en évidence en phase gazeuse par spectroscopie photoélectronique [79 Wes] et [79 Esh].

Au laboratoire de chimie structurale de Rennes, de nouvelles méthodes de synthèse des phosphaalcènes et des phosphaalcynes cinétiquement non stabilisés, et donc extrêmement réactifs, ont été mises au point et ont fait l'objet de plusieurs thèses et publications. Citons par exemple : [89 Pel], [89 Cab], [89 Gui] et [90 Den 1], et plus récemment [92 Gui 1].

L'objet de ce chapitre est d'analyser par spectroscopie microonde des phosphaalcènes et phosphaalcynes non stabilisés (Cl-C≡P, H_2C=CH(PH_2), (CH_3)CH=PH), entités qui ont déjà été caractérisées par d'autres méthodes spectroscopiques (RMN ^1H, ^{13}C, ^{31}P [91 Gui], [91Gau], [89 Cab], photoélectrons [91 Den], [91 Lac], etc).

Il a été montré d'autre part que des espèces chimiques de très courte durée de vie, comme par exemple Si_2H_2, pouvaient être analysées par spectroscopie microonde [91 Bog]. Nous avons donc utilisé cette technique dans l'espoir de mettre en évidence le phosphaallène (H_2C=C=PH), entité non détectée directement mais postulée comme intermédiaire réactionnel dans l'isomérisation de l'yne phosphine en méthylphosphaalcyne.

Comme nous ne disposions d'aucune donnée bibliographique, ni expérimentale, sur ces molécules, nous avons tout d'abord estimé certaines de leurs caractéristiques physiques à l'aide de calculs "ab initio" (constantes de rotation, moments dipolaires, ...). Nous les avons ensuite étudiées dans le domaine centimétrique où l'identification des raies est plus facile.

bibliographie p. 197

1°) Recherche du chlorophosphaalcyne : Cl-C≡P

L'analyse du spectre microonde du chlorophosphaalcyne obtenu par bideshydrochloration de la trichlorométhylphosphine sur un banc de chaux chauffé à 250°C a posé un certain nombre de problèmes. En effet, la synthèse du précurseur est effectuée dans l'éther éthylique

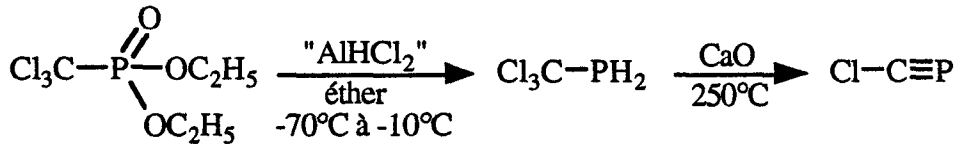

et bien que la solution ait été concentrée, l'éther résiduel a énormément géné l'interprétation du spectre du fait qu'il possède de nombreuses raies intenses dans la gamme de fréquences balayée alors que celles du chlorophosphaalcyne sont petites.

Au même moment, deux publications de Kroto et collaborateurs sont parues sur l'analyse du chlorophosphaalcyne par spectroscopie microonde [90 Den 2] et spectroscopie photo-électronique [91 Den]. Nous avons alors décidé d'interrompre nos recherches puisqu'elles confirmaient le fait que nous devions utiliser un précurseur en l'absence totale d'éther et donc envisager une autre synthèse de celui-ci. En effet, Kroto et collaborateurs ont pu analyser le spectre de très faible intensité de Cl-C≡P grâce à une méthode de synthèse qui consiste à réaliser une thermolyse éclair à 530°C de la pentachlorophosphine :

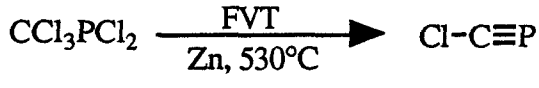

2°) Recherche d'une tautomérie entre la vinylphosphine et le méthylphospha alcène

* Rappels de la littérature :

Le méthylphosphaalcène a été obtenu dans la littérature par deshydrochloration en phase gazeuse de l'α-chlorophosphine sur un banc de carbonate de potassium chauffé à 250°C [89 Cab].

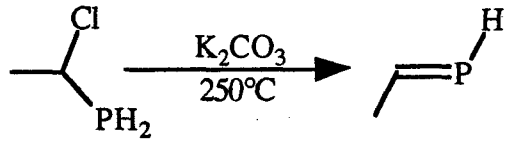

bibliographie p. 197

Si on chauffe à une température de 350°C, la vinylphosphine est obtenue [91 Gui 2].

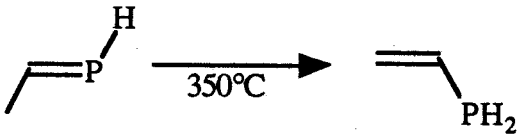

On peut en conséquence penser que cette formation provient d'une isomérisation du phosphaalcène sur base solide à haute température et qu'il peut exister un équilibre entrre ces deux entités :

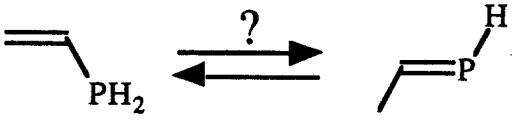

L'objet de cette étude était d'obtenir les spectres microondes de ces deux entités et de chercher leur présence simultanée éventuelle.

2.1. Calculs "ab initio" et recherche de la structure de la vinylphosphine

Nous avons émis l'hypothèse que la vinylphosphine présente dans la cellule existait sous la forme de l'un des trois conformères "décalés" représentés ci-dessous selon la représentation de Newman :

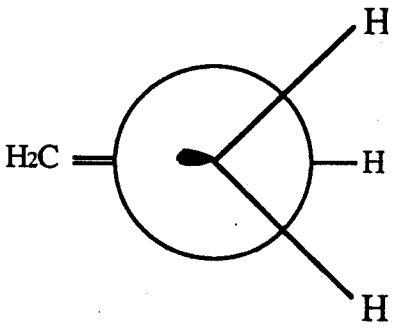

conformère N°1

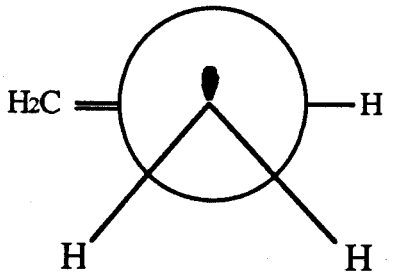

conformère N°2

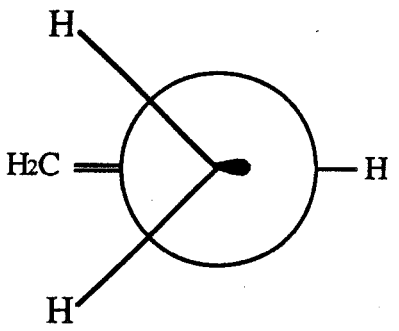

conformère N°3

Nous avons effectué des calculs "ab initio" dans la base 3.21G* sur ces trois conformères afin de savoir :

- si la phosphine la plus stable possède, comme chez l'amine $H_2C=CH(NH_2)$ [82 Sae], [84 Ham], les deux hydrogènes du même côté du plan, c'est à dire si elle correspond au conformère N°2,
- ou si les effets stériques sont minimisés par la présence d'un hydrogène de chaque côté du plan vinylique (conformère N°1).

bibliographie p. 197

Le tableau ci-dessous nous permet non seulement de voir que la forme la plus stable est la première, où la paire libre du phosphore se conjugue avec la liaison π, mais aussi que les niveaux d'énergie des deux autres formes sont suffisamment proches pour que leur existence soit possible.

Le tableau EI regroupe également les différentes caractéristiques qui nous sont nécessaires pour faire une prévision de spectre. Les constantes de rotation ont été obtenues à partir de la structure représentée figure EIII.

Confomère N°	1	2	3
E (Hartrees)	-417,270869	-417,269096	-417,266614
$\Delta E = E_i - E_1$	-	389 cm^{-1} 6,65 kJ Mol^{-1}	934 cm^{-1} 11,2 kJ Mol^{-1}
A (MHz)	41 615	41 560	40 430
B (MHz)	5 511	5 479	5 455
C (MHz)	5 074	5 009	5 011
défaut d'inertie ($uÅ^2$)	-4,25	-3,51	-4,29
μ_a (D)	0,83	0,45	1,30
μ_b (D)	0,82	0,86	-0,62
μ_c (D)	0	0,61	0

(1 Hartree = $2,195.10^5$ cm^{-1} = $6,272.10^5$ cal.Mol^{-1} = $26,217\ 10^5$ J Mol^{-1})

Tableau EI : Energie, constantes de rotation, défaut d'inertie et moments dipolaires "ab initio" (base 3.21G*) des différents conformères de $H_2C{=}CH(PH_2)$

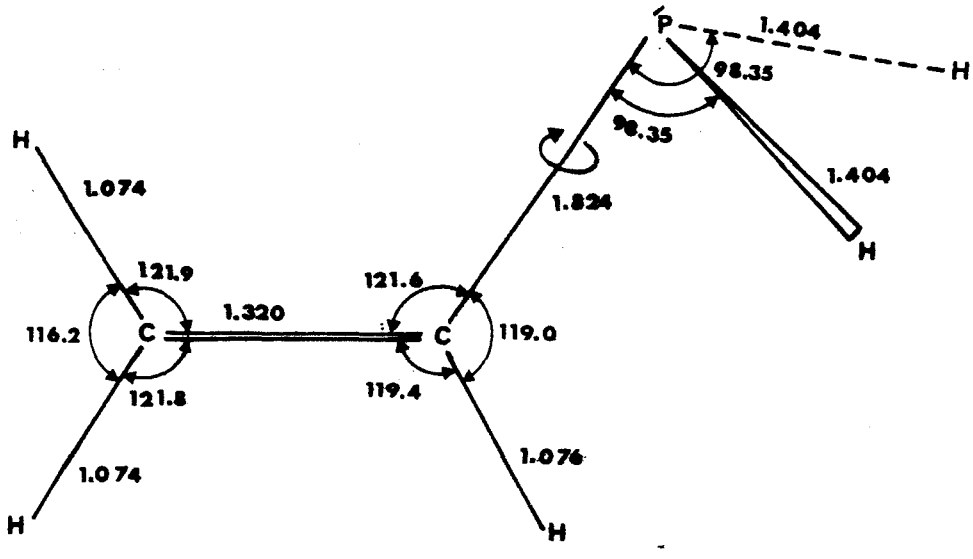

bibliographie p. 197

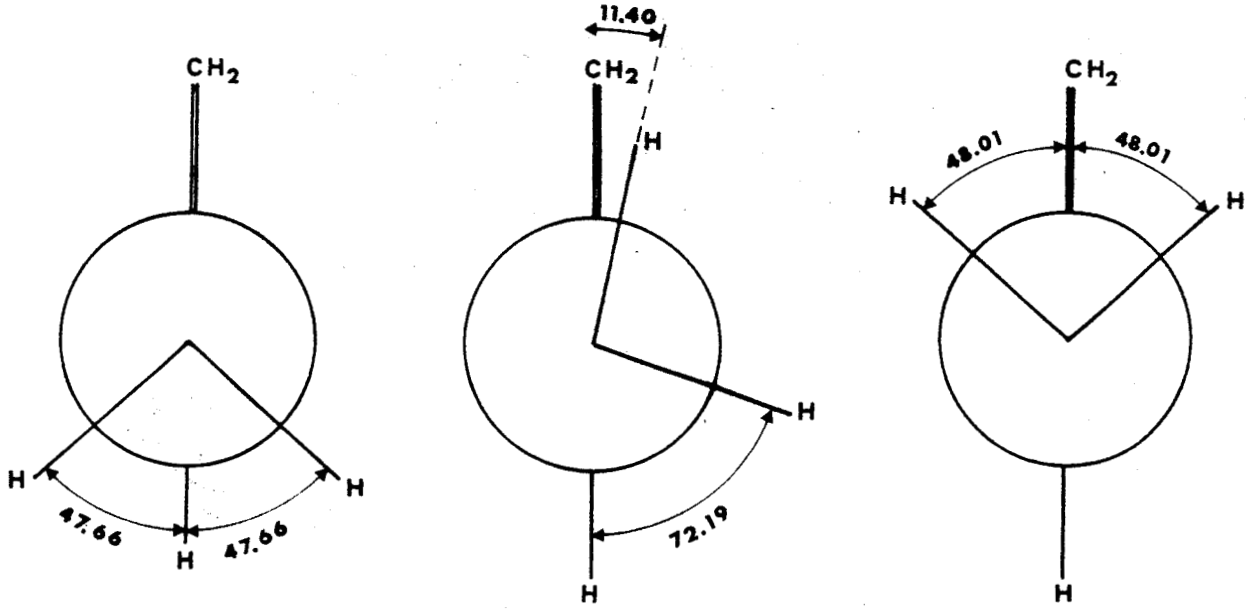

Figure EIII : Structure géométrique de $H_2C{=}CH(PH_2)$ obtenue à partir de calculs "ab initio" (base 3.21G*) ; longueurs de liaison en Å et angles en degrés

2.2. Spectrométrie centimétrique à modulation Stark

Parmi les nombreuses raies présentes dans la gamme balayée et dûes aux impuretés (C_2H_5OH, C_2H_5Cl, $C_2H_5(PH_2)$, ...) nous avons réussi à identifier douze raies appartenant à la vinylphosphine (exemple figure EIV), qui nous ont permis de déterminer, dans la réduction A et la représentation I^r, les constantes de rotation A, B, C et la constante de distorsion centrifuge Δ_J (tableau EII).

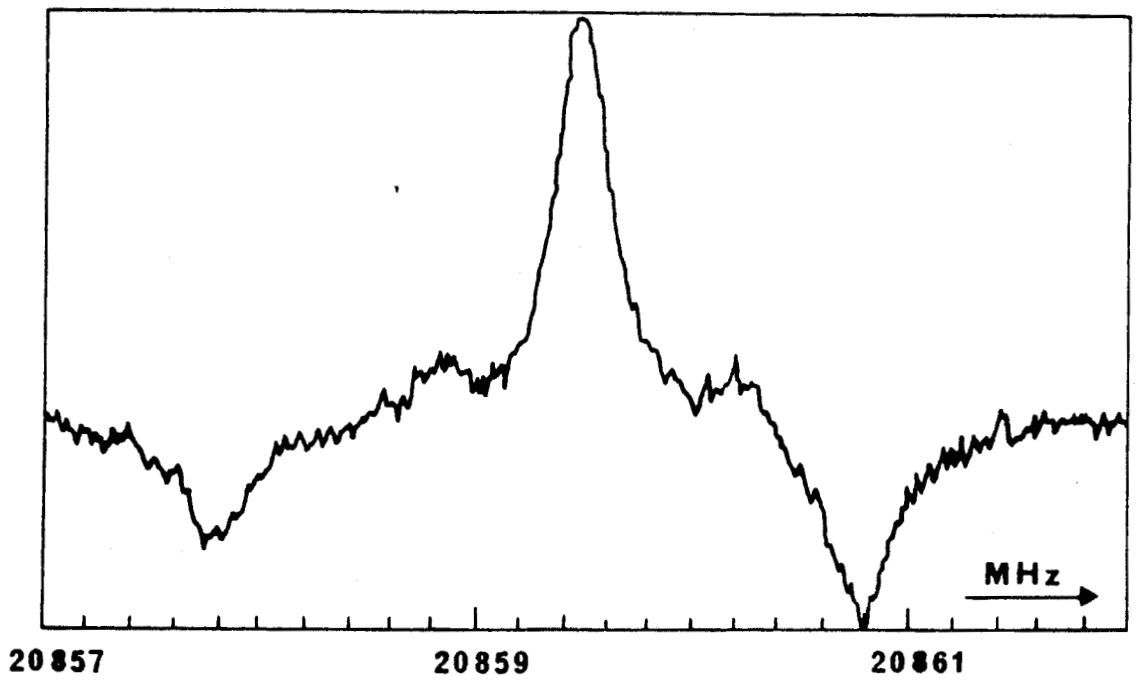

Figure EIV : Transition $2_{0,2}$-$1_{0,1}$ de $H_2C{=}CH(PH_2)$ et ses composantes Stark M=0 à gauche et M=1 à droite (Tension Stark = 500 V)

bibliographie p. 197

Transition	Fréquence expérimentale (MHz)	e.- c. (MHz)
$2_{1,2} - 1_{1,1}$	20 380,641	-0,018
$2_{0,2} - 1_{0,1}$	20 859,473	-0,067
$2_{1,1} - 1_{1,0}$	21 348,430	0,001
$3_{1,3} - 2_{1,2}$	30 567,799	0,066
$3_{0,3} - 2_{0,2}$	31 276,543	-0,117
$3_{1,2} - 2_{1,1}$	32 019,388	0,030
$4_{0,4} - 3_{0,3}$	41 678,622	0,004
$4_{2,2} - 3_{2,1}$	41 774,756	0,009
$4_{1,3} - 3_{1,2}$	42 686,409	0,115
$5_{1,5} - 4_{1,4}$	50 929,077	-0,006
$5_{0,5} - 4_{0,4}$	52 060,465	0,035
$5_{1,4} - 4_{1,3}$	53 347,750	-0,083
Ecart type	0,0732	
A (MHz)	40 306 (26)	1,000
B (MHz)	5 458,098 (11)	0,430 1,000
C (MHz)	4 974,211 (11)	0,162 0,158 1,000
Δ_J (kHz)	2,38 (22)	0,631 0,808 0,799 1,000
Défaut d'inertie (uÅ^2)	-3,531	

Tableau EII : Fréquences d'absorption et constantes moléculaires de l'état fondamental de $H_2C{=}CH(PH_2)$

Arrivés à ce stade, il ne nous est pas possible de savoir quel conformère est présent dans la cellule. Nous avons alors déterminé à l'aide de l'effet Stark [84 Gor] les composantes du moment dipolaire : $\mu_a = 0{,}63\ (6)$ D

$\mu_b = 0{,}51\ (5)$ D

μ_c fixé à 0 D

L'interprétation de tous les résultats obtenus (tableau EIII) va maintenant nous permettre de déterminer le conformère de la vinylphosphine présent dans la cellule.

bibliographie p. 197

Conformère N°	1	2	3
$(A_{exp.} - A_{ab\ initio}) / A_{exp.}$	-3,14 %	-3,02%	-0,31%
$(B_{exp.} - B_{ab\ initio}) / B_{exp.}$	-0,96 %	-0,38%	0,06%
$(C_{exp.} - C_{ab\ initio}) / C_{exp.}$	-1,97 %	-0,69%	-0,73%
$*\Delta_{exp.} - \Delta_{ab\ initio}$	-16,9 %	0,60%	-21,8%
$(\mu_{a\ exp.} - \mu_{a\ ab\ initio}) / \mu_{aexp.}$	-21,4 %	40,0%	-51,5%
$(\mu_{b\ exp.} - \mu_{b\ ab\ initio}) / \mu_{bexp.}$	-37,8 %	-40,7%	-17,7%
$(\mu_{c\ exp.} - \mu_{c\ ab\ initio}) / \mu_{cexp.}$	0 %	-100%	0%
$E_i - E_1$	-	6,65 kJ Mol^{-1}	11,2 kJ Mol^{-1}

* Δ = défaut d'inertie

Tableau EIII : Comparaison entre les résultats "ab initio" et expérimentaux de la vinylphosphine

Nous pouvons très facilement dire que nous ne sommes pas en présence du conformère N°2 puisque sa symétrie n'est pas favorable et que son moment dipolaire possède trois composantes alors qu'expérimentalement $\mu_c = 0$ Debye. Von Ragué Schleyer [87 Sch] explique de plus la différence d'énergie par le fait que le groupement pyramidal $-PH_2$ se comporte comme un groupement attracteur et que la délocalisation des électrons du système π est plus grande pour le confomère N°1 que pour le conformèe N°2.

Il n'existe pas de critère expérimental qui permette d'éliminer catégoriquement l'un ou l'autre des deux conformères restants. Cependant, lorsque l'on regarde les énergies électroniques, on s'aperçoit qu'il existe une différence significative de stabilité entre les conformères 1 et 3. Pfister-Guillouzo et collaborateurs expliquent la stabilisation conduisant à la forme 1 par l'interaction existant entre la paire libre du phosphore et l'orbitale π*(C=C) [88 Gon]. Nous pouvons alors affirmer que la vinylphosphine présente dans la cellule est sous sa forme la plus stable, c'est à dire :

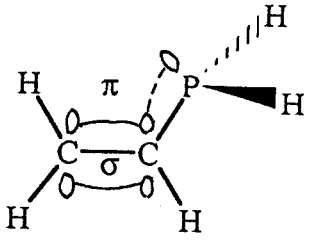

Figure EV : Conformère de $H_2C=CH(PH_2)$ observé

bibliographie p. 197

Comme nous ne disposons que de trois constantes de rotation, il n'est possible de déterminer qu'au maximum trois paramètres. Différents essais ont été effectués et nous n'avons pu déterminer que que deux paramètres : r(C-P) = 1,846 Å

$\angle$(CCP) = 120,7°

Les autres paramètres ont été quant à eux fixés d'une part aux valeurs de la vinylamine [75 Lov] pour le radical vinylique, et d'autre part à des valeurs obtenues à partir de calculs "ab initio" en base 6.31G* pour les valeurs manquantes (c'est à dire r(P-H) = 1,403 Å, $\angle$(CPH) = 99,25° et l'angle dièdre φ = 48,36°).

Les calculs "ab initio" donnent des angles avec une bonne précision (de l'ordre du degré), mais malheureusement les longueurs de liaisons sont affectées d'une erreur systématique. Pour évaluer l'influence de la liaison P-H sur les valeurs déterminées, nous avons effectué un essai en variant légèrement sa valeur (r(P-H) = 1,41 Å) et nous avons observé que les paramètres variaient très peu : r(C-P) = 1,848 Å

$\angle$(CCP) = 120,7°

2.3. Recherche du C-Méthylphosphaalcène : $(CH_3)CH{=}PH$

Nous avons déterminé par calculs "ab initio" de nombreuses caractéristiques physiques du C-méthylphosphaalcène :

- sa structure optimisée (figure EVI)
- ses constantes de rotation : A = 42 348 MHz
  B = 5 517 MHz
  C = 5 032 MHz
- les composantes de son moment dipolaire : μ_a = -1,26 D
  μ_b = 0,96 D
  μ_c = 0 D
- son énergie électronique : E = -417,268979 Hartrees

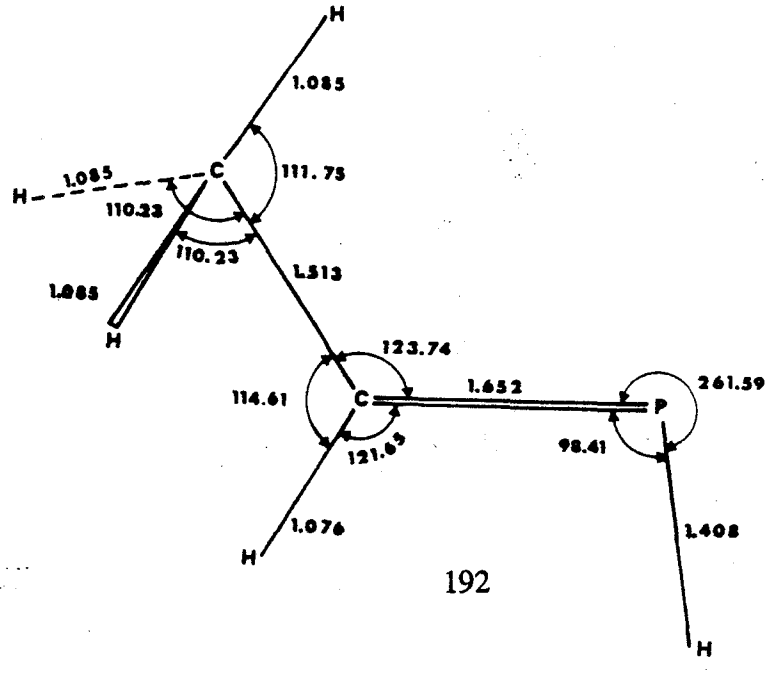

bibliographie p. 197

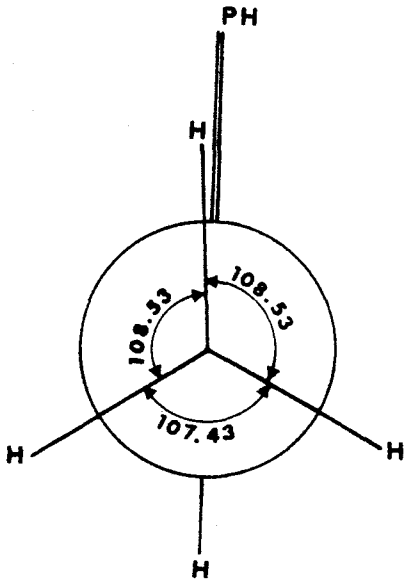

Figure EVI : structure géométrique de $(H_3C)HC{=}PH$ obtenue à partir de calculs "ab initio" (base 3.21G*) : a) longueurs de liaison en Å et angles de valence en degrés ; b) angles dièdres en degrés

Parmi les nombreuses raies présentes dans la gamme balayée (30-32 GHz), nous n'avons pas réussi à identifier les raies appartenant au C-méthylphosphaalcène.

En effet, comme il a été signalé dans le chapitre C-1, les conditions expérimentales sont différentes de celles décrites dans la littérature et l'on observe par conséquent beaucoup de raies appartenant à des impuretés identifiées ou non (C_2H_5OH, C_2H_5Cl, $C_2H_5(PH_2)$, ...). De plus, du fait de sa très grande réactivité, le C-méthylphosphaalcène a eu tendance à se polymériser dès sa formation (observation d'un polymère blanc à la sortie du four),

Toutes ces conditions ont fait que la réaction n'a pas été facilement reproductible et qu'il n'a pas été possible de caractériser le C-méthylphosphaalcène par spectroscopie microonde.

2.4. Conclusion

Il n'a pas été possible de mettre en évidence l'équilibre entre la vinylphosphine et le C-méthylphosphaalcène.

Nous avons observé la présence de nombreuses impuretés qui rendent difficilement interprétables les spectres microondes de ces espèces. Il est donc souhaitable de purifier les précurseurs à l'avance avant de pouvoir obtenir des spectres suffisamment clairs qui permettraient de mettre en évidence une tautomérie.

Ce travail sera repris avec une synthèse séparée des précurseurs et des tests de pureté.

bibliographie p. 197

3°) Tentative de mise en évidence d'un intermédiaire réactionnel : $H_2C{=}C{=}PH$

L'intermédiaire réactionnel que nous voulons étudier est issu de la réaction suivante [92 Gui 1] :

$$H{-}C{\equiv}C{-}PH_2 \xrightarrow[100°C]{K_2CO_3} \left[H_2C{=}C{=}PH\right] \longrightarrow CH_3CP$$

Nous avons dans un premier temps mis en évidence la formation de l'éthynylphosphine par réduction du phosphonate correspondant, en l'absence du banc basique et nous avons visualisé les raies prédites par Cohen et al [87 Coh].

En faisant ensuite passer l'yne phosphine sur un banc de carbonate de potassium chauffé à 100°C, nous avons détecté le méthylphosphaalcyne [79 Kro].

3.1. Calculs "ab initio"

Nous avons déterminé par calculs "ab initio" de nombreuses caractéristiques physiques concernant le phosphaallène :

- sa structure optimisée (figure EI) dont on tire
- les constantes de rotation : A = 140 260 MHz
  B = 5 318 MHz
  C = 5 307 MHz
- les composantes de son moment dipolaire : μ_a = 1,47 D
  μ_b = 0,56 D
  μ_c = 0,14 D
- son énergie électronique : E = - 416,072668 Hartrees
- ainsi que d'autres caractéristiques (champ de force, coordonnées atomiques, ...) qui ne sont pas indispensables dans le cadre de ce travail.

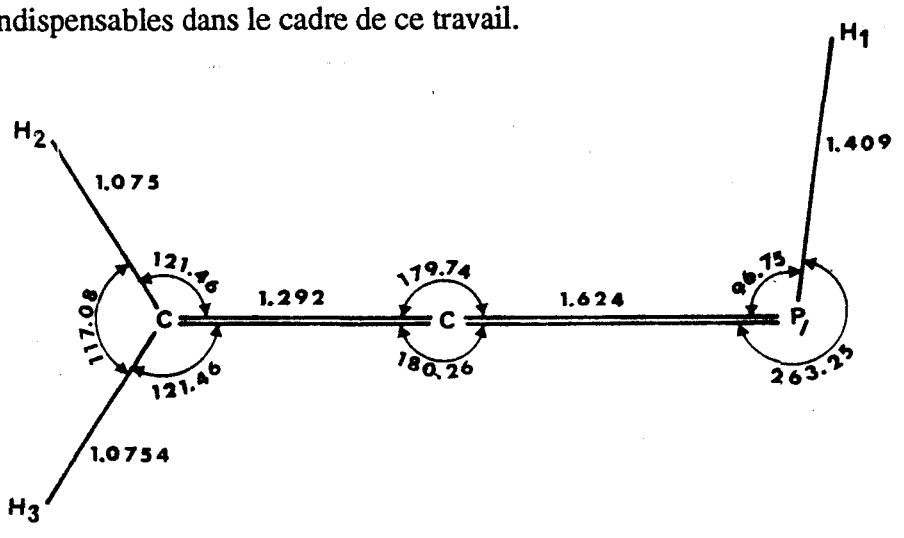

bibliographie p. 197

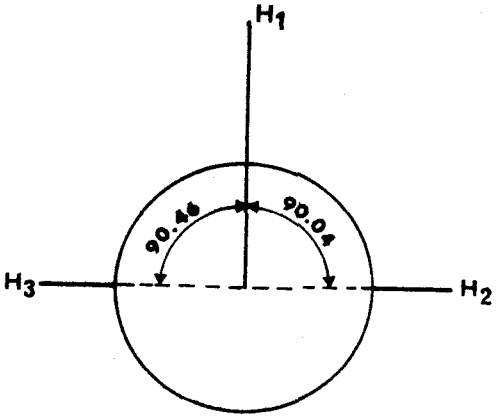

Figure EI : Structure géométrique de $H_2C=C=PH$ obtenue à partir de calculs "ab initio" (base 3.21G*) : a) longueurs de liaison en Å et angles de valence en degrés ; b) angles dièdres en degrés

Nous avons alors pu prévoir le type de spectre de la molécule (essentiellement type μ_a) ainsi que la fréquence approximative des raies d'absorption. Il faut toutefois noter un handicap important : la très haute instabilité de l'espèce que nous voulons étudier dans des conditions de manipulation qui ne sont pas très bien adaptées.

3.2. Recherche de l'intermédiaire phosphallènique :

Pour essayer de mettre en évidence le phosphaallène $H_2C=C=PH$, nous avons effectué plusieurs essais en montant progressivement la température du banc de carbonate de potassium :
- lorsque la température du four est inférieure à 75°C, la réaction n'a pas lieu et CH_3CP ne se forme pas,
- lorsque la température est de 75°C, on observe une petite quantité de CH_3CP,
- lorsque la température est de 100°C, on observe une grande quantité de CH_3CP dans la cellule.

La suite des analyses a donc été effectuée après un chauffage à 75°C, en flux réalisé à l'aide de deux pièges à des températures différentes : pièges A à -110°C et B à la température de l'azote liquide (voir figure CII).

La large gamme balayée (18-20 GHz) n'a malheureusement pas permis de mettre en évidence l'intermédiaire phosphallénique. Plusieurs hypothèses peuvent être avancées pour expliquer cet échec :

* Du fait de son énergie élevée, cette molécule est très instable et les conditions expérimentales utilisées ne lui sont pas bien adaptées :
- le trajet entre le four, où $H_2C=C=PH$ se forme, et l'entrée de la cellule, bien que raccourci au maximum est peut être trop long (environ 70 cm),

bibliographie p. 197

- le flux gazeux réalisé à l'aide d'un jeu des deux pièges thermiques A et B, refroidis à des températures différentes, n'est peut-être pas assez rapide,
- la présence, sur le parcours, d'une vanne d'arrêt qui possède un diamètre de quelques millimètres, introduit une perte de charge importante et augmente en conséquence le temps de séjour des espèces formées sur la base et dans le réacteur.

* Un autre aspect important est d'ordre cinétique. Il a été montré que la vitesse de réarrangement était fonction de l'acidité de la phosphine [92 Gui 1]. Pfister-Guillouzo a montré récemment que l'acidité *P-H* du phosphaallène était du même ordre de grandeur que celle de l'yne phosphine [91 Pfi]. Il est donc vraisemblable que les deux réarrangements interviennent presque simultanément ; le phosphaallène ne serait donc pas observable dans ces conditions.

En conclusion, il n'a pas été possible de mettre en évidence l'intermédiaire phosphallènique dans les conditions expérimentales utilisées ; ce qui n'exclut pas pour autant son existence qui a été montrée récemment par piégeage chimique [92 Gui 1].

bibliographie p. 197

BIBLIOGRAPHIE

[61 Gie] T. E. GIER
J. Am. Chem. Soc. 1961, 83, 1769 -1770

[75 Lov] F. J. LOVAS, F. O. CLARK & E. TIEMANN
J. Chem. Phys. 1975, 62, 1925-1931

[79 Esh] H. ESHTIAGH - HOSSEINI & H. W. KROTO
J. Chem. Soc., Chem. Comm. 1979, 653 -654

[79 Kro] H. W. KROTO, J. F. NIXON & N. P. C. SIMMONS
J. Mol. Spectrosc. 1979, 77, 270-285

[79 Wes] N. P. C. WESTWOOD, H. W. KROTO, J. F. NIXON & N. P. C. SIMMONS
J. Chem. Soc. Dalton Trans. 1979, 1405 -1408

[82 Sae] S. SAEBØ & L. RADOM
J. Mol. Struct. 1982, 89, 227-233

[84 Ham] Y. HAMADA, K. HASHIGUCHI, M. TSUBOI, Y. KOGA & S. KONDO
J. Mol. Spectrosc. 1984, 105, 93-104

[84 Gor] W. GORDY & R. L. COOK
"Microwave Molecular Spectra"
Wiley, New York 1984, vol XVIII, chap. X

[87 Coh] E. A. COHEN, G. A. MC RAE, H. GOLDWHITE, S. DiSTEFANO
& R. A. BEAUDET
Inorg. Chem. 1987, 26, 4000-4003

[87 Sch] C. SCHADE & P. VON RAGUE SCHLEYER
J. Chem. Soc., Chem. Comm. 1987, 1339-1401

[88 Gon] D. GONBEAU, S. LACOMBE, M. C. LASNES, J. L. RIPOLL & G. PFISTER-GUILLOUZO
J. Am. Chem. Soc. 1988, 110, 2730-2735

[88 Nix] J. F. NIXON
Chem. Rev. 1988, 88, 1327-1362

[89 Cab] J. L. CABIOCH

Thèse de Doctorat, Avril 1989, Université de Rennes (France)

[89 Gui] J. C. GUILLEMIN, M. LE GUENNEC & J. M DENIS
J. Chem. Soc., Chem. Comm. 1989, 988-990

[89 Pel] B. PELLERIN
Thèse de Doctorat, Avril 1989, Université de Rennes (France)

[90 Den 1] J. M. DENIS, J. C. GUILLEMIN & M. LE GUENNEC
Phosphorus, Sulfur & Silicon 1990, 49/50, 317-320

[90 Den 2] T. J. DENNIS, S. FIRTH, H. W. KROTO, D. R. M. WALTON & R. J. SUFFOLK
J. Chem. Soc., Chem. Comm. 1990, 1430-1431

[90 Maa] M. J. MAAH & J. F. NIXON
"The Chemistry of organophosphorus Compounds"
Ed. F. R. Hartley, J. Wiley & Sons Ltd 1990

[90 Reg] M. REGITZ
"Multiple Bonds and Low Coordination in Phosphorus Chemistry"
Ed. M. Regitz and O. J. Scherer, New York 1990

[91 Bog] M. BOGEY, H. BOLVIN, C. DEMUYNCK & J. L. DESTOMBES
Phys. Rev. Letters 1991, 66, 413-416

[91 Den] T. J. DENNIS, S. FIRTH, H. W. KROTO, G.Y. MATTI, C. Y. MOK,
R. J. SUFFOLK & D. R. M. WALTON
J. Chem. Soc. Farad. Trans. 1991, 87, 917-920

[91 Gau] A. C. GAUMONT
Thèse de Doctorat, Juillet 1991, Université de Rennes (France)

[91 Gui] J. C. GUILLEMIN, T. JANATI, P. GUENOT, P. SAVIGNAC & J. M. DENIS
Angew. Chem. Int. Ed. Engl. 1991, 30, 196-198

[91 Lac] S. LACOMBE, G. PFISTER-GUILLOUZO, J. C. GUILLEMIN, & J. M. DENIS
J. Chem. Soc., Chem. Comm. 1991, 403-405

[91 Pfi] G. PFISTER-GUILLOUZO
résultat non publié

[92 Gui 1] J. C. GUILLEMIN, T. JANATI & J. M. DENIS
J. Chem. Soc., Chem. Comm. 1992, sous presse

J. C. GUILLEMIN, T. JANATI, P. GUENOT & J. M. DENIS
J. Chem. Soc., Chem. Comm. 1992, sous presse

[92 Gui 2] J. C. GUILLEMIN
résultat non publié

Conclusion

Nous avons déterminé avec une très grande précision les constantes de rotation de nombreux isotopomères de plusieurs molécules simples : deux linéaires triatomiques (BrCN et OCSe) et trois symétriques ($FClO_3$, GeH_3F et CH_3CN). Cela nous a permis de déterminer et de comparer plusieurs types de structures.

Nous avons montré que la structure $r_{\varepsilon,I}$ est facile à utiliser et qu'elle fournit des résultats de qualité égale ou supérieure à la structure r_s. En outre, elle est d'application plus générale, en particulier la structure reste déterminable si les atomes ne sont pas substituables ou s'ils sont près d'un axe principal d'inertie.

Nous avons montré également que la structure r_s pouvait être très différente de la structure r_e, même pour une molécule lourde (molécule sans hydrogène). Nous avons analysé les causes de cette différence et nous avons déterminé les différents termes du développement en série de Taylor de la correction vibrationnelle aux moments d'inertie. Ce développement ne converge pas très rapidement .

Cela explique aussi pourquoi la structure de double substitution fournit parfois des résultats inacceptables.

Enfin, nous avons étudié la variation de la correction vibrationnelle ε lors des substitutions isotopiques. Nous avons montré que dans les cas favorables (beaucoup d'isotopomères disponibles), il était possible de trouver une loi de variation simple et, en conséquence, d'en déduire une structure de qualité r_e.

Par ailleurs nous avons pu identifier une nouvelle molécule organique phosphorée instable : la vinylphosphine. Nous avons analysé son spectre de rotation mais nous n'avons pas déterminé sa structure. En effet, la synthèse et l'analyse des différentes espèces isotopiques est un travail de longue haleine qui sera poursuivi ultérieurement .

Finalement, notre analyse des spectres de rotation de CH_2DCN et $CH_2DC{\equiv}CH$ a permis leur identification dans le milieu interstellaire : Orion A pour CH_2DCN et TMC1 pour $CH_2DC{\equiv}CH$.

Annexe

ANNEXE

Spectroscopie de rotation de CH_2DCCH et CH_3CCD

La première étude du propyne remonte aux années 50 où Trambarulo et Gordy se sont déjà intéressés à certaines formes isotopiques, deutérées ou non [50 Tra]. Par la suite, de nombreuses équipes ont mesuré les spectres des états fondamentaux et des états excités dans les domaines centimétrique, millimétrique, submillimétrique ou infra-rouge ; citons par exemple parmi les plus récents : [82 Cog] pour CH_3CCD et CD_3CCH, [88 Wlo] pour CH_3CCH et les isotopes en ^{13}C, ...

L'analyse des spectres rotationnels des propynes-1D et -3D et de leurs formes isotopiques en ^{13}C, a été réalisée entre 145 et 470 GHz.

L'identification des transitions a été relativement facile grâce à l'intensité des raies des états fondamentaux et au fait que le spectre n'est pas trop dense. Les fréquences d'absorption mesurées sont rassemblées dans les tableaux AnI et AnII et les paramètres moléculaires dans le tableau AnIII et AnIV.

BIBLIOGRAPHIE :

[50 Tra] R. TRAMBARULO & W. GORDY
J. Chem. Phys. 1950, 18, 1613-1616

[82 Cog] C. D. COGLEY, L. N. TACK & S. G. KUKOLICH
J. Chem. Phys. 1982, 76, 5669-5671

[88 Wlo] G. WLODARCZAK, R. BOCQUET, A. BAUER & J. DEMAISON
J. Mol. Spectrosc. 1988, 129, 371-380

J	K	Fréquence	e. - c.
		CH_3CCD	
0	0	15576.329	0.000
1	0	31152.560	-0.043
1	1	31152.000	-0.032
2	0	46728.720	-0.046
2	1	46727.860	-0.049
2	2	46725.320	-0.020
9	0	155754.182	-0.002
9	1	155751.299	-0.033
9	2	155742.762	-0.012
9	3	155728.557	0.041
9	4	155708.533	-0.028
9	5	155682.963	0.046
9	6	155651.601	0.008
9	7	155614.596	-0.005
9	8	155571.934	-0.020
9	9	155523.669	0.002
12	0	202472.207	0.017
12	1	202468.492	0.008
12	2	202457.386	0.019
12	3	202438.855	0.011
12	4	202412.907	-0.013
12	5	202379.610	0.004
12	6	202338.933	0.019
12	7	202290.845	-0.012
12	8	202235.435	-0.019
12	9	202172.700	-0.024
12	10	202102.696	0.005
12	11	202025.384	0.005
12	12	201940.831	0.014
28	0	451489.504	0.005
28	1	451481.295	0.008
28	2	451456.660	0.005
28	3	451415.615	0.004
28	4	451358.173	0.002
28	5	451284.352	-0.004
28	6	451194.181	-0.010
28	9	450825.936	-0.025
28	11	450499.467	-0.023
28	12	450312.142	0.013
28	15	449654.423	0.039
28	18	448854.881	-0.017
		$CH_3C^{13}CD$	
9	0	151849.602	0.006
9	1	151846.864	-0.002
9	2	151838.711	0.037
9	3	151825.055	0.031
9	4	151805.926	0.005
9	5	151781.395	0.023
9	6	151751.357	-0.028
9	7	151715.945	-0.026
12	0	197396.670	0.019
12	1	197393.003	-0.100
12	2	197382.473	0.012
12	3	197364.735	0.007
12	4	197339.910	-0.001
12	6	197269.119	0.058
12	7	197223.009	-0.044
12	8	197170.002	-0.010
12	9	197109.977	0.022
28	0	440176.370	-0.004
28	1	440168.523	0.012
28	2	440144.935	0.011
28	3	440105.584	-0.038
28	6	439893.615	0.022
28	9	439540.959	-0.007
29	0	455339.436	0.007
29	1	455331.290	-0.010
29	3	455266.300	0.021
29	4	455209.384	-0.028
29	5	455136.140	-0.192
29	6	455047.090	0.026
29	9	454682.650	-0.058
29	12	454173.737	0.017
		$CH_3{}^{13}CCD$	
9	0	155731.328	0.012
9	2	155719.958	0.029
9	3	155705.682	-0.018
9	4	155685.755	-0.031
9	6	155628.951	0.016
9	7	155592.030	0.010
12	0	202442.461	0.001
12	2	202427.690	0.023
12	3	202409.154	-0.027
12	4	202383.272	-0.039
12	6	202309.456	-0.001
12	7	202261.493	-0.007
12	8	202206.191	-0.021
12	9	202143.640	0.025
27	0	435871.511	-0.002
27	2	435839.877	0.029
27	3	435800.264	-0.015
27	6	435586.863	0.049
27	9	435231.736	-0.091
28	0	451423.117	-0.030
28	2	451390.350	-0.021
28	3	451349.418	0.007
28	4	451292.130	0.040
28	6	451128.415	-0.035
28	9	450760.996	-0.001
28	12	450248.284	0.006
		$^{13}CH_3CCD$	
9	0	151527.202	-0.007
9	1	151524.488	-0.012
9	2	151516.390	0.015
9	3	151502.828	-0.008
9	4	151483.887	-0.002
9	6	151429.809	0.010
9	7	151394.674	-0.002
9	5	151459.540	-0.001
9	8	151354.172	-0.011
9	9	151308.337	0.001
12	0	196977.498	0.016
12	1	196973.985	0.022
12	2	196963.432	0.025
12	3	196945.783	-0.036
12	4	196921.258	0.054
12	5	196889.556	-0.016
12	6	196850.914	-0.020
12	7	196805.267	-0.037
12	8	196752.720	0.022
12	9	196693.170	0.033
28	0	439240.005	0.102
28	1	439232.096	-0.008
28	2	439208.737	0.028
28	3	439169.746	0.019
28	6	438959.461	0.031
28	8	438741.763	0.053
28	12	438121.704	-0.005
29	0	454370.530	-0.009
29	1	454362.461	-0.015
29	2	454338.323	0.035
29	3	454297.876	-0.109
29	4	454241.576	-0.005
29	5	454169.024	-0.073
29	6	454080.536	-0.024
29	9	453718.947	-0.037

Tableau AnI : Fréquences d'absorption (MHz) de CH_3CCD dans l'état fondamental

J'	K'_+	K'_-	J	K_+	K_-	Fréquence	e.- c.
				CH_2DCCH			
1	0	1	0	0	0	16181.120	-.031
2	0	2	1	0	1	32362.080	-.045
2	1	1	1	1	0	32491.860	-.051
2	1	2	1	1	1	32231.440	-.065
3	0	3	2	0	2	48542.620	-.125
3	1	2	2	1	1	48737.520	-.112
3	1	3	2	1	2	48346.900	-.129
3	2	1	2	2	0	48540.330	-.140
3	2	2	2	2	1	48539.960	-.064
11	1	10	10	1	9	178685.218	-.055
11	2	9	10	2	8	177987.562	.042
11	2	10	10	2	9	177963.012	.029
11	0	11	10	0	10	177953.843	.026
11	3	8	10	3	7	177955.608	-.014
11	4	8	10	4	7	177933.816	-.009
11	5	6	10	5	5	177907.033	-.053
11	6	5	10	6	4	177874.869	.038
11	7	5	10	7	4	177836.944	.050
11	8	3	10	8	2	177793.243	.035
11	9	2	10	9	1	177743.788	.050
11	10	2	10	10	1	177688.499	.036
11	1	11	10	1	10	177253.736	.010
14	1	13	13	1	12	227401.085	.024
14	2	12	13	2	11	226534.525	.047
14	2	13	13	2	12	226483.829	.061
14	3	12	13	3	11	226480.098	.178
14	0	14	13	0	13	226455.832	.014
14	4	10	13	4	9	226451.230	-.010
14	5	9	13	5	8	226416.721	-.026
14	6	9	13	6	8	226375.439	-.035
14	7	8	13	7	7	226327.078	-.003
14	8	7	13	8	6	226271.451	.020
14	9	6	13	9	5	226208.500	.044
14	10	5	13	10	4	226138.171	.052
14	11	4	13	11	3	226060.415	.022
14	12	2	13	12	1	225975.168	-.092
14	1	14	13	1	13	225579.764	.009
18	1	18	17	1	17	289996.376	.022
18	1	17	17	1	16	292336.405	.058
18	2	16	17	2	15	291269.297	.042
18	3	16	17	3	15	291168.677	-.020
18	3	15	17	3	14	291169.580	-.040
18	2	17	17	2	16	291161.433	-.007
18	4	14	17	4	13	291129.621	-.044
18	0	18	17	0	17	291089.924	.025
18	5	14	17	5	13	291084.290	-.017
18	6	13	17	6	12	291030.706	-.051
18	7	11	17	7	10	290968.264	-.031
18	8	10	17	8	9	290896.661	.025
18	9	10	17	9	9	290815.682	.040
18	10	9	17	10	8	290725.343	.106
18	11	8	17	11	7	290625.413	.040
18	12	7	17	12	6	290515.891	-.127
27	1	27	26	1	26	434831.093	.021
27	0	27	26	0	26	436316.878	-.001
27	2	26	26	2	25	436590.420	-.068
27	3	25	26	3	24	436657.745	-.004
27	3	24	26	3	23	436664.791	-.005
27	2	25	26	2	24	436951.668	.015
27	1	26	26	1	25	438330.211	.024
28	1	28	27	1	27	450913.105	.018
28	0	28	27	0	27	452432.439	-.008
28	2	27	27	2	26	452739.203	.047
28	3	26	27	3	25	452816.648	-.014
28	3	25	27	3	24	452825.104	-.011
28	2	26	27	2	25	453141.337	.022
28	1	27	27	1	26	454539.924	.004
28	4	24	27	4	23	452745.702	-.073
28	5	24	27	5	23	452669.491	-.065
28	6	22	27	6	21	452583.488	-.062
28	7	21	27	7	20	452485.004	-.037
28	8	21	27	8	20	452372.977	.011
28	9	20	27	9	19	452246.908	.083
28	10	19	27	10	18	452106.485	.129
28	11	18	27	11	17	451951.493	.092
29	1	29	28	1	28	466992.670	.013
29	0	29	28	0	28	468543.332	.001
29	2	28	28	2	27	468885.559	.060
29	3	27	28	3	26	468974.166	.119
29	3	26	28	3	25	468984.101	-.019
29	2	27	28	2	26	469331.529	.017
29	1	28	28	1	27	470746.929	.015
				$CH_2DC^{13}CH$			
10	2	8	9	2	7	156937.202	-.011
10	2	9	9	2	8	156920.975	.029
10	0	10	9	0	9	156917.168	.009
10	3	7	9	3	6	156913.088	-.049
10	4	6	9	4	5	156894.607	-.005
10	5	5	9	5	4	156871.644	.003
10	1	9	9	1	8	157539.440	.001
10	1	10	9	1	9	156314.560	.005
10	7	3	9	7	2	156811.144	.003
10	8	3	9	8	2	156773.476	.014
10	9	2	9	9	1	156730.750	-.046
10	6	5	9	6	4	156843.831	-.023
13	2	11	12	2	10	204021.559	-.015
13	2	12	12	2	11	203985.661	-.047
13	5	8	12	5	7	203924.807	.081
13	1	13	12	1	12	203196.392	-.004
13	1	12	12	1	11	204788.248	-.005
13	6	7	12	6	6	203888.490	.054
28	1	28	27	1	27	437415.843	-.029
28	0	28	27	0	27	438863.142	-.005
28	1	27	27	1	26	440830.227	.002
28	3	26	27	3	25	439199.112	.040
28	3	25	27	3	24	439206.093	.007
28	5	23	27	5	22	439061.050	-.008
28	9	19	27	9	18	438660.459	-.037
29	1	29	28	1	28	453015.313	.046

Tableau AnII : Fréquences d'absorption (MHz) de CH_3CCD dans l'état fondamental

J'	K'+	K'-	J	K+	K-	Fréquence	e.- c.
29	9	20	28	9	19	454310.918	.007
29	8	22	28	8	21	454434.868	.049
29	0	29	28	0	28	454493.853	-.003
29	7	23	28	7	22	454544.984	.040
29	5	24	28	5	23	454726.193	-.118
29	2	28	28	2	27	454794.918	.008
29	4	25	28	4	24	454801.210	-.034
29	3	27	28	3	26	454870.904	.006
29	3	26	28	3	25	454879.250	-.006
29	2	27	28	2	26	455189.681	.009
29	1	28	28	1	27	456549.760	.019

$CH_2D^{13}CCH$

9	2	7	8	2	6	145532.491	.001
9	0	9	8	0	8	145517.175	-.006
9	2	8	8	2	7	145519.122	-.008
9	3	6	8	3	5	145511.166	-.038
9	4	6	8	4	5	145493.887	.003
9	5	4	8	5	3	145472.278	-.032
9	6	3	8	6	2	145446.163	-.016
9	7	3	8	7	2	145415.390	-.012
9	8	2	8	8	1	145379.962	.019
9	1	9	8	1	8	144939.780	-.020
9	1	8	8	1	7	146110.202	.034
13	2	11	12	2	10	210218.922	.005
13	2	12	12	2	11	210178.430	.009
13	0	13	12	0	12	210157.873	-.007
13	4	9	12	4	8	210146.921	-.012
13	5	8	12	5	7	210115.394	.126
13	6	7	12	6	6	210077.279	-.001
13	7	7	12	7	6	210032.705	.003
13	1	13	12	1	12	209340.158	.009
13	1	12	12	1	11	211030.006	.002
28	9	19	27	9	18	451964.322	-.158
28	8	21	27	8	20	452089.579	-.116
28	0	28	27	0	27	452146.757	-.066
28	6	23	27	6	22	452298.980	.139
28	5	24	27	5	23	452384.299	-.008
28	2	27	27	2	26	452453.114	-.022
28	4	24	27	4	23	452460.002	-.085
28	3	26	27	3	25	452530.572	-.053
28	3	25	27	3	24	452538.998	-.050
28	2	26	27	2	25	452854.456	-.033
28	1	28	27	1	27	450628.678	.085
28	1	27	27	1	26	454251.947	-.215
29	1	29	28	1	28	466698.111	.111
29	10	20	28	10	19	467944.623	.016
29	9	20	28	9	19	468089.052	.095
29	8	22	28	8	21	468218.746	.078
29	0	29	28	0	28	468247.471	-.076
29	7	23	28	7	22	468334.072	.055
29	6	24	28	6	23	468435.564	.022
29	5	24	28	5	23	468524.392	-.017
29	4	25	28	4	24	468603.540	-.086
29	3	27	28	3	26	468677.735	-.044
29	3	26	28	3	25	468687.777	-.040
29	2	27	28	2	26	469034.404	.015
29	1	28	28	1	27	470449.272	.380

$^{13}CH_2DCCH$

10	2	8	9	2	7	157885.103	.014
10	2	9	9	2	8	157868.318	.023
10	0	10	9	0	9	157864.219	.030
10	3	7	9	3	6	157860.469	-.009
10	4	6	9	4	5	157841.692	-.001
10	5	5	9	5	4	157818.443	.025
10	1	9	9	1	8	158496.349	.018
10	6	5	9	6	4	157790.262	-.005
10	7	3	9	7	2	157757.131	.002
10	8	3	9	8	2	157718.939	-.022
10	9	2	9	9	1	157675.892	.151
10	1	10	9	1	9	157252.472	.013
13	2	11	12	2	10	205254.031	.005
13	2	12	12	2	11	205216.972	-.026
13	0	13	12	0	12	205198.969	.017
13	4	9	12	4	8	205185.982	-.005
13	5	8	12	5	7	205155.378	.008
13	6	7	12	6	6	205118.572	-.029
13	7	6	12	7	5	205075.385	-.050
13	8	6	12	8	5	205025.747	-.030
13	1	12	12	1	11	206031.916	.015
13	1	13	12	1	12	204415.347	-.025
28	0	28	27	0	27	441500.835	-.051
28	1	28	27	1	27	440036.041	.288
28	1	27	27	1	26	443502.791	.052
28	2	26	27	2	25	442146.714	-.315
28	3	26	27	3	25	441848.733	-.008
28	3	25	27	3	24	441856.158	.006
28	5	24	27	5	23	441708.407	-.073
28	6	22	27	6	21	441625.897	-.084
28	7	21	27	7	20	441531.263	-.099
28	8	21	27	8	20	441423.297	-.366
29	0	29	28	0	28	457224.570	-.065
29	2	28	28	2	27	457535.858	-.037
29	4	25	28	4	24	457544.050	-.044
29	3	27	28	3	26	457614.920	-.015
29	3	26	28	3	25	457623.681	-.087
29	1	29	28	1	28	455728.074	-.116
29	7	22	28	7	21	457284.105	.045
29	6	23	28	6	22	457382.380	.165
29	5	24	28	5	23	457468.043	.065
29	9	21	28	9	20	457046.869	-.006
29	8	22	28	8	21	457172.791	.347
29	2	27	28	2	26	457943.548	.251
29	1	28	28	1	27	459317.186	.084

Tableau AnII : Fréquences d'absorption (MHz) de CH_3CCD dans l'état fondamental

	CH_3CCD					
B (MHz)	7788.16907 (20)	1.000				
D_J (kHz)	2.29926 (16)	0.755	1.000			
D_{JK} (kHz)	142.7840 (50)	0.473	0.262	1.000		
H_{JK} (Hz)	0.7127 (34)	0.414	0.522	0.745	1.000	
H_{KJ} (Hz)	4.281 (13)	0.009	-0.328	0.209	-0.465	1.000
n	41					
	$CH_3C^{13}CD$					
B (MHz)	7592.91599 (70)	1.000				
D_J (kHz)	2.18083 (41)	0.980	1.000			
D_{JK} (kHz)	136.680 (20)	0.685	0.655	1.000		
H_{JK} (Hz)	0.656 (12)	0.665	0.689	0.907	1.000	
H_{KJ} (Hz)	4.020 (77)	-0.015	-0.109	0.142	-0.258	1.000
n	31					
	$CH_3{}^{13}CCD$					
B (MHz)	7787.02573 (93)	1.000				
D_J (kHz)	2.29966 (58)	0.981	1.000			
D_{JK} (kHz)	143.495 (25)	0.722	0.691	1.000		
H_{JK} (Hz)	0.713 (15)	0.704	0.725	0.923	1.000	
H_{KJ} (Hz)	4.346 (72)	-0.025	-0.130	0.094	-0.281	1.000
n	26					
	$^{13}CH_3CCD$					
B (MHz)	7576.80020 (41)	1.000				
D_J (kHz)	2.19882 (26)	0.903	1.000			
D_{JK} (kHz)	135.569 (12)	0.694	0.538	1.000		
H_{JK} (Hz)	0.6508 (70)	0.592	0.698	0.617	1.000	
H_{KJ} (Hz)	4.100 (73)	0.112	-0.134	0.454	-0.374	1.000
n	35					

Tableau AnIII : Constantes moléculaires de CH_3CCD

	CH_2DCCH									
A (MHz)	121834.2 (84)	1.000								
B (MHz)	8155.7341 (48)	-0.360	1.000							
C (MHz)	8025.4273 (47)	0.349	-0.968	1.000						
Δ_J (kHz)	2.70869 (72)	-0.400	0.794	-0.660	1.000					
Δ_{JK} (kHz)	132.006 (20)	-0.049	-0.005	0.162	0.192	1.000				
δ_J (kHz)	0.05957 (77)	0.095	0.463	-0.462	0.040	0.012	1.000			
δ_K (kHz)	25.4 (21)	-0.507	0.881	-0.881	0.821	-0.103	0.037	1.000		
H_{JK} (Hz)	0.7584 (84)	0.029	0.068	0.082	0.348	0.669	0.014	-0.015	1.000	
H_{KJ} (Hz)	-1.29 (13)	-0.176	0.137	-0.046	0.196	0.844	0.014	0.099	0.269	1.000
n	82									
	$CH_2DC^{13}CH$									
A (MHz)	121814.0 (90)	1.000								
B (MHz)	7908.5008 (54)	-0.349	1.000							
C (MHz)	7785..8574 (54)	0.349	-0.977	1.000						
Δ_J (kHz)	2.53908 (77)	-0.329	0.856	-0.755	1.000					
Δ_{JK} (kHz)	125.424 (20)	0.081	-0.104	0.239	0.138	1.000				
δ_J (kHz)	0.05493 (63)	0.062	0.355	-0.355	0.037	-0.004	1.000			
δ_K (kHz)	26.8 (25)	-0.435	0.935	-0.935	0.862	-0.185	0.042	1.000		
H_{JK} (Hz)	0.703 (13)	0.015	0.163	-0.033	0.413	0.909	0.008	0.104	1.000	
n	37									
	$CH_2D^{13}CCH$									
A (MHz)	121829 (18)	1.000								
B (MHz)	8150.567 (12)	-0.449	1.000							
C (MHz)	8020.371 (12)	0.448	-0.975	1.000						
Δ_J (kHz)	2.7108 (17)	-0.470	0.844	-0.735	1.000					
Δ_{JK} (kHz)	131.147 (53)	0.083	-0.074	0.222	0.177	1.000				
δ_J (kHz)	0.0587 (15)	0.074	0.393	-0.389	0.049	0.006	1.000			
δ_K (kHz)	28.3 (54)	-0.566	0.921	-0.923	0.854	-0.166	0.048	1.000		
H_{JK} (Hz)	0.715 (33)	-0.024	0.138	0.009	0.397	0.950	0.017	0.065	1.000	
n	45									
	$^{13}CH_2DCCH$									
A (MHz)	121918 (26)	1.000								
B (MHz)	7956.896 (16)	-0.445	1.000							
C (MHz)	7832.239 (16)	0.445	-0.977	1.000						
Δ_J (kHz)	2.5913 (22)	-0.454	0.847	-0.746	1.000					
Δ_{JK} (kHz)	127.037 (52)	0.115	-0.125	0.265	0.128	1.000				
δ_J (kHz)	0.0559 (20)	0.066	0.380	-0.378	0.043	0.003	1.000			
δ_K (kHz)	55.1 (72)	-0.554	0.925	-0.925	0.859	-0.216	0.042	1.000		
H_{JK} (Hz)	0.682 (34)	0.070	0.023	0.111	0.300	0.922	0.010	-0.052	1.000	
n	45									

Tableau AnIV : Constantes moléculaires de CH_2DCCH